University of Nottingham

UK | CHINA | MALAYSIA

Microwave-Enhanced Thermal Processing of Algae

Yu HONG, BEng.

Thesis submitted to the University of Nottingham

for the degree of Doctor of Philosophy

July 2017

Abstract

Algae are promising substitutes to the widely-used fossil fuels. The thermochemical conversion of algae has been investigated extensively in the past two decades. In this study, systematic investigation of microwave-enhanced pyrolysis of algae together with catalytic reforming was conducted aiming at developing a new approach for the production of more syngas-enriched gas product from algae and other marine biomass.

Firstly, the characterisation of algae was conducted to show the nature of the raw materials followed by the kinetic study of the decomposition of a suite of micro- and macro-algae, i.e., spirulina, chlorella and porphyra. The kinetic study was carried out using model algae, i.e. the use of ovalbumin as protein, oil droplets as lipid and cellulose as polysaccharides or carbohydrate to simulate a real alga. The thermogravimetric characteristics of algal samples were studied based on the analysis of TG and DTG curves. Kissinger-Akahira-Sunose method was used to derive the activation energy and pre-exponential factor. Moreover, the optimal reaction mechanism was determined by using Coats-Redfern method of the decomposition of different samples. The morphology and composition of char after TG analysis were characterised by using SEM/EDS. By comparing the characteristics of chars prepared in N_2 and CO_2 atmosphere, it was found that CO_2 atmosphere favored the pyrolysis of algal protein with

lower required activation energy (about 235 kJ mol^{-1}) and shortened the pyrolysis time by 5.9-20.2%. But it was also found that the algal lipid increased the difficulty for the pyrolysis of algae with relatively higher activation energy around 200 kJ mol^{-1} (>180 kJ mol^{-1} under N_2). However, the activation energy of cellulose decomposition remained almost the same around 310 kJ mol^{-1} in N_2 and CO_2. Therefore, CO_2 atmosphere is more suitable for the pyrolysis of algae with high protein content and low lipid content. It was also found that protein in algae decomposes first, which is followed by the decomposition of carbohydrates and then lipids.

Secondly, in order to obtain a high yield of syngas-enriched gas product from algae, microwave-enhanced pyrolysis of algae (spirulina, chlorella, dunaliella, laminaria and porphyra) and primary model algal compounds, i.e. cellulose and ovalbumin, at 400, 550 and 700°C in N_2 atmosphere was conducted. The distribution and composition of gaseous, liquid and solid products were also studied in detail. Amongst the five algae, porphyra is the most promising raw material for high syngas-enriched gas production with more than 85 wt.%, while protein-rich spirulina and chlorella favored bio-oil production which yielded in about 10 wt.%. Meanwhile, with 94 wt.% carbohydrate, dunaliella converted most of its carbohydrates into C1-C3 gases. With a high portion of incombustible components (14.7-23.3 vol.% of CO_2), laminaria has relatively lower gaseous production

which was less than 80 wt.%. It also found that the optimal pyrolysis temperature was in the range of 400 to 550 °C for most of the samples except for spirulina which was at 700 °C. For the production of bio-oil, microalgae, with high protein content, were favored to be the raw materials (oil yield of 5.2-15.4 wt.%), compared to macroalgae (oil yield of 1.8-5.2 wt.%). Moreover, microalgae-spirulina and chlorella-favoured the formation of more phenols and nitrogenated compounds (10.8-17.8% and 20.9- 28.7% respectively) primarily from protein content, while less PAHs of 11.4-29.9% which mainly derived from algal carbohydrates.

Finally, microwave-enhanced reforming of algae under CO_2 atmosphere was conducted at 400, 550 and 700°C, together with the comparison of the results including the distribution and composition of gas, bio-oil and char in N_2 and CO_2 atmospheres. Compared with the product distribution derived under N_2, the bio-oil yield from most algae in CO_2 increased by 50- 170%, whilst the production of gas slightly decreased by 1-7%. Under CO_2 atmosphere, the syngas in spirulina and chlorella gas product dramatically decreased by 60.8-69.7% and 7.1-17.6% respectively, while that from dunaliella increased by 23.4-30.4%. The percentage of syngas for the other samples remained similar. For the bio-oil derived from all the five algae samples, there were nearly no PAHs contained.

In addition, the ash of algae was used as catalyst and introduced into the pyrolysis of five algae respectively under N_2 atmosphere at 550°C. Compared with the non-catalytic pyrolysis, the weight percent of char from most algae increased by 20-90% using laminaria and porphyra ash, due to the decomposition of compounds in bio-oil. The syngas percentage from microalgae significantly increased by 6-45%, while that from macroalgae slightly decreased by 2-15% with the addition of spirulina, chlorella and porphyra ash. The content of PAHs in the bio-oil of spirulina, chlorella, laminaria and porphyra considerably reduced by 29-94%, while the amount of aromatics from spirulina and chlorella increased to around 1.3-7.1 times.

In summary, the microwave-enhanced pyrolysis of algae favored the production of more CO/H_2 rich gas at lower pyrolysis temperature under N_2 atmosphere, while under CO_2 atmosphere the yield of bio-oil increased. With the addition of algal ash as catalysts, the CO+H_2 percentage in gas production from microalgae increased significantly. Therefore, it can be concluded that the microwave-enhanced pyrolysis of algae is an effective and efficient process for the conversion of algal biomass into value-added fuels.

Achievements

Journal papers

- **Yu Hong**, Wanru Chen, Xiang Luo, Chengheng Pang, Edward Lester, Tao Wu*, Microwave-enhanced pyrolysis of macroalgae and microalgae for syngas production. Bioresource Technology, 2017. **237**: p. 47-56.
- Xiang Luo, **Yu Hong**, Fuchen Wang, Siqi Hao, Chengheng Pang, Edward Lester, Tao Wu*, Development of nano NixMgyO solid solutions with outstanding anti-carbon deposition capability for the steam reforming of methanol. Applied Catalysis B: Environmental, 2016, 194(0): 84-97.
- Ashak Mahmud Parvez, **Yu Hong**, Edward Lester, Tao Wu*, Enhancing the Reactivity of Petroleum Coke in CO2 via Co-Processing with Selected Carbonaceous Materials. Energy & Fuels, 2017. 31(2): p. 1555-1563.

Patent

- Chengheng Pang, Tao Wu, Edward Lester, Yang Meng, **Yu Hong**, Zhixuan Wu, Ling Huang, Yukuan Xu. A method for examining and determining the characteristic curve of ash fusion behaviours. Appl. No. 201610871164.0. Serial No. 2016122101831200.
- ChengHeng Pang, Tao Wu, Yang Meng, Luyao Tang, Yuxin Yan, **Yu Hong**. A method for preparing heavy metal adsorbent for

gasification process and gasification process. Appl. No. 201710346393.5, pending.

- ChengHeng Pang, Tao Wu, Yang Meng, Luyao Tang, Yuxin Yan, **Yu Hong**, Nusrat Sharmin. A method for preparing graphene based on mechano-chemical method using biomass derivative. Appl. No. 201710346395.4, pending.

Conference publications

- **Yu Hong**, Wanru Chen, Kaiqi Shi, Yang Meng, Luyao Tang, Chengheng Pang, Tao Wu.(2017). Kinetic Study of the Pyrolysis of Microalgae-Spirulina and Macroalgae-Porphyra under Nitrogen and Carbon Dioxide Atmosphere. 16th International Conference on Sustainable Energy Technologies, Bologna, Italy.

- **Yu Hong**, Xiang Luo, Tao Wu. (2016). Microwave-enhanced pyrolysis and catalytic reforming of algae for the production of syngas (Poster). 1st International Conference on Bioresource Technology, Sitges, Spain.

- Xiang Luo, **Yu Hong**, Kaiqi Shi, Edward Lester, Tao Wu. (2016). Hydrogen production from steam reforming of acetic acid over the promoted NixMgyO catalysts (Poster). 1st International Conference on Bioresource Technology, Sitges, Spain.

- Kaiqi Shi, Jiefeng Yan, Wanru Chen, **Yu Hong**, Xiang Luo, Edward Lester, Tao Wu. (2016). Microwave-assisted biomass pyrolysis

and reforming with activated carbon for hydrogen-rich syngas (Poster). 1st International Conference on Bioresource Technology, Sitges, Spain.

Acknowledgement

First of all, I would like to thank my supervisor, Professor Tao Wu for providing me this great opportunity to carry out research on this topic. He also selflessly supervised my research work.

My thanks also extend to the staff members who helped and gave me suggestions with practical work, especially Dr Chengheng Pang, Dr Bencan Tang, Dr Kaiqi Shi, Dr Haitao Zhao, Dr Xiang Luo, Professor Chuang Peng, Dr Cheng-gong Sun, Professor Colin Snape, Carey Tao, Gang Yang, Kelly Yao, Jessica Wang, Julian Zhu, Jane Zhang, Helen Xu, Xi Gao, etc. I also want to express my appreciation to all my colleagues for their support to my work and our friendship, Dr Jiefeng Yan, Dr Honglei Zhang, Dr Ashak Mahmud Parvez, Wanru Chen, Pengfei Cao, Yang Meng, Luyao Tang, Xueliang Mu, Yipei Chen, Siqi Hao, Minghua Liu, Jingsha Xu, Bin Dong, Jenny Fan, etc.

Moreover, the International Doctoral Innovation Centre is acknowledged for the provision of a full PhD scholarship.

Most important of all, I want to thank my parents and my whole family for their encouragement and trust, as well as their support on my PhD study and life.

Table of Contents

List of Figures

List of Tables

Chapter 1. Introduction

1.1 Research background

Whilst the social economy is fast developing with living conditions greatly improved, the consumption of energy has increased significantly and the demand for sustainable alternative energy source is far greater than ever before. Fossil fuels, the primary energy form, are non-renewable with its large-scale utilization closely associated with severe GHG emissions. Many substitutes have been explored to alleviate the dependence on traditional energy source, among which biomass energy is regarded as one of the most promising alternatives to fossil fuels.

Marine-based biomass, such as micro- and macro-algae, are known to be the third generation bioenergy feedstock to replace the conventional arable crops, woody crops and agricultural wastes as energy source [1]. The main composition of algae are lipid, protein and carbohydrate, whilst terrestrial biomass is primarily comprised of lignin, cellulose and hemicellulose. Compared with terrestrial biomass, the shorter growth cycle, higher photosynthetic efficiency, marginal land cultivation, lipid-rich nature and valuable commercial products of microalgae have made it popular in research [2, 3]. However, the high-energy requirement for dehydration, the difficulty in harvesting

and the high cost for cultivation impede the large-scale utilisation of microalgae in biofuel production [4]

The conversion of biomass has two main approaches, i.e., biochemical and thermochemical conversion. The biochemical conversion can then be divided into fermentation and transesterification involving microorganisms, whilst the thermochemical conversion can be further subdivided into gasification, pyrolysis, liquefaction and hydrogenation. Pyrolysis is a thermochemical process for the conversion of fuels (e.g., biomass), into char, bio-oil and gaseous fraction by heating the raw materials to high temperatures under anaerobic atmosphere [5, 6]. It is generally the first stage of fuel utilization processes such as combustion [7-13] , gasification [14, 15] and carbon activation [16], but it is also commonly used as the primary process to produce fuel products. The use of biomass in energy production is perhaps even more dependent on the pyrolysis step due to the relatively high moisture and volatiles content [13].

Microwave-enhanced thermal processing applies electromagnetic waves to interact with matter and has several advantages including shorter preparation time, highly automated, volumetric and instantaneous heating [17]. During pyrolysis, biomass decomposes into char, pyrolytic bio-oil and gaseous fraction with a high fuel-to-feed ratio of 95.5% [18]. Due to high lipid concentration in algae [19-

21], previous studies were mainly focused on the production of high-quality bio-oil [22]. However, after lipid extraction, numerous algal residues including protein, soluble polysaccharide, etc., are commonly treated as wastes or low value products such as animal feeds [23]. Moreover, most algal oil can hardly satisfy the requirements of the European standards for biodiesel, such as high iodine value for heating oil and high linolenic acid methyl ester content for vehicle biodiesel [23]. With energy density of approximately 50% that of natural gas, syngas is considered as a promising fuel source or raw material for the production of chemicals, especially for the direct synthesis of methanol and ethylene glycol based on the attractive ratio of hydrogen to carbon monoxide [24].

To date, numerous efforts have been made to maximize and optimize the yield of algal oil from lipid-rich microalgae, particularly chlorella and spirulina [25-28]. While recent decades, pollutions from industry, agriculture, and other human activities have caused severe oceanic environmental problems, e.g., red tides. The cultivation of macroalgae (i.e., laminaria and porphyra) is a promising approach to relieve this eutrophication phenomenon since it consumes excessive amount of nutrient in water in a low cost and environmental-friendly manner [29]. Among seaweed categories, porphyra has a harvest cycle of only 15 days with high tolerance and strong ability in the consumption of nutrients. It has therefore drawn most attention in

many studies that are targeted at relieving eutrophication and improving the water environment [30]. However, there is not much work that has been carried out on the study of microwave-enhanced pyrolysis (MEP) of algae for syngas production and its mechanism by using model compounds.

Therefore, this study is to investigate microwave-enhanced pyrolysis of algae as well as the catalytic reforming process to gain a high selectivity of $CO+H_2$ in gaseous products. Meanwhile, kinetic study of the pyrolysis of representative algae together with its model compounds will also be carried out to discuss the mechanism of algal pyrolysis under N_2 and CO_2 atmosphere. The improvement of pyrolysis and catalytic reforming conducted under effects of microwave irradiation could be found according to the characterization of pyrolytic products from algal biomass.

1.2 Aim and objectives

The aim of this research is to investigate the microwave-enhanced pyrolysis coupled with catalytic reforming for algae processing to minimize the production of pyrolytic char and bio-oil while maximize gaseous product yield with high $CO+H_2$ content. There are four objectives to accomplish this project as follows,

- To characterize algae by conducting proximate analysis, intrinsic analysis, ultimate analysis, composition tests, morphologies and algal ash characterization.

- To understand the mechanism of algae pyrolysis. Kinetic study of five algal biomasses will be carried out using a thermogravimetric analyser at heating rates of 5, 10, 20 and 50 °C min^{-1} respectively. Kinetic parameters as well as the reaction mechanism under nitrogen or carbon dioxide atmosphere will be studied.
- To investigate the effects of microwave irradiation on the pyrolysis of algae, microwave-enhanced pyrolysis of five algae samples will be conducted at 400, 550 and 700 °C respectively. The pyrolytic gaseous, liquid and solid products will be collected and further analyzed.
- To increase the selectivity of syngas in gaseous fraction together with reducing char yield, reforming under CO_2 atmosphere will be delivered under microwave at 400, 550 and 700 °C respectively. The distribution and characterization of gas product, bio-oil and char will be further compared with that derived under N_2 atmosphere. Meanwhile, the ash content of four algae will be recycled and used as catalysts to investigate the influence of minerals contained in algae on the reforming of algal biomass at 550 °C under N_2. The result obtained will be compared with that from non-catalytic pyrolysis process.

1.3 Thesis structure

There are eight chapters in this thesis:

Chapter 1 introduces the background, aim and objectives, and structure of this thesis.

Chapter 2 carries out the comprehensive review of recent literature. It includes the current conversion technologies of biomass, kinetic analysis of the pyrolysis of biomass, microwave-enhanced pyrolysis and catalytic reforming of biomass.

Chapter 3 describes the algae samples and their systematic characterization. Methods adopted in the kinetic analysis of algae pyrolysis, microwave-enhanced pyrolysis and catalytic reforming are illustrated together with the methodologies used for the characterization of pyrolytic gaseous, liquid and solid products.

Chapter 4 covers the characteristics of algae samples and algal model compounds including proximate, intrinsic, ultimate features, lipid, carbohydrate and protein contents, density, morphologies as well as their ash characteristics.

Chapter 5 illustrates the kinetic study of algae pyrolysis together with three model compounds to reveal the mechanism of pyrolysis reaction using a thermogravimetric analyser at heating rates of 5, 10, 20 and 50 °C min^{-1} under N_2 or CO_2 atmosphere.

Chapter 6 focuses on the microwave-enhanced pyrolysis of algae and their pseudo-carbohydrate and protein components at 400, 550 and 700 °C in N_2, together with the characterization of pyrolytic gaseous fraction, bio-oil and char.

Chapter 7 discusses the microwave-enhanced reforming of algae and their primary model compounds, i.e., ovalbumin and cellulose under CO_2 atmosphere at 400, 550 and 700 °C, coupled with the characteristics of gas, liquid and solid products. Moreover, the ash of spirulina, chlorella, laminaria and porphyra are used as the catalysts to assist the microwave-enhanced pyrolysis of five algae under N_2 at 550 °C.

Chapter 8 summarizes the findings described in the thesis and suggestions for future studies.

Chapter 2. Literature review

2.1 Algae and its thermochemical conversion technologies

2.1.1 Introduction

The increasing energy demand and limited reserves of fossil fuels have motivated the investigation of alternative energy sources. Biomass has been considered as one of the most promising renewable energy substitutes to mitigate the reliance on fossil fuels, which constitutes 14% of the global primary energy and ranks as the fourth largest energy source, following coal, oil and natural gas [31, 32]. Biomass is a carbon neutral material, the utilization of which can reduce the emission of greenhouse gas effectively [33]. Therefore, bio-energy has become popular globally [34]. Agricultural resources including crops and oil-rich biomass have been commercialized as the first generation of biofuel feedstocks due to their carbon neutral nature and adaptability to existing infrastructure, devices and systems [35, 36]. However, the application of these resources has aroused unexpected ethical dilemmas and increasing the price of crops [37, 38]. Therefore, the second and third generation of bio-energy, which are inedible and marine biomass, have been introduced to soothe the side effects imposed by edible biomass, but

there are still technical barriers for commercialization of these feedstocks [39-41].

Terrestrial biomass is composed of three major components, i.e., cellulose, hemicellulose, and lignin, and a variety of minor components, such as inorganic matters. Cellulose (40-80 wt.% of biomass) is a crystalline, high molecular weight polymer of glucose which decomposes at 240-350 °C to produce anhydrocellulose and levoglucosan. Hemicellulose (15–30 wt.% of biomass) is an amorphous, shorter polymer of various sugars, decomposing at 200–260 °C to produce more volatiles, less tars and less char, compared to cellulose. Lignin (10-25 wt.%) is an aromatic polymer, which decays at 280-500 °C to produce phenols, and more char than cellulose [42]. Many studies reported that the activation energy of three compositions is in order of cellulose> hemicellulose > lignin [43-45].

2.1.2 Algae

Algae, as marine-based biomass, have recently deemed being the ideal alternative energy source to conventional fossil fuels [46, 47]. Unlike lignocellulosic biomass, the main compositions of algae are protein, lipid, and carbohydrates. Thermogravimetric analysis (TGA) shows that the pyrolytic profile of algal biomass normally has three stages [48]. The first step is attributed to moisture loss (below 110 °C) [48, 49]. The decomposition of carbohydrates leads to a mass loss

between 200 and 270 °C, due to its structure of unstable polysaccarides, whilst the protein decomposed below 350 °C [47]. The mass loss at higher temperatures (above 600 °C) was resulted from the degradation of lipid.

Compared with other biomass, the benefits of using algae as the energy sources are listed as follows,

- Higher photosynthetic efficiency

  Among the biomasses, algae have a higher photosynthetic efficiency than other bioenergy sources such as trees and plants [50]. The average photosynthetic efficiency of aquatic biomass is 6-8% [51], while that of terrestrial biomass is in the vicinity of 1.8-2.2%.

- Shorter growth cycle

  The growth rate of algae far exceeds that of terrestrial biomass [52]. Microalgae can be harvested in a very short cycle around 1-10 days, whilst traditional crop plants are harvested once or twice a year[53].

- Lower cultivation requirement

  Compared to other bioenergy sources, algae can be cultivated on non-arable land or even wastewater. Since algae are not traditional food or feedstocks, it will not compete for the arable land with traditional agriculture [54].

- Higher oil yield

Algae have the highest oil yield with up to 100,000 L oil per ha year, while oil palm, coconut, corn produce up to 5950, 2689 and 172 L per ha year[19]. Oil yield from algae is 1000-4000 gallon per acre per year, which is significantly higher than that from soybean and oil palm with much lower land area to produce certain amount of oil [55].

Because of these advantages, the energy production from algae could provide both economic and environmental benefits. However, drawbacks including the relatively greater cost of algae cultivation and harvest, the pretreatment of high-moisture algae, the lower efficiency of energy conversion, etc. post challenges to the large-scale commercialization of algae [20, 23].

2.1.3 Biomass thermochemical conversion technologies

Owing to the world-widely growing demands for energy and attempts to relieve the environmental pollutions from utilization of fossil fuels, biomass as one of renewable energy sources have been revisited [56]. Biochemical (fermentation and transesterification) and thermochemical (gasification, combustion, pyrolysis, liquefaction and hydrogenation) conversion are the two mechanisms of energy conversion from algae [57-59]. Biochemical conversion involves the use of enzymes, microorganisms or chemicals to decompose biomass at only ambient temperature with high selectivity of products. However, disadvantages such as essential pre-treatment, long

processing time, secondary waste production, etc. make this technology less competitive in energy generation from biomasses [60]. The high lipid concentration in algae has drawn most concerns to produce bio-oil of high quality via biochemical technologies [19-21]. Conversely, after lipid extraction, numerous algal residues involving protein, soluble polysaccharide, etc. have been treated as waste or animal feeds [23]. Since most algae have high moisture content, not all conversion processes can be utilized [61]; therefore, each technology for energy extraction from algae would be discussed substantially in following sections.

2.1.3.1 Combustion

Direct combustion is the burning of biomass in aerobic atmosphere which convert the internal chemical energy into heat, mechanical power, or electricity. At present, combustion represents more than 97% of the world's bio-energy production [62]. The most commonly-used biomass energy application is for heating. In industry, biomass combustion normally occurs in furnaces for heat generation, boilers for steam generation to drive turbines [63]. Based on environmental considerations, the combustion of biomass is undesirably adopted which might emit NO_x, SO_x, CO_2, particulate matters or ash [34, 64] at much lower levels compared with coal-firing processes. But for long-term consideration, biomass is regarded to be carbon neutral,

since the CO_2 released during combustion process could be converted via photosynthesis by plants.

2.1.3.2 Liquefaction

Liquefaction, or hydrothermal liquefaction (HTL) is a thermal process to convert biomass directly into bio-oil in the presence of water under medium temperature (250–550 °C) and high pressure (5-25 MPa) [65], sometimes with the assistance of catalysts. Water at high temperatures can act as a reactant which provides hydrogen ions and reforms biomass into hydrocarbons. Algae with high moisture content, require a significant amount of energy to vaporize the water contained during drying process, which makes it unsuitable as a feedstock on the considerations of energy consumption. Compared with pyrolysis and gasification, HTL directly converts this wet algal biomass to liquid fuels without preliminary drying [66]. Further upgrading strategies of the oil to reach transportation fuel standards, such as distillation, solvent extraction, catalytic cracking and hydrodeoxygenation, could be conducted to modify the properties of bio-oil, such as its density, heating value, sulfur content, etc. [67]. Previous studies on the production of bio-oil from algae via HTL were mainly focused on optimizing particle size, residence time, solvent type, biomass category and composition, temperature and biomass-to-solvent ratio for higher yield and the understanding of its mechanism [68-71]. However, the selection of parameters for HTL

could either have positive or negative effects on the final product yield and also there is no optimal selection because of different conditions in each experiment. Overall, HTL is certainly a promising technology for the conversion and level-up of biomass energy into liquid fuels.

2.1.3.3 Gasification

Gasification is a partial oxidation process converting carbonaceous materials such as fossil fuels, biomass, etc. into syngas as the main gas product at high temperatures (>700 °C), with a controlled amount of gasifying agents such as air, oxygen or steam [72]. The syngas produced could be converted into long-chain hydrocarbons via the Fischer-Tropsch process [73, 74]. There are various advantages of gasification technology over other thermochemical processes. A combined cycle system has been introduced to the biomass gasification power plant to sufficiently utilize the energy generated in gasification process to motivate gas turbines, which creates a more efficient pathway to convert biomass (up to about 50%) [75]. By concerns of environmental protection, the gasification of biomass generates extremely low production of SO_x and NO_x, as well as particulates. Meanwhile, CO_2 could be easily captured and stored because it is highly concentrated in syngas production at high temperatures, which reduce the GHG emissions [76].

The air gasification of biomass has already been developed in industry; however, the gaseous fraction is highly diluted by nitrogen and is of low hydrogen content (8-14 vol. %) [77-79]. Oxygen-rich air gasification was capable of generating gas product with medium heating value, but the oxygen production equipment would increase the cost of gasification process. Steam gasification would provide H_2 –enriched gas product with a content of 30-60 vol. % and heating value of 10-16 MJ/m^3, while the endothermic reaction could reduce the bed temperature which required additional energy input to maintain the set temperature [80]. The steam-oxygen gasification process could produce a fuel gas with high proportion of H_2, whilst the expensive cost of providing pure oxygen makes it infeasible in industrial application [78]. Therefore, the gasifying agent for biomass gasification could largely affect the final gas production and quality. Most of these processes contain oxygen production equipment which increase the difficulty of application in industry.

2.1.3.4 Pyrolysis

It is proved that the algal lipid could be converted into biodiesel via liquefaction process, only if the lipid content is high (up to about 70 wt.%) [74, 81]. However, the growth of these algae species is slow, while algae with lower lipid content conversely grow fast [82]. Algae with low lipid content can be exploited as the feedstock of pyrolysis to derive syngas for further use [74]. Pyrolysis is a conversion

process of biomass to char, bio-oil and gaseous fraction by heating biomass under anaerobic atmosphere at high temperatures [5, 6] or by heating with addition of catalysts to optimize the high-value fuel products from biomass [83]. Via pyrolysis, biomass will generally decompose into charcoal and volatile matters, which further form pyrolytic bio-oil, biogas or methanol production with high fuel-to-feed ratio at 95.5% [18]. Various pyrolytic products derived from different compositions of biomass have been concluded in **Figure 2-1** [84], with rare generation of SO_x and NO_x, meanwhile low emission of CO_2.

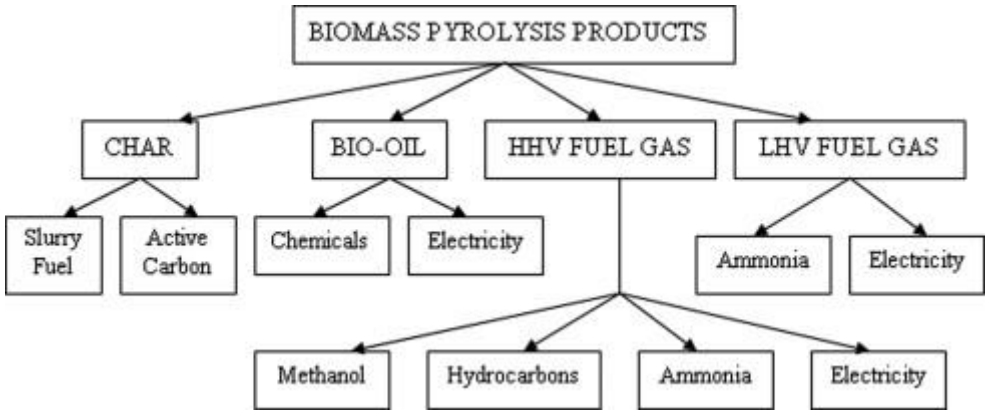

Figure 2-1 Fractionation of biomass pyrolysis products[84].

Depending on the process conditions (i.e., temperature and residence time), pyrolysis could be further subdivided into six categories, fast pyrolysis, slow pyrolysis, intermediate pyrolysis, flash pyrolysis, vacuum pyrolysis, and ablative pyrolysis. The conditions of each pyrolysis category are summarized in **Table 2-1** [85]. Previous studies mostly concentrated on the bio-oil production, especially from fast pyrolysis with high heating rate at 10^3 to 10^4 K/s and short gas

residence time which reduces the cracking into short chain molecules but condensing to liquid fuels [22]. Pyrolysis has been selected by many researchers as the biomass conversion technique due to its high production of bio-oil (about 80 wt.%) at a moderate temperature around 500°C [86]. However, most algal oil is unlikely to comply with the European biodiesel standards, because of high iodine value for heating oil requirement and too high linolenic acid methyl ester content for vehicle biodiesel. However, the gaseous fraction produced via pyrolysis is of high calorific value which can be reused to supply energy [87]. Meanwhile, it is very easy and flexible for recycling the gas product back to the system, which does not require further separation process thus reduces the equipment and labour cost [88].

Table 2-1 Summary of biomass pyrolysis conditions [85].

Conversion Technology	Process Condition	Product yield		
Pyrolysis		Liquid (wt %)	Gas (wt %)	Solid (wt %)
Fast Pyrolysis	Atmospheric pressure, small particle size (< 3mm), short residence time (0.5-2s), moderate temperature (400-550^{0}C) in absence of oxygen	65-75	13-25	12-19
Slow pyrolysis	Low heating rate, moderate temperature (350-750^{0}C), atmospheric pressure, long residence time in absence of oxygen	30-50	15-30	30-60
Intermediate Pyrolysis	Moderate temperature (< 500^{0}C), moderate vapor residence time (4-10s) and atmospheric pressure	45-55	25-35	15-25
Flash Pyrolysis	Rapid heating (< 0.5s), very small particle sizes (< 0.5mm), temperature (400-1000^{0}C)	60-70	10-15	15-25
Vacuum Pyrolysis	Moderate temperature (300-500^{0}C), pressure below atmospheric (< 50kPa)	45-60	17-27	19-27
Ablative Pyrolysis	Moderate temperature (450 -600^{0}C), atmospheric pressure, particle size < 3.5mm	60-80	6-10	12-20

2.1.3.5 Microwave-assisted pyrolysis

There are many variables affecting the microwave-assisted pyrolysis process, involving the product yield and quality [89]. In order to enhance the process and obtain the maximum desired conversion, main factors are required to be optimized listed below:

- Category and size of input materials
- Moisture content of input materials
- Reaction(pyrolysis) temperature
- Microwave power input
- Microwave mode type (multimode or single-mode)
- Reactor design
- Microwave absorber type, size and amount
- Catalyst type and amount
- Flowrate and type of carrier gas
- Reaction time

2.2 Kinetics of algae pyrolysis

2.2.1 Kinetic analysis of pyrolysis

As a renewable carbonaceous resource, biomass has attracted significant interests and is accessible widely nowadays. Algae has a great potential to replace the terrestrial biomass which mainly consists of cellulose, hemicellulose and lignin with complex structure [90, 91]. Algal biomass is comprised of proteins, carbohydrates, lipids, and minerals in ash content, which has been investigated in literatures for its various conversion to biofuels [26, 27, 92, 93].

Thermogravimetric analysis (TG) and differential thermogravimetric analysis (DTG) are two important profiles to study the features of thermal decomposition of algae and its model components, i.e., ovalbumin, cellulose and oil droplets. Previous research, based on TG

and DTG profiles derived under different heating rates using a thermogravimetric analyser [94], investigated the thermal degradation of biomass via observing the weight loss changing along with the temperature. By applying Arrhenius Law, Flynn-Wall-Ozawa (FWO) and Kissinger-Akahria-Sunose (KAS), as two representative iso-conversional methods, were widely adopted to study the kinetics of pyrolysis and define parameters including activation energy (E_a) and pre-exponential factor (A) [91, 95]. However, the difference in the decomposition of each biomass constituent makes the pyrolysis of biomass extremely complicated. Therefore, to analyse the complex reaction system, those iso-conversional methods are relatively inappropriate [96]. Model fitting method is introduced to simulate kinetics of pyrolysis of biomass [97], by substituting different reaction models into Coats-Redfern function. The highest regression value corresponded to the fittest mechanism model for each pyrolysis Event.

Traditional pyrolysis using nitrogen as carrier gas to maintain anaerobic atmosphere and kinetic study of the pyrolysis of biomass under nitrogen has been discussed in previous literatures [91, 95, 96, 98-100]. Microalgae-chlorella variables were investigated by TGA-MS under argon atmosphere (40 mL min^{-1}) for its thermal decomposition and analysis of released gas product via non-isothermal pyrolysis at heating rates of 5, 10, 20 and 35 °C min^{-1}, from room temperature

to 900°C. According to the TG and DTG curves, it was found that three stages of decomposition (0-100, 100-550, and 550-900 °C) and three zones of volatilization (100-400, 400-550, and 600-750 °C) existed during pyrolysis. Based on iso-conversional (FWO and KAS) and model fitting (Coats- Redfern) methods, E_a values for each stage or zone have been calculated to derive the possible reaction model [91]. Kinetic analysis of the pyrolysis of biomass main components (cellulose, hemicellulose, and lignin) has been conducted by using a TGA with non-isothermal method at four linear heating rates of 5, 10, 20 and 40 °C min^{-1}, from 25 to 800 °C. Nitrogen as carrier gas was purged into the system at a flowrate of 40 mL min^{-1}. The correlation between conversion rate and activation energy was detected by iso-conversional (KAS) method and model fitting (Coats-Redfern and Kissinger) methods were further introduced to derive the reaction model for each pyrolysis stage. It has been concluded that the pyrolysis of lignin and hemicellulose followed the reaction-order model, while the pyrolysis of cellulose was in Avrami-Erofeev nucleation model (A2) [95]. Since most of the previous work focused on the kinetics of conventional pyrolysis, the microwave pyrolysis of seven representative lignocellulosic biomass, i.e., corn stover, rice straw, etc., was studied for investigating their kinetics. It draw a conclusion that the power of microwave had linear relationship with heating rate, as well as the maximum temperature, while a breakpoint was found when the power level reached 250 W.

Compared with conventional pyrolysis, the activation energy and pre-exponential factor of microwave pyrolysis were much lower, coupled with higher rate constant. Therefore, heating performance of microwave pyrolysis was better than conventional pyrolysis, due to less input energy and processing time [101]. But it is found that compared to N_2, CO_2 could assist in the pyrolysis of carbonaceous materials with higher thermal efficiency, reduction of tar formation, higher production of syngas (especially CO) [102-104], etc. However, there is not much work that has been carried out about the kinetics of the pyrolysis of algae and its model compounds under CO_2 atmosphere, as well as the comparison of results obtained under N_2 and CO_2.

2.2.2 Determination of kinetic parameters

The thermal decomposition of algae is a typical solid decomposition reaction, which can be expressed by $Algae \rightarrow Volatiles + Char$. The conversion rate of algae is defined as Eq. (a),

$$\alpha = \frac{m_0 - m_T}{m_0 - m_f} \quad \text{(a)}$$

Where m_0 is the initial mass of test material, m_f is the final mass of solid material after pyrolysis, m_T is the mass of material at reaction temperature of T.

The kinetic study is based on the Arrhenius law. According to Eq. (a), the conversion rate only depends on the reaction temperature. The thermal dynamic formula can be described as Eq. (b),

$$\frac{d\alpha}{f(\alpha)} = \frac{A}{\beta}\exp(\frac{-E_a}{RT})dT \quad (b)$$

Where $f(\alpha)$ is the conversion, α-dependent function; $\beta = \frac{dT}{dt}$ is the heating rate, K/min; E_a is the activation energy, J/mol; A is the pre-exponential factor, min^{-1}; R is universal gas constant, 8.314 J/mol·K; T is the absolute temperature, K.

Integrating Eq. (b) over α is generally expressed as Eq. (c),

$$G(\alpha) = \int_0^{\alpha} \frac{d\alpha}{f(\alpha)} = \frac{A}{\beta}\int_0^{T} exp\left(\frac{-E_a}{RT}\right) dT \quad (c)$$

Where $G(\alpha)$ is the integrated form of$f(\alpha)$.

2.2.2.1 Iso-conversional method: Kissinger- Akahira-Sunose (KAS) and Flynn-Wall-Ozawa (FWO)

It is generally agreed that the activation energy and pre-exponential factor of one-step fluid state reactions remain constant, but these parameters would change depending on the conversion rate (α) for reactions involving solid, due to its internal heterogeneity of solid samples and complicated reaction mechanism. Therefore, iso-conversional methods can be applied to determine the kinetic parameters of solid state reactions.

KAS method is based on Arrhenius equation using differential method [105],

$$G(\alpha) = \frac{AE}{\beta R} p(\frac{E_a}{RT}) \quad \text{(d)}$$

Combined with eq. (c), the variables of A, E_a and $f(\alpha)$ are related to T whilst A and E_a are independent of α. Hence, Eq. (c) can be further integrated into the following form,

$$ln\frac{\beta}{T^2} = \ln\left(\frac{RA}{E_a G(\alpha)}\right) - \frac{E_a}{RT} \quad \text{(e)}$$

The plot of $ln\frac{\beta}{T^2}$ versus $-\frac{1}{RT}$ for constant α will derive a linear relationship.

FWO method can also be applied to calculate the activation energy of algae and its pseudo-components.

$$ln\beta = \ln\left(\frac{AE_a}{RG(\alpha)}\right) - \frac{E_a}{RT} \quad \text{(f)}$$

The plot of $ln\beta$ versus $-\frac{1}{RT}$ for constant α will derive a linear relationship.

To investigate the correlation between E_a and α specifically, 19 conversion rates from 5 to 95% were selected. The E_a can be determined by the gradient of the straight line.

2.2.2.2 Model fitting method: Coats-Redfern method

The Coats-Redfern method is one of the model fitting approaches, which can be used to calculate the kinetic parameters and determine the order and mechanism of reaction [106].

Coats-Redfern approximation was applied and further rearranged as Eq. (g),

$$ln\frac{G(\alpha)}{T^2} = \ln\left[\frac{AR}{\beta E_a}(1-\frac{2RT}{E_a})\right] - \frac{E_a}{RT} \quad (g)$$

The function $G(\alpha)$ depends on different reaction models[107] and can be summarized in **Table 2-2**.

Table 2-2 Commonly-used mechanism models of solid-state reaction

Reaction models	Differential form $\boldsymbol{f(\alpha)}$	Integral form $\boldsymbol{G(\alpha)}$
1-D diffusion (D1)	$1/(2a)$	a^2
2-D diffusion (D2)	$-[\ln(1-a)]^{-1}$	$(1-a)\ln(1-a)+a$
3-D diffusion (D3)	$3/2[1-(1-a)^{1/3}]^{-1}(1-a)^{2/3}$	$[1-(1-a)^{1/3}]^2$
4-D diffusion (D4)	$3/2[1-(1-a)^{1/3}]^{-1}$	$1-(2a/3)-(1-a)^{2/3}$
Phase boundary contracting reaction (R2)	$2(1-a)^{1/2}$	$1-(1-a)^{1/2}$
Phase boundary contracting reaction (R3)	$3(1-a)^{2/3}$	$1-(1-a)^{1/3}$
Avrami–Erofeev equation (A2)	$2(1-a)[-\ln(1-a)]^{1/2}$	$[-\ln(1-a)]^{1/2}$
Avrami–Erofeev equation (A3)	$3(1-a)[-\ln(1-a)]^{2/3}$	$[-\ln(1-a)]^{1/3}$
First-order chemical reaction (F1)	$1-a$	$-\ln(1-a)$
Second-order chemical reaction (F2)	$(1-a)^2$	$(1-a)^{-1}-1$

The usual value of $\frac{2RT}{E_a}$ is far less than 1 and thus can be disregarded.

Therefore, the equation could be simplified as Eq. (h),

$$ln\frac{G(\alpha)}{T^2} = \ln(\frac{AR}{\beta E_a}) - \frac{E_a}{RT} \quad (h)$$

By substituting different forms of $G(\alpha)$ in **Table 2-2** into Eq.(h), a plot of $ln\frac{G(\alpha)}{T^2}$ versus $-\frac{1}{RT}$ would give a straight line with a slope equal to E_a and the intercept point providing values of E_a and A.

2.3 Microwave-assisted heating V.S. Conventional heating

Microwave is electromagnetic radiation with frequencies ranging from 300 MHz to 300 GHz and wavelengths in the range of 1 mm to 1 m [108, 109]. In case of interference with other radio services, household microwave frequency for heating is 2.45 GHz with a wavelength of 12.2 cm, while large industrial ovens often use microwave with a frequency of 915 MHz and a wavelength of 32.8 cm wavelength [110]. Dielectric or microwave heating means that object is heated up by high-frequency electromagnetic radiation. The materials will be heated via the interaction between internal charged particles. Microwave processing is considered to be one of the most promising modern heating technologies [111] and has been applied in various domains [112].

Microwave heating bases on dipolar and interfacial polarization effects [113]. Molecular rotation will align polar molecules in materials (e.g. water) in the electromagnetic field, which is so-called dipolar polarization. As the electric field oscillating, these molecules rotate accordingly, even reverse their direction when the field changes. The heat energy appears when the molecules rotate and collide [114]. The heating temperature is related to the kinetic energy

of polar molecules movement including vibration, rotation and conversion [115]. Maxwell–Wagner–Sillars polarization or interfacial polarization is dissipated in the form of heat [116]. It is generally agreed that introducing materials with larger polarity would be greatly influenced by microwave energy, which could significantly improve the uniform and volumetric heating. Therefore, based on the mechanism of heating, microwave heating is considered to have great potential as a biomass treatment method [117].

Dielectric loss tangent parameter (DLTP) quantifies a dielectric material's inherent dissipation of electromagnetic energy into heat. The ability to be heated in the presence of a microwave field can be expressed in terms of $\tan\delta = \varepsilon'' / \varepsilon'$. DLTP consists of two parameters, the dielectric constant or real permittivity, ε', and the dielectric loss factor or imaginary permittivity, ε''. ε' defines the amount of energy retarded or reflected as it passes through, whilst ε'' determines the amount of microwave energy dissipated or lost in the form of heat within the material [114, 116]. For optimum microwave heating, ε' shall be moderate with high values of ε''; therefore, the high values of DLTP ($\tan\delta$) will be derived, which can convert more microwave energy into thermal energy [118, 119]. Hence, materials with high ε'' could be heated by microwave energy easily [113].

On the basis of the interactions between materials and microwave irradiation, the materials can be categorized into three groups, which

are insulator, conductor and absorber. Metals cannot be heated up by microwaves due to the reflection on the surface, and are categorized as conductors. Conductors are often used as waveguide for microwaves. Material which are transparent to microwave irradiation are classed as insulator, and generally used to support materials to be heated in microwave ovens (e.g., quartz). Absorbers can be easily heated up by the microwave energy (e.g., water, biomass, silicon carbide, carbon) [120, 121].

The microwave heating of materials with dielectric properties, which involves conversion of electromagnetic energy into heat, provides several advantages compared to conventional heating methods, but not limited to, as follows:

- **Homogeneous/ volumetric heating**

  Microwave can use electromagnetic radiation to evenly heat the entire volume of substances [122]. Regardless of the sample geometry, microwave can penetrate the object and heat can be generated throughout the whole volume [123, 124]. It is possible for microwave to achieve consistent and instant heating of thick materials [125].

  Although the microwave transferred energy throughout the material simultaneously, the heat would easily accumulate inside the interior material because of the relatively lower thermal conductivity of biomass and slower energy transfer

process from inner to outer layer. This is an opposite energy transfer direction to conventional heating methods, which transfers heat from outside to inside. Therefore, under the combined effects of microwave transmission and transformation, heat and mass transfer, and chemical reaction (pyrolysis), the internal temperature of the material is normally higher than outer temperature when using microwave [126].

- **Selective heating**

  The dielectric properties of different materials decide their absorption of microwave radiation [127, 128]. As a result of considering DLTPs of different materials, inhomogeneous energy dissipation will be observed in the microwave heating leading to possible temperature gradient or hot spots, which is so-called selective heating [129]. Due to relatively slow heat transfer rate, the presence of hot spots might accelerate the chemical reaction in the hot zone. Hot spot effects have been demonstrated and clarified for using heterogeneous catalysts. Meanwhile, the materials with low dielectric properties mixed with strong microwave absorbing ability would be heated selectively and thus less overall energy consumption [130].

  Water as an excellent microwave absorber with high complex dielectric permittivity, is highly contained in algae sample and will evaporate at the early stage of microwave-assisted pyrolysis [131]. This explained the fact that the conversion

reaction between water and carbon existed coupled with less gas products such as methane and carbon monoxide (water shift gas reaction). Compared to microwave-assisted thermal processing, the sample drying process and volatiles generation occur simultaneously during traditional pyrolysis process, which could absorb energy and thus reduce the heating rate and terminal temperature of pyrolysis [126].

Water gas reaction: $C+H_2O \leftrightarrow CO+H_2$ $\Delta H_{298K}=132\ kJmol^{-1}$

Water gas shift reaction: $CO+H_2O \leftrightarrow CO_2+H_2$

$\Delta H_{298K}=-41.5\ kJmol^{-1}$

Methane gasification: $CH_4+H_2O \leftrightarrow CO+3H_2$ $\Delta H_{298K}=206.1\ kJmol^{-1}$

- **Instant heating and higher thermal efficiency**

  The energy is generated from interior of the material on a molecular level transferred by microwave irradiation, rather heat transfer from outer layer, which is considered to be non-contact heating. The microwave energy carried by irradiation could fast interact with the molecules; thus, the molecules would generate much greater heat instantaneously, compared to the bulk reactants [132].

- **Higher heating penetrating ablility**

  The ability of an electromagnetic wave to pass through a medium is the penetrating capability. When the electromagnetic wave enters the medium from the surface and propagates through it, the microwave energy is absorbed and

continuously converted into heat energy. This heat energy decays exponentially as it goes deeper into the surface of the medium.

- **Safe and easily controllable**

  Since the microwave radiation is generated and transferred in closure space, without any radioactive rays, it is reliable to use microwave heating method. Meanwhile, the microwave heating power can be easily controlled with instantaneously start-up and shut-down through the working panel, which can be simply applied in automatic system [133].

Figure 2-2 shows the energy transformation and heat and mass transfer mechanism in the ideal microwave heating. The microwave irradiation penetrates the material and continuously decays. During the penetration propagating, the microwave energy is converted into heat. Due to the "selective heating" of microwave heating, the temperature difference between the material and container is normally very large, which result in heat loss from the surface of material. Meanwhile, those heat generated would be accumulated inside the materal and transferred outwards with smaller thermal conductivity and slower heat transfer process, leading to higher internal temperature while lower external temperature.

The pyrolysis is conducted layer by layer from inside materal to outside. The biomass particles in the internal of material, which is called "complete pyrolysis zone", are heated rapidly and decomposed

into volatiles and carbons at first. Those products would pass through a lower temperature zone- "reaction zone", where some intermediate material occurs via secondary cracking. With heat transfer, the particles produced in the external would be heated and pyrolyzed further, and the volatiles would diffuse to the low temperature zone outside, while a few would diffuse to the internal high temperature zone[126].

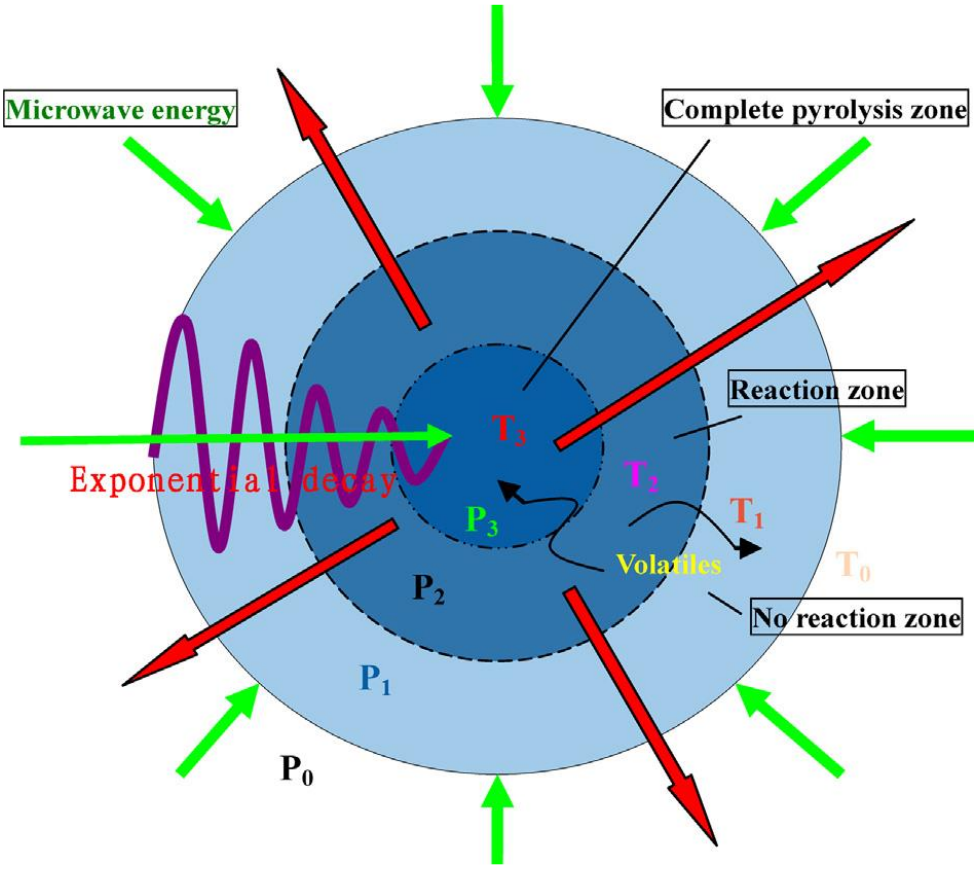

Figure 2-2 Schematic diagram of energy conversion and heat and mass transfer process during microwave heating (T- Temperature, $T_3 > T_2 > T_1 > T_0$; P- Press, $P_3 > P_2 > P_1 > P_0$). [126]

Unlike microwave heating, heat from traditional thermal processing can be transferred between substances by conduction, convection and radiation [134]. Energy is transferred into the interior of the

material from outer surface by thermal conduction, which depends on its thermal conductivity, specific heat, etc. [135] Therefore, it requires higher external surface temperature to generate desired temperature gradient, which is in the opposite transfer direction to the microwave heating.

The microwave heating is regarded to be a preferable heating process, compared with traditional heating. However, the measured temperature of reaction bed during process for microwave is not always reliable. Normally, an optical pyrometer and thermocouple are equipped with microwave to measure the temperature. Optical pyrometer (i.e., infrared thermometer) can only detect surface temperature, which is much lower than the actual temperature in reaction bed [113]. In conventional heating, the temperature is calibrated by thermocouple, but it would be interfered with the radio frequency field and cause energy loss [136]. Apart from the difficulty in detecting temperature, the feasibility of process scaling-up from laboratory-scale operation is of uncertainty. Based on available microwave technologies, as the scale becomes larger, the power from microwave have to penetrate a longer distance from the waveguide, which would lead to significant overheating at the surfaces to form hot spots. It also exists much more problems of measurement and control as the scale of work is increased [137]. Moreover, the addition of microwave absorbers is compulsory for processing materials with

poor dielectric properties. Non-homogenous material heating may present, that is, the temperature of some parts in the materials can rise faster than others, which is so-called thermal runaway [112]. But this phenomenon can be controlled by keeping the sample well-mixed.

2.4 Microwave absorbers

Biomass is generally regarded as a poor absorber of microwave irradiation. Although water content and inorganic matter in biomass may contribute in absorbing microwave energy, it is relatively difficult for biomass to reach the target heating rate and final pyrolysis temperature. This results in an intermediate pyrolysis rate rather than fast pyrolysis [31]. Therefore, materials with outstanding dielectric properties would be selected as microwave absorbents, which may also act as catalysts [138]. Microwave absorbers act as a pivotal role both in heat transfer and reaction, due to effects of catalysis and energy absorbing.

2.4.1 Water

Water is considered to be an excellent microwave absorber and could create interior heat via microwave irradiation because of its dielectric properties and polarity nature [131, 139]. The water molecules in biomass absorb microwaves and generate polarization which align the molecules according to the radiation. This could generate heat via the friction between molecules. Therefore, when the instant microwave radiation occurs, the moisture reaches super-heated point

and evaporates from the biomass [140]. However, the temperature of reaction bed stabilizes after the vaporization of moisture, while the other matters in biomass do not absorb the microwave radiation readily. Hence, other materials should be input into the system to enhance the ability of microwave radiation absorption.

2.4.2 Metal based microwave absorbers (MMWAs)

Previous researches focus on different microwave absorbers, among which, the most commonly-used are elemental metals, metal oxides, hydroxides, carbonates and chlorides, including aluminum (Al), iron (Fe), copper oxide (CuO), calcium oxide (CaO), magnesium oxide (MgO), nickel oxide (NiO), iron oxide (Fe_3O_4), sodium hydroxide (NaOH), potassium hydroxide (KOH), sodium carbonate (Na_2CO_3), potassium carbonate (K_2CO_3), calcium carbonate ($CaCO_3$), iron chloride ($FeCl_3$), zinc chloride ($ZnCl_2$), etc. [141]. These absorbents, as well as catalysts, would help in catalyzing and cracking the vapor or gas generated simultaneously as secondary reaction. Compared with carbon based microwave absorbers, these added metal ones could significantly improve the temperature profile and the yield, distribution and quality of products. However, besides the recycle of MMWAs, reuse or disposal of char containing these additives is one of primary concerns. Furthermore, the characteristics and properties of char may be changed with the addition of MMWAs.

2.4.3 Carbon based microwave absorbers (CMWAs)

Carbonaceous microwave absorbers including charcoal, activated carbon (AC), graphite, silicon carbide (SiC), etc. are important materials promoting fast heat transfer to biomass during microwave processing [42, 118, 142]. The values of DLTPs for different carbonaceous materials are concluded in **Table 2-3** [118]. With better dielectric properties, the addition of CMWAs can considerably improve the heating rate and reduce the power input to reach desired temperature. Since the microwave absorbers need to be pre-mixed with biomass, CMWAs are much easier to mix with biomass uniformly, compared with MMWAs, due to similar density, size and shape properties between biomass and CMWAs. Hence, heat transfer, reactor temperature and heating rate are all well-improved. Moreover, the biochar produced by using CMWAs can be reused as a cost effective MWA without any further treatment. However, it is difficult to distinguish the catalyst effects of CMWAs from gasification of carbon, which affecting yields and quality of products.

Table 2-3 Dielectric loss tangents for different carbonaceous materials at room temperature (298 K) and a frequency of 2.45 GHz

Carbonaceous material	tanδ = ε'' / ε'
Coal	0.02–0.08
Carbon foam	0.05–0.20
Charcoal	0.11–0.29
Carbon black	0.35–0.83
Activated carbon	0.57–0.80
Activated carbon at 398K	0.22–2.95
Carbon nanotube	0.25–1.14
CSi nanofibres	0.58–1.00

Char and graphite have been used as absorbers in different types of microwave oven in both single and multi-modes [143]. They concluded that the type of microwave absorbers used have almost no effect on the elemental composition of the sludge oil product (C, H, N, S, O contents). By analyzing the proportions of main pyrolysis compounds in the oil using GC-MS, the product oil derived using char as the microwave absorber contained the highest content of hexadecanoic acid which is up to 24.6 wt.%. However, using graphite as absorbers, the oil produced has more cracking in the large aliphatic chains, including more monoaromatic than aliphatic compounds, whilst using char as absorbers can increase the proportions of these two compounds likewise. Lignite char was utilized to increase the absorption of microwave radiation by chlorella vulgaris from 200 °C (without microwave receptors) to 1015 °C in 2 min [42]. With addition of 5 wt.% carbonaceous char into sewage sludge, the

maximum temperature (900 °C) was achieved within 2 mins using microwave processing, while reached only 200 °C without char [144]. About 0.5 wt.% carbon grains were well mixed with oil shales and then pyrolyzed under microwave radiation [145].

Silicon carbide (SiC), in general, acts as a considerable microwave absorbents in microwave-enhanced pyrolysis of biomass. SiC was applied in the microwave-assisted pyrolysis of wood sawdust and corn stover, which investigated in the size effect of SiC on the pyrolysis [146]. Absorbers with larger particle size reduce the heat exchange with biomass, while smaller absorbents would agglomerate and reduce the heating process. The fMAP of chlorella sp. and nannochloropsis was conducted with silicon carbide as microwave absorbent [147].

2.4.4 Mass ratio of biomass to microwave absorber and distribution of microwave absorber

The mass ratio of biomass to microwave absorbers is one of the effective parameters determining solid, liquid and gas products of biomass pyrolysis. The pyrolysis of shell and fibers of oil palm has been carried out using microwave with assistance of char obtained from traditional pyrolysis of oil palm shell as microwave absorber at three ratios of biomass to microwave absorber (4:1, 2:1 and 1:1) [140]. The oil palm biomass yielded the highest amount of bio-oil and lowest amount of char at the ratio of 2:1. Different ratios of activated

carbon (AC to biomass, 1.32 to 4.86) were added into biomass-douglas fir as catalysts as well as microwave absorbers in fixed total amount. The production of gas rose from 35 to 52 wt.% when the ratio increased continuously, while the amount of char decreased significantly from 35 to 10 wt.%. Maximum of liquid and volatile yield and minimum of solid remained was observed when the ratio increased from 3 to 4, which considered to be the optimal pyrolysis condition [148]. However, this kind of non-uniform distribution of microwave absorber mixed with biomass could easily create hot spots, which might lead to uneven heating process and lower quality of products [149]. With uniformly-distributed coconut activated carbon as microwave absorbers which have improved heating profiles, oil yield and microwave penetration depth at 35, 55, 75 and 91.2 wt.% carbon loading, oil palm shell waste was pyrolyzed under microwave [150]. There was no significant difference in the heating rate as the loading ratio increasing, while the final pyrolysis temperature achieved was rising.

2.5 Temperature profile

The heating rate and pyrolysis temperature are key characteristics affecting the microwave-induced pyrolysis and final products [151-153]. The power level of microwave affects these two factors significantly. It is widely acknowledged that the higher the microwave power, the greater the inner energy generated in the sample, the

faster the increase in temperature and therefore the higher the final pyrolysis temperature. A single-mode device at power levels from 200 to 500 W was used to study the productivity of H_2-rich gas from rice straw. As the loaded power increasing, the higher maximum temperature could be reached in shorter period. This phenomenon implied that as the microwave power increased, the density of microwave irradiation in cavity and the energy absorption of biomass became stronger; meanwhile, the inter-molecule movement was greater [154]. Similar conclusion have been drawn [155], which is microwave oven under higher power level could attribute to larger heating rate and shorter low temperature duration time, thus greater yield of gas. After investigating the heating rates at different time intervals under various microwave powers, it is apparent that the temperature increases primarily in the first 10 mins particularly during 300-500 W [124, 151]. The highest heating rates were achieved in the first 5mins, possibly due to the quick reactivity of microwave pyrolysis, which was similar to heating behaviour in previous works [142, 145]. In most cases, the first 2 mins of reaction has a lower heating rates than that at 3-5 mins. This might be resulted from the drying process of biomass (<100 °C) in the beginning of pyrolysis since moisture could absorb microwave irradiation tremendously [131]. After biomass was fully dried and its temperature significantly rose, an excellent microwave energy absorbent –char-would be formed, which significantly assisted in

microwave-induced pyrolysis [145]. Du, Li [156] carried out the pyrolysis of chlorella sp. in a microwave oven with the power increased from 500 to 1250 W. It is found that the temperature increased significantly during the first 8-9 mins and then it became relatively stable which might due to the balance between heat loss and heat generated.

With the addition of catalysts, the maximum temperature and heating rates decreased slightly [157]. Among metal oxides, CaO reduced the reaction temperature mostly, due to its influence on the dielectric heating of the system [158]. The amount of catalysts loaded would affect the reaction system as well [124], because of the competition of microwave energy absorption between catalysts and biomass.

2.6 Products distribution

Algal biomass contains protein, lipid, carbohydrates and moisture. Based on previous studies, microwave-enhanced pyrolysis of biomass-related feedstocks can generate a wide range of biofuels and bio-based products including bio-char, bio-oil, gaseous fraction, syngas, hydrogen [159]. The distribution of these products mainly depends on the biomass categories, pyrolysis conditions, microwave power level, microwave absorbents, and the design of microwave reactor, which can be referred to **Table 2-1**.

Pyrolysis is a de-volatilization in inert atmosphere leading to the decomposition of amorphous compounds and the release of hydrogen

and oxygen-rich gases [160]. H_2, CO and CH_4 are major gaseous products of microwave-induced pyrolysis of algal biomass. These gases are particularly used for the production of syngas, thus making biomass pyrolysis highly desirable. Microwave-assisted pyrolysis of microalgae, such as scenedesmus almeriensis, was carried out to obtain high production of gaseous fraction with high proportion of H_2 (c.a. 50 vol. %) and syngas (c.a. 94 vol. %) at 800 °C via pyrolyzing algae extraction residue [92]. A microwave plasma reactor was used at the power levels of 800, 900 and 1000 W under nitrogen purge and produced 36.75-45.13 vol. % hydrogen gas from 1 g dry spirulina algae. As microwave power level increased, the reaction temperature rose which resulted in the decrease of CO_2 and CO formation and increase of H_2 in the gaseous products [161].

Bio-oil is a crucial product from microwave-enhanced pyrolysis of algae. The microwave-enhanced pyrolysis of natural algae from water blooms under different reaction conditions was conducted (algal biomass particle size, microwave power input, microwave absorber, carrier gas and catalysts) to optimize the bio-oil production. The maximum liquid production was obtained under CO_2 atmosphere, which was 54.3 wt.%[27]. The pyrolysis of Chlorella sp. was studied by using a microwave oven and the maximum yield of bio-oil was achieved as 28.6 wt.% under the power level of 750 W. Aliphatic hydrocarbons and aromatic hydrocarbons which accounted for 22.2%

of the bio-oil, are highly desirable compounds. The results of GC-MS showed that the bio-oil mainly contained aromatic hydrocarbons and aliphatic hydrocarbons (22.2% of the spectrum area), phenols, long chain fatty acids and nitrogenated compounds [156]. However, bio-oil collected after pyrolysis of biomass is normally a mixture of unstable compounds. This presents some challenges to the large scale utilization of bio-oil due to their high oxygen content, viscosity, corrosiveness and requirement of upgrading process [22, 162].

Bio-char is the solid residue after the algae pyrolysis and generally regarded as worthless material where many researches made great efforts to reduce its amount [163]. Lower power level of microwave as well as lower heating rate led to higher yield of char, while higher power level with higher heating rate resulted in more gasification [164, 165].

2.7 Pyrolysis under carbon dioxide atmosphere

Overwhelming carbon dioxide emission, especially from combustion of fossil fuels, has been a global issue attributed to greenhouse effect by trapping the solar heat and increasing the earth surface temperature, thus melting iceberg and raised sea level [166, 167]. Hence, various studies focus on the technology of capture, storage, and utilization of carbon dioxide. Carbon dioxide has mainly used by the food industry (food additive in beverages, dry ice for wine

making), oil recovery, agriculture (photosynthesis of plant) and the chemical industry (urea and methanol production) [168, 169].

Pyrolysis was carried out under nitrogen to maintain the anaerobic atmosphere generally [31, 101, 170, 171]. Recently, carbon dioxide was proposed to have a fast cycle of carbon and result in higher syngas yield especially CO from pyrolysis of biomass [103]. The influence of CO_2 was investigated to have significant improvement of the microalgae pyrolysis with CO concentration increased up to 30 times at 670 °C. This might be achieved by the expedited thermal-cracking of volatile organic compounds (VOCs) by both increasing release of VOCs from algae pyrolysis with the presence of CO_2 and unidentified direct reaction between VOCs and CO_2. It was also found that the effectiveness of CO_2 was initiated from 530 °C [73]. Similar achievement has been found in the microwave-enhanced pyrolysis of biomass waste (spent coffee ground) with great enhancement of CO yield (~3000%) and tar reduction (~40-60%), which could be explained by similar reaction. Furthermore, the bio-char processed under CO_2 was observed to have larger pores in SEM images, compared to char derived under N_2 [37, 103], which was hypothesized that after the depletion of VOCs, the further modification of char under CO_2 occurred [172]. Additionally, the microwave-enhanced pyrolysis of natural algae under CO_2 derived bio-oil with 66.6% carboxylic acids because of the inhibition of

decarboxylation by CO_2 [27]. Since pyrolysis is an intermediate step of gasification process, CO_2 has also been introduced into gasification as the gas medium. The microwave-enhanced gasification of oil palm shell (OPS) char in packed bed under CO_2 to produce CO via the Boudouard reaction ($C+CO_2 \rightarrow 2CO$) was investigated. Higher CO_2 flowrate (50-125 mL/min) led to lower CO_2 conversion rate (93-58%) but larger cumulative CO production (3.74-6.83 mmol/min). Moreover, as the gasification temperature increased (750-900 °C), the average CO_2 conversion rate was improved from 28 to 74% [173].

However, biochar derived under CO_2 has less active sites as absorbents or catalysts because of the destruction of functional groups, though it has larger porosity [174]. CO_2 also favored the yield of bio-oil, rather gas product [27]. CO_2 is still believed to enhance the thermal efficiency, improve thermal cracking of VOCs, reduce the tar yield and modify the morphologies of char.

2.8 Microwave-enhanced catalytic reforming

Catalysis is widely applied in science and engineering. The production of most industrially important chemicals involves catalysis at some point. Similarly, most biochemically significant processes are catalyzed. Thus, research into catalysis is a major field in applied science and involves many areas of chemistry, particularly organometallic chemistry and material science. More recently, catalysis is applied during microwave-enhanced pyrolysis of biomass

to improve the yield and quality of gaseous fraction or bio-oil. Such potential brings about many benefits and interests worldwide; however, it is still in its infancy [123, 175].

The microwave-enhanced pyrolysis as a promising approach for promoting pyrolysis process, is fast becoming popular which is believed to be more efficient compared to conventional pyrolysis [31, 120]. More importantly, microwave-insisted heating can bring about higher gas production with a larger proportion of syngas (CO and H_2), along with better quality of bio-oil compared to conventional ways [176, 177].

2.8.1 Molecular sieves as catalysts

Molecular sieves are heterogeneous catalysts commonly used in the petroleum industry, particularly in the gas stream purification and interconversion of hydrocarbons. Many previous research reported molecular sieves in catalytic pyrolysis of lignocellulosic biomass improved the quality of bio-oils, but seldom concerning the pyrolysis or catalytic pyrolysis of algae to produce bio-products.

ZSM-5 is an aluminosilicate zeolite with a high silicon to aluminium ratio, which is one of the most favoured molecular sieves. With addition of H^+ as the cation, the HZSM-5 has strong acidity, to facilitate the conversion of hydrocarbons involving thermal cracking reaction [178]. Borges, Xie [146] conducted fast microwave-assisted pyrolysis of microalgae (chlorella sp. strain and nannochloropsis

strain) with the presence of catalyst HZSM-5. The use of this catalyst for both algal biomass increased the moisture content in the liquid product and the amount of char. Moreover, without usage of HZSM-5 catalyst, higher carbon and hydrogen proportions were exhibited, thus higher HHV of bio-oil was derived. Therefore, this HZSM-5 catalyst may not be appropriate for the bio-oil fuel production from algae. It was also used to maximize and upgrade the pyrolysis vapours from a mixed biomass waste via 3hr-catalysis, meanwhile reducing the formation of coke [179]. Pan, Hu [180] carried out pyrolysis of nannochloropsis sp. residue in a fixed bed reactor with different HZSM-5 catalyst to material ratios, which created a noteworthy decrease in liquid yield while simultaneous increase in char together with gas due to coking. The volatile intermediates generated pass through the micropores or remain on catalyst surface and enhance secondary reaction. Hence, apart from more production of gaseous fraction, coke deposits accumulate on the surface and micropores of catalysts [181]. As the catalyst-to-material ratio increased, the interaction between catalyst and material have been enhanced with larger production of gas from greater thermal cracking and secondary reactions.

Anand, Sunjeev [182] investigated fast pyrolysis of A. platensis (spirulina) algae with zeolites including ZSM-5, zeolite-β and zeolite-Y catalysts in a single shot micropyrolyzer to upgrade the

bio-oil. After characterization, the activity of these zeolite catalysts is considered to be affected by the acidity (TPD, ammonia-temperature programmed desorption), specific surface area, pore size (BET, Brunauer-Emmett-Teller method) and structure [183, 184].

2.8.2 Metal oxides as catalysts

The effects of four metal oxides, i.e., NiO, CuO, CaO, and MgO, on the pyrolysis of corn stover under the microwave irradiation was studied [124]. Except for MgO, the addition of other three metal oxides at lower addition ratio (3%), raised the maximum temperatures reached. The addition of CaO could increase the H_2 production by 5-10%. Meanwhile, the use of the four metal oxides decreased the production of CO and CO_2 for up to 30%. It was concluded that the addition of these catalysts could reduce the formation of PAHs in the microwave pyrolysis of biomass, and thus lower the toxicity of bio-oil. Generally, the introduction of alkaline metal oxides as catalysts could change the distribution of three-phase biomass products, which increasing the liquid products while reducing gaseous and solid yields. Same four metal oxides, NiO, CuO, CaO, and MgO, were selected as catalysts to process microwave-enhanced pyrolysis of sugarcane bagasse [157]. Similar results showed that the addition of metal oxide catalysts improved the reaction results including mass reduction ratio and reaction rate. The introduction of either NiO or CaO could slightly increase the H_2 production, whilst

adding either CuO or MgO would marginally decrease that amount. When CaO and MgO served as catalysts, the gas production could be enhanced, and NiO and CuO would increase the bio-oil yield.

Six catalysts (CaO, $CaCO_3$, NiO, Ni_2O_3, γ-Al_2O_3 and TiO_2) for the microwave pyrolysis of sewage sludge were investigated [158]. The catalysts could raise the temperature growth rates of sewage sludge besides CaO, and the decreasing order for temperature growth rates was $Ni_2O_3 \approx \gamma$ -Al_2O_3> TiO_2>NiO> $CaCO_3$. Ni-based catalysts particularly Ni_2O_3, showed relatively higher reactivity in decomposition of organic matters, and significantly increased the yields of pyrolytic biogas (especially CO-rich syngas) and bio-oil. But CaO promoted the production of H_2-rich syngas from sewage sludge. Both of γ-Al_2O_3 and TiO_2 also increased the decomposition of organic matters, but almost no influence on the combustible gas production and the H_2/CO ratio.

Three metal oxides with microwave absorption effects of MgO>CaO>CuO and three metal salts with effects of $ZnCl_2$ > NaH_2PO_3 > $MgCl_2$ were added into the microwave-induced pyrolysis of algae, gulfweed, at a power level of 1500 W [185]. After 5 wt.% of metal oxides mixed with algae, the production of solid residue showed the greatest decrease of 14.35% and that of bio-oil appeared to be 11.04%, while gaseous product increased. The chemical composition and physical structure inside the material might

be changed by the addition of CuO, due to the formation of high temperature nucleus which pyroylzed more macro-molecules into micro-molecules. The remained char was reduced and more gas product generated because of the alteration from micropores into mesopores[186]. Under high temperatures, MgO and CaO could form complex compounds and significantly affect the stability of π electron cloud in tar component, which promoted the second pyrolysis of the tar molecules. Therefore, the yield of bio-oil increased, whilst the gas production decreased [187, 188]. Meanwhile, electrical energy consumption after the addition of CuO and MgO were detected to increase by 1.44% and saved by 40.76% separately. When the algae was added with 5 wt.% $MgCl_2$, $ZnCl_2$ and NaH_2PO_3, respectively, the amount of solid residue increased by 3.98, 1.13 and 2.31%, and the yield of bio-oil increased by 6.3, 16.92 and 0.71%, separately.

Other categories of salts have also been used to catalyze the pyrolysis of biomass. Chloride salts can improve the bio-oil yield, which simplify the chemical compositions of bio-oils and enhance the products selectivity of the pyrolysis process [189]. Microwave-assisted pyrolysis of pine wood sawdust was conducted at 470 °C with catalytic effects of eight inorganic additives (i.e., NaOH, Na_2CO_3, Na_2SiO_3, NaCl, TiO_2, HZSM-5, H_3PO_4, $Fe_2(SO_4)_3$) [175]. All of the eight additives have significantly increased yields of solid products while decreased yields of gaseous products correspondingly. The

production of bio-oil have not subjected to dramatic changes. The effect of copper (Cu) on the pyrolyzed bio-oil from demineralized wood dust, which is a terrestrial biomass and composed of cellulose, hemicellulose and lignin, has been discussed. Copper inhibited the final step of cellulose decomposition into light compounds, and promoted the pyrolysis of hemicellulose. Meanwhile, copper could partially reduce the degradation of lignin intermediates [190]. K_2CO_3, CaO, Na_2CO_3 have been added into the microwave pyrolysis of wheat straw [155]. The catalyst of K_2CO_3 improved the transformation of tar and increased the syngas yield at higher temperature, but at low temperatures, it would increase the heat and mass transfer resistance between biomass particles which limited the pyrolysis reaction. The addition of CaO would decrease around 35% of the CO_2 content by absorbing CO_2 and forming $CaCO_3$ to produce more hydrogen in microwave pyrolysis [191].

2.8.3 Char as a catalyst

Catalysis in the pyrolysis of biomass was primarily used to crack the heavy compounds and generate valuable lighter gases. The catalysts used for pyrolysis of biomass are generally metal oxides (i.e., Al_2O_3) or natural materials (i.e., dolomite, olivine) as catalysts or catalytic supports [192]. These catalysts or carriers are relatively expensive and the preparation for catalysts are time and energy consuming. Char is a good carbonaceous microwave absorber which could

improve the absorption of microwave irradiation. This inexpensive catalytic support or catalyst would be simply gasified to recover the energy rather regeneration [193].

Zhang, Dong [193] focused on maximizing the gas yield and the optimum syngas production from microwave pyrolysis of rice husk by using its char and char-supported metallic (Ni, Fe, and Cu) catalyst. The char as a catalytic support with pore structure and catalytic activity favored the production of gas and conversion of tar. The three rice husk char-supported metallic catalysts improved the capability of microwave absorption and thus increased the heating rate as well as final temperature. Among four catalysts, it is noteworthy that Ni-char catalyst gave the highest gas production and lowest liquid yield, due to high activation ability of C-H and C-C bonds in the tar molecules on the Ni metal surface. They also found that the effects of increasing Ni content in catalyst on pyrolysis could accelerate the cracking and reforming process and so as the production of syngas by creating more active sites on the catalysts. However, higher Ni loading catalyst was considered inappropriate due to its high cost, risk of environmental pollution and ordinary performance. Moreover, rice husk char and Ni-char, Fe-char, Ni-Fe/char (with calcination) and Ni-Fe char (without calcination) were also used as catalysts to improve the conversion of tar during biomass pyrolysis [194]. After high temperature pyrolysis, the char became highly porous structure

and could act as a catalyst support or microwave absorbent according to SEM image and BET result. Similarly, the Ni-char catalysts could increase the reforming activity of hydrocarbons, compared with Fe-char catalysts, due to the higher activation ability of C-H and C-C bonds in the hydrocarbons on the surface of Ni-based catalysts. Additionally, the tar from biomass pyrolysis converted effectively with the addition of rice husk char/rice husk ash supported nickel-iron catalysts was investigated at the temperature of 800 °C [195]. The tar conversion efficiency could be as high as 92.3% with rice husk char Ni-Fe and reached about 93% by the rice husk ash Ni.

However, the char catalysts prepared by conventional pyrolysis methods have large and deep cracks, while pores were found in microwave pyrolyzed char without cracks [140] as **Figure 2-3**. Since the heat transferred from inferior to interior biomass for conventional pyrolysis, the outer temperature is much higher than the core of material, and thus creates many cracks which make the char more fragile. But the volumetric heating feature of microwave led to the generation of heat from inner core, which formed many small pores on the surface of char and might benefit catalysis [186, 196, 197].

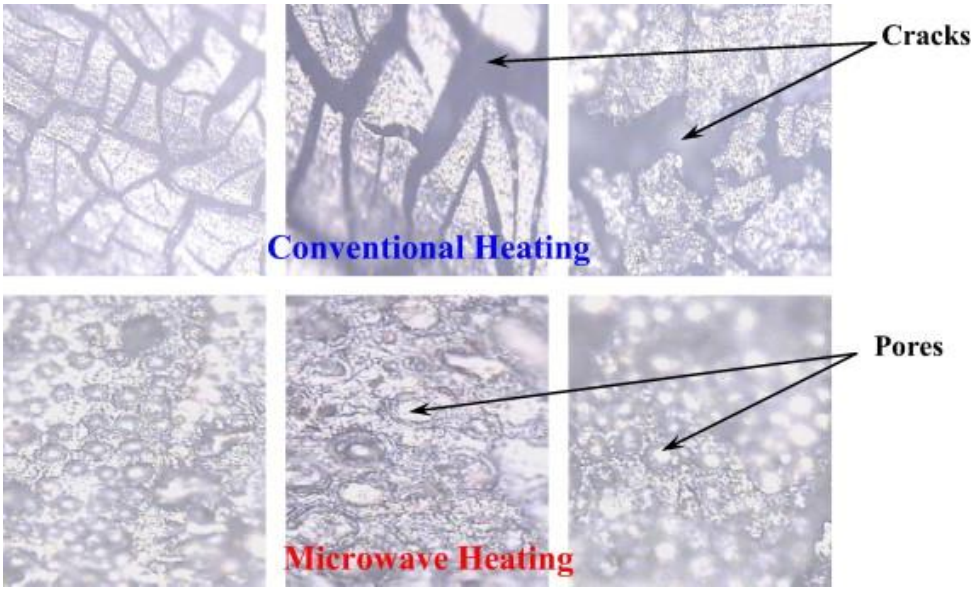

Figure 2-3 Surface image analysis of oil palm chars after conventional heating and microwave heating

2.8.4 Ash as catalysts

All biomass contain ash-forming minerals in the forms of cations which could further bound onto phenolic or carboxylic groups, or form precipitates [198]. The main constituents of ash normally include oxides of Al_2O_3, CaO, Fe_2O_3, K_2O, MgO, MnO, MnO_2, Na_2O, SiO_2, TiO_2, P_2O_5, SO_3, etc. [199]. It is found that the presence of ash has several effects on catalyzed pyrolysis of biomass. Firstly, the biomass ash affects ultimate compositions of the products via interaction with the volatiles, which increases the yield of non-condensable gases [200]. Secondly, the biomass ash is capable of cracking larger vapor molecules into smaller ones which could access the interior pore structure of catalysts. Thirdly, the reforming of cracked smaller vapors may be further promoted by catalysts. Last but not least, some ash compounds are regarded to be good microwave absorbers,

i.e. Fe_2O_3 and TiO_2, whereas some ash compounds have lower performance in absorption of microwave radiation, i.e. MgO and SiO_2 [199, 201-203]. Although the heating rate together with the pyrolysis temperature could be enhanced by ash components and so as the oil production, sometimes the oil production would be reduce, since ash itself cannot be pyrolyzed into bio-oil [204, 205]. It also implies that the deactivation of the catalysts used in catalyzed pyrolysis normally caused by the deposition of coke and biomass originated metals via poisoning the active sites or blocking the pores of catalysts, which influences the conversion of vapors as well as pyrolysis reaction [206, 207].

The fast pyrolysis of pine wood in a stirred bed reactor at 500 °C was conducted and the results were compared with each other, including non-catalytic pyrolysis, addition of pine wood ash, catalytic pyrolysis using ZSM-5 based catalysts, catalytic pyrolysis using ZSM-5 based catalysts together with ash, and catalytic pyrolysis with catalysts recycled after eight pyrolysis. About 3 wt.% of biomass weight was biomass ash added to the catalytic pyrolysis and aroused a reduction of 2 wt.% organics and coke, while increased the moisture and non-condensable gases by 1 wt.% and 4 wt.% respectively [208]. Oil sludge, i.e. oil field sludge and oil tank sludge, can be recovered and recycled by applying the oil sludge ash-catalysed pyrolysis-reforming processes. The highest yield of oil was 35.5 wt.% achieved by oil tank

sludge with oil field sludge ash, which might be attributed by the higher iron and sulphur elements contained in this ash. Due to the higher metal contents in the oil field sludge ash, especially iron, the vapor produced after pyrolysis could be upgraded by using this catalyst [209]. Oil sludge ash and some metal oxides (Al_2O_3, CaO, SiO_2 and Fe_2O_3) have been added into the pyrolysis of oil sludge in a stirred tank reactor to investigate the catalytic effects on the oil yield. It is observed that Al_2O_3, CaO, Fe_2O_3 and ash which contained these metal oxides, reduced the char amount and alteration of S, O and N elements from oil sludge into the oil, while improved the oil quality [210].

Although some investigations have been carried out on the catalytic pyrolysis of biomass, a very limited number of reports were found in open literature on the use of algae ash which consists of minerals as catalysts for the microwave-pyrolysis of algae itself.

2.9 Conclusions and prospect

The yield of products from microwave-enhanced pyrolysis depends largely on the properties of biomass, operating conditions, types of microwave absorbers and catalysts used. Higher microwave power results in larger heating rate as well as pyrolysis processing temperature, which favours the formation of volatiles, especially for syngas production.

Kinetic analysis of pyrolysis could help in comprehension the pyrolysis mechanism together with selecting and improving the biomass feedstocks into the system to obtain desirable products. Meanwhile, carbon dioxide atmosphere has been introduced into both conventional and microwave-induced pyrolysis of biomass. Thus, the effects of CO_2 on pyrolysis, compared with N_2 is worth investigation.

It has been found out that the introduction of microwave absorbers, the use of CO_2 as the carrier gas and the presence of catalysts in the pyrolysis process could improve the yield and selectivity of final pyrolysis products. Therefore, it is worthwhile to try different types of microwave absorbers, different atmosphere, and the recycling of the solid residue (char/ash) back to the reaction system as catalysts for improvement of the product yield.

Chapter 3. Experimental

This chapter introduces the algae studied and the systematic characterisation of these samples. The kinetic analysis of samples to investigate the mechanism of algae pyrolysis is described in details. The microwave-enhanced pyrolysis of algae and its model compounds is explicated as well as the methodologies used in this thesis for the characterization of gaseous, liquid and solid products. Moreover, catalytic reforming process of algae under microwave heating mode with the addition of algal recycled char as a catalyst are stated. All experiments were repeated at least once to confirm the validity of results and the averages of results were taken for further analysis.

3.1 Materials

Algae and its model compounds

Three microalgae (chlorella, spirulina, dunaliella) and two macroalgae (laminaria japonica and porphyra) were used in the experiment. Chlorella and spirulina were provided by Shandong Binzhou Tianjian Biotechnology Co.Ltd. (Shandong Province, China). Dunaliella and Laminaria japonica were purchased from Shanxi Sciphar Natural Products Co. Ltd. (Shanxi Province, China). Porphyra was supplied by Fuqing Riji Food Co. Ltd. (Fujian Province, China). Oil droplets (Optima 339 powdered vegetable fat), α- Cellulose ($(C_6H_{10}O_5)_n$, Aladdin®, product code C104844) and ovalbumin (Sinopharm Chemical Reagent Co., Ltd, product code 69003835) were taken as

model constituents of algae representing lipid, carbohydrate and protein respectively. All the five algae and the model compounds were dried at 105 °C for 24 h prior to milling (Retsch ZM200 Ultra-Centrifugal mill) and were ground to a size smaller than 212 μm.

Microwave absorbent

Silicon carbide (SiC, Sinopharm Chemical Reagent Co., Ltd, product code 200723752) was added into the reactor as a microwave absorbent. The size of SiC particles was greater than 600 μm, which could be easily separated from char after the completion of pyrolysis.

3.2 Characterization of algae

3.2.1 Proximate analysis

Moisture content, volatile matters, fixed carbon and ash content were determined by a thermogravimetric analyser (TGA, NETZSCH STA449F3, Germany) based on BS ISO 17246:2010 following procedures described elsewhere [211, 212] . Samples were manually grounded to smaller size at first and weighed about 10mg for each test. The sample was heated from 40 °C to 105 °C at a heating rate of 20 °C min^{-1} under 20 ml min^{-1} nitrogen (N_2) purging. The temperature was held at 105 °C for 30 min to completely drive off moisture and raised to 900 °C at 50 °C min^{-1} with 20 ml min^{-1} N_2 purge. After being held at 900 °C for 30 min to remove all volatiles, the temperature was then lowered to 850 °C in air with a flowrate of

20ml min^{-1}. The temperature was then kept isothermal for 30 min. The proximate analysis was carried out by analyzing weigh loss curve (TG curve) extracted from the TGA.

3.2.2 Intrinsic analysis

Ignition, peak and burnout temperatures can be determined by using the thermogravimetric (TG) and differential thermogravimetric (DTG) profiles [213, 214]. Meanwhile, LHV (Lower Heating Value) of the sample was also calculated by exothermic peak area from Differential Scanning Calorimetry (DSC) analysis.

Approximately 10mg of sample was weighed firstly and heated from 40 to 105 °C. After being held at 105 °C for 30 min to drive off all the moisture, the temperature was then raised up to 900 °C and maintained at 900 °C for 30 min. The whole process was carried out at a heating rate of 20 °C min^{-1} under 20 ml min^{-1} air purging [215].

3.2.3 Ultimate analysis

Carbon (C), hydrogen (H), nitrogen (N) and sulphur (S) contents of algae samples were derived using a CHNS/O Elemental Analyser (Euro Vector EA3000, Italy). The standard sample was used to calibrate the analyser at first, and about 1.5 mg of pre-treated sample was applied for testing. The content of oxygen (O) was derived by difference on the basis of dry and ash free [212].

3.2.4 Higher Heating Value

Bomb Calorimeter (IKA C200, Germany) was used to determine the calorific value of algae and model compounds. The samples were firstly compressed into tablets using tablet press machine in case of blowing away after introducing oxygen. After samples ignition, the temperature in vessel increased and the calorific value was calculated and recorded in software Calwin.

3.2.5 Density

Automatic density analyser (ULTRAPYC 1200e, Quantachrome Instruments, U.S.) was applied to test the true volume and density of algae and model compounds with helium purging to ensure maximum accuracy. The density of solid was calibrated for 6 runs to minimize the deviation from mean value.

3.2.6 Lipid, protein, carbohydrate contents

Protein content was determined according to Kjeldahl method (BS EN ISO 20483:2013) while the lipid content was determined according to Soxhlet extraction (GB/T 5009.6-2003). Carbohydrate was calculated by difference (GB/Z 21922-2008). Ovalbumin, cellulose and powered oil samples were used to represent pure protein, carbohydrates and lipids, respectively, and were used as model compounds for comparison purposes.

3.3 Algae ash preparation and characterization

In this study, ash samples of the five algae were used as catalysts. The preparation of algae ash was based on BS EN ISO 18122:2015 standard. Algae samples after pre-treatment were placed in crucibles into muffle furnace (5E-MF 6000, Changsha Kaiyuan Instruments Co. Ltd., China) and its temperature rose evenly from room temperature to 250 °C at a heating rate of 7.5 °C min^{-1}. The furnace temperature maintained at 250 °C for 60 mins and increased steadily to 550 ± 10 °C over a period of 30 mins with a heating rate of 10 °C min^{-1}. Then the temperature was kept at this level for 120 mins. After cooling down, the remaining solid materials were the ash samples for further use.

Scanning Electron Microscope (SEM, Sigma VP, Zeiss, Germany) was applied to study the morphology of algae ash samples. According to the electronic conductivity of samples, the voltage was set between 2 and 5 kV, and the working distance was normally around 7.5 mm. Secondary electron detector (SE2) was used for taking SEM images. Qualitative and quantitative analyses of elemental composition in ash was determined by Energy Dispersive X-ray Spectrometer (EDS, Oxford, UK), which was equipped with the SEM. 15-20 kV was normally applied to generate adequate X-ray from the sample to reach the EDS detector. For each char sample, 20 points were

scanned and the averages of the char compositions were recorded [216, 217].

Surface area of algae ash was measured via the BET analysis (ASAP-2000, Micrometrics Corp, USA) by nitrogen multilayer adsorption measured as a function of relative pressure. The technique encompasses external area and pore area evaluations to determine the total specific surface area in m^2/g yielding important information in studying the effects of surface porosity and particle size in catalysis. Also, pore size distribution and pore volume can be characterized by adsorption and desorption techniques [218].

The elemental oxides in algal ash was detected by X Ray Fluorescence (XRF, Shimadzu XRF-1800, Japan). Approximately 1 g of sample was pressed into tablets and it was placed into cavity testing for 10 s. The composition of each oxide in ash would be shown directly.

3.4 Kinetic study method

Pyrolysis of pre-dried algae and its three pseudo-compositions via traditional electric heating method were carried out using a thermogravimetric analyser (TGA, NETZSCH STA449F3, Germany) via non-isothermal process. Four linear heating rates from 50 to 900 °C, which were 5, 10, 20 and 50 °C min^{-1}, to conduct pyrolysis of the five algae and three pseudo-components (oil droplets, α-cellulose and ovalbumin), as well as the char of samples to derive weight loss profiles (TG curves). Pure nitrogen or carbon dioxide with

a flowrate of 20 mL min^{-1} was introduced into the system as carrier gas and provided an anaerobic atmosphere. The sample for each experiment was milled to a particle size less than 106 μm and spread as a thin layer in crucible (2±0.5 mg). In order to investigate the effects of CO_2 on carbon content of solid residue, the char was firstly prepared by tube furnace (SG-GL1200K, Shanghai) with the same heating programme in TGA. The sample was heated from 50 to 900 °C with a heating rate of 5 °C min^{-1} under N_2 purge at a flowrate of 100 mL min^{-1}. After cooling down and collected, the kinetic analysis of the pyrolysis of char under CO_2 was further performed by TGA using same procedure.

3.5 Microwave-enhanced pyrolysis

Microwave-enhanced pyrolysis of algae and its main model compounds (α-cellulose and ovalbumin) was conducted in a 2.45 GHz multi-mode microwave (Nanjing Jiequan Microwave Co., Ltd., China). The system has two control modes, namely temperature control and power input control. The maximum power input of the testing system was 3 kW. There are two devices to monitor the reaction bed temperature – infrared thermometer and thermocouple. The infrared thermometer with lower penetrating capability could only detect the surface temperature of the reaction bed, which is considered to be inaccurate. The operating temperature was determined by using a stainless steel-sheathed K-type thermocouple to avoid arcing, which

showed more accurate bed temperature (±10°C). The thermocouple would be inserted into the reaction bed with a detecting range of 0-1300 °C. A quartz fixed bed reactor (315 mm length, 34 mm diameter) was placed in the cavity and sheathed with an outer quartz reactor (44 mm diameter) to guarantee an inert atmosphere during the experiment. The experimental setup is shown as **Figure 3-1**.

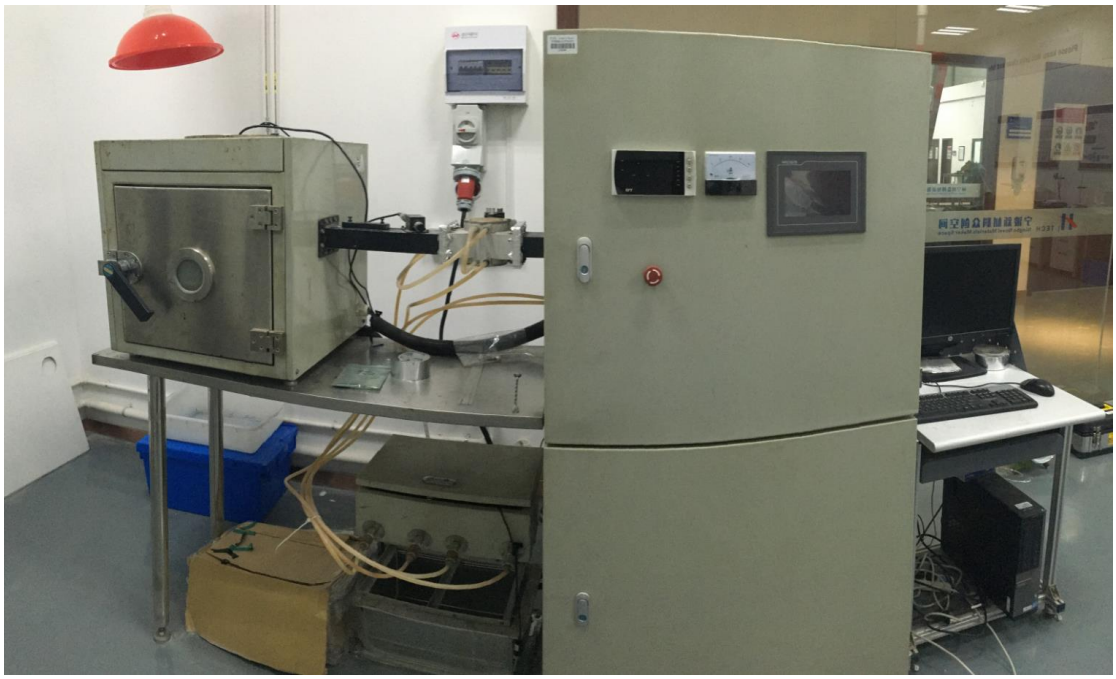

Figure 3-1 Multi-mode microwave experimental rig

The schematic diagram of microwave-enhanced pyrolysis is shown in **Figure 3-2**. In each test, 10 ± 0.5 g of sample (<212 μm) was mixed with 50 ± 0.5 g of SiC (>600 μm) and placed in the quartz reactor. The temperature-controlled mode was used when the pyrolysis temperature set at 400, 550, and 700 °C. With the assistance of SiC, the temperature can be raised to set value from room temperature in approximately 10 min and maintain at that temperature for 20 min.

The microwave input power was automatically adjusted to achieve the set temperature. After 30 min, the microwave stopped automatically. A nitrogen purge at a flowrate of 100 ml min^{-1} was introduced to the rig for 15 min before each experiment start to ensure an oxygen-free atmosphere and was turned off after the experiment. After pyrolysis, bio-oil, including those trapped in the reaction system, was dissolved in dichloromethane while non-condensable gaseous fraction was collected in 20 L Tedlar® gasbag. The remaining char was separated from SiC by sieving for 30min using a GZS-1 High-frequency Sieve Shaker. The liquid and solid yields were weighed, while the gaseous fraction was determined by difference on the basis of mass balance [42, 49]. The solid, liquid and gaseous products were collected and subjected to further analysis in **Section 3.6**.

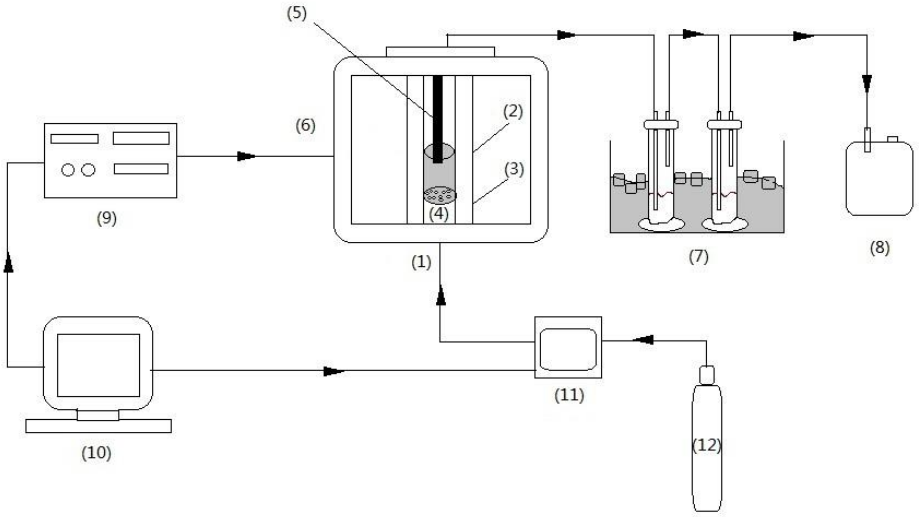

Figure 3-2 Experimental rig: (1) microwave generator and cuboid cavity; (2) cylindrical quartz reactor; (3) hollow quartz tube with larger diameter to ensure the anaerobic atmosphere in reaction bed; (4) reaction bed with microwave absorbers; (5) K-type thermocouple which insert into the reaction bed with a detecting range of 0- 1300°C; (6) infrared temperature measurement for detecting the cavity temperature in the backside of cavity; (7) liquid fraction collectors in ice bath; (8) gas collection bag; (9) microwave controller system; (10) computer;(11) gas flowmeter; (12) carrier gas supplier.

3.6 Microwave-enhanced catalytic reforming

The ash of algae as catalyst was prepared and characterized as described in **Section 3.3**. Approximately 3± 0.5 g of the ash catalyst was mixed sufficiently with algae placed in the same pyrolytic quartz reactor as indicated in **Figure 3-2** with 100 ml min^{-1} nitrogen purge. Other procedures remained the same as microwave-enhanced pyrolysis in **Section 3.5**. After reforming, the catalyst was separated (>212 mm) and char was collected for further characterization (**Section 3.6**).

3.7 Characterization of pyrolytic products

Two condensers contained 100 mL organic solvent-dichloromethane each to dissolve the condensable vapours and form into bio-oil products. However, some of the tar was found to adhere to the pipes, tube wall, lid of cavity, condensers. Hence, after each experiment, they were washed by dichloromethane and collected in the end, to minimize the loss of oil product. After washing by dichloromethane, the weight error of bio-oil was measured to be around 10%. The oil was then measured for 20 ml in bottle and put in fume cupboard for 24 h. After vaporization of dichloromethane, the weight difference was calculated as the mass of bio-oil. After sieving, the weight of char can be derived. Because of the difficulty in completely distinguish the gaseous product compositions from carrier gas and dichloromethane vapour, its yield was calculated by the difference based on mass balance due to ignorable error[49].

3.7.1 Characterization of gas

A gas chromatograph (GC, Shimadzu GC-2014, Japan) was used to determine the gaseous product from pyrolysis of algae. The GC consists of 1 FID detector, 2 TCD detectors, 8 molecular sieve columns and 1 HP-AL/s capillary column. GC could detect volume percentage of C1-C5 hydrocarbons (CH_4, C_2H_6, C_2H_4, C_3H_8, C_3H_6, C_4H_{10}, C_4H_8, C_4H_6, i-C_5H_{12} and n-C_5H_{12}, etc.) and permanent gas (O_2, N_2, H_2, CO, CH_4, and CO_2, etc.).

3.7.2 Characterization of bio-oil

The compositions of bio-oil were analyzed by using a gas chromatograph mass spectrometry (GC-MS, Agilent 7890-5975C, USA). The GC-MS was equipped with an HP-5ms capillary column (30m length, 0.25mm internal diameter, 0.25 μm film thickness). Initial oven temperature of the GC was kept at 60°C for 2 min. Oven temperature was then programmed to increase to 280 °C at a heating rate of 10 °C min^{-1} and kept for a further 2 min. A split/splitless injector operated in the split mode was installed with the GC. The split ratio was 50:1. By comparing the mass spectra with NIST 2011 library database, the chromatogram peaks could be categorized. The GC-MS technique cannot deliver the actual quantitative analysis of bio-oil, rather the actual compound concentrations. However, according to previous literatures [156, 219-221], GC-MS could detect the peak retention time and peak area for each corresponding compounds in bio-oil. Relative molar content of each substance in the bio-oil was estimated proportional to the calculated percentage of associated chromatographic area. Meanwhile, the intrinsic analysis were carried out using TGA using the method described in **Section 3.2.2**.

3.7.3 Characterization of char

Pyrolytic char was firstly separated from microwave absorbents by sieving for 30min using a GZS-1 High-frequency Sieve Shaker.

Proximate and intrinsic analyses were conducted to characterize char by TGA, as described in **Section 3.2.1** and **3.2.2**. Morphologies of char determined by SEM/EDS following the procedure described in **Section 3.3**.

Chapter 4. Characterization of algae and its model compounds

This chapter demonstrates the characterization of algal biomass together with the three model compounds, including proximate analysis, intrinsic analysis, ultimate analysis, higher heating values (HHVs), morphology and composition of algae ash. These properties of biomass samples are essential for the understanding of thermal behaviours of different samples upon heating.

4.1 Proximate analysis

Proximate analysis was carried out by using a TGA and results are shown in **Table 4-1**. Moisture content of air-dried algal biomass varies between 5 to 10 wt.%. Volatile matters of algae are more than 67 wt.%, and fixed carbon is around 11.5-18.5 wt.%. The volatile content of algae is much higher than normal coals [222]. Ash content of algae varies between 0.2 and 6.7 wt.%. The predicted pyrolytic char amount including ash and fixed carbon, is around 12 to 25 wt.%. The volatile matters in algae can be easily converted into bio-oil and gaseous fraction during pyrolysis process. The potential production of bio-oil and gaseous fraction largely depends on the volatiles contained [223], as well as heating rates, etc. Three algae model compounds have over 85 wt.% of volatiles, especially for oil droplets, which contains 100 wt.% of volatiles, but less ash (less than 10 wt.%) and moisture content (1.1 wt.% of cellulose).

Table 4-1 Proximate analysis of algae and the model compounds

Algae	Moisture (wt.%)	Volatile (wt.%)	Fixed carbon (wt.%)	Ash (wt.%)
Spirulina	6.7	73.5	13.2	6.6
Chlorella	8.0	70.7	15.2	6.1
Dunaliella	5.7	82.4	11.7	0.2
Laminaria	7.4	67.7	18.3	6.6
Porphyra	9.3	70.8	16.9	3.0
α-Cellulose	2.7	88.6	7.6	1.1
Ovalbumin	2.0	86.6	9.9	1.5
Oil droplets	0.0	100.0	0.0	0.0

4.2 Intrinsic analysis

Intrinsic analysis of algae was conducted by using a TGA, the results of which are illustrated in **Table 4-2**. It investigated ignition temperature, peak temperature, burnout temperature and lower heating value (LHV) of the five algal biomass samples together with the model compounds. The ignition temperature of algae is around 220 to 270 °C, which are much lower than that of coal [224], since the hemicellulose in biomass is easily burnt around 280 °C. The combustion profile of algal biomass generally has two peak temperatures, which due to the burning of carbohydrates at 270-310 °C and proteins above 440 °C respectively. Similarly, the burnout temperatures of algae vary between 520 and 740 °C, which are still lower than that of coal samples. Moreover, by comparing LHVs of different samples, dunaliella and porphyra with larger carbohydrate

content are more reactive due to their higher LHVs (around 10 MJ/kg). But spirulina, chlorella and laminaria with smaller amount of carbohydrates while larger protein content, are found to be less reactive because of their LHVs (about 6 MJ/kg).

Table 4-2 Intrinsic analysis of algae and the model compounds

Algae	Ignition Temperature (°C)	Peak Temperature 1 (°C)	Peak Temperature 2 (°C)	Burnout Temperature (°C)	LHV (MJ/kg)
Spirulina	256	297	576	643	5.5
Chlorella	241	279	566	598	6.3
Dunaliella	262	312	442	529	9.4
Laminaria	224	275	469	597	5.9
Porphyra	271	292	580	734	10.7
Cellulose	325	343	-	563	4.1
Ovalbumin	200	232	519	625	6.4
Oil droplets	349	398	-	469	4.9

4.3 Ultimate analysis

Ultimate analysis results are indicated in **Table 4-3**, together with the calculated molar ratios of C: H: O. Carbon (C), hydrogen (H), nitrogen (N), sulfur (S) and oxygen (O) contents of spirulina and chlorella are around 50.9, 6.9, 10.3, 0.8 and 31.2 wt.% respectively. Dunaliella has similar amount of C and H contents (46.6 and 6.9 wt.%), whilst no N and S in this alga. Laminaria has the lowest compositions of C, H, N, S, but the highest O content with over 60 wt.%. Porphyra has the largest amount of S which is more than 2 wt.%, whereas others are comparable to chlorella. Oil droplets, as

one of the model compounds, has the highest C and H content about 75.8 and 11.8 wt.% respectively, while ovalbumin and cellulose have similar C and H content, which are 42.2 and 6.8 wt.% respectively.

Table 4-3 Ultimate analysis of algae and the model compounds*

Algae	C (wt.%)	H (wt.%)	N (wt.%)	S (wt.%)	O (by difference wt.%)	C:H:O molar ratio
Spirulina	49.8	6.6	11.0	0.7	31.9	1: 1.6: 0.3
Chlorella	51.9	7.1	9.6	0.9	30.5	1: 1.6: 0.3
Dunaliella	46.6	6.9	0.1	0.0	46.4	1: 1.8: 0.4
Laminaria	25.3	4.1	0.4	0.8	69.4	1: 2.0: 1.0
Porphyra	42.5	6.2	6.0	2.3	43.0	1: 1.8: 0.4
Cellulose	42.7	6.5	0.0	0.0	50.8	1: 1.6: 0.5
Ovalbumin	41.6	7.0	12.2	1.2	38.0	1: 2.0: 0.7
Oil droplets	75.8	11.8	0	0	12.4	1: 1.9: 0.1

*dry and ash free basis

4.4 Heating Value

The calorific value of algae was measured as illustrated in **Table 4-4**. The HHV of microalgae is around 18-22 MJ/kg, but that value of macroalgae is less than 17 MJ/kg. It can be concluded that the microalgae generally have greater energy content compared with macroalgae. Oil droplets, as pseudo-lipid component of algae, has the highest HHV of 39.1 MJ/kg, whilst cellulose and ovalbumin have relatively lower HHVs around 17 MJ/kg, which are similar to the HHV of chlorella. It has been found that the HHVs largely depend on carbon and hydrogen content of samples[225]. Therefore, laminaria,

with the lowest C and H proportions amongst the five algae, has the lowest HHV of 9.8 MJ/kg.

Table 4-4 HHV of algae and the model compounds

Algae	HHVs (MJ/kg)
Spirulina	20.6
Chlorella	18.5
Dunaliella	21.9
Laminaria	9.8
Porphyra	16.3
Cellulose	17.0
Ovalbumin	18.7
Oil droplets	39.1

4.5 Lipid, carbohydrate and protein contents

The weight percentages of lipid, carbohydrate and protein are shown in **Table 4-5**. Spirulina and chlorella contain large amount of protein, which are more than 55 wt.%, while dunaliella and laminaria have almost no protein (0.4 and 3.2 wt.% respectively). However, the carbohydrate content of dunaliella and macroalgae are much higher than spirulina and chlorella, particularly for dunaliella, which has 94 wt.% of carbohydrate. In terms of lipid content, the five algae contain less than 5 wt.%, especially for dunaliella and laminaria which rarely contain lipid. Cellulose, as the model compound representing carbohydrate, has a percentage of 97 wt.%, while ovalbumin contains

81.6 wt.% of protein. The oil droplets is comprised of 99.6 wt.% lipid. Therefore, these three materials were taken as model constituents of algae representing carbohydrate, protein and lipid respectively.

Table 4-5 Lipid, carbohydrate and protein contents of algae and the model compounds

	Carbohydrate (wt.%)	Protein (wt.%)	Lipid (wt.%)
Spirulina	23.4	57.8	2.9
Chlorella	26.1	55.6	5.4
Dunaliella	94.0	0.4	0.3
Laminaria	51.8	3.2	0.4
Porphyra	47.7	35.7	1.5
Cellulose	97.1	0	1.2
Ovalbumin	7.9	81.6	1.1
Oil droplets	0.1	0	99.6

4.6 Density

Density of the five algae and model compounds was measured as shown in **Table 4-6**. It can be seen that the density of samples is in the range of 1 to 1.7 g/cm^3.

Table 4-6 Density of algae and the model compounds

Algae	Density (g/cm^3)
Spirulina	1.3
Chlorella	1.2
Dunaliella	1.0
Laminaria	1.7
Porphyra	1.5
Cellulose	1.7
Ovalbumin	1.4
Oil droplets	1.0

4.7 Morphology of algae and its model compounds

Figure 4-1 shows the morphology images of the five algae with a magnification 100 for of A and 1000 for B respectively. Spirulina, chlorella and dunaliella have spherical micro-structure (B), since they all belong to microalgae, whereas milled macro-algae (laminaria and porphyra) have blocky and platy structures. Similar to macroalgae, cellulose is in slice while ovalbumin and oil droplets are in spherical shapes, which are similar to microalgae morphology. Some bright areas in SEM images resulted from poor electrical conductivity of algal biomass samples.

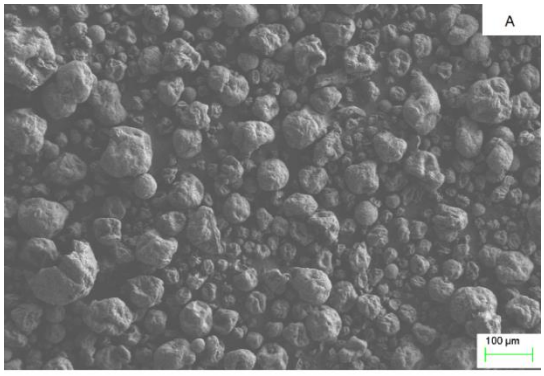

Spirulina x 100

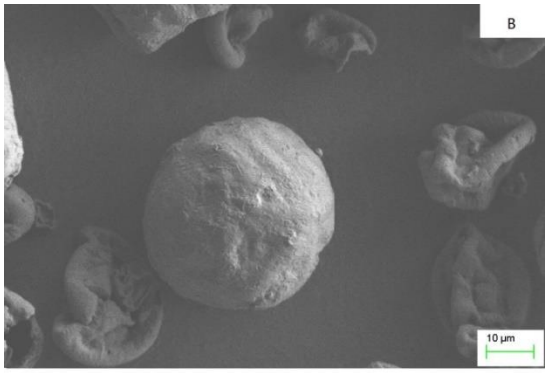

Spirulina x 1000

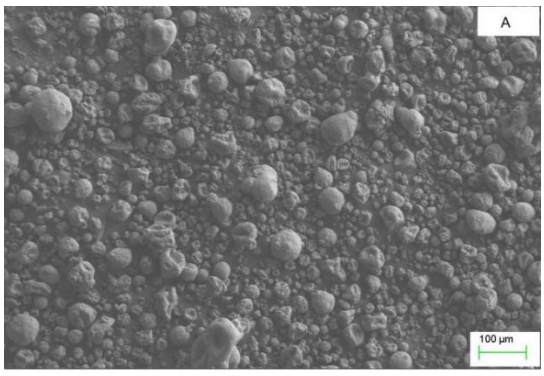

Chlorella x 100

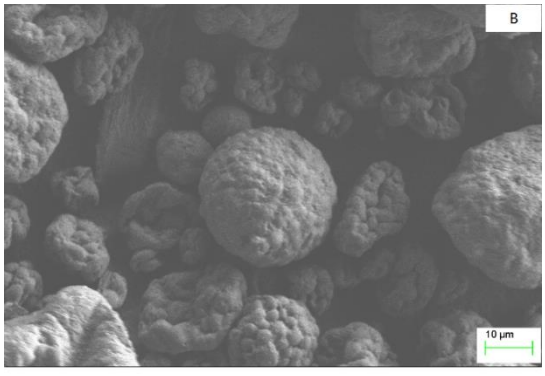

Chlorella x 1000

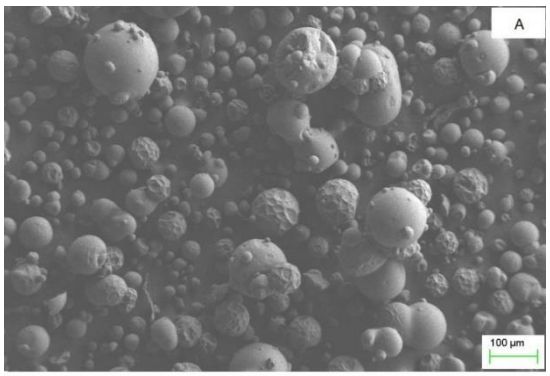

Dunaliella x 100

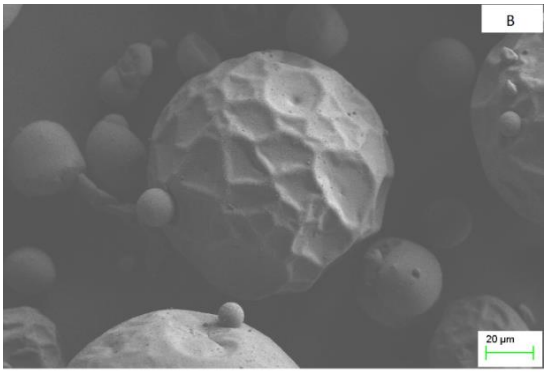

Dunaliella x 1000

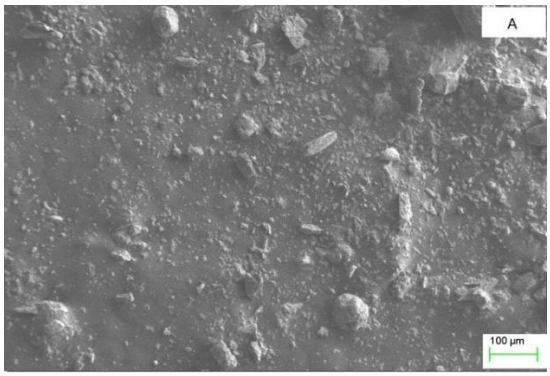

Laminaria x 100

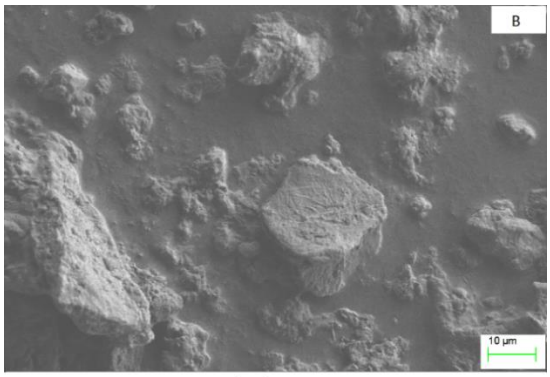

Laminaria x 1000

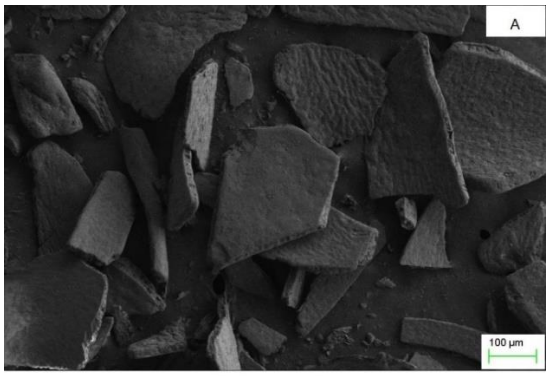

Porphyra x 100

Porphyra x 1000

Cellulose X 100

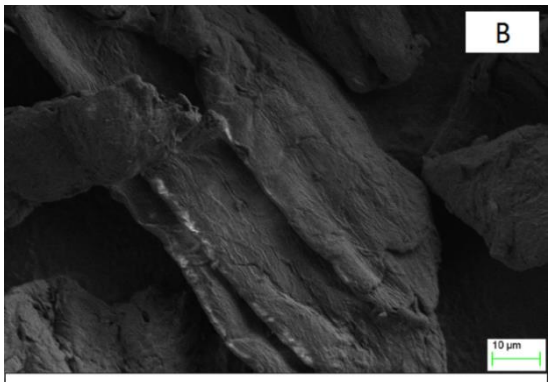

Cellulose X 1000

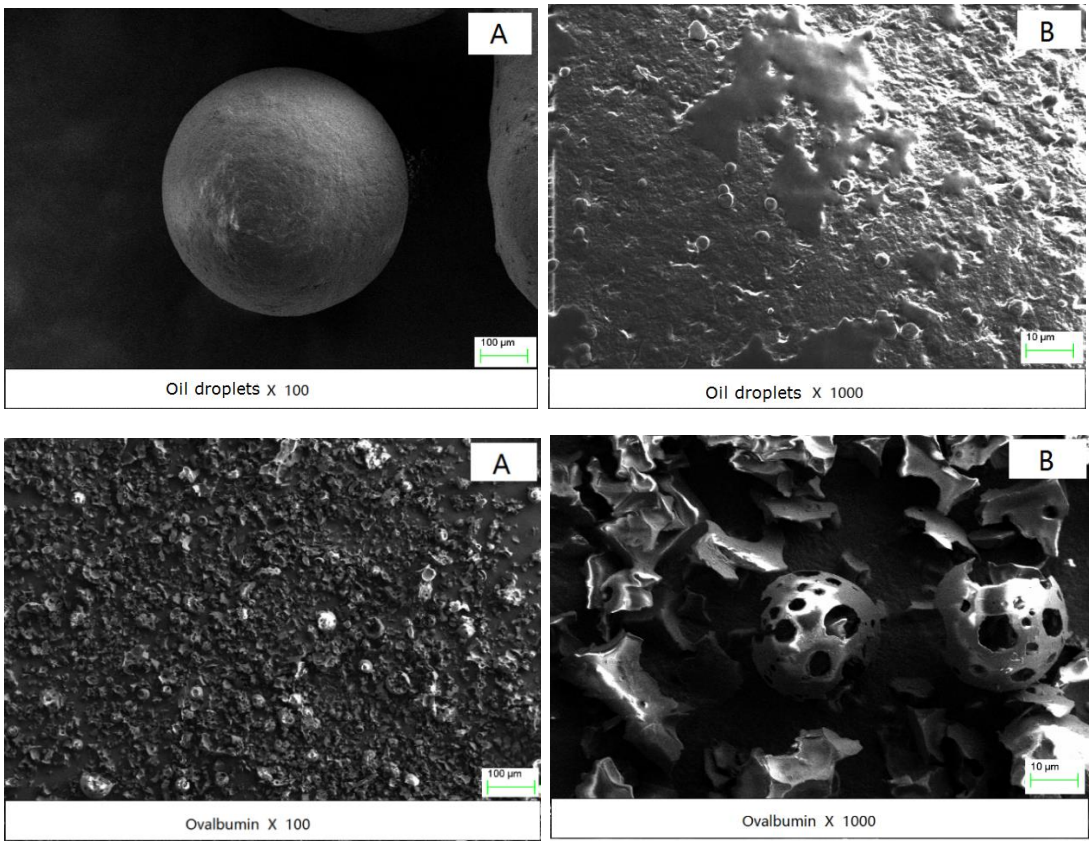

Figure 4-1 SEM images of five algae with magnification of A x 100 and B x 1000

4.8 Algal ash characterization

The five algae ash samples are prepared by using a muffle furnace and characterized using SEM, BET and XRF. To investigate the morphology of ash samples in powder (A x 100, B x 1000) and block (C x 100, D x 1000) states, SEM was used which is shown in **Figure 4-2** to **Figure 4-6**. The portion on the top, which was fully exposed to air and under high temperature, could combust at first and form into ash. The algae underneath the top layer, would be separated from air and pyrolyze in inert atmosphere. Therefore, compared with the powdered ash, the ash samples in blocks contained relatively higher level of carbon and they also have been characterized

separately from powder ash samples. Meanwhile, the minerals in biomass can potentially act as catalysts and lead to synergetic effects on biomass pyrolysis process.

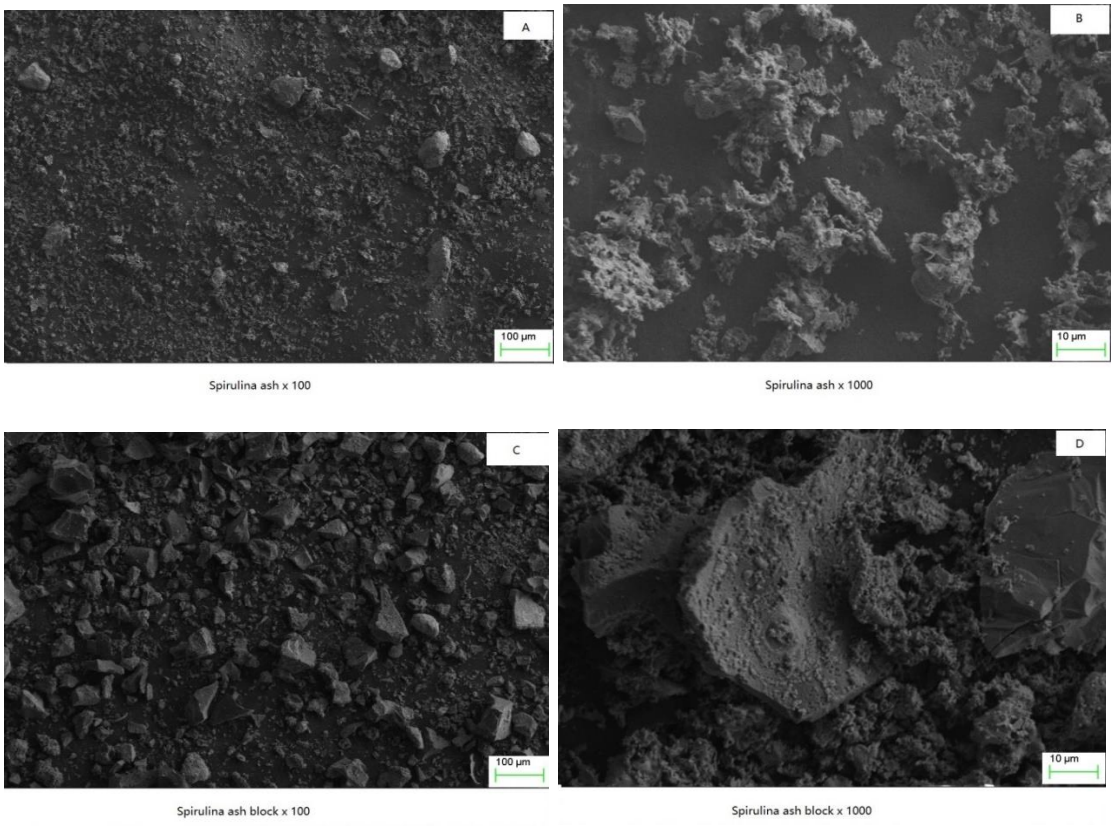

Figure 4-2 SEM images of spirulina ash and spirulina ash in blocks

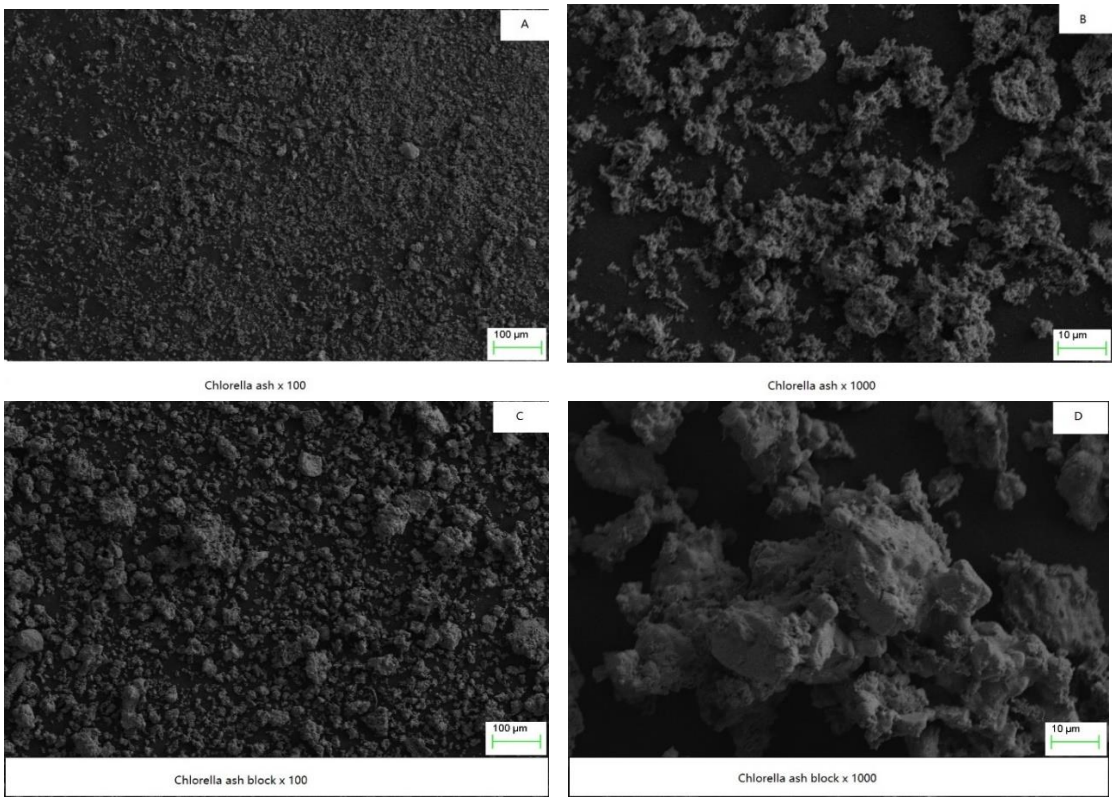

Figure 4-3 SEM images of chlorella ash and chlorella ash in blocks

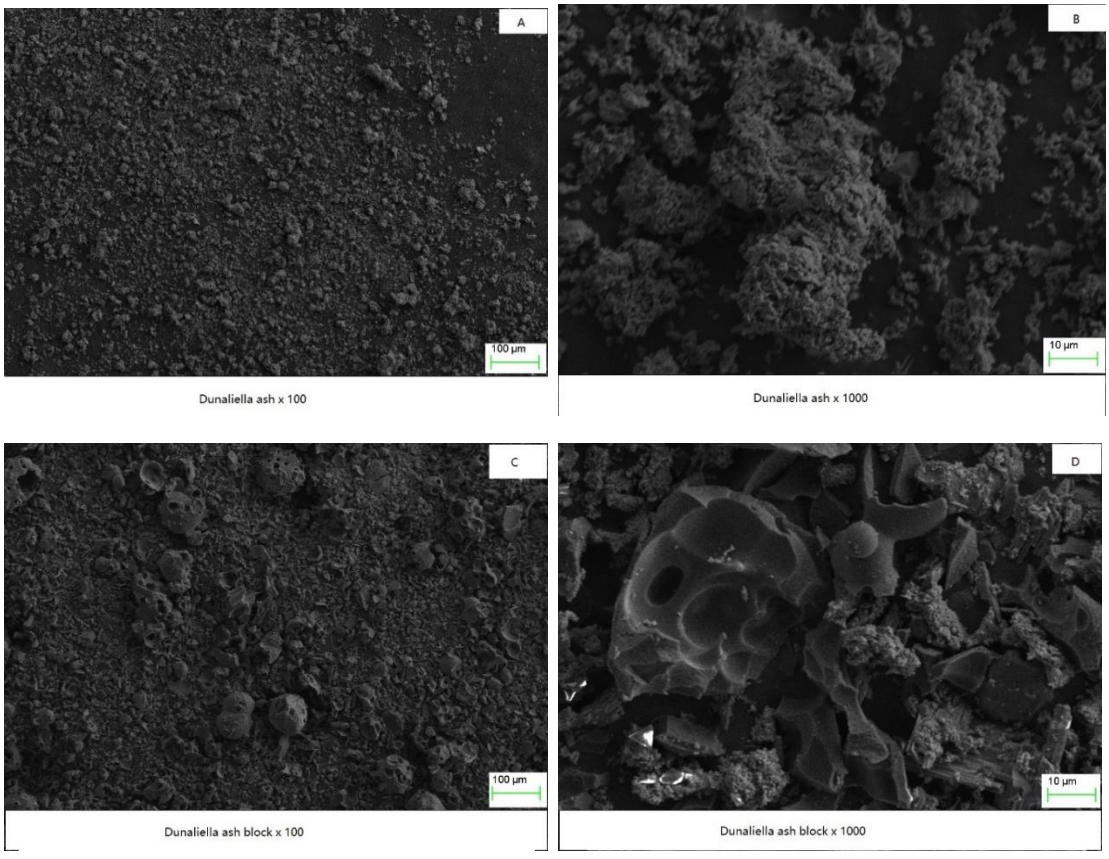

Figure 4-4 SEM images of dunaliella ash and dunaliella ash in blocks

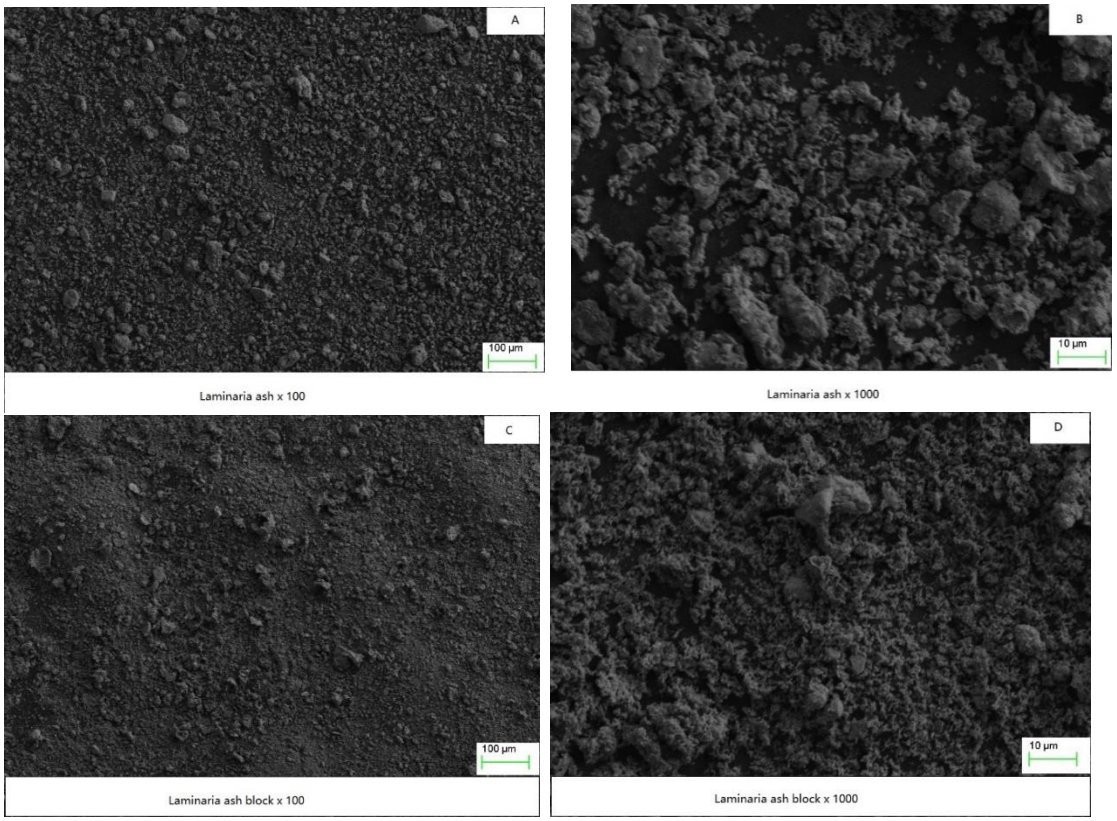

Figure 4-5 SEM images of laminaria ash and laminaria ash in blocks

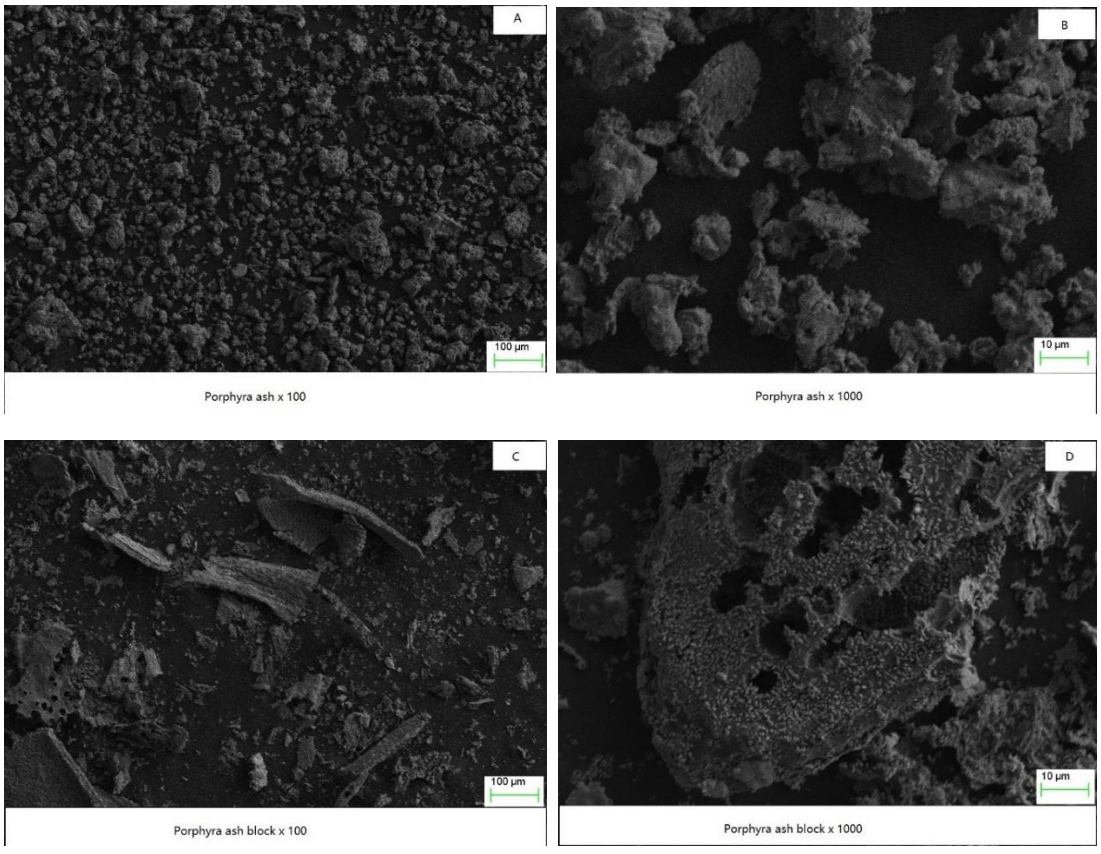

Figure 4-6 SEM images of porphyra ash and porphyra ash in blocks

Table 4-7 shows the surface area, pore volume and pore size of ash in both block and powder. Blocky ash has larger surface area and pore volume, but smaller pore size, except chlorella ash. Massive dunaliella ash powder has extremely high surface area and pore volume (323.61 m^2/g and 126.26 mm^3/g respectively).

Table 4-7 Physical properties of ash in block and powder

	BET Surface area(m^2/g)	T-Plot micropore volume (mm^3/g)	Adsorption average pore width (nm)
Spirulina ash powder	1.9	0.1	2.3
Spirulina ash block	22.9	6.6	2.0
Chlorella ash powder	5.3	-0.1	11.0
Chlorella ash block	2.1	-0.8	3.6
Dunaliella ash powder	7.3	-1.4	14.5
Dunaliella ash block	323.6	126.3	2.3
Laminaria ash powder	0.5	0.6	/
Laminaria ash block	12.8	3.1	0.4
Porphyra ash powder	1.9	-0.1	7.2
Porphyra ash block	4.8	-1.1	2.1

Table 4-8 shows minerals of the five algae ash samples, mostly in the form of mineral oxides in both powder and block states. Some of these minerals can perform as catalysts, such as, CaO, MgO, Al_2O_3, Fe_2O_3, TiO_2, Na_2O, whilst others are inert. Some even contribute to negative catalysis. Spirulina in both forms was rich in P_2O_5, K_2O and CaO, while K_2O, SO_3, P_2O_5 were the most abundant components in

porphyra. Three major components in both chlorella and laminaria ash were Cl, CaO and P_2O_5. Dunaliella massive ash contains 46.5 wt.% of P_2O_5, followed by SiO_2 and CaO, while powdered dunaliella ash had plenty amount of CaO (33.8 wt.%), SiO_2 and Cl.

Table 4-8 XRF analysis of powder and block algae ash samples (wt.%)

	Na_2O	MgO	Al_2O_3	SiO_2	P_2O_5	SO_3	Cl	K_2O	CaO	TiO_2	Cr_2O_3	MnO	Fe_2O_3	SrO	Sb_2O_3
spirulina ash powder	nd	1.6	nd	5.0	34.1	1.7	5.0	28.8	14.1	0.3	nd	0.3	7.6	0.3	1.1
spirulina ash block	nd	2.3	0.7	3.9	28.9	1.8	7.3	29.7	15.1	0.6	0.1	0.3	8.1	0.4	0.8
chlorella ash powder	nd	1.7	nd	1.8	24.4	6.5	16.5	9.3	27.0	0.2	0.0	0.3	10.3	0.9	0.9
chlorella ash block	nd	0.2	nd	1.6	1.5	3.5	76.1	3.5	11.8	nd	0.2	0.0	0.7	0.7	nd
Dunaliella ash powder	6.7	nd	0.6	29.1	nd	2.2	13.5	11.1	33.8	0.5	0.1	0.3	0.8	0.2	nd
Dunaliella ash block	nd	nd	nd	29.3	46.5	nd	nd	nd	13.1	nd	0.8	0.2	0.7	nd	9.0
Laminaria ash powder	0.5	0.8	0.1	1.3	1.3	3.4	76.5	3.6	10.9	nd	0.1	0.0	0.5	0.7	nd
Laminaria ash block	nd	0.9	nd	1.6	20.4	4.9	21.7	9.3	27.3	0.2	0.1	0.4	11.7	0.9	0.3
Porphyra ash powder	nd	0.7	nd	2.4	10.9	26.7	7.4	44.7	4.1	nd	nd	0.1	1.0	0.0	1.4
Porphyra ash block	nd	1.0	0.3	1.3	9.3	23.5	11.0	47.0	4.3	nd	0.1	0.1	1.2	0.1	0.2

nd – not detected

4.9 Summary

The major characteristics of the five algae and three model compounds have been summarized in this chapter, which would assist in the selection of feedstock, as well as comprehending thermal behaviours of samples. The proximate analysis indicated dunaliella has the highest amount of volatiles among the five algae with rare ash content, which represents its great potential to pyrolyze into gaseous and oil products, while less char output. According to the intrinsic analysis, the combustion characteristics of each sample were studied, which showed the influence of lipid, carbohydrate and protein content on featured temperatures and LHVs. Porphyra is the last to be fully decomposed and has the highest LHV. Moreover, the C, H, N, S and O composition of samples were determined by ultimate analysis. With higher C and H content, the sample is anticipated to be more reactive, while lower S and N content lead to less emission of SO_x and NO_x. Microalgae have relatively higher C and H content; thus, the HHVs of microalgae are much higher than those of macroalgae, on the basis of heating value assessment. The characterization of algal ash indicates their morphology, compositions, surface area and porosity, which could attribute to the selection of ash catalysts applied in pyrolysis of algae in the following session. The effective composition of ash which have been determined, would contribute to the pyrolysis process.

Chapter 5. Kinetic study of the pyrolysis of algae under nitrogen and carbon dioxide atmosphere

In this chapter, kinetics of the pyrolysis of the three representative algae (microalgae- spirulina and chlorella; macroalgae- porphyra) under N_2 and CO_2 atmosphere are conducted together with the pyrolysis of the three model components, carbohydrate, lipid and protein. Firstly, the thermogravimetric characteristics of samples are explored by analyzing the TG and DTG profiles. Iso-conversional method, Kissinger- Akahira-Sunose (KAS) is applied to derive the activation energy (E_a) and pre-exponential factor (A). Furthermore, the model fitting method (Coats-Redfern) is used to obtain reaction mechanism as well as other kinetic parameters. The parameters and EDS analysis of the composition of char obtained under N_2 and CO_2 atmosphere are compared, together with the morphology and compositions of solid residue from SEM/EDS.

5.1 Thermogravimetric analysis

The TG and DTG curves derived from non-isothermal pyrolysis of three representative algae (microalgae- spirulina and chlorella; macroalgae- porphyra) and three algal model compounds under N_2 and CO_2 atmosphere at heating rates of 5, 10, 20 and 50 °C min^{-1} were presented in **Figure 5-1** and **Figure 5-2**. Although the heating rates were different, the TG curves were analogous with similar initial and final temperatures. However, the peak value of DTG curve shifted

to high temperature zone as the heating rate increasing and reached its maximum at 50 °C min^{-1}. Because the higher heating rate would extend the temperature gradient of reactants, which resulted in the thermal lag between theoretical and experimental temperatures [226]. This phenomenon means that to obtain same level of weight loss rate, the pyrolysis temperature would be higher as the heating rate increasing.

Figure 5-1 and **Figure 5-2** showed that the degradation trends of six samples were similar with three stages, involving dehydration, volatilization and carbonization under both N_2 and CO_2 atmosphere. The first stage started from ambient temperature to the temperature where light volatiles began to release, during which the moisture in biomass evaporated around 105 °C. Although only slight weight loss has been observed during this stage, the structure of algal cells has changed. A major weight loss was observed in the second stage ranging from 150 to 500 °C, primarily due to the devolatilization of organic matters. This period was regarded as the main pyrolysis stage. The third stage (500-800 °C) showed a steady weight loss which resulted from the decomposition of non-volatile carbonaceous residues and finally formed char while CO_2 and CO vaporized.

Primary pyrolysis parameters including Y_{char}, the weight percentage of char residue; T_i, the initial temperature when volatile matters start to release; D_m, the maximum weight loss rate; T_m, the peak

temperature; $\Delta T_{1/2}$, the half peak width temperature; r, the volatile release index, r= D_m/ (T_i T_m $\Delta T_{1/2}$) have been summarized in **Table 5-1** and **Table 5-2** (N_2 and CO_2), which were derived from TG and DTG curves (**Figure 5-1** and **Figure 5-2**). From **Table 5-1**, the char residue of spirulina, chlorella, porphyra, oil droplets, cellulose and ovalbumin after pyrolysis remained almost the same under N_2 at the four different heating rates (26.7, 22.1, 23.5, 0.6, 5.8, 12.7 wt.% respectively). However, when the carrier gas was changed to CO_2, the amount of char from pyrolysis of all six samples increased gradually as the rising of heating rate, which is generally known that lower heating rate resulted in longer processing time for carbon gasification with CO_2. The volatiles and ash content in sample have significant influence on the pyrolysis performance. Higher ash content in spirulina, chlorella and ovalbumin reduced T_m and larger volatiles in oil droplets and cellulose increased D_m. Due to the thermal lag, the values of D_m, T_m and T_i increased as the heating rate getting larger in both atmosphere. The larger heating rate could reduce the reaction time and postponed the pyrolysis. The volatile release index, r, described the effect of pyrolysis and that value showed similar trend which means more sufficient pyrolysis is conducted as the heating rate grows. The r values of porphyra, oil droplets and cellulose obtained under CO_2 are larger than those under N_2 which indicated CO_2 assisted in the pyrolysis of algae, while others remained almost the same value under two atmospheres.

Table 5-1 Thermogravimetric features of pyrolysis of spirulina, chlorella, porphyra, cellulose, ovalbumin and oil droplets under N_2

Sample	β (°C min^{-1})	5	10	20	50
Spirulina	Y_{char} (%)	25.3	25.8	26.2	29.5
	T_i (°C)	225	235	243	255
	T_m (°C)	300	310	322	338
	D_m (%min^{-1})	-2.9	-5.8	-11.5	-27.6
	$\Delta T_{1/2}$(°C)	125	146	169	192
	r ($\times 10^{-7}$%min^{-1}°C^{-3})	-3.4	-5.5	-8.7	-16.7
Chlorella	Y_{char} (%)	21.2	21.4	20.4	25.3
	T_i (°C)	212	220	228	233
	T_m (°C)	316	277	330	354
	D_m (%min^{-1})	-2.1	-4.1	-8.5	-19.2
	$\Delta T_{1/2}$(°C)	169	135	213	216
	r ($\times 10^{-7}$%min^{-1}°C^{-3})	-1.9	-5.0	-5.3	-10.8
Porphyra	Y_{char} (%)	27.8	25.8	15.8	24.7
	T_i (°C)	227	236	245	254
	T_m (°C)	263	274	283	293
	D_m (%min^{-1})	-2.9	-6.2	-13.0	-29.1
	$\Delta T_{1/2}$(°C)	83	98	134	153
	r ($\times 10^{-7}$%min^{-1}°C^{-3})	-5.9	-9.8	-14.0	-25.6
Oil droplets	Y_{char} (%)	0.4	0.5	0.6	0.7
	T_i (°C)	240	255	261	274
	T_m (°C)	410	422	437	455
	D_m (%min^{-1})	-13.5	-25.9	-53.0	-114.2
	$\Delta T_{1/2}$(°C)	91	106	114	135
	r ($\times 10^{-7}$%min^{-1}°C^{-3})	-15.0	-22.7	-40.8	-67.8
Cellulose	Y_{char} (%)	5.1	5.8	4.5	7.8
	T_i (°C)	299	309	319	330
	T_m (°C)	326	338	349	364
	D_m (%min^{-1})	-13.6	-25.2	-47.4	-100.1

	$\Delta T_{1/2}$(°C)	67	85	125	176
	r ($\times 10^{-7}$%min^{-1}°C^{-3})	-20.8	-28.4	-34.1	-47.3
Ovalbumin	Y_{char} (%)	11.8	11.8	9.5	17.6
	T_i (°C)	186	193	197	208
	T_m (°C)	219	228	232	242
	D_m (%min^{-1})	-2.3	-4.7	-9.7	-23.9
	$\Delta T_{1/2}$(°C)	78	92	123	137
	r ($\times 10^{-7}$%min^{-1}°C^{-3})	-7.2	-11.6	-17.3	-34.7

* Y_{char} is the weight percentage of char residue; T_i is the initial temperature when volatile matters start to release at conversion rate of 5%; D_m is the maximum weight loss rate; T_m is the corresponding peak temperature; $\Delta T_{1/2}$ is the half peak width temperature; r is the volatile release index, r= D_m/ (T_i T_m $\Delta T_{1/2}$).

Table 5-2 Thermogravimetric features of pyrolysis of spirulina, chlorella, porphyra, cellulose, ovalbumin and oil droplets under CO_2

Sample	**β (°C min^{-1})**	**5**	**10**	**20**	**50**
Spirulina	Y_{char} (%)	12.1	19.0	25.7	29.3
	T_i (°C)	227	236	243	254
	T_m (°C)	296	306	322	337
	D_m (%min^{-1})	-2.8	-5.8	-10.9	-24.8
	$\Delta T_{1/2}$(°C)	131	143	178	194
	r ($\times 10^{-7}$%min^{-1}°C^{-3})	-3.2	-5.6	-7.8	-14.9
Chlorella	Y_{char} (%)	13.7	21.3	22.8	25.0
	T_i (°C)	198	218	224	235
	T_m (°C)	262	272	282	353
	D_m (%min^{-1})	-2.1	-4.0	-7.8	-19.3
	$\Delta T_{1/2}$(°C)	138	132	147	213
	r ($\times 10^{-7}$%min^{-1}°C^{-3})	-2.9	-5.1	-8.4	-10.9
Porphyra	Y_{char} (%)	7.6	8.5	12.8	20.6
	T_i (°C)	227	240	249	258
	T_m (°C)	261	272	282	294
	D_m (%min^{-1})	-3.0	-6.2	-12.8	-29.2
	$\Delta T_{1/2}$(°C)	83	93	132	118

	r ($\times 10^{-7}$%min^{-1}°C^{-3})	-6.1	-10.2	-13.8	-32.6
Oil droplets	Y_{char} (%)	0.2	0.5	0.7	0.8
	T_i (°C)	209	223	226	233
	T_m (°C)	410	423	435	449
	D_m (%min^{-1})	-13.1	-25.7	-51.4	-115.0
	$\Delta T_{1/2}$(°C)	108	119	115	107
	r ($\times 10^{-7}$%min^{-1}°C^{-3})	-14.2	-22.9	-45.5	-102.7
Cellulose	Y_{char} (%)	4.8	7.9	8.0	8.5
	T_i (°C)	297	289	318	330
	T_m (°C)	325	338	350	364
	D_m (%min^{-1})	-13.9	-25.5	-47.8	-101.5
	$\Delta T_{1/2}$(°C)	67	81	90	143
	r ($\times 10^{-7}$%min^{-1}°C^{-3})	-21.5	-32.2	-47.7	-59.1
Ovalbumin	Y_{char} (%)	0.4	1.3	6.2	16.3
	T_i (°C)	187	197	202	214
	T_m (°C)	216	224	231	245
	D_m (%min^{-1})	-2.3	-4.4	-9.0	-25.1
	$\Delta T_{1/2}$(°C)	87	93	98	140
	r ($\times 10^{-7}$%min^{-1}°C^{-3})	-6.5	-10.7	-19.7	-34.2

* Y_{char} is the weight percentage of char residue; T_i is the initial temperature when volatile matters start to release at conversion rate of 5%; D_m is the maximum weight loss rate; T_m is the corresponding peak temperature; $\Delta T_{1/2}$ is the half peak width temperature; r is the volatile release index, $r= D_m/ (T_i T_m \Delta T_{1/2})$.

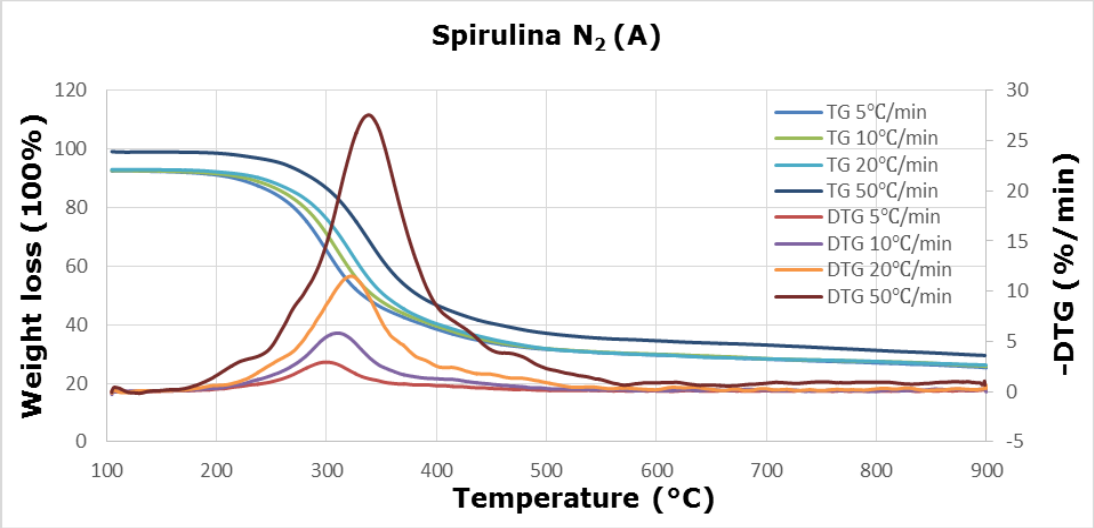
Spirulina N2 (A)
Weight loss (100%)
-DTG (%/min)
Temperature (°C)
TG 5°C/min
TG 10°C/min
TG 20°C/min
TG 50°C/min
DTG 5°C/min
DTG 10°C/min
DTG 20°C/min
DTG 50°C/min

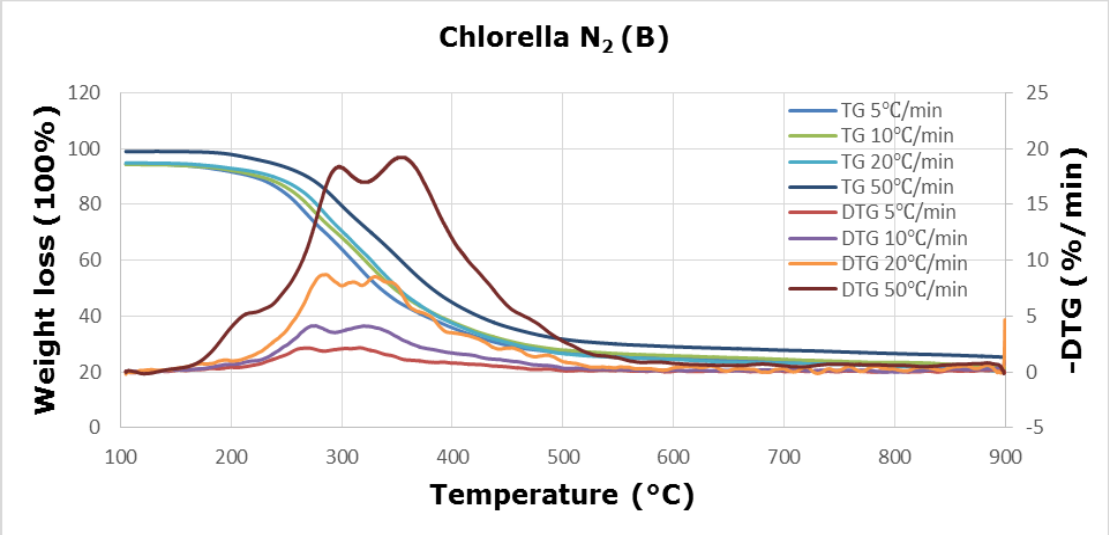
Chlorella N2 (B)
Weight loss (100%)
-DTG (%/min)
Temperature (°C)
TG 5°C/min
TG 10°C/min
TG 20°C/min
TG 50°C/min
DTG 5°C/min
DTG 10°C/min
DTG 20°C/min
DTG 50°C/min

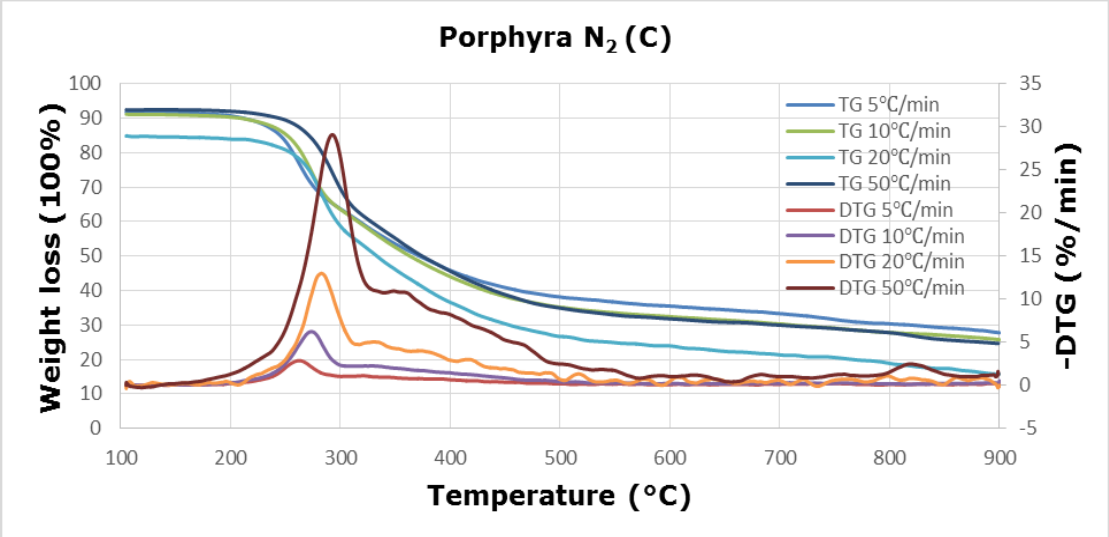
Porphyra N2 (C)
Weight loss (100%)
-DTG (%/min)
Temperature (°C)
TG 5°C/min
TG 10°C/min
TG 20°C/min
TG 50°C/min
DTG 5°C/min
DTG 10°C/min
DTG 20°C/min
DTG 50°C/min

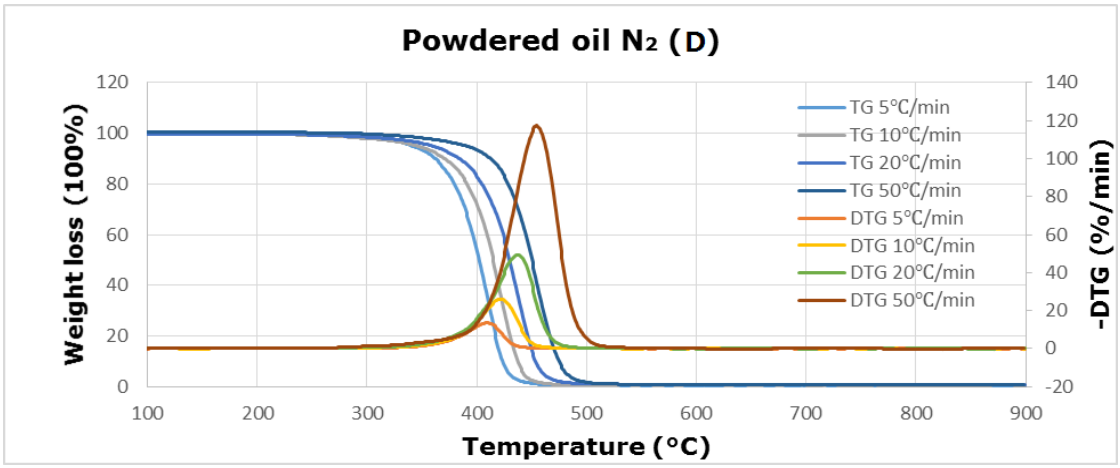

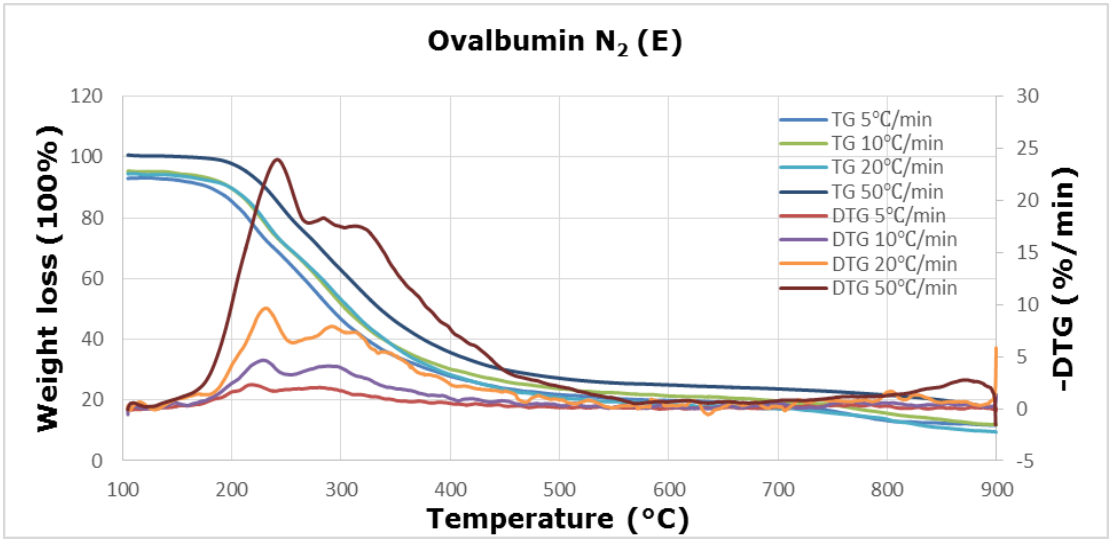

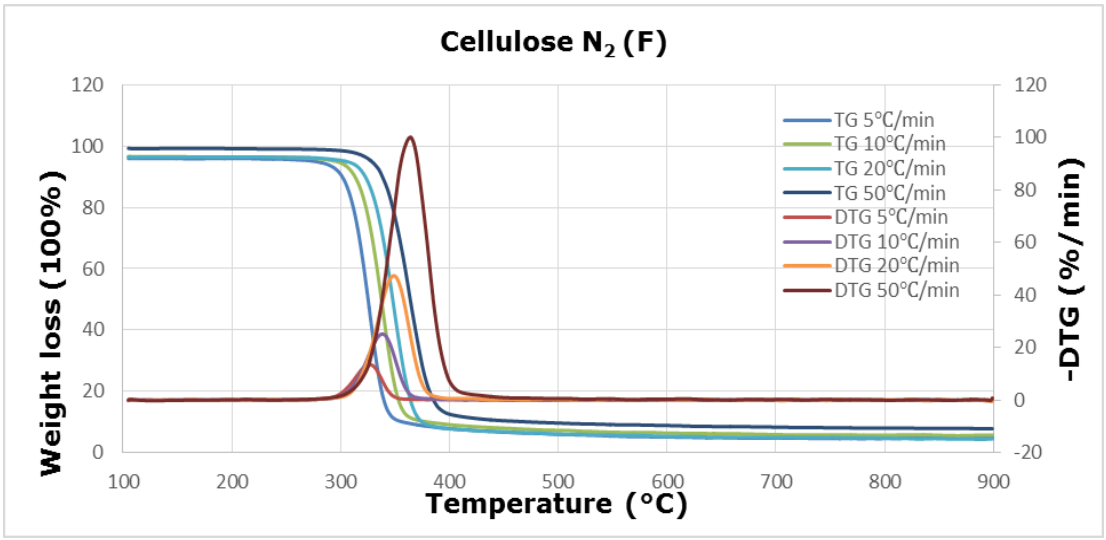

Figure 5-1 TG and DTG curves of the pyrolysis of spirulina (A), chlorella (B), porphyra (C), oil droplets (D), ovalbumin (E), and cellulose (F) under N_2 at different heating rates of 5, 10, 20, and 50°C /min

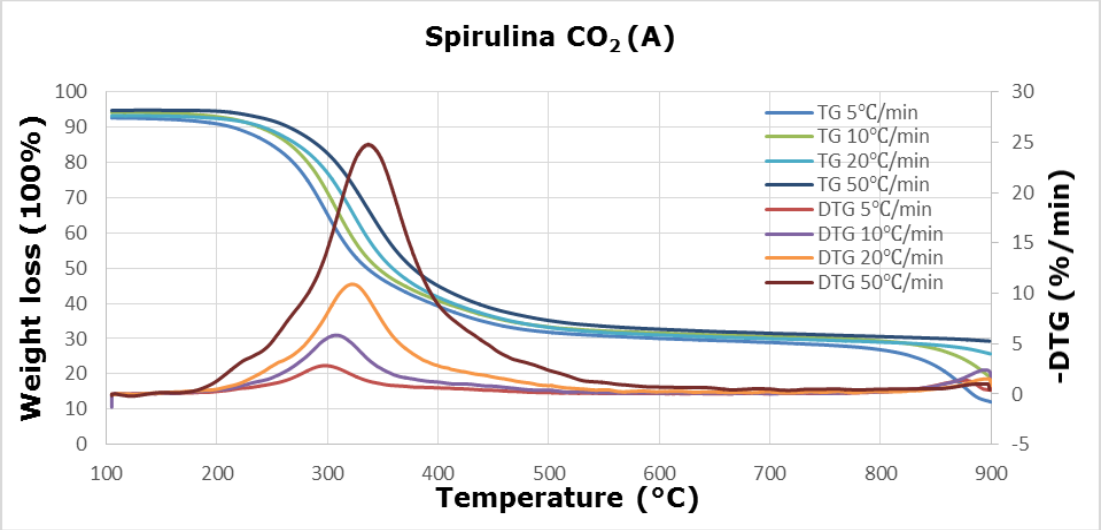
Spirulina CO_2 (A)
Weight loss (100%)
-DTG (%/min)
Temperature (°C)
TG 5°C/min
TG 10°C/min
TG 20°C/min
TG 50°C/min
DTG 5°C/min
DTG 10°C/min
DTG 20°C/min
DTG 50°C/min

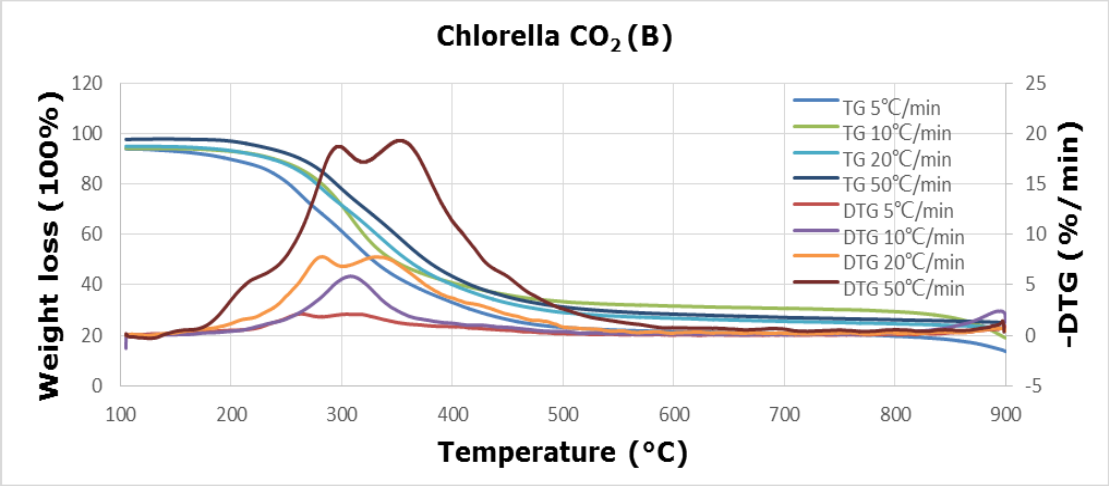
Chlorella CO_2 (B)
Weight loss (100%)
-DTG (%/min)
Temperature (°C)
TG 5°C/min
TG 10°C/min
TG 20°C/min
TG 50°C/min
DTG 5°C/min
DTG 10°C/min
DTG 20°C/min
DTG 50°C/min

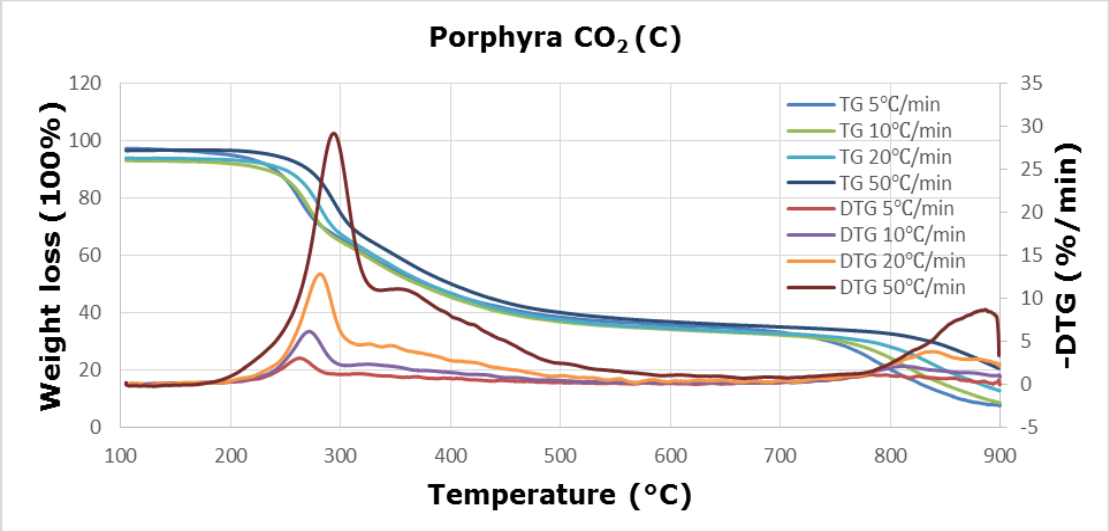
Porphyra CO_2 (C)
Weight loss (100%)
-DTG (%/min)
Temperature (°C)
TG 5°C/min
TG 10°C/min
TG 20°C/min
TG 50°C/min
DTG 5°C/min
DTG 10°C/min
DTG 20°C/min
DTG 50°C/min

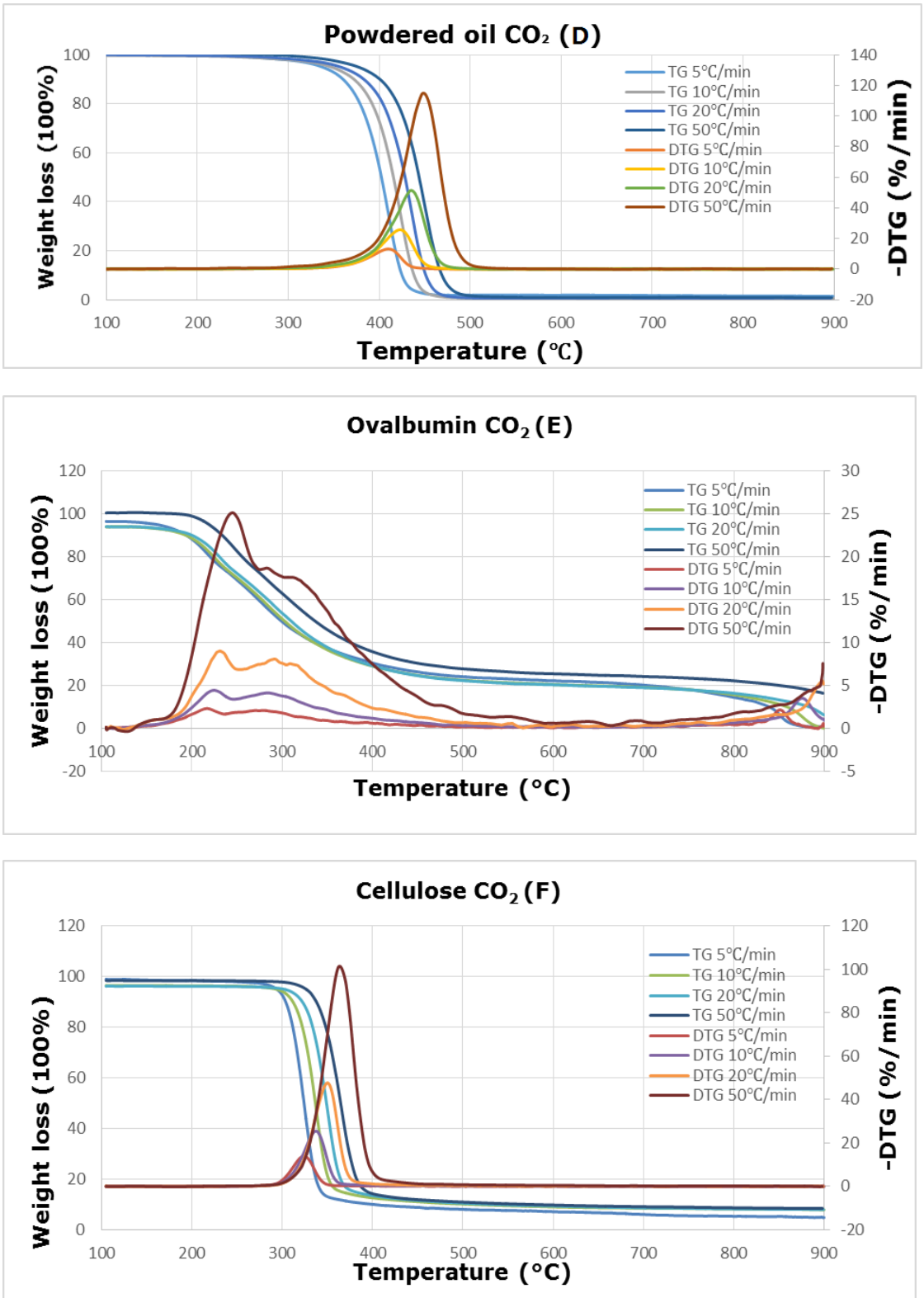

Figure 5-2 TG and DTG curves of the pyrolysis of spirulina (A), chlorella (B), porphyra (C), oil droplets (D), ovalbumin (E), and cellulose (F) under CO_2 at different heating rates of 5, 10, 20, and 50°C /min

Table 5-3 Start and end temperature, start and end time, and pyrolysis time of samples under N_2 at different heating rates of 5, 10, 20, and 50°C /min.

Sample	β (°C min^{-1})	5	10	20	50
Spirulina	Start temperature (°C)	181	167	172	188
	End Temperature (°C)	498	622	582	645
	Start time (min)	56.2	41.8	36.1	32.7
	End time (min)	119.6	87.3	56.6	41.9
	Pyrolysis time (min)	63.4	45.5	20.5	9.2
Chlorella	Start temperature (°C)	123	135	146	159
	End Temperature (°C)	570	541	653	753
	Start time (min)	34.7	38.5	34.8	32.3
	End time (min)	134.1	79.1	60.2	44.1
	Pyrolysis time (min)	99.4	40.6	25.4	11.8
Porphyra	Start temperature (°C)	181	159	173	194
	End Temperature (°C)	547	634	638	648
	Start time (min)	56.1	40.9	36.2	32.9
	End time (min)	129.4	88.4	59.9	42.0
	Pyrolysis time (min)	73.3	47.5	23.7	9.1
Oil droplets	Start temperature (°C)	273	199	195	113
	End Temperature (°C)	464	484	549	594
	Start time (min)	74.6	44.9	37.2	31.5
	End time (min)	112.7	73.4	55.0	40.9
	Pyrolysis time (min)	38.1	28.5	17.8	9.4
Cellulose	Start temperature (°C)	247	265	243	264
	End Temperature (°C)	434	475	613	614
	Start time (min)	69.5	51.5	39.7	34.2
	End time (min)	106.9	72.5	58.2	41.3
	Pyrolysis time (min)	37.4	21.0	18.5	7.1
Ovalbumin	Start temperature (°C)	132	123	135	183
	End Temperature (°C)	503	597	547	629
	Start time (min)	46.5	37.6	34.6	32.6
	End time (min)	120.8	85.8	54.9	41.6
	Pyrolysis time (min)	74.3	48.2	20.3	9.0

Table 5-4 Start and end temperature, start and end time, and pyrolysis time of samples under CO_2 at different heating rates of 5, 10, 20, and 50°C /min.

Sample	β (°C min^{-1})	5	10	20	50
Spirulina	Start temperature (°C)	165	163	144	143
	End Temperature (°C)	522	634	577	665
	Start time (min)	53.1	41.3	34.9	32.3
	End time (min)	115.2	84.2	54.9	40.0
	Pyrolysis time (min)	62.1	42.9	20.0	7.7
Chlorella	Start temperature (°C)	124	140	135	140
	End Temperature (°C)	522	625	597	771
	Start time (min)	44.8	39.0	34.6	32.3
	End time (min)	124.5	87.5	57.4	43.3
	Pyrolysis time (min)	79.7	48.5	22.8	11.0
Porphyra	Start temperature (°C)	129	170	150	175
	End Temperature (°C)	555	570	567	707
	Start time (min)	45.9	42.0	35.1	32.8
	End time (min)	112.3	82.1	55.9	41.7
	Pyrolysis time (min)	66.4	40.1	20.8	8.9
Oil droplets	Start temperature (°C)	236	216	207	121
	End Temperature (°C)	463	495	509	595
	Start time (min)	67.2	46.7	37.9	31.7
	End time (min)	112.6	79.4	59.1	42.1
	Pyrolysis time (min)	45.4	32.7	21.2	10.4
Cellulose	Start temperature (°C)	258	257	260	221
	End Temperature (°C)	428	549	543	721
	Start time (min)	71.6	50.7	40.5	33.5
	End time (min)	105.7	79.9	54.7	43.4
	Pyrolysis time (min)	34.1	29.2	14.2	9.9
Ovalbumin	Start temperature (°C)	129	131	133	138
	End Temperature (°C)	517	607	564	665
	Start time (min)	45.9	38.2	34.5	32.2
	End time (min)	115.8	78.5	50.7	40.3
	Pyrolysis time (min)	69.9	40.3	16.2	8.1

5.2 Kinetic study

5.2.1 Determination of activation energy via Kissinger-Akahira-Sunose Method (KAS)

Among the three stages of pyrolysis, the second stage-evolatilization was worthwhile investigation, since it is regarded as the major step in algae decomposition. Based on the start and end temperature (**Table 5-3** and **Table 5-4**), under both atmospheres, ovalbumin firstly decomposed around 120°C and pyrolyzed until 600°C where the weight loss rate was nearly zero, followed by cellulose (250 - 500°C). Then oil droplets was the last to initiate its pyrolysis at 300°C and finish around 550°. The three algae samples started the pyrolysis from 120°C until the temperature reached 650°C. Therefore, after considering all six samples pyrolysis, temperature range of applying KAS method was selected as 120 to 650°C, which included the temperatures of the whole conversion process.

Table 5-5 and Table 5-6 showed the activation energy and correlation factor of the pyrolysis of the six samples under N_2 and CO_2 at conversion rate of 5 to 95% respectively. At the beginning of pyrolysis, cellulose showed the highest activation energy amongst the three model compounds, which was corresponding to the T_i values order in TG analysis. During the major weight loss stage, the activation energy of cellulose decreased steadily from 200 to 170 kJ/mol, while oil droplets increased gradually and fluctuated around

180 kJ/mol. However, the activation energy of spirulina, chlorella, porphyra and ovalbumin were gradually increasing from around 160, 200, 180 and 190 kJ/mol, then surged up to 340, 400, 550 and 330 kJ/mol after 300 °C.

Since the pyrolysis carried out by TGA is a fixed bed reaction, and the feed into the bed gradually reduces as the pyrolysis progressing. Thus, the results calculated when the conversion rate beyond 80% are inaccurate. Overall, during the pyrolysis, the activation energy derived via KAS method can be deployed for analysis. **Table 5-5** show the activation energy obtained from KAS method at different conversion rates under N_2 atmosphere for the pyrolysis of three algae and three algal model compounds. For pyrolysis under N_2 atmosphere, the activation energy of oil droplets gradually increased from 123 to 175 kJ mol^{-1} ($5\% < \alpha < 45\%$) and fluctuated around 183 kJ mol^{-1}. Contrary trend has been found in the pyrolysis of cellulose under N_2 atmosphere, where the activation energy decreased progressively from 202 to 170 kJ mol^{-1} in the pyrolysis process ($5\% < \alpha < 90\%$). But it surged to 200 kJ mol^{-1} in the end of pyrolysis at the conversion of 95%. The routine for decomposition of ovalbumin has increasing activation energy from 188 to 230 kJ mol^{-1} ($5\% < \alpha < 25\%$). Then the value rose slightly to 240 kJ mol^{-1} ($30\% < \alpha < 60\%$) and rocketed to 330 kJ mol^{-1} ($\alpha = 75\%$). However, the energy value reduced significantly until below zero, which means the depletion of reactants

in TGA. For spirulina pyrolysis under N_2, the activation energy grew from 160 to 180 kJ mol^{-1} ($5\% < \alpha < 15\%$) and increased steadily to 190 kJ mol^{-1} ($20\% < \alpha < 50\%$), after which the value surged to 335 kJ mol^{-1} ($55\% < \alpha < 80\%$). Similar to ovalbumin pyrolysis, the activation energy then decreased dramatically about to zero, which represented the exhaustion of raw materials after the conversion rate of 85%. The activation energy profile of chlorella showed similar trend as spirulina with steady increase from 206 to 215 kJ mol^{-1} ($5\% < \alpha < 60\%$). But rapid growth of E_a occurred after conversion rate of 65% to 395 kJ mol^{-1}, followed by significant drop to below zero. As other two algae, E_a of porphyra pyrolysis increased gradually from 178 to 200 kJ mol^{-1} ($5\% < \alpha < 25\%$) but started to surge until 550 kJ mol^{-1}(α=75%), then reduced to less than zero.

When the carrier gas changed to CO_2, the required energy to activate the pyrolysis for different samples are various as **Table 5-6** indicated. The activation energy of oil droplets decomposition increased slightly from 157 to 209.5 kJ mol^{-1} ($5\% < \alpha < 95\%$), which required 5.3-27.5% more energy to pyrolyze the oil droplets with CO_2 carrier gas. For pyrolysis of cellulose, the activation energy decreased from 188 to 170 kJ mol^{-1} ($5\% < \alpha < 40\%$) while maintained around 172 kJ mol^{-1} ($45\% < \alpha < 85\%$), then surged to 343 kJ mol^{-1} ($\alpha = 95\%$). Slight reduced amount of activation energy (1.5-7.4% lower) is required for pyrolysis of cellulose under CO_2, in comparison with the energy

calculated using N_2 as carrier gas. However, the activation energy distribution of ovalbumin under CO_2 indicated a different pattern, which is much higher than E_a under N_2. The energy required surged from 149 to 572 kJ mol^{-1} ($5\% < \alpha < 50\%$), after which the activation energy declined to lower than zero. This indicates although the pyrolysis of ovalbumin under CO_2 was much difficult to carry out, the pyrolysis process finished ahead, compared with N_2 as carrier gas. Since spirulina has a protein content of 57.8 wt. %, the alternation of activation energy for the pyrolysis of this algae followed a similar trend as shown in ovalbumin. The value increased at initial stage from 178 to 317 kJ mol^{-1} ($5\% < \alpha < 55\%$), which required higher activation energy during pyrolysis compared to N_2 as carrier gas but ended earlier (2.1-16.3% time ahead). It is similar for the activation energy of porphyra pyrolysis, which surged from 152 to 723 kJ mol^{-1} ($5\% < \alpha < 35\%$), but became smaller until less than zero ($40\% < \alpha < 95\%$), after the depletion of reactants in fixed bed. For chlorella, the energy to activate was comparably lower than E_a under N_2 ($5\% < \alpha < 25\%$), but grew slightly larger after that. The pyrolysis of chlorella was estimated to finish at the conversion rate of 70%.

Based on the activation energy calculation of six samples under two atmospheres, the degradation of algae was composed of the protein, carbohydrate and lipid content, which represented by ovalbumin, cellulose and oil droplets. Lipids are long chains of hydrocarbon

molecules with a carboxyl group in one end. They play both structural and energy storage roles as they are present as phospholipids, glycolipids, fatty acids and triglycerides. Fatty acid chains commonly contain 14 to 20 carbon atoms, and 18 carbon fatty acids are the most frequent [227]. Weight composition of typical fatty acids found in algae show very similar elemental composition (H = 11-13% and C = 73-78%), with moderate variations with carbon number and unsaturation degree [228] . Unsaturated fatty acids are the most abundant [229].

Proteins are long chains of polymerized amino acids, also involved in cell structure. There are various species of protein contained in algae, since one single cell produces thousands of different proteins with different amino acid composition.The nitrogen-released compounds are mainly in the form of organic nitrites, nitriles, amines, amides, indoles, pyrroles and their derivatives [230].

The degradation of algae carbohydrate is different from cellulose pyrolysis. Alginates are linear unbranched polymers constituted by (1, 4)-linked D-mannuronic and L-guluronic acid residues. This polymer decomposes in a different way than cellulose, which consists of D-glucose monomers linked by β-glycosidic bonds. There are two main types of carbohydrates in brown seaweed, those with β-1,3 linkages (e.g. laminarin and mannitol) and those with β-1,4 linkages (e.g. amylopectin, amylose) roughly equivalent to starch in lignocellulosic

biomass. These structural differences explain the large formation of anhydrous mannitol rather than levoglucosan [47].

Overall, by comparison of the activation energy derived from the pyrolysis of three model compounds and three algae under N_2 and CO_2, although the ovalbumin and three algae required higher amount of energy to start pyrolysis but ended the process earlier (2.1-20.2 % time ahead) under CO_2 atmosphere, which indicated the CO_2 could assist in the pyrolysis of spirulina, chlorella, porphyra and their protein content. However, the activation energy remained almost the same for the pyrolysis of cellulose under two carrier gas, while the higher energy request of oil droplets showed the difficulty for lipid content in algae to pyrolyze under CO_2.

Table 5-5 The activation energy (E_a, kJ/mol) and correlation factor (R^2) of algae and model compounds under N_2 at increasing conversion rate (α) using KAS method.

	Spirulina		Chlorella		Porphyra		Ovalbumin		α-Cellulose		Oil droplets	
α	E_a	R^2	E_a	R^2	E_a	R^2	E_a	R^2	E_a	R^2	E_a	R^2
5%	162.5	0.9978	205.8	0.9595	178.2	0.9885	188.4	0.9880	202.5	0.9915	123.1	0.9323
10%	177.5	0.9987	210.4	0.9821	192.3	0.9649	202.4	0.9881	198.9	0.9963	136.1	0.9763
15%	183.2	0.9996	202.4	0.9938	193.4	0.9668	209.7	0.9892	196.2	0.9970	147.0	0.9905
20%	183.0	0.9998	202.8	0.9975	196.9	0.9739	209.9	0.9836	194.7	0.9972	154.9	0.9934
25%	182.2	0.9997	204.1	0.9982	202.7	0.9783	231.6	0.9920	193.6	0.9974	163.2	0.9965
30%	182.1	0.9998	207.0	0.9952	211.4	0.9788	232.0	0.9921	191.7	0.9977	166.0	0.9973
35%	182.0	0.9997	212.0	0.9910	230.1	0.9730	234.6	0.9808	189.9	0.9979	169.8	0.9979
40%	182.6	0.9995	210.5	0.9859	281.4	0.9574	237.9	0.9654	188.1	0.9982	173.0	0.9981
45%	183.9	0.9990	206.6	0.9878	334.8	0.9077	237.9	0.9675	186.8	0.9984	175.2	0.9987
50%	186.8	0.9985	206.6	0.9848	372.0	0.9331	233.4	0.9696	185.6	0.9984	186.1	0.9936
55%	191.2	0.9974	207.7	0.9827	389.4	0.9519	231.7	0.9658	184.5	0.9985	189.6	0.9920
60%	200.0	0.9956	214.9	0.9762	423.9	0.9143	240.8	0.9490	182.9	0.9987	183.0	0.9980
65%	218.0	0.9914	229.7	0.9702	486.3	0.8878	255.0	0.9195	181.0	0.9990	179.5	0.9988
70%	249.2	0.9842	259.7	0.9564	525.7	0.8370	278.5	0.8695	179.3	0.9990	180.9	0.9987
75%	299.5	0.9436	307.2	0.9242	548.5	0.6922	331.6	0.7119	178.2	0.9992	182.1	0.9985
80%	335.5	0.9228	367.4	0.9038	257.2	0.1508	165.2	0.1812	176.2	0.9992	183.6	0.9986
85%	305.7	0.8717	395.0	0.8341	-143.9	0.1788	-29.8	0.0157	174.1	0.9994	183.6	0.9985
90%	203.2	0.4713	345.9	0.6092	-147.2	0.2812	-64.7	0.3252	171.4	0.9994	185.3	0.9980
95%	28.8	0.0255	-57.7	0.0620	305.6	0.4821	334.3	0.6023	198.4	0.9582	180.6	0.9972

Table 5-6 The activation energy (E_a, kJ/mol) and correlation factor (R_2) of algae and model compounds under CO_2 at increasing conversion rate (α) using KAS method.

	Spirulina		Chlorella		Porphyra		Ovalbumin		α-Cellulose		Oil droplets	
α	E_a	R^2	E_a	R^2	E_a	R^2	E_a	R^2	E_a	R^2	E_a	R^2
5%	178.1	0.9981	115.2	0.9150	152.0	0.9607	148.9	0.9820	187.6	0.9975	156.9	0.9918
10%	223.2	0.9955	165.4	0.9707	228.8	0.9915	183.8	0.9844	189.9	0.9777	168.6	0.9945
15%	233.2	0.9996	178.5	0.9865	269.8	0.8268	202.3	0.9838	187.1	0.9955	173.8	0.9957
20%	234.9	0.9978	187.0	0.9926	254.9	0.5756	231.5	0.9698	183.6	0.9980	181.1	0.9962
25%	235.2	0.9957	195.7	0.9953	245.6	0.4299	315.0	0.9291	180.6	0.9985	184.4	0.9959
30%	237.6	0.9924	210.3	0.9961	352.7	0.4842	376.4	0.8623	178.5	0.9988	188.5	0.9960
35%	243.6	0.9883	225.8	0.9962	723.4	0.8563	420.8	0.8267	177.6	0.9987	192.5	0.9962
40%	255.5	0.9776	232.2	0.9968	227.3	0.3897	462.5	0.7931	175.6	0.9988	193.4	0.9970
45%	278.2	0.9533	236.3	0.9985	141.3	0.3696	504.4	0.7552	174.7	0.9990	197.3	0.9967
50%	314.7	0.8680	244.6	0.9992	96.4	0.2947	572.0	0.6446	173.6	0.9990	198.6	0.9971
55%	316.7	0.5007	204.3	0.8454	63.5	0.1805	298.5	0.0759	172.5	0.9993	199.6	0.9975
60%	-52.2	0.0139	214.8	0.7933	47.8	0.4481	-485.6	0.5018	172.2	0.9994	202.2	0.9973
65%	-182.0	0.4655	224.0	0.6634	9.3	0.0067	-291.7	0.8597	172.0	0.9995	203.7	0.9975
70%	-147.9	0.7375	206.8	0.4292	-16.0	0.0632	-168.0	0.9059	171.7	0.9997	204.2	0.9977
75%	-97.0	0.8374	136.2	0.1611	-16.5	0.1037	-96.8	0.9426	170.9	0.9999	205.1	0.9978
80%	-45.8	0.8669	45.2	0.0194	-96.5	0.5376	-47.0	0.9233	170.4	1.0000	206.0	0.9980
85%	-43.8	0.9261	-17.5	0.0053	-694.2	0.6118	-53.3	0.9153	171.5	1.0000	206.4	0.9981
90%	-47.4	0.9196	-113.4	0.7196	-229.2	0.0512	-88.1	0.7844	179.0	0.9998	208.0	0.9977
95%	-75.2	0.8890	-83.9	0.9993	274.5	0.0210	-205.3	0.1403	342.8	0.2799	209.5	0.9984

5.2.2 Determination of reaction model via Coats- Redfern method

According to TG/DTG analysis, the heating rate affected the pyrolysis process significantly. Due to the thermal hysteresis, the kinetic factors calculated based on the high heating rate were usually underestimated, compared to the real parameters [231, 232]. The total pyrolysis time would be reduced by the rising heating rate; thus, the temperature of decomposition will drift to higher temperature which requested more activation energy. Hence, to minimize this influence from thermal lag, the result collected under low pyrolysis heating rate of 5°C/min was adopted to determine the reaction model. Similar analysis was reported most literature [91, 95]. Commonly-used mechanism models (**Table 2-2**) were substituted into Coats-Redfern method to plot $ln\frac{G(\alpha)}{T^2}$ against $-\frac{1}{RT}$ for the major pyrolysis stage (Event I and II). On the basis of R^2 fitting method summarized in **Table 5-7** and **Table 5-8**, the category of mechanism, activation energy, E_a and pre-exponential, A corresponding to the best regression value, among the application of each form, $G(\alpha)$ were listed in **Table 5-9**.

According to **Section 5.2.1**, the activation energy of spirulina, chlorella, porphyra, cellulose and ovalbumin would increase gradually at the initial decomposition stage and rocketed to high values in the end, which indicated that two reaction mechanism took place in this

stage of pyrolysis. The carbonaceous matters of ovalbumin firstly started to decompose from 180°C and fitted the Second-order chemical reaction (F2) model, which required the smallest activation energy of 74.4 kJ/mol. As the pyrolysis temperature increasing, the activation energy of ovalbumin in Event II reduced to 41.5 kJ/mol from 220°C, which was much lower than the value derived by KAS method, and the mechanism of ovalbumin pyrolysis remained as F2 model. Cellulose was the second model compound to decompose into volatiles from 300 to 360°C, which requested higher activation energy of F2 model (302.3kJ/mol). Compared with results concluded from KAS method, the activation energy showed apparent difference, which varied around 175 kJ/mol during the whole period of pyrolysis and decreased to about 170 kJ/mol at α=90%. Powered oil didn't alter evidently and therefore, one reaction model was involved in the pyrolysis process, which appeared to be D1 model. It was the last model substance beginning to disassemble at 340 until 440°C, with activation energy of 227.8 kJ/mol, which was higher than the value obtained via KAS method (approximately 180 kJ/mol).

Hence, the protein in algae was the first primary component to decompose during the second stage, followed by carbohydrate which need more energy. Lipid in algae was the last component to decompose, which required less energy input and was decomposed with remaining carbohydrate and protein simultaneously. Unlike

cellulose, the decomposition of spirulina was in D1 model with an activation energy of 122.6 kJ/mol from 220 to 270°C at first. After 270°C, the mechanism was changed to F2 model and reduced E required with amount of 53.0 kJ/mol. Likely, the breakdown of chlorella and porphyra also showed two events, and the first event in D1 and F2 model started with an activation energy of 108.9 and 92.6 kJ/mol from 200 and 220°C respectively. After 250 and 300°C, less energy required for the continuity of pyrolysis which reduced to 47.0 and 26.3 kJ/mol both in F2 model. It is apparent that decomposition of most samples was controlled by diffusion mechanism in lower operating temperature and then changed to second-order chemical reaction mechanism in higher pyrolysis temperature.

When transferring to the CO_2 atmosphere, spirulina, chlorella and ovalbumin required less energy to proceed the decomposition, while E_a of porphyra, powedered oil and cellulose pyrolysis raised by 5.3-32.1%, compared to the decomposition of substances under N_2 atmosphere. Spirulina required 83.1 and 31.3% less energy to proceed the decomposition under CO_2, which decomposed in D1 model with 20.7 kJ/mol for Event I, and altered to F2 mechanism with E of 36.4 kJ/mol, compared to the decomposition of substances under N_2 atmosphere. The pyrolysis of chlorella began with Event I in D1 model from 200°C with lower requirement of energy amount (87.7 kJ/mol), followed by Event II from 250°C with smaller activation

energy of 38.9 kJ/mol, compared to N_2 atmosphere. However, the initial decomposition of porphyra requested higher energy 122.3 kJ/mol in D3 model, while decreased to 18.7 kJ/mol in Event II.

Ovalbumin decayed firstly in F2 mechanism which is the same as the decomposition under N_2 with only 66.8 kJ/mol activation energy from 180 °C. After 220 °C, the activation energy would follow the same decreasing trend as in N_2 to 24.4 kJ/mol. Meanwhile, cellulose started the decomposition from 300 °C with moderately higher energy consumption of 318.4 kJ/mol in F2 mechanism. With higher activation energy of 266.5 kJ/mol, compared to the value under N_2 atmosphere, the degradation of oil droplets performed in the meantime (340-440 °C). Therefore, similar decomposition sequence of the three model compounds can be performed under CO_2, compared to N_2 as carrier gas. The decomposition of ovalbumin required lower amount of activation energy, which means that CO_2 atmosphere favours the pyrolysis of protein content in algae. However, the E_a of cellulose and oil droplets decomposition increased by 5.3 and 17.0% respectively, which indicated the decomposition of lipid and carbohydrate part in algal samples was relatively difficult to undertake in CO_2. Therefore, same conclusion can be drawn which described in **Section 5.2.1**.

Table 5-7 The activation energy (E_a, kJ/mol), pre-exponential factor (A) and correlation factor (R^2) of algae and model compounds under N_2 in different model mechanisms using Coats-Redfern method.

Model	Spirulina			Chlorella			Porphyra			Ovalbumin			α-Cellulose			Oil droplets		
	E_a	A	R^2	E_a	A	R^2	E_a	A	R^2	E_a	A	R^2	E_a	A	R^2	E_a	A	R^2
D1	38.8	23.3	0.5573	43.2	69.4	0.7011	26.2	1.0	0.4876	24.9	1.2	0.5132	296.1	$5.73 X10^{24}$	0.8260	227.8	$1.43X10^{16}$	0.9902
D2	44.7	55.9	0.6169	49.2	$1.7 X10^{2}$	0.7550	30.8	1.9	0.5612	29.1	2.2	0.5854	329.0	$3.06 X10^{27}$	0.8561	248.8	$4.04X10^{17}$	0.9869
D3	52.9	99.8	0.6915	57.4	$3.0 X10^{2}$	0.8189	37.1	2.3	0.6506	35.0	2.7	0.6735	373.5	$7.77 X10^{30}$	0.8927	275.8	$1.56 X10^{19}$	0.9771
D4	47.4	24.6	0.6431	51.9	74.9	0.7779	32.9	0.7	0.5926	31.0	0.9	0.6164	343.5	$1.43 X10^{28}$	0.8693	257.7	$4.88 X10^{17}$	0.9843
R2	19.0	0.3	0.5213	21.5	0.7	0.6952	11.3	$3.8 X10^{-2}$	0.3912	10.7	$4.2 X10^{-2}$	0.4096	170.8	$5.74 X10^{13}$	0.8698	125.7	$1.75 X10^{8}$	0.9813
R3	132.4	$4.3 X10^{8}$	0.9754	23.5	0.8	0.7386	12.9	$4.1 X10^{-2}$	0.4541	12.1	$4.6 X10^{-2}$	0.4731	181.7	$3.93 X10^{14}$	0.8872	132.4	$4.27 X10^{8}$	0.9754
A2	7.3	0.0	0.3664	8.8	0.1	0.6060	2.5	$4.7 X10^{-3}$	0.0990	2.3	$5.1 X10^{-3}$	0.1006	98.2	$4.82 X10^{7}$	0.9106	68.0	$1.13 X10^{4}$	0.9526
A3	1.2	0.0	0.0307	2.4	0.0	0.1829	-2.1	$-1.8 X10^{-3}$	0.1392	-2.0	$-2.0 X10^{-3}$	0.1418	62.1	$2.35 X10^{4}$	0.9012	41.7	7.17 X10	0.9452
F1	25.6	4.1	0.6657	28.0	8.0	0.8176	16.4	0.4	0.5789	15.4	0.4	0.5988	206.4	$2.21 X10^{17}$	0.9188	147.1	$2.23 X10^{10}$	0.9585
F2	43.6	$4.3 X10^{2}$	0.8738	45.8	$7.9 X10^{2}$	0.9607	30.1	16.3	0.8502	28.1	18.0	0.8691	302.3	$1.30 X10^{26}$	0.9734	202.5	$9.21 X10^{14}$	0.8775

Table 5-8 The activation energy (E_a, kJ/mol), pre-exponential factor (A) and correlation factor (R^2) of algae and model compounds under CO_2 in different model mechanisms using Coats-Redfern method.

Model	Spirulina			Chlorella			Porphyra			Ovalbumin			α-Cellulose			Oil droplets		
	E_a	A	R^2	E_a	A	R^2	E_a	A	R^2	E_a	A	R^2	E_a	A	R^2	E_a	A	R^2
D1	1.8	8.9 X10^{-4}	0.7834	27.5	1.6	0.5330	17.0	7.9 X10^{-2}	0.3565	15.2	6.6 X10^{-2}	0.4063	145.0	1.7 X10^{11}	0.4920	243.5	5.29 X10^{17}	0.9933
D2	4.1	2.3 X10^{-3}	0.9387	32.1	2.9	0.6011	20.6	0.1	0.4381	18.4	9.5 X10^{-2}	0.4951	164.1	5.5 X10^{12}	0.5286	266.5	2.29 X10^{19}	0.9948
D3	8.5	3.6 X10^{-3}	0.9545	38.4	3.6	0.6848	25.5	0.1	0.5371	22.7	7.9 X10^{-2}	0.5994	190.8	4.1 X10^{14}	0.5791	296.2	1.56 X10^{21}	0.9909
D4	5.5	1.0 X10^{-3}	0.9497	34.2	1.1	0.6306	22.2	4.2 X10^{-2}	0.4727	19.8	3.3 X10^{-2}	0.5319	172.8	8.1 X10^{12}	0.5460	276.2	3.32 X10^{19}	0.9943
R2	1.8	7.4 X10^{-4}	0.6501	11.9	4.8 X10^{-2}	0.4275	5.3	4.4 X10^{-3}	0.1555	4.4	3.6 X10^{-3}	0.1668	83.6	6.6 X10^{5}	0.5249	135.3	1.60 X10^{9}	0.9933
R3	2.9	1.1 X10^{-3}	0.8038	13.5	5.3 X10^{-2}	0.4884	6.5	4.8 X10^{-3}	0.2150	5.5	4.0 X10^{-3}	0.2353	90.2	1.9 X10^{6}	0.5505	142.6	4.49 X10^{9}	0.9903
A2	1.4	1.2 X10^{-3}	0.4381	2.8	5.9 X10^{-3}	0.1179	-1.7	-1.2 X10^{-3}	0.0559	-1.9	-1.5 X10^{-3}	0.1091	47.5	8.4 X10^{2}	0.5499	73.9	4.55 X10^{4}	0.9762
A3	0.0	-4.57 X10^{-6}	0.0000	-2.0	-1.8 X10^{-3}	0.1088	-5.3	-2.2 X10^{-3}	0.5348	-5.2	-2.3 X10^{-3}	0.6168	28.2	11.3	0.4901	45.7	1.89 X10^{2}	0.9728
F1	5.6	1.3 X10^{-2}	0.8993	17.0	0.5	0.6086	9.2	3.9 X10^{-2}	0.3499	7.9	3.1 X10^{-2}	0.3898	105.3	1.6 X10^{8}	0.6026	158.8	3.20 X10^{11}	0.9789
F2	18.1	0.9	0.9295	30.7	21.2	0.8668	19.8	1.0	0.6927	17.1	0.7	0.7535	165.8	7.9 X10^{13}	0.7359	219.9	4.42 X10^{16}	0.9104

Table 5-9 Values of activation energy, pre-exponential factor and related kinetic models of Event I and II under N_2 and CO_2

N_2							
	Parameters	**Spirulina**	**Chlorella**	**Porphyra**	**Oil droplets**	**Ovalbumin**	**Cellulose**
Event I	**Range(°C)**	220-270	200-250	220-300	340-440	180-220	300-360
	E (kJ mol^{-1})	122.6	108.9	92.6	227.8	74.4	302.3
	Mechanism	1-D diffusion (D1)	1-D diffusion (D1)	Second-order chemical reaction (F2)	1-D diffusion (D1)	Second-order chemical reaction (F2)	Second-order chemical reaction (F2)
	A (s^{-1})	5.3 X10^{9}	3.8× 10^{8}	5.7× 10^{7}	1.4× 10^{16}	3.3× 10^{6}	1.30 X10^{26}
Event II	**Range(°C)**	270-400	250-460	300-450		220-400	
	E (kJ mol^{-1})	53.0	47.0	26.3		41.5	
	Mechanism	Second-order chemical reaction (F2)	Second-order chemical reaction (F2)	Second-order chemical reaction (F2)		Second-order chemical reaction (F2)	
	A (s^{-1})	4.7 X10^{3}	1.2× 10^{3}	0.9		164.7	
CO_2							
	Parameters	**Spirulina**	**Chlorella**	**Porphyra**	**Oil droplets**	**Ovalbumin**	**Cellulose**
Event I	**Range(°C)**	220-300	200-250	220-330	340-430	180-220	300-350
	E (kJ mol^{-1})	20.7	87.7	122.3	266.5	66.8	318.4
	Mechanism	1-D diffusion (D1)	1-D diffusion (D1)	3-D diffusion (D3)	2-D diffusion (D2)	Second-order chemical reaction (F2)	Second-order chemical reaction (F2)
	A (s^{-1})	0.3	2.9× 10^{6}	7.7× 10^{9}	2.29× 10^{19}	4.0× 10^{5}	4.2 × 10^{27}
Event II	**Range(°C)**	300-490	250-460	330-430		220-400	
	E (kJ mol^{-1})	36.4	38.9	18.7		24.4	
	Mechanism	Second-order chemical reaction (F2)	Second-order chemical reaction (F2)	Second-order chemical reaction (F2)		Second-order chemical reaction (F2)	
	A (s^{-1})	94.9	37.7	1.4		0.6	

5.2.3 Characterisation of solid residues

5.2.3.1 Morphology of solid residues

The morphology of solid residue of each algae (spirulina, chlorella, porphyra) and its primary model compounds (cellulose and ovalbumin) after thermal processing in TGA was indicated in **Figure 5-3** to **Figure 5-7** under N_2 and **Figure 5-8** to **Figure 5-12** under CO_2. Since oil droplets has neither fixed carbon nor ash content, almost no char left in the crucibles after pyrolysis of oil droplets; therefore, no results for char of algal pseudo-lipid content. When under nitrogen atmosphere, different heating rates (5, 10, 20 and 50 °C min^{-1}) appeared to be have little influence on the formation of solid remains. However, lower heating rate such as 5 and 10°C min^{-1}, improved the cracking and decomposing of samples, especially for porphyra and chlorella. The morphology of porphyra and cellulose char obtained under CO_2 remained the same as those derived under N_2. But ovalbumin char is found to have more fibres under N_2, particular at lower heating rates. Moreover, the char of spirulina and chlorella aggregates and forms into more blocks under CO_2.

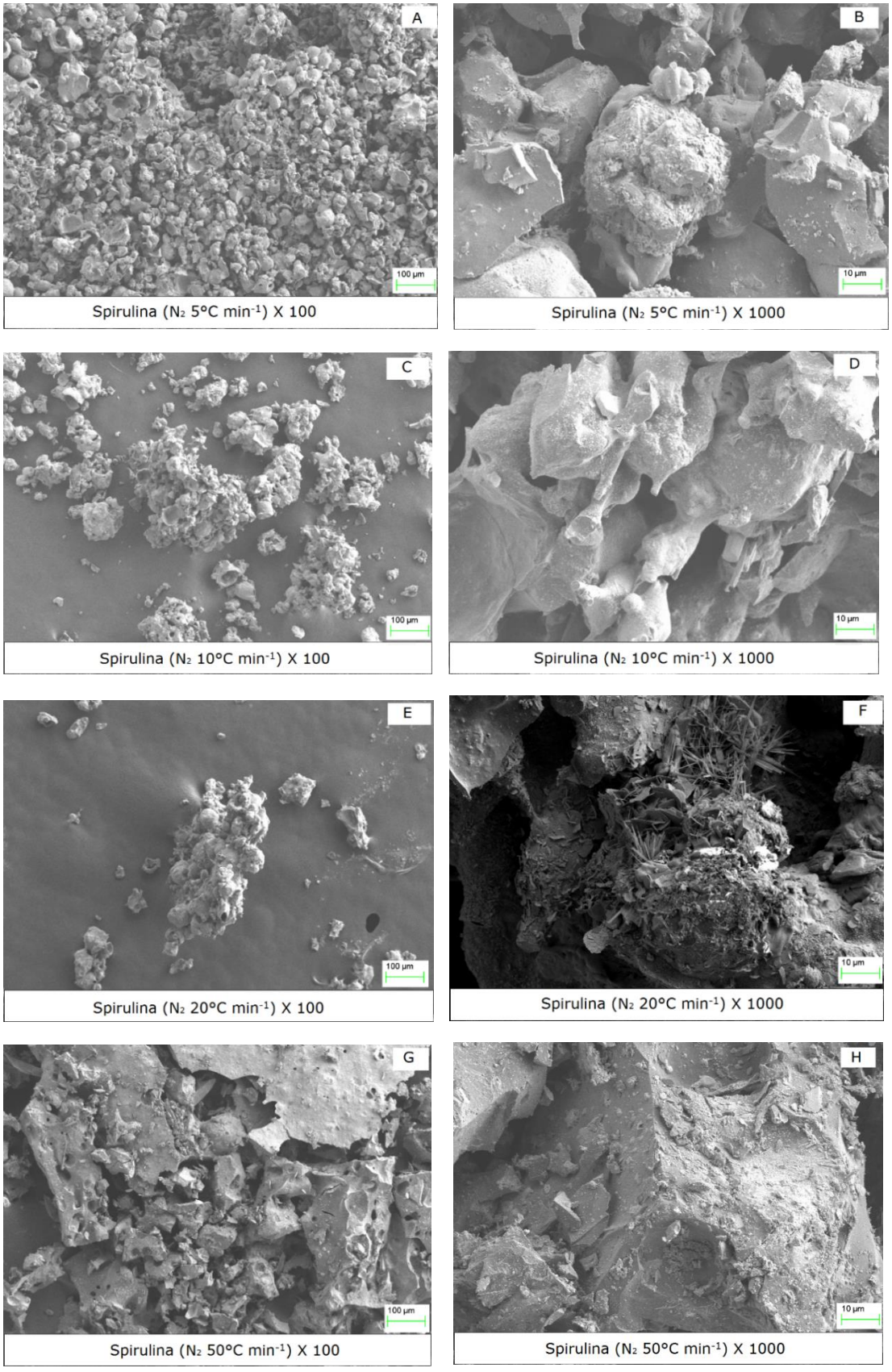

Figure 5-3 SEM images of char from kinetic studies of spirulina under N_2 at 5 °C min^{-1} with magnification of A x 100, B x 1000; at 10 °C min^{-1}, C x 100, D x 1000; at 20 °C min^{-1}, E x 100, F x 1000; at 50 °C min^{-1}, G x 100, H x 1000.

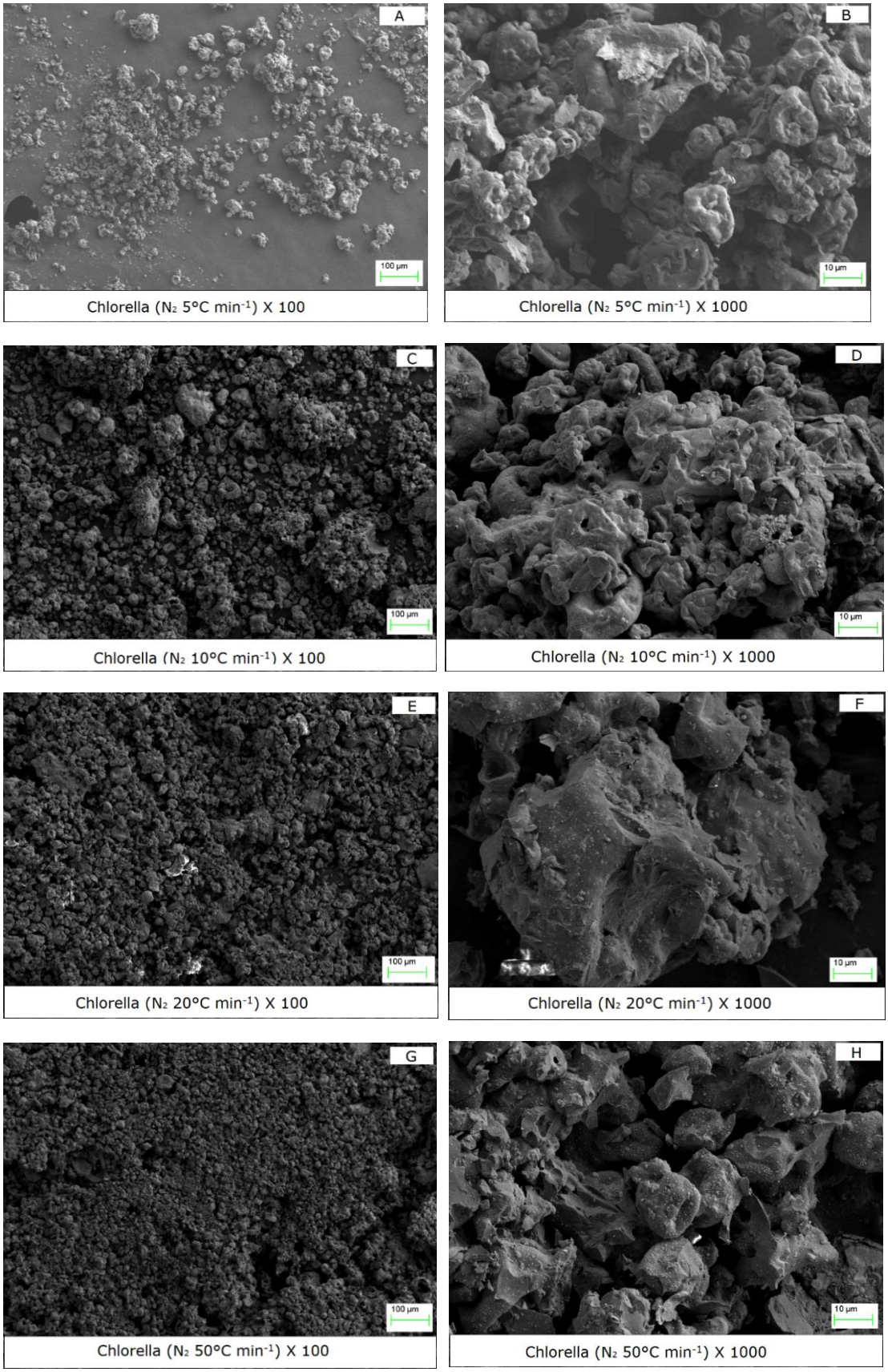

Figure 5-4 SEM images of char from kinetic studies of chlorella under N_2 at 5 °C min^{-1} with magnification of A x 100, B x 1000; at 10 °C min^{-1}, C x 100, D x 1000; at 20 °C min^{-1}, E x 100, F x 1000; at 50 °C min^{-1}, G x 100, H x 1000.

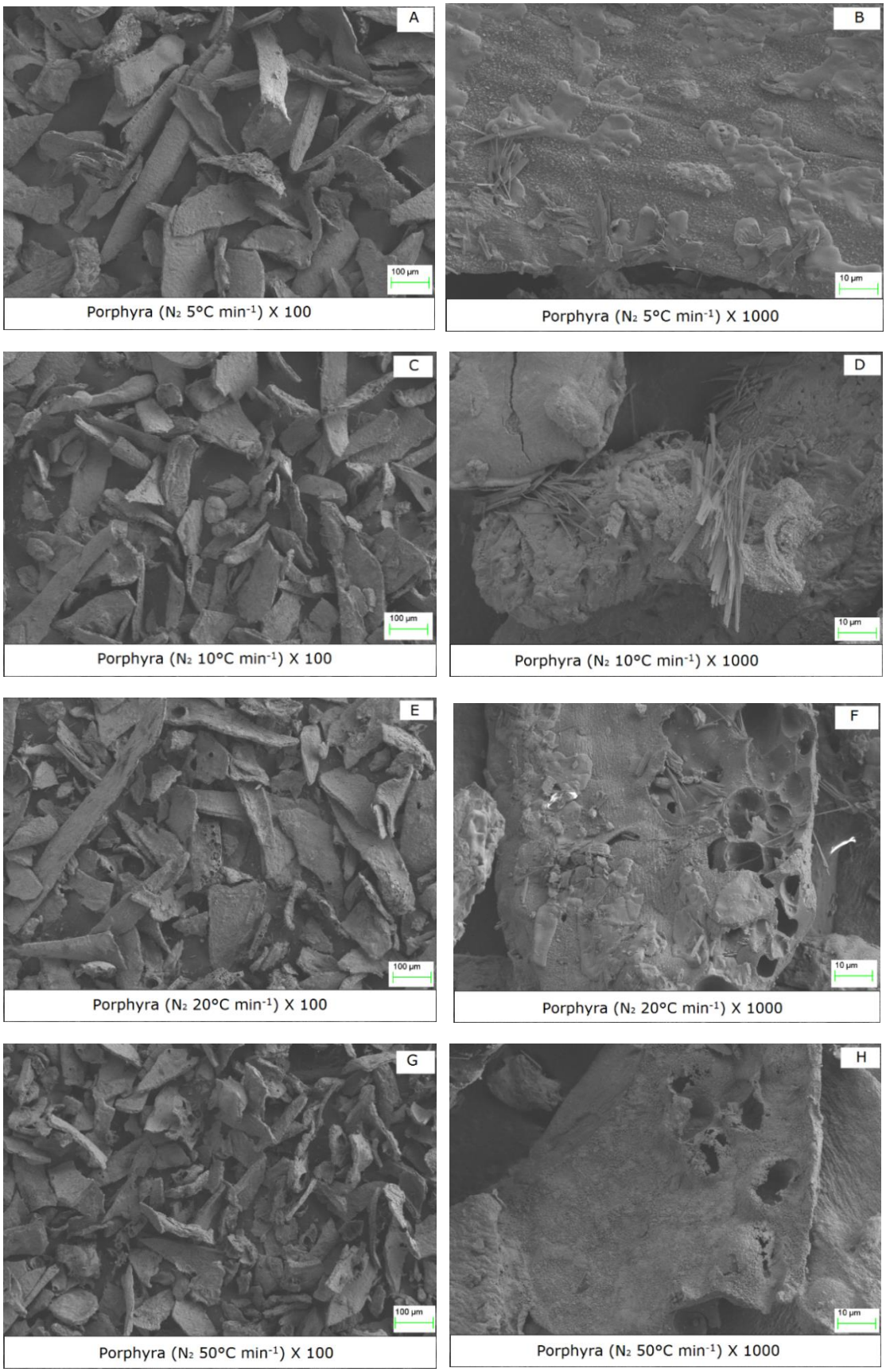

Figure 5-5 SEM images of char from kinetic studies of porphyra under N_2 at 5 °C min^{-1} with magnification of A x 100, B x 1000; at 10 °C min^{-1}, C x 100, D x 1000; at 20 °C min^{-1}, E x 100, F x 1000; at 50 °C min^{-1}, G x 100, H x 1000.

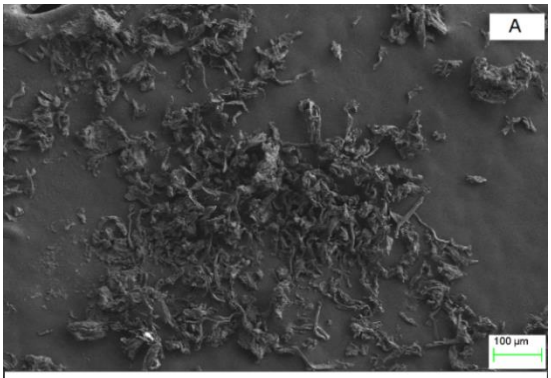

Cellulose (N_2 5°C min^{-1}) X 100

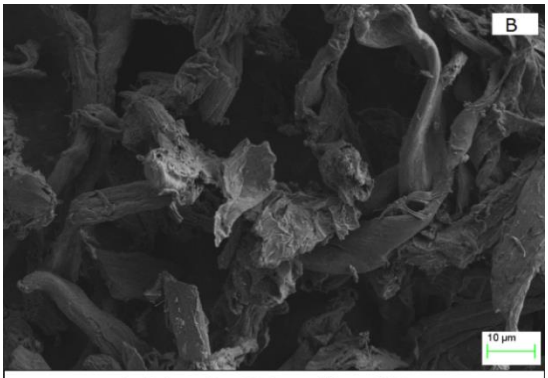

Cellulose (N_2 5°C min^{-1}) X 1000

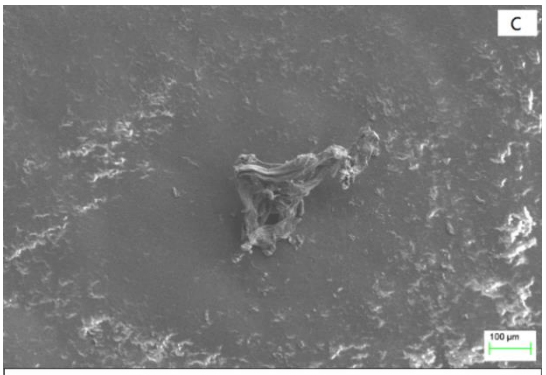

Cellulose (N_2 10°C min^{-1}) X 100

Cellulose (N_2 10°C min^{-1}) X 1000

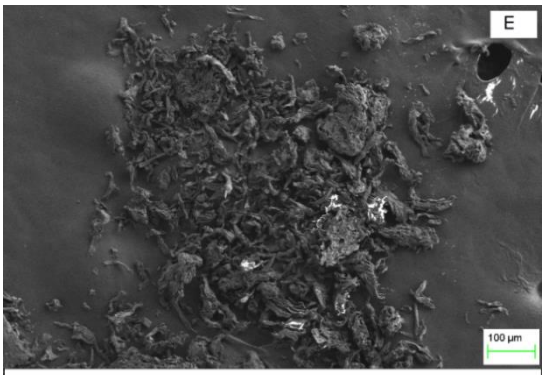

Cellulose (N_2 20°C min^{-1}) X 100

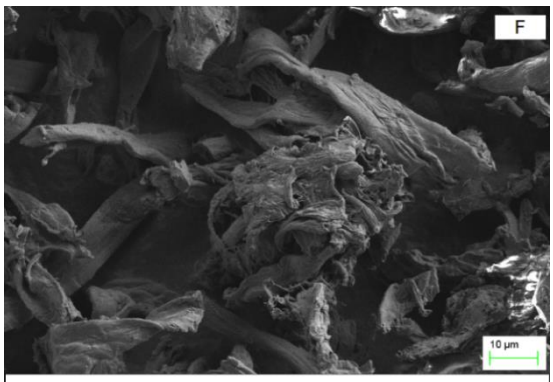

Cellulose (N_2 20°C min^{-1}) X 1000

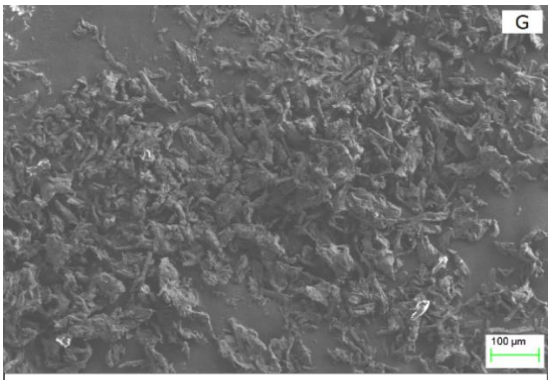

Cellulose (N_2 50°C min^{-1}) X 100

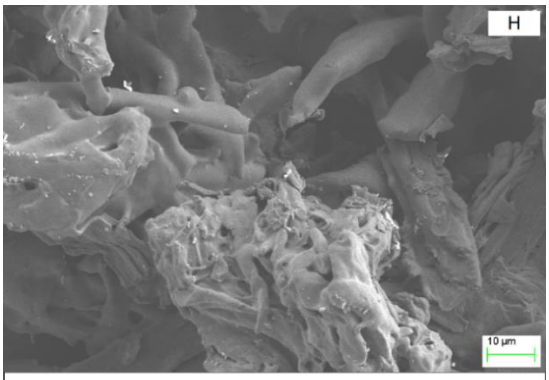

Cellulose (N_2 50°C min^{-1}) X 1000

Figure 5-6 SEM images of char from kinetic studies of cellulose under N_2 at 5 °C min^{-1} with magnification of A x 100, B x 1000; at 10 °C min^{-1}, C x 100, D x 1000; at 20 °C min^{-1}, E x 100, F x 1000; at 50 °C min^{-1}, G x 100, H x 1000.

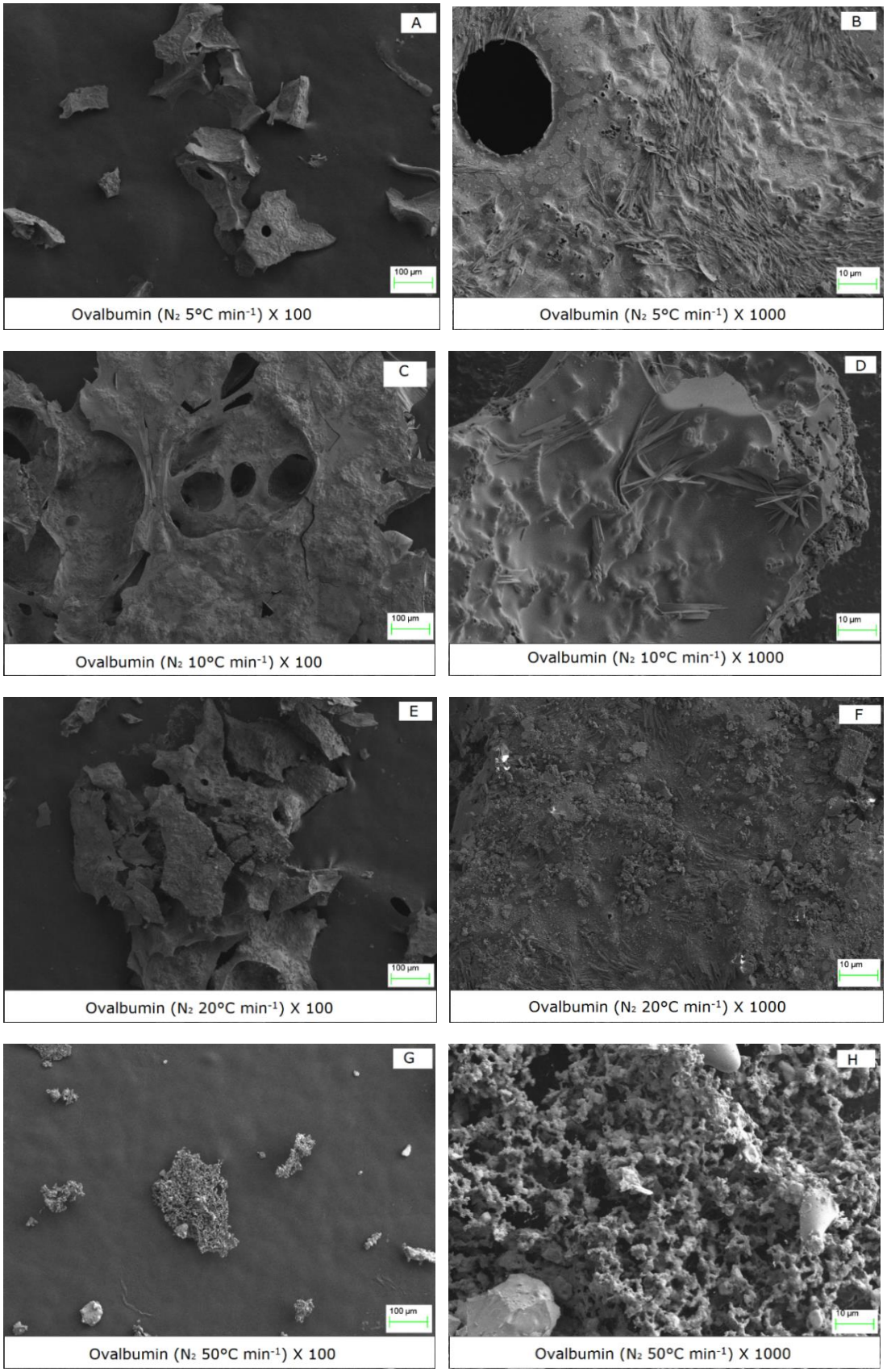

Figure 5-7 SEM images of char from kinetic studies of ovalbumin under N_2 at 5 °C min^{-1} with magnification of A x 100, B x 1000; at 10 °C min^{-1}, C x 100, D x 1000; at 20 °C min^{-1}, E x 100, F x 1000; at 50 °C min^{-1}, G x 100, H x 1000.

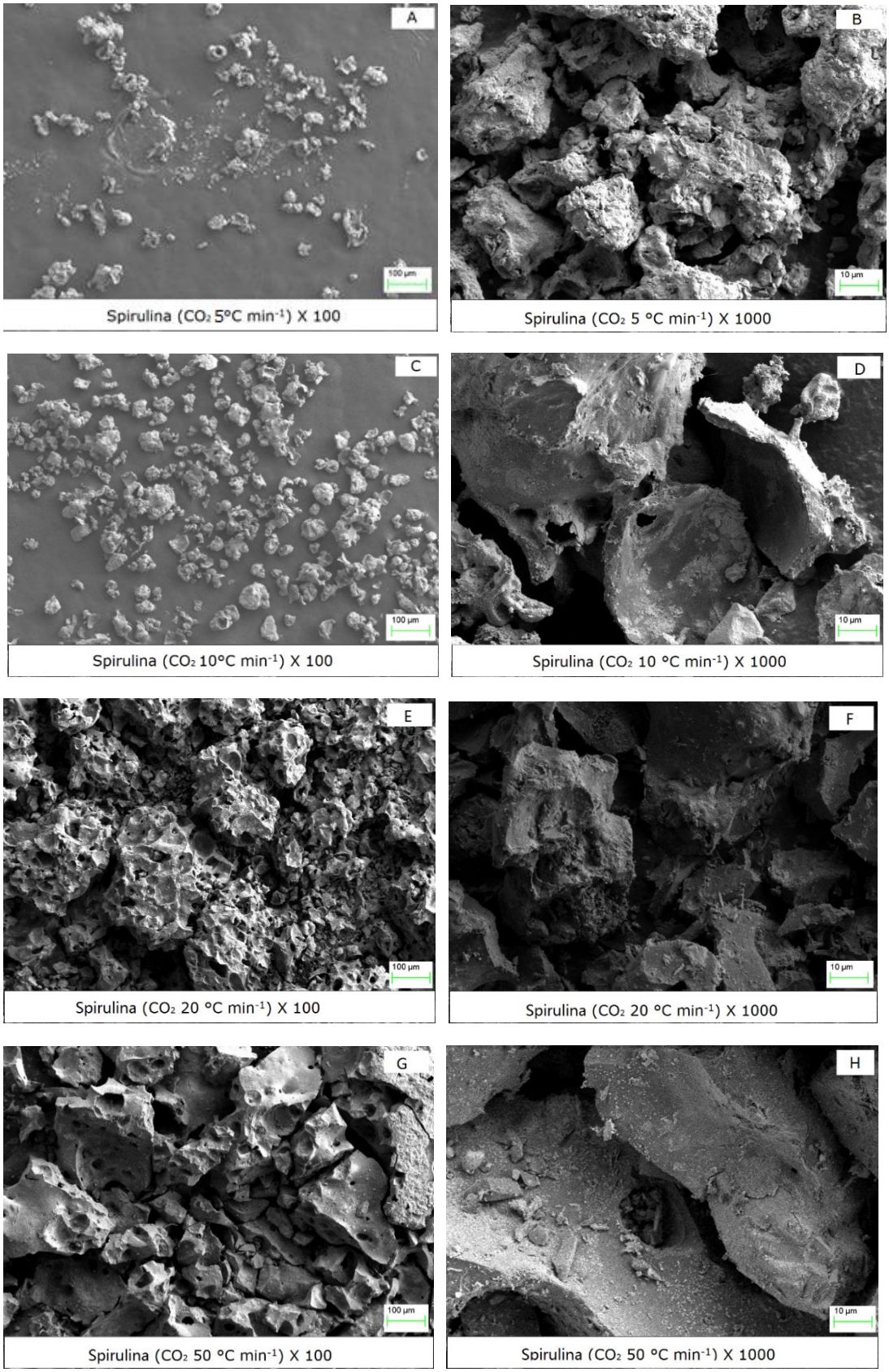

Figure 5-8 SEM images of char from kinetic studies of spirulina under CO_2 at 5 °C min^{-1} with magnification of A x 100, B x 1000; at 10 °C min^{-1}, C x 100, D x 1000; at 20 °C min^{-1}, E x 100, F x 1000; at 50 °C min^{-1}, G x 100, H x 1000.

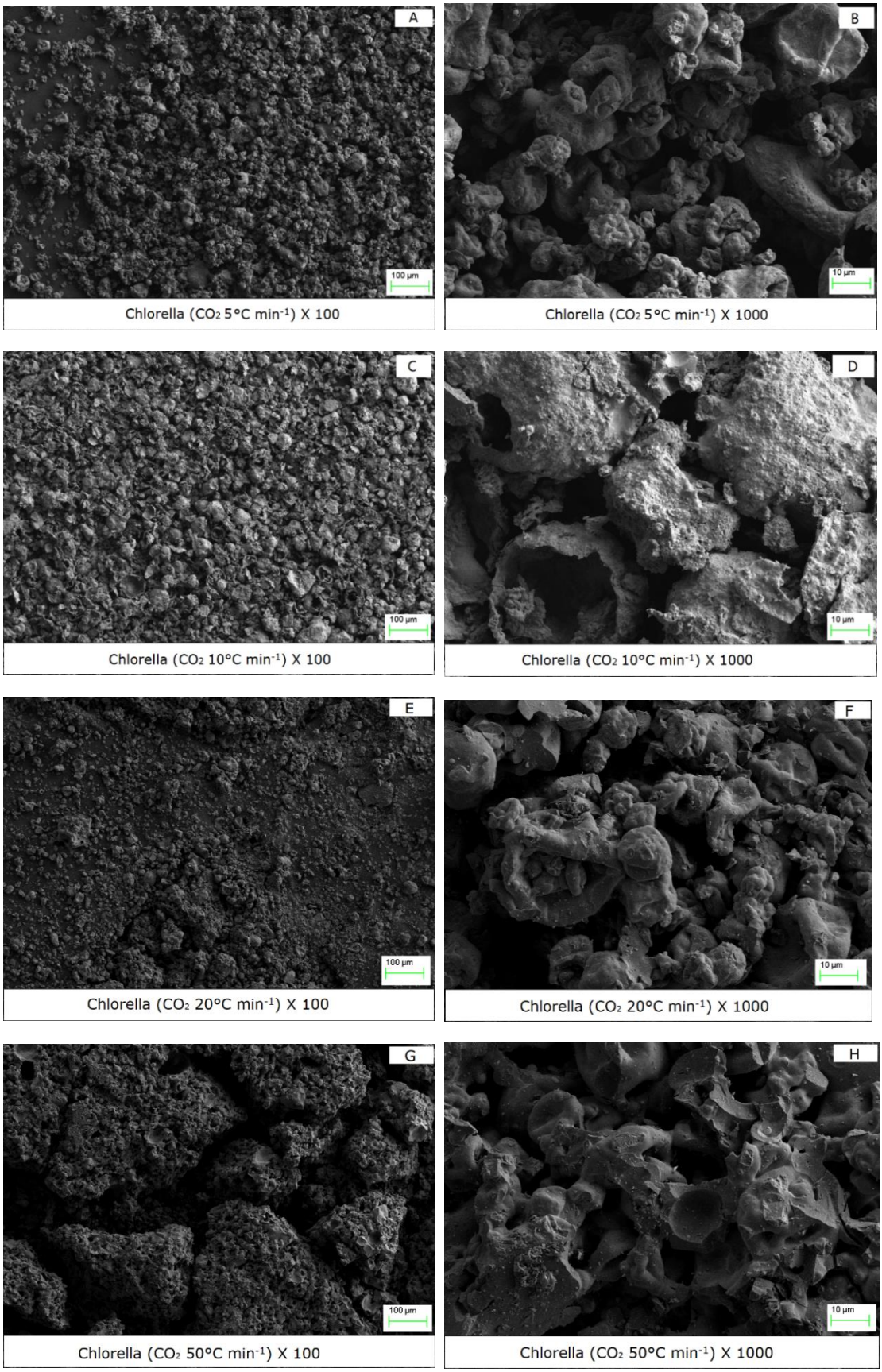

Figure 5-9 SEM images of char from kinetic studies of chlorella under CO_2 at 5 °C min^{-1} with magnification of A x 100, B x 1000; at 10 °C min^{-1}, C x 100, D x 1000; at 20 °C min^{-1}, E x 100, F x 1000; at 50 °C min^{-1}, G x 100, H x 1000.

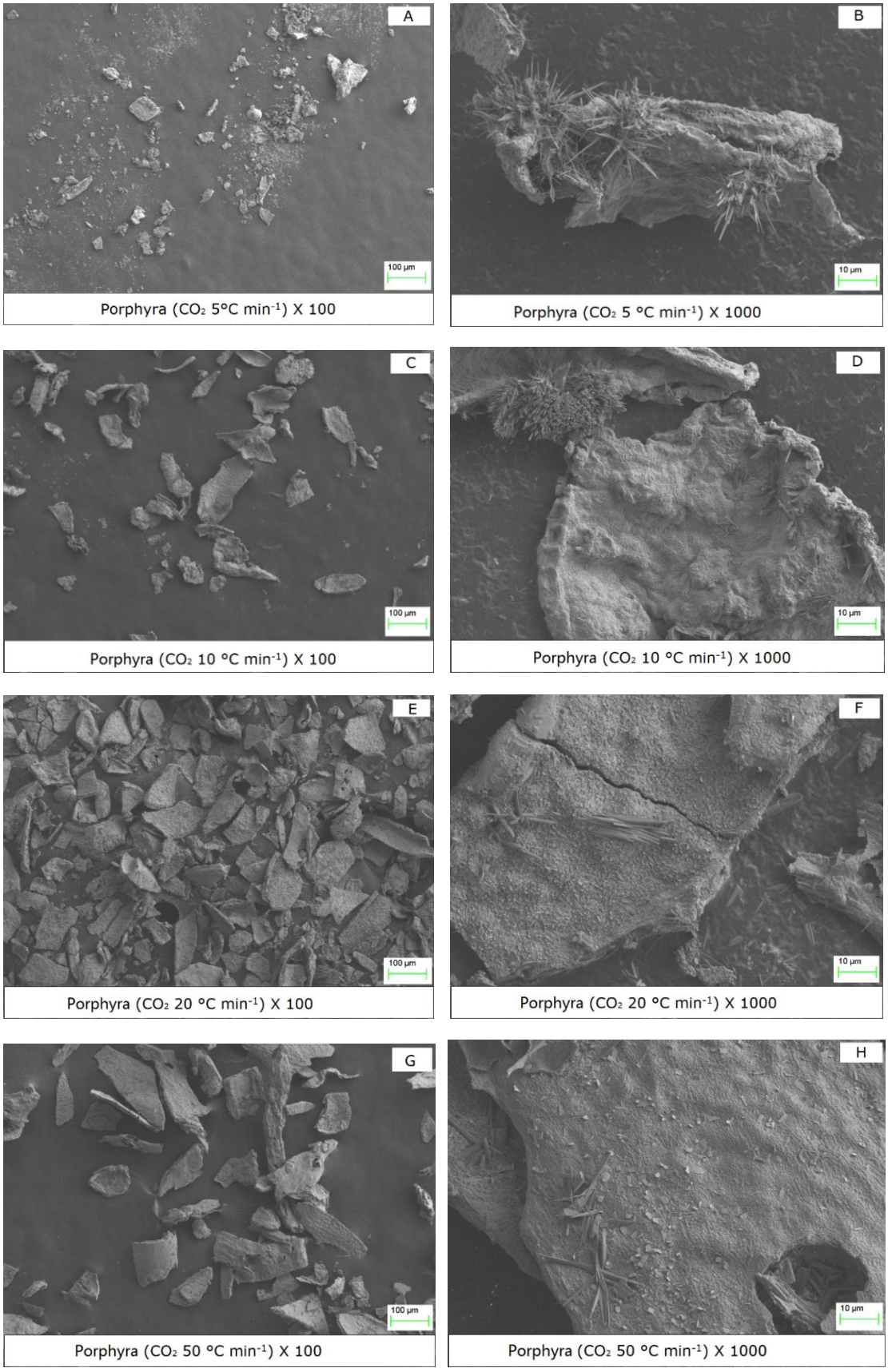

Figure 5-10 SEM images of char from kinetic studies of porphyra under CO_2 at 5 °C min^{-1} with magnification of A x 100, B x 1000; at 10 °C min^{-1}, C x 100, D x 1000; at 20 °C min^{-1}, E x 100, F x 1000; at 50 °C min^{-1}, G x 100, H x 1000.

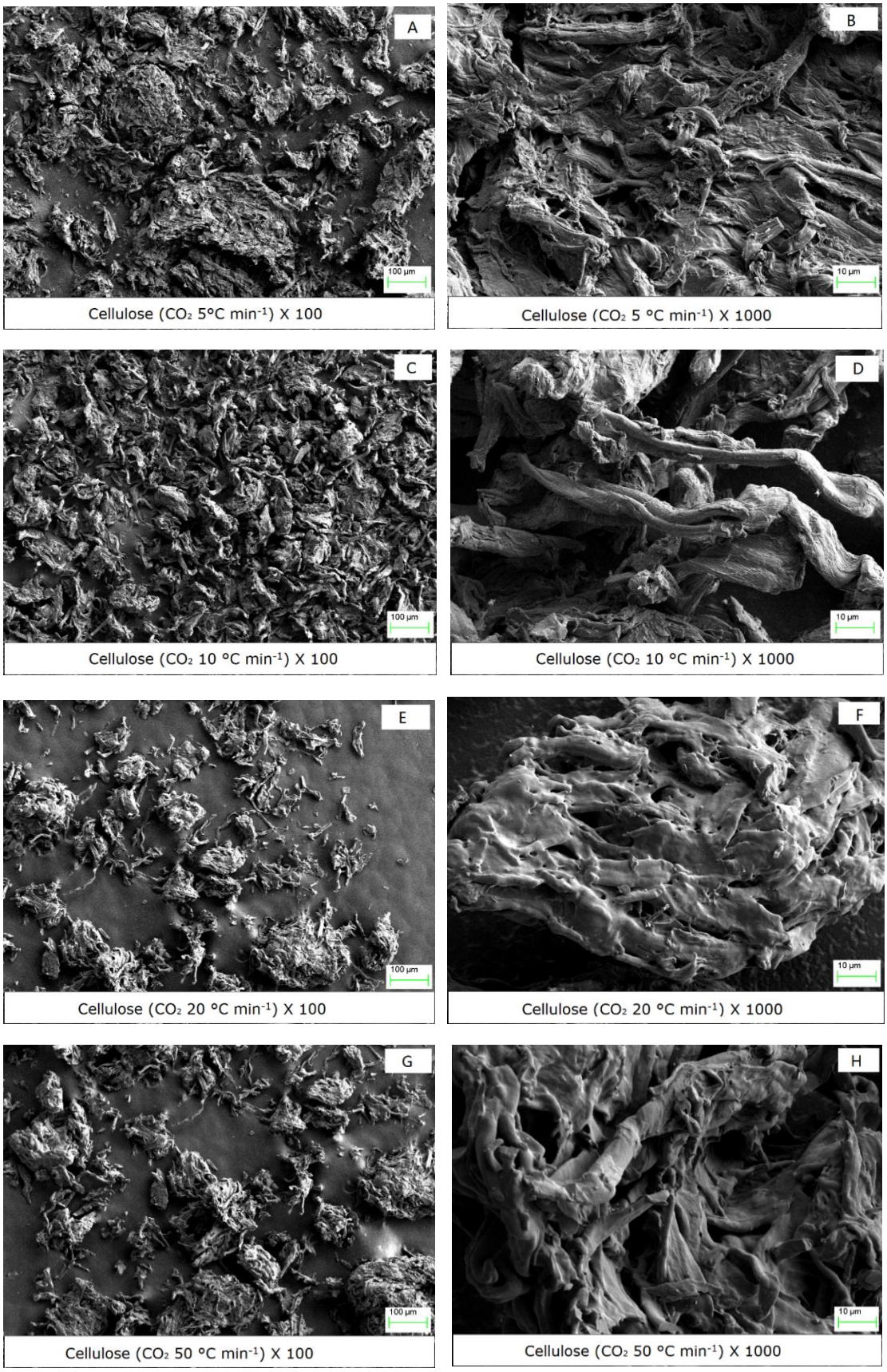

Figure 5-11 SEM images of char from kinetic studies of cellulose under CO_2 at 5 °C min^{-1} with magnification of A x 100, B x 1000; at 10 °C min^{-1}, C x 100, D x 1000; at 20 °C min^{-1}, E x 100, F x 1000; at 50 °C min^{-1}, G x 100, H x 1000.

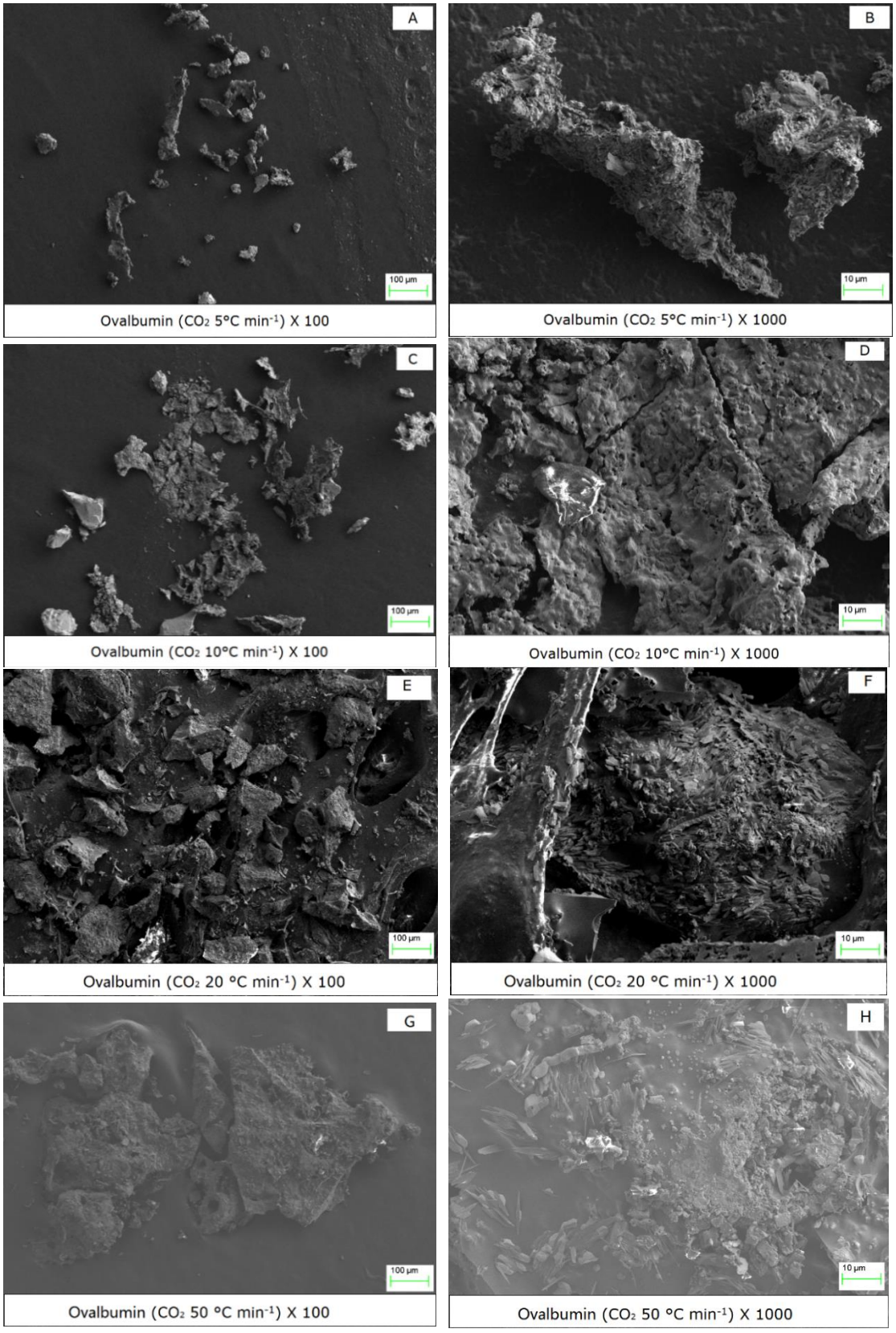

Figure 5-12 SEM images of char from kinetic studies of ovalbumin under CO_2 at 5 °C min^{-1} with magnification of A x 100, B x 1000; at 10 °C min^{-1}, C x 100, D x 1000; at 20 °C min^{-1}, E x 100, F x 1000; at 50 °C min^{-1}, G x 100, H x 1000.

5.2.3.2 Composition of solid residues

Table 5-1 and **Table 5-2** elucidated the compositions of char remained after pyrolysis of spirulina, chlorella, porphyra, ovalbumin and cellulose under N_2 and CO_2 in four different heating rates. Most compositions of algae char (spirulina, chlorella and porphyra) varied slightly after pyrolyzed under N_2 in four different heating rates. Carbon and oxygen content of the char fluctuated around 25 and 70 wt.% respectively, which is similar to the char compositions of ovalbumin. But after pyrolysis in CO_2, the carbon content in solid residue increased as the heating rate getting larger and became similar to the percentage derived under N_2 (3.7-24.5wt.% for spirulina; 0-24.5 wt.% for chlorella; 10.1-19.7 wt.% for porphyra), so as the oxygen content (45.2-69.8wt.% for spirulina; 47.5-70.6 wt.% for chlorella; 51.6-62.8 wt.% for porphyra). It is generally agreed that using CO_2 as carrier gas could reduce the carbon and oxygen content in algal char residue as well as its remaining amount, which is corresponding to Y_{char} in **Table 5-2**. Moreover, the pyrolysis of algae finished earlier and required less activation energy under CO_2 in **Section 5.2.1**. Such elements including Na, Mg, Al, Si, P, K, Ca, and Fe, in the char of algae pyrolyzed under CO_2 declined as the heating rate rising. At the heating rate of 5 °C min^{-1}, these elements were significantly larger than the amount derived under N_2, especially for P, K, Ca, and Fe. Similar trend has been found in the pyrolysis of ovalbumin under CO_2 for elements such as Mg, P, K, and Ca.

However, for cellulose, the elements in char kept the same for processing under both N_2 and CO_2 in various heating rates (carbon, 27.3wt.%; oxygen, 72.7 wt.%), which is corresponding to the relatively unchanged activation energy calculated in **Table 5-6** as well as the derived r values. This indicated CO_2 rarely participated in the pyrolysis of carbohydrate content in algae.

The different heating rate have significant influence on the carbon content in char after the pyrolysis under CO_2 atmosphere, since CO_2 atmosphere could improve the cracking of VOCs and the reaction between VOCs and CO_2. The carbon content will increase as the increment of heating rate. In order to investigate the effects of processing time on carbon content of solid residue, the pyrolysis of char which was prepared by the tube furnace (using a simulated TGA process under 5 °C min^{-1}) was conducted under four heating rates in CO_2 atmosphere. As the heating rate increased from 5 to 50 °C/min, the carbon content of the newly-prepared char from spirulina and ovalbumin increased from 2.0 to 9.1 wt. % and 15.1 to 29.0 wt. %, while that of chlorella and porphyra char decreased from 62.1 to 9.9 wt. % and 23.4 to 5.3 wt. %. The carbon content of cellulose char remained steady around 93 wt. %. This indicated CO_2 atmosphere would participate in the reaction with carbon contained in char as the pyrolysis progressing, mainly due to the gasification of CO_2 and carbon content $[C(s) + CO_2(g) \leftrightarrow 2CO(g)]$. That reaction of spirulina

and ovalbumin char became more severe at longer processing time or lower heating rate.

Therefore, the pyrolysis of under CO_2 would favor the pyrolysis of protein content in algae but have no effects on the decomposition of carbohydrate. Longer processing time or lower heating rate under CO_2 could diminish the amount of char residue from algal protein component.

Table 5-10 The elemental compositions of solid residues of spirulina, chlorella, porphyra, ovalbumin and cellulose derived by EDS (Wt.%).

Spirulina												
Heating rate (°C min^{-1})	N_2				CO_2				Char CO_2			
	5	10	20	50	5	10	20	50	5	10	20	50
C	25.4	23.1	24.1	25.0	3.7	15.2	23.8	24.5	2.0	7.7	9.2	9.1
N	-	-	0.7	0.8	-	-	-	-	-	-	-	-
Na	0.4	0.5	0.6	0.4	2.5	1.7	0.8	0.7	4.7	2.6	4.3	2.9
Mg	0.5	0.8	0.6	0.4	4.5	2.3	0.8	0.7	5.9	6.8	4.8	4.9
Al	0.1	0.3	0.3	0.2	3.0	0.9	0.6	0.1	2.2	1.8	2.9	3.1
Si	0.40	0.4	0.2	0.2	2.8	1.0	0.9	0.3	5.2	2.5	5.4	4.1
P	1.41	2.5	1.2	0.9	14.9	5.9	1.8	1.3	13.1	12.1	11.2	11.6
S	0.1	0.1	-	-	-	0.1	0.1	-	-	0.1	-	-
Cl	-	-	-	-	-	0.1	-	-	0.1	-	-	-
K	0.9	1.5	1.0	0.8	13.7	7.0	1.8	1.6	9.4	9.7	7.7	10.3
Ca	0.3	2.1	0.7	0.2	3.4	2.0	0.8	0.4	5.2	10.4	4.2	6.7
Fe	0.1	1.0	0.3	0.4	3.6	1.8	1.1	0.4	4.2	5.6	3.0	4.3
O	70.8	67.8	70.2	70.9	45.2	56.3	68.0	69.8	47.7	34.4	47.3	42.8
Chlorella												
Heating rate (°C min^{-1})	N_2				CO_2				Char CO_2			
	5	10	20	50	5	10	20	50	5	10	20	50
C	25.0	25.5	24.9	25.2	-	21.8	24.7	24.5	62.1	25.8	42.5	9.9
N	-	-	-	-	-	-	0.6	0.8	-	-	-	-
Na	0.4	0.3	0.4	0.4	5.3	1.3	0.4	0.5	1.5	3.0	2.5	3.6
Mg	0.5	0.3	0.3	0.3	5.8	1.2	0.3	0.3	1.1	2.5	2.3	4.4
Si	0.1	-	-	-	4.0	0.2	0.1	-	0.2	0.9	0.3	7.6
P	2.3	1.5	2.3	2.0	13.5	7.9	1.3	1.9	5.8	14.0	9.8	9.2
K	0.9	1.3	1.6	1.3	7.9	7.1	0.8	1.2	4.1	9.6	0.3	7.2

Ca	0.3	0.2	0.3	0.2	6.4	1.1	1.3	0.1	0.7	2.8	1.5	3.2
Fe	0.1	0.1	0.1	0.1	6.3	0.4	-	0.1	0.2	0.5	0.5	4.1
O	70.5	70.7	70.1	70.5	47.5	58.5	70.5	70.6	24.1	39.7	33.2	47.5
Porphyra												
Heating rate (°C min^{-1})	N_2				CO_2				Char CO_2			
	5	10	20	50	5	10	20	50	5	10	20	50
C	24.4	24.3	21.9	22.6	10.1	14.3	15.0	19.7	23.4	8.4	4.8	5.3
Na	0.5	2.1	0.8	0.7	4.3	3.9	3.9	2.2	4.9	7.0	8.5	7.7
Mg	0.4	0.3	0.8	0.4	4.9	5.1	1.9	1.1	3.0	2.9	4.5	3.2
Si	0.3	0.0	0.3	0.2	2.6	1.3	1.2	0.2	5.1	3.5	1.9	8.1
P	0.5	0.5	1.6	1.2	4.9	6.4	4.2	2.2	6.5	13.7	14.8	10.0
S	0.1	-	-	0.5	-	-	-	-	1.5	1.9	0.5	0.2
K	0.2				4.2	-	-	0.9	15.4	20.7	14.7	18.4
Ca	0.1	0.3	0.7	0.5	3.6	1.4	1.4	0.4	2.3	4.6	4.6	3.7
Fe	0.1		0.3	0.3	2.5	0.5	0.5	0.2	4.2	1.8	1.6	1.5
O	62.0	68.6	65.5	66.2	51.6	57.9	56.9	62.8	32.8	34.5	42.9	41.3
Ovalbumin												
Heating rate (°C min^{-1})	N_2				CO_2				Char CO_2			
	5	10	20	50	5	10	20	50	5	10	20	50
C	25.4	25.6	25.6	25.5	14.9	20.0	22.2	22.2	15.1	28.6	29.6	29.0
N	-	-	0.4	0.3	-	0.9	0.9	1.7	-	-	-	-
Na	-	-	-	-	0.3	-	-	-	9.5	7.2	5.7	5.3
Mg	0.4	0.4	0.4	0.3	2.1	0.9	0.5	0.4	6.3	6.8	4.4	4.5
Si	-	-	-	-	0.1	-	-	-	-	0.1	0.1	-
P	1.4	1.2	1.2	1.0	8.0	2.8	2.2	1.5	13.2	11.9	9.6	11.6
S	-	-	-	0.1	-	-	-	-	-	-	-	-
Cl	-	-	-	-	-	0.1	-	-	-	-	-	-
K	2.2	2.1	1.8	1.4	10.3	4.5	3.6	1.8	0.3	0.4	0.4	0.6

Ca	0.4	0.2	0.2	0.2	1.6	0.4	0.7	0.2	11.6	11.9	12.9	16.5
Fe	-	-	-	0.1	-	-	-	-	0.2	0.6	0.2	0.3
O	70.3	70.5	70.6	70.8	55.9	62.9	66.4	67.6	43.0	31.8	36.6	31.6
Cellulose												
Heating rate (°C min^{-1})	N_2				CO_2				Char CO_2			
	5	10	20	50	5	10	20	50	5	10	20	50
C	27.3	27.3	27.3	27.3	27.3	27.3	27.3	27.3	92.9	90.5	94.3	94.0
O	72.7	72.7	72.7	72.7	72.7	72.7	72.7	72.7	7.1	9.5	5.7	6.0

5.3 Summary

The pyrolysis behaviour and the kinetic characteristic of three primary algae components (lipid, carbohydrate and protein) and three representative algae, i.e. microalgae-spirulina and chlorella, macroalgae-porphyra, pyrolyzed under nitrogen and carbon dioxide were investigated using a thermogravimetric analyzer (TGA) in this study. The iso-conversional method, Kissinger- Akahira-Sunose (KAS) was employed based on the Arrhenius Law to determine activation energy and pre-exponential factor from the weight loss profiles. On the other hand, the model fitting Coats-Redfern method was used to calculate the kinetic parameters and determine the order and mechanism of reaction. Upon comparison of the activation energy derived from the pyrolysis processes, ovalbumin and spirulina required the least amount of energy (66.8 and 20.7 kJ/mol) to initiate pyrolysis under CO_2. Moreover, the time required to complete the pyrolysis under CO_2 atmosphere was shortened by 2.1-20.2% which indicated that CO_2 could assist in the pyrolysis of algae and its protein contents. On the contrary, oil droplets required higher activation energy thus suggesting the difficulty of algal lipid to pyrolyze under CO_2 atmosphere. However, the activation energy appeared similar for the pyrolysis of cellulose under the two carrier gas tested. It was also found that the protein components in algae are the first to decompose followed by carbohydrates and lastly lipids. This study shows that CO_2

atmosphere is favourable for algae pyrolysis when the protein content is high whilst lipid content is low.

Chapter 6. Microwave-enhanced pyrolysis of algae for syngas production

In this chapter, microwave-enhanced pyrolysis of microalgae (spirulina, chlorella and dunaliella), macroalgae (laminaria and porphyra) is carried out together with the pyrolysis of model algae prepared by using α-Cellulose and ovalbumin to represent the primary constituents of algae [233]. The reaction pathways for five algae to yield syngas-rich gaseous fraction via microwave-enhanced pyrolysis are investigated. The difference in syngas production between microwave-enhanced pyrolysis of macroalgae (porphyra, laminaria) and microalgae (spirulina, chlorella, dunaliella) is investigated. Meanwhile, the characterisation of pyrolytic bio-oil and char is also conducted.

6.1 Influences of heating rate

The pyrolysis temperature was measured and regulated by using a thermocouple inserted in the reaction bed when it was under temperature-controlled mode. The microwave input power level was regulated based on the pre-set temperature. It is generally agreed that the higher the microwave power, the greater the inner energy generated within the sample and thus higher heating rate. From the microwave heating profiles, it was found that the temperature increased significantly during the first 8-9 min and then became

relatively steady due to the balance between heat generation and heat loss [156]. Since the instant heating property of microwave heating, algae absorbed much energy to start decomposition. As the depletion of reactants and the release of products, the amount of energy absorbed reduced and then maintained around the same level. The poor microwave absorption capability of algal biomass resulted in the slow increase in pyrolysis temperature. The addition of sufficient amount of microwave absorbents enhanced heat transfer during the pyrolysis process and reduced the time required to reach the set point of pyrolysis temperature due to their outstanding dielectric properties [140]. The SiC is heated up first and then energy is transferred to the samples resulting in the samples being heated up via conventional heating and microwave heating simultaneously. The biomass is thus decomposed into vapour and char at high temperatures. The high temperature vapour was then cooled down to form bio-oil and gaseous fraction.

Figure 6-1 shows that the average heating rate (β_i), which was the instant temperature (T_i) divided by time (t) to reach that temperature, changes with time at three targeted pyrolysis temperatures. At the initial stage of pyrolysis, the heating rate was extremely high at around 160 °C min^{-1} but sharply reduced to about 30 °C min^{-1} within one minute. The curves are characteristics of different samples. However, after 7-15 min, the heating rates of different samples

decreased steadily to the same level, which corresponds to the period that target temperature was achieved and kept fluctuating around this temperature.

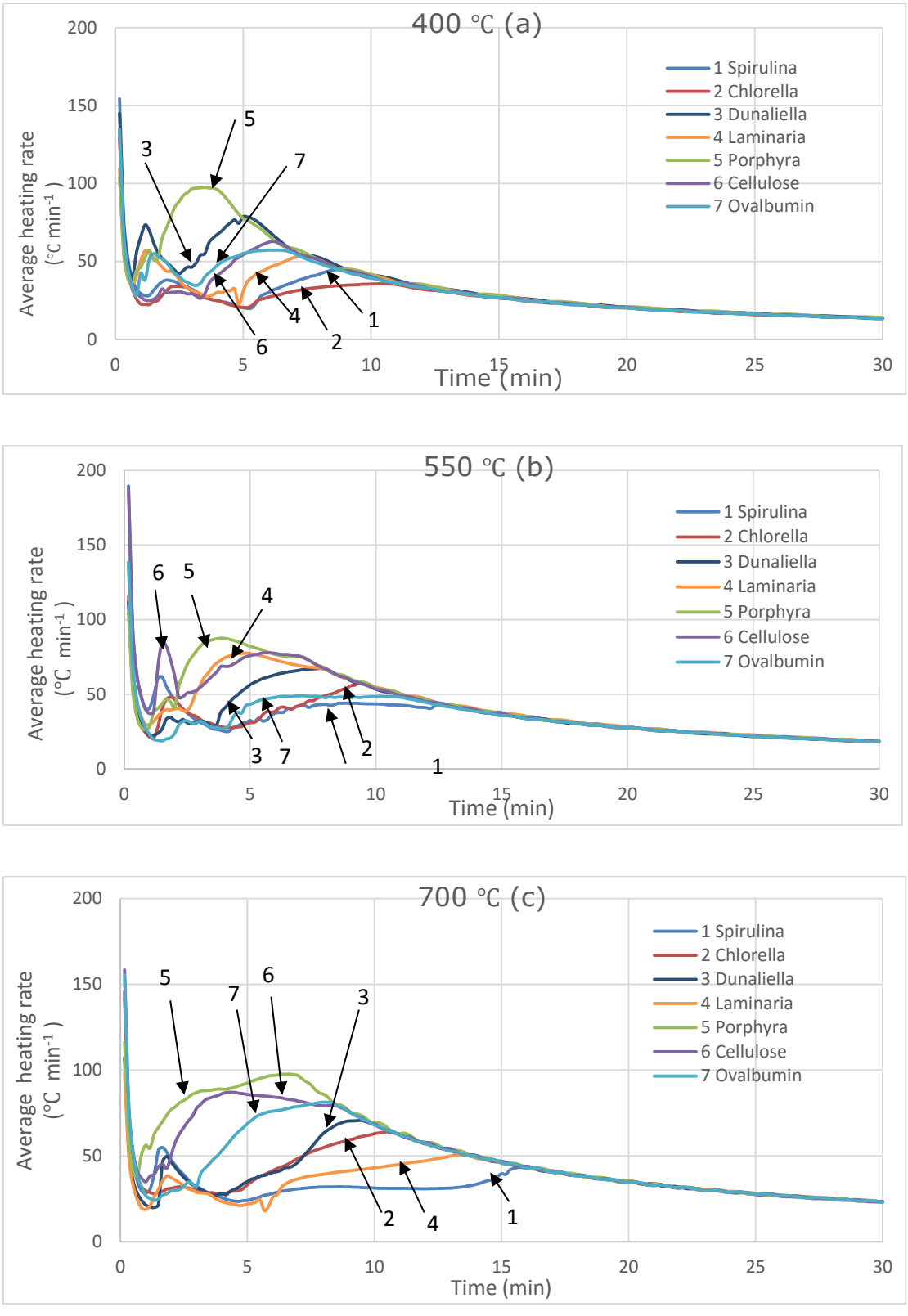

Figure 6-1 Average heating rate of spirulina, chlorella, dunaliella, laminaria, porphyra, cellulose and ovalbumin at target temperatures of 400℃ (a), 550℃ (b) and 700℃ (c)

In the first 7 min, the heating rate profiles of the seven samples differed from each other, due to their various content of moistures and volatiles. β_i curve for cellulose was lower than that of ovalbumin at 400 °C, but increased and became higher than that of ovalbumin when the target temperature was changed to 550 °C. At 700 °C, the β_i values of cellulose were much greater than those of ovalbumin. Similar correlation was found in the curves of β_i between spirulina and chlorella. This might be due to the higher carbohydrate content in chlorella and the relatively high protein composition in spirulina. Both of dunaliella and laminaria contained high level of carbohydrate; hence, the temperature followed similar pattern as shown by cellulose. As the target temperature rose to 550 °C, the value of β_i increased significantly, but reduced slightly after the aiming temperature changed to 700 °C. It was clear that porphyra achieved the highest rate among all the samples at the three operating temperature levels.

Normally, heating rate is highly correlated with the combustible content (volatiles and fixed carbon) of the feedstocks, and increases with the increase in combustible content [234]. Therefore, porphyra with the largest combustible content among the five algae (87. 7 wt.%) demonstrated the highest heating rate. Meanwhile, moisture content is found to be a dominant factor in raising dielectric properties as well as heating rate in this pyrolysis of algae since water is an excellent microwave absorber owing to its dielectric property

and polar nature [139]. Porphyra with the highest moisture content depicted the fastest increase in temperature compared with the other four algae samples as well as the two model compounds.

The conversion of electromagnetic energy into heat is dependent largely on the dielectric properties of the materials [235]. The dielectric properties of algal vary insignificantly at lower temperatures. After being heated to a temperature beyond 350-450°C, biomass is transformed into carbonaceous material and its dielectric properties would be changed significantly [236]. Bio-char has been proven to have good microwave absorbing properties due to its high carbon content [235]. In addition, the density of biomass also favors the increase in dielectric properties [237]. The heating rate of porphyra pyrolysis was the highest, which can be attributed to its higher density and thus higher dielectric properties. The low thermal conductivity of materials to be processed using microwave irradiation is considered to limit heat transfer or high heating rate of the process [238]. However, algal biomass has extremely low thermal conductivity (<< 1.0 W/ (m·K)); therefore, it has insignificant influence on the heating rate when algae is processed alone under microwave irradiation.

6.2 Differences in product yield

The yields of gas, liquid and solid product from spirulina, chlorella, dunaliella, laminaria, porphyra, cellulose and ovalbumin at different

pyrolysis temperatures (400, 550 and 700 °C) are presented in **Table 6-1**. When the pyrolysis temperature was raised from 400 to 700 °C, cellulose led to the formation of approximately 7 wt.% of char, 3 wt.% of bio-oil and 90 wt.% of gaseous fraction, whilst around 4 wt.% of char, 15 wt.% of bio-oil and 81 wt.% of gas product were generated from ovalbumin. Dunaliella with extremely high carbohydrate content (94 wt.%) showed a similar product distribution with gas product over 85 wt.% as cellulose, which had low oil production around 7 wt.%, but more than 89 wt.% gas yield. Similar product distribution with more than 85 wt.% of gaseous fraction was also found in the pyrolysis of porphyra which have relatively high carbohydrate content of 47.7 wt.%. For protein-rich microalgae-spirulina and chlorella (around 56 wt.%), the product distribution was comparable to that of ovalbumin with a higher oil production around 6-15 wt.% and less gas production at about 79-84 wt.%. The lowest amount of gas product was yielded from the pyrolysis of laminaria at 400°C which was less than 75 wt.%, although it contained high percentage of carbohydrate (51.8 wt.%). This might be due to the high proportion of ash and fixed carbon in laminaria (about 25 wt.%), which was difficult to be converted into volatiles. The maximum gaseous fraction was 90.1 wt.% for dunaliella as observed at 400 °C, followed by porphyra. It produced 87 wt.% of gaseous faction at 700 °C, while for spirulina the largest gas production was 83.7 wt.% at the same temperature. As for chlorella, 84 wt.% of the product yield was

gaseous fraction at 400 °C. Therefore, it appeared that dunaliella had the highest gas yield among the five algae due to its greater carbohydrate whilst lower protein led to lower oil yield.

Table 6-1 Product distribution of MEP of algae at 400, 550 and 700°C (100 wt.%)

	Temperature(°C)	Solid	Liquid	Gas
Spirulina	400	9.2±1.9	10.9±2.1	79.9±4.0
	550	5.4±0.4	12.8±1.1	81.8±1.5
	700	9.9±1.3	6.3±1.7	83.8±3.0
Chlorella	400	8.0±1.4	8.0±0.9	84.0±2.3
	550	11.7±2.4	8.9±0.8	79.5±3.2
	700	5.8±0.2	15.4±2.3	78.9±2.5
Dunaliella	400	4.7±0.4	5.2±1.0	90.1±1.4
	550	6.0±0.9	9.3±2.0	84.7±2.9
	700	5.2±1.1	7.4±0.9	87.4±2.0
Laminaria	400	20.4±2.9	5.2±0.7	74.4±3.6
	550	18.9±3.1	2.2±0.5	79.0±3.6
	700	20.7±2.2	3.7±0.6	75.6±2.8
Porphyra	400	12.6±1.3	1.8±0.2	85.6±1.5
	550	11.2±2.1	2.4±0.1	86.4±2.2
	700	10.7±1.1	2.2±0.1	87.1±1.2
Cellulose	400	7.5±1.0	3.5±0.4	89.0±1.4
	550	5.3±0.5	2.7±0.1	92.0±0.6
	700	5.4±0.7	2.6±0.1	92.0±0.8
Ovalbumin	400	3.5±0.3	15.3±1.5	81.2±1.8
	550	3.1±0.4	13.3±2.0	83.6±2.4
	700	4.9±0.7	16.3±1.3	78.8±2.0

In general, a lower pyrolysis temperature leads to a higher production of char while higher temperature favours the yield of gaseous fraction [239]. This has been observed where the production of gas from spirulina and porphyra increased over the pyrolysis temperatures investigated. Meanwhile, a smaller amount of pyrolyzed char derived from porphyra was formed when the operating temperature was raised to a higher level. The gaseous fraction pyrolyzed from

dunaliella decreased slightly when the target temperature rose to 550 °C, but increased immediately after the temperature changed to 700 °C, which had opposite trend with that of laminaria. For spirulina, dunaliella and porphyra, the bio-oil production reached the maximum at 550 °C, which is similar to the results of most previous studies about temperature effects on pyrolysis, which reported that optimal pyrolysis temperature for bio-oil yield was between 450-550 °C [240-242]. Beyond that temperature, secondary cracking of oil vapours into incondensable gaseous fractions lead to the reduction of bio-oil and growth of gas yield [156]. Conversely, the gas yield from the pyrolysis of chlorella decreased when the temperature increased over the same range; meanwhile the yield of bio-oil decreased when the temperature was raised to higher levels. The significant variation of char yield for different species is speculated to be depended on the mineral contents in algae. It was reported that higher alkali content normally results a greater amount of char being formed after pyrolysis [243].

6.3 Characteristics of gas products and reaction pathways

According to **Table 6-2**, CO and CO_2 were the main permanent gaseous products due to the high oxygen content of the feedstock. CO_2 was mainly produced from carboxyl groups in protein and from the decomposition of cellulose and hemicellulose for terrestrial

biomass [244]. It is generally believed that when the sample is heated to higher temperatures, the secondary cracking reactions of gaseous products take place and a larger amount of incondensable gas is formed, which subsequently results in a higher yield of pyrolyzed gaseous fraction. The primary and secondary cracking reactions (R.1 - 11) are listed as follow [245],

$$\mathrm{Tar(g)} \rightarrow \mathrm{CH_4}(g) + H_2O(g) + H_2(g) + C_mH_n(g) \quad (1)$$

$$\mathrm{CH_4}(g) + H_2O(g) \leftrightarrow \mathrm{CO(g)} + 3H_2(g) \quad (2)$$

$$\mathrm{C}(s) + H_2O(g) \leftrightarrow \mathrm{CO(g)} + H_2(g) \quad (3)$$

$$\mathrm{C}_m\mathrm{H}_n(g) + 2mH_2O(g) \rightarrow \mathrm{mCO_2(g)} + [2\mathrm{m} + \tfrac{\mathrm{n}}{2}]H_2(g) \quad (4)$$

$$\mathrm{C}_m\mathrm{H}_n(g) + mH_2O(g) \rightarrow \mathrm{mCO(g)} + [\mathrm{m} + \tfrac{\mathrm{n}}{2}]H_2(g) \quad (5)$$

$$\mathrm{CO}(g) + H_2O(g) \leftrightarrow \mathrm{CO_2(g)} + H_2(g) \quad (6)$$

$$C(s) + CO_2(g) \leftrightarrow 2CO(g) \quad (7)$$

$$\mathrm{CH_4}(g) \leftrightarrow \mathrm{C(s)} + 2H_2(g) \quad (8)$$

$$\mathrm{CH_4}(g) + CO_2(g) \leftrightarrow \mathrm{2CO(g)} + 2H_2(g) \quad (9)$$

$$\mathrm{C}_m\mathrm{H}_n(g) + mCO_2(g) \rightarrow \mathrm{2mCO(g)} + [\tfrac{\mathrm{n}}{2}]H_2(g) \quad (10)$$

$$\mathrm{C}_m\mathrm{H}_n(g) \rightarrow \mathrm{mC(s)} + [\tfrac{\mathrm{n}}{2}]H_2(g) \quad (11)$$

Table 6-2 Compositions of gaseous fraction from different algae at 400, 550 and 700°C. (100 vol. %)

	Temperature(°C)	CH_4	C_2H_6	C_2H_4	C_3H_8	CO_2	CO	H_2	Others	Syngas (CO+ H_2)	HHV (MJ/Nm^3)
Spirulina	400	16.5	6.1	1.4	1.0	14.3	20.4	26.2	14.1	46.6	18.7
	550	16.8	5.4	2.0	0.7	18.1	22.1	26.9	8.1	49.0	18.6
	700	10.9	3.3	0.5	0.2	6.4	33.3	26.1	19.3	59.4	14.7
Chlorella	400	14.2	5.7	1.6	0.8	19.1	22.2	31.1	5.3	53.3	18.3
	550	16.6	5.6	1.3	0.7	12.4	23.6	26.1	13.7	49.7	18.4
	700	16.8	5.6	1.3	0.4	15.1	27.8	31.9	1.1	59.7	19.4
Dunaliella	400	10.5	5.8	0.9	0.6	13.3	34.3	21.2	13.4	55.5	16.5
	550	9.6	2.6	1.2	0.3	17.5	33.3	22.6	12.9	55.9	13.8
	700	11.6	5.2	0.6	0.7	11.2	34.6	26.3	9.8	60.9	17.1
Laminaria	400	8.3	1.1	1.1	0.1	23.3	29.0	30.4	6.7	59.4	12.4
	550	6.5	1.3	0.5	0.2	14.7	31.0	40.4	5.5	71.4	13.0
	700	7.1	1.3	1.1	0.1	21.3	29.2	30.0	9.9	59.2	12.1
Porphyra	400	8.1	2.6	0.3	0.3	11.1	35.6	33.2	8.8	68.8	14.3
	550	6.4	0.3	0.1	0.1	7.5	40.7	38.6	6.3	79.3	13.0
	700	7.2	1.6	0.2	0.2	11.5	34.5	38.8	6.0	73.3	13.6
Cellulose	400	9.2	0.4	3.2	0.0	7.3	53.3	16.9	9.7	70.2	14.9
	550	8.1	0.5	1.7	0.0	15.1	42.8	23.8	8.0	66.5	13.1
	700	10.0	0.6	3.3	0.0	10.9	45.6	19.4	10.2	65.0	14.7
Ovalbumin	400	11.0	1.5	3.4	0.6	27.6	30.7	14.1	11.0	44.9	14.0
	550	15.7	1.8	4.4	0.6	25.9	18.8	17.3	15.4	36.1	15.6
	700	10.5	0.4	2.2	0.0	2.5	55.6	24.1	4.7	79.7	16.0

Water is known to have outstanding dielectric properties and absorbs microwave energy and evaporates immediately after formation. Therefore, heterogeneous reactions involving H_2O such as R. 3 are less favoured during the course of microwave-enhanced pyrolysis in a fixed-bed reactor. Microwave-enhanced pyrolysis could assist in the cracking reaction of C1 to C3 hydrocarbons (R.11), particularly the cracking of CH_4 on the surface of char via R.8. This would result in a higher amount of carbon deposits remaining as solid residues when pyrolysis proceeds further. When the temperature was raised to 800 °C or above, carbon deposits start to react with CO_2 and generate CO in an anaerobic atmosphere (R. 7), which suggests that high pyrolysis temperatures result in the formation of less char and favour the formation of more CO. At high pyrolysis temperatures, the reaction between CH_4 and CO_2 (R.9) is enhanced, and leads to the formation of more CO and H_2, so does R10. It is also clear in this study that the CO content of microwave pyrolytic gaseous fraction increased with the increase in temperature, the same as H_2. CO_2 derived from cellulose increased from 7.3 to 15.1 vol. % at lower temperatures but decreased to 10.9 vol. % as the pyrolysis temperature increased, which was the same for CO and H_2. Similar trend was observed in the MEP of ovalbumin, spirulina, dunaliella and laminaria. But porphyra has increasing amount of CO and H_2 with decreasing content of CO_2 along with the growing target temperature.

When the pyrolysis temperature was raised to higher levels, the amount of syngas produced from cellulose decreased slightly from 70.2 vol. % at 400 °C to 65.0 vol. % at 700 °C. On the contrary, the syngas yield from ovalbumin increased significantly from 44.9 to 79.7 vol. %. Compared with other algae, porphyra led to the formation of a significant amount of syngas with a 23.4 - 61.8 % improvement compared with spirulina and 22.8 - 59. 6 % improvement compared with chlorella due to its high carbohydrate content, which favours the formation of PAHs and small gas molecules under high temperatures according to **Section 6.4**. However, both of laminaria and dunaliella contained much more carbohydrates with 52 and 94 wt.% respectively, while yielded 10-20% and 17- 30% lower volume of syngas compared with porphyra. Reactions 9 and 10 could explicate the formation of considerable lower amount of C1-C3 hydrocarbons (6.9-11.3 vol. %) and CO_2 in the final gas yield from macroalgae (laminaria and porphyra), which was less than half of that of the C1-C3 gas yield from microalgae, i.e., spirulina (14.9-25.0 vol. %), chlorella (22.3-24.2 vol. %) and dunaliella (13.7-18.1 vol. %). Meanwhile, the ratio of H_2 to CO for macroalgae was around 1 (0.8-1.1). Compared with syngas produced via coal water slurry gasification (80-84%) and pulverized coal gasification (90-93 %) [246], the pyrolysis of porphyra showed similar $CO+H_2$ content in the gaseous fraction. With further steam reforming of C1-C3 hydrocarbons, the percentage of syngas ($CO+H_2$) might be

comparable with the yield of commercial gasification processes. It can therefore be concluded that the pyrolysis of macroalgae-porphyra is an approach of great potential for the production of syngas in large scale.

However, the gaseous fraction derived from macroalgae (laminaria and porphyra) have relatively lower heating value at different temperatures (12.1-13.0 and 13.0-14.3 MJ/Nm^3 respectively), which were calculated to be 6 to 38 % lower compared with gas derived from spirulina (14.7-18.7 MJ/Nm^3), chlorella (18.3-19.4 MJ/Nm^3) and dunaliella (13.8-17.1 MJ/Nm^3). This is because the gaseous fraction derived from macroalgae contained less C1-C3 components which have higher heating values. But all the HHVs of gas products obtained from algae showed much higher value compared with the HHVs of clean gases from gasification processes of coal water slurry and pulverized coal (9.5-13.2 MJ/Nm^3).

6.4 Dependence of bio-oil composition on raw materials

Algae-derived oils are red brown colour with strong odour, similar to oils derived from other biomasses. GC-MS analysis was carried out in this study to determine the percentage of major compounds present in the pyrolytic bio-oil derived from the five algae samples and the two primary model compounds at different temperatures, which was calculated based on the relative percentage of chromatographic area of individual compounds. Compounds such as phenols, polycyclic

aromatic hydrocarbons (PAHs), nitrogenated compounds, aromatic hydrocarbons, aliphatic hydrocarbons and acids, were analyzed. **Table 6-3** shows composition of the bio-oils, which were derived from the five algae and the model compounds pyrolyzed at 400, 550 and 700 °C respectively. It is obvious from **Table 6-3** that at the lowest temperature tested (400 °C), the bio-oil mainly contained phenol, p-Cresol, indole, quinoline, benzene, xylene, naphthalene and their derivatives. When samples were pyrolyzed at 550 °C, fluoranthene, indene and their derivatives were found in algae-derived bio-oil while more acids, naphthalene, biphenylene, phenanthrene, pyrene and their derivatives were produced in algae-derived bio-oil compared with model compounds. However, as the temperature rising up to 700 °C, the fraction of nitrogenated compounds including indole, nitriles decreased slightly, so as phenols (i.e. phenol and p-Cresol), while the amount of aromatics (i.e. ethylbenzene and styrene) kept increasing. More PAHs were formed from microalgae in bio-oil when pyrolysis temperature was raised to higher levels, while that content in bio-oil obtained from macro-algae decreased.

Table 6-3 GC-MS: Bio-oil compositions of α- Cellulose, ovalbumin, spirulina, chlorella, dunaliella, laminaria, porphyra at different pyrolytic temperatures of 400, 550 and 700°C. (100% area)

		α- Cellulose			Ovalbumins			Spirulina			Chlorella			Dunaliella			Laminaria			Porphyra		
Category	**Compounds**	**400**	**550**	**700**	**400**	**550**	**700**	**400**	**550**	**700**	**400**	**550**	**700**	**400**	**550**	**700**	**400**	**550**	**700**	**400**	**550**	**700**
Aromatics	Benzene, 1,3-dimethyl-	-	-	1.7	5.2	1.0	1.4	-	-	-	-	-	-	4.6	1.6	3.9	-	-	-	3.9	2.3	-
	Benzene, 1-ethynyl-4-methyl-	-	-	-	-	-	-	-	-	-	-	-	-	-	-	-	-	-	-	3.1	3.3	-
	Styrene/1,3,5,7-Cyclooctatetraene	0.9	1.8	1.4	1.1	0.9	1.2	2.9	1.5	3.1	1.1	2.9	1.3	3.4	-	-	3.1	8.8	3.1	8.1	5.4	9.6
	o-Xylene	-	-	-	-	-	-	-	-	1.6	-	-	-	4.6	0.4	-	3.3	5.2	3.3	3.9	2.3	4.6
	Ethylbenzene	0.4	1.6	1.7	1.2	1.0	1.4	1.9	0.6	1.5	0.9	1.4	0.7	2.6	-	2.4	3.1	1.5	3.4	1.8	1.2	2.0
	t-Butylhydroquinone	-	-	-	-	-	-	-	-	-	-	-	-	8.8	10.8	9.9	-	-	-	-	-	-
	2-Furanmethanol	-	-	-	-	-	-	-	-	-	-	-	-	5.4	7.0	6.8	-	-	-	-	-	-
	tert-Butyl-p-benzoquinone	-	-	-	-	-	-	-	-	-	-	-	-	0.9	7.0	-	-	-	-	-	-	-
	1-Dodecanol, 3,7,11-trimethyl-	-	-	-	-	-	-	-	-	-	-	-	-	3.3	4.6	-	-	-	-	-	-	-
	Total	**1.3**	**3.4**	**4.8**	**7.4**	**3.0**	**4.0**	**4.8**	**2.1**	**6.2**	**2.0**	**4.3**	**2.0**	**33.6**	**31.4**	**23.0**	**9.5**	**15.5**	**9.8**	**20.8**	**14.5**	**16.2**
Aliphatics	Heptadecane	-	-	-	-	-	-	3.8	4.1	-	-	-	-	-	-	-	-	-	-	-	-	-
Phenols	p-Cresol	2.4	2.4	1.0	4.9	7.0	5.3	8.8	8.5	6.0	11.1	8.5	6.8	1.7	1.2	-	5.6	2.0	4.3	6.4	4.6	3.2
	Phenol	6.5	5.4	3.0	3.2	4.8	3.3	7.9	9.3	9.2	6.0	4.0	4.0	1.9	1.4	1.6	6.4	1.9	4.6	3.6	2.2	-
	Total	**8.9**	**7.8**	**4.0**	**8.1**	**11.8**	**8.6**	**16.7**	**17.8**	**15.2**	**17.1**	**12.5**	**10.8**	**3.6**	**2.6**	**1.6**	**12.0**	**3.9**	**8.9**	**10.0**	**6.8**	**3.2**
Nitrogenated compounds	Indole	-	-	-	5.2	7.2	6.4	14.6	12.8	9.7	13.9	10.1	10.5	-	-	-	8.1	5.2	7.3	6.0	4.5	2.5
	1H-Indole, 4-methyl-	-	-	-	1.7	2.2	1.6	3.8	3.7	3.9	3.2	2.8	2.1	-	-	-	-	-	2.1	-	-	-
	Benzyl nitrile	-	-	-	1.0	1.1	1.0	2.5	2.5	2.0	1.8	2.2	1.6	-	-	-	-	0.5	-	-	-	-
	Benzonitrile	-	-	-	0.4	0.9	1.9	3.0	2.5	3.5	1.5	2.1	3.0	-	-	-	-	-	-	3.0	3.6	2.8
	Quinoline	-	-	-	0.7	1.2	1.8	4.8	4.1	3.8	3.7	3.7	4.4	-	-	-	2.7	-	2.5	3.3	2.3	-
	Total	**0**	**0**	**0**	**9.0**	**12.6**	**12.7**	**28.7**	**25.6**	**22.9**	**24.1**	**20.9**	**21.6**	**-**	**-**	**-**	**10.8**	**5.7**	**11.9**	**12.3**	**10.4**	**5.3**
Acids	n-Hexadecanoic acid	-	-	-	-	-	-	3.4	5.2	3.0	1.0	1.8	0.5	-	-	-	-	-	-	-	-	-
	Benzoic acid	-	-	-	-	-	-	-	-	-	-	-	-	0.3	3.0	1.4	-	-	-	-	-	-
	Total	**-**	**-**	**-**	**-**	**-**	**-**	**3.4**	**5.2**	**3.0**	**1.0**	**1.8**	**0.5**	**0.3**	**3.0**	**1.4**	**-**	**-**	**-**	**-**	**-**	**-**
PAHs	Naphthalene	2.7	2.4	1.6	0.9	2.1	3.5	6.9	6.4	6.1	8.3	9.2	14.5	10.5	6.4	11.2	8.2	11.7	7.4	15.2	19.7	14.6
	Anthracene	3.2	3.8	1.4	0.4	0.5	1.0	3.1	1.4	3.6	2.8	4.3	6.2	3.7	1.2	5.2	2.4	7.1	5.4	7.0	8.1	6.5
	Pyrene	0.4	0.4	1.2	-	-	0.4	-	-	-	0.6	1.1	0.7	1.6	-	3.0	1.0	2.5	3.9	2.1	3.2	3.5
	Fluoranthene	1.3	1.6	1.5	-	-	0.3	0.7	0.5	1.8	-	1.5	1.9	1.4	-	2.7	-	2.6	2.5	2.0	3.4	3.9
	Indene	-	-	-	-	-	-	1.0	1.3	0.5	0.7	1.4	1.2	2.9	-	-	1.4	4.2	-	-	-	4.9
	Biphenylene	2.4	2.8	0.7	-	0.3	0.8	2.3	1.8	3.0	2.8	3.2	5.3	4.5	1.1	6.1	-	7.3	6.4	7.4	9.4	5.8
	Total	**10.0**	**11.0**	**6.4**	**1.3**	**2.9**	**6.0**	**14.0**	**11.4**	**15.0**	**15.2**	**20.7**	**29.9**	**24.6**	**8.7**	**28.2**	**13.0**	**35.4**	**25.6**	**33.7**	**43.8**	**39.2**
HHVs (MJ/kg)		**5.4**	**5.0**	**6.9**	**3.5**	**4.3**	**4.4**	**3.3**	**3.1**	**2.9**	**5.6**	**3.8**	**4.5**	**4.2**	**3.6**	**1.8**	**3.8**	**1.9**	**3.1**	**2.4**	**3.3**	**3.1**

The bio-oil obtained from the pyrolysis of spirulina contained significantly higher amount of phenols, quinolone, indole, nitriles, fatty acids, heptadecane. The bio-oil derived from chlorella largely consisted of indole, phenols, quinolone, nitriles, styrene, long carbon chain acids and PAHs (naphthalene, anthracene, biphenylene, pyrene). The bio-oil from dunaliella involved considerably large amount of aromatics (t-Butylhydroquinone, 2-Furanmethanol, tert-Butyl-p-benzoquinone, 1-Dodecanol, 3, 7, 11-trimethyl-, benzene) than oil from porphyra and more PAHs (naphthalene, anthracene, biphenylene). A much greater amount of PAHs (naphthalene, biphenylene, and anthracene) and styrene was observed in the bio-oil derived from porphyra, which contained greater carbohydrate content compared with spirulina, chlorella and laminaria. Compared to porphyra, bio-oil derived from laminaria has relatively lower amount of aromatics (styrene, xylene, and ethylbenzene), phenols and PAHs (naphthalene, anthracene, biphenylene). Small quantity of nitrogenated compounds was spotted in the bio-oil from dunaliella, laminaria and porphyra because of their low protein content. This could be explained by none nitrogenated compounds detected in bio-oil from cellulose. Light organics, such as aldehydes, organic acids, ketones and alcohols, which were obtained from carbohydrate compounds in biomass, were deoxygenated and decomposed into C2–C6 olefins [247]. Carbohydrate contents in algae have significant influence on the formation of gaseous fractions. Therefore, dunaliella,

with the highest portion of carbohydrate, produced the largest amount of syngas-rich gaseous fraction.

Unlike terrestrial biomass that consists of lignin, cellulose and hemicellulose as the main compounds, algae are mainly composed of proteins, lipids and carbohydrates, which is shown in **Table 4-5**. Normally, the aromatics in algae derived bio-oil are mainly formed via the decomposition of lipids followed by carbohydrates, while protein has the least contribution to the formation of aromatics under all reaction conditions [233]. For algae, the yield of aromatic hydrocarbons was primarily derived from the lipid fraction at lower operating temperature. However, as the temperature increases, the carbohydrate content in algae dominates the yield of aromatics. Dunaliella has the highest amount of t-Butylhydroquinone, 2-Furanmethanol, tert-Butyl-p-benzoquinone, 1-Dodecanol, 3, 7, 11-trimethyl-, benzene, as well as the total amount of aromatics, while porphyra has the highest amount of styrene, benzene derivatives, xylene, which can be attributed to their high carbohydrate content. Normally, aromatics are desirable products if the products are to be used directly as fuel. In particular, the bio-oil from porphyra has extremely high ratio of styrene (5.4-9.6 %), compared with the other two microalgae (1.1-3.1%). With low viscosity and broad melting temperature range, styrene is generally applied in plastic manufacture as raw materials.

It is also clear that nitrogenated compounds, such as indole, quinoline, benzonitrile, (1H-Indole, 4-methyl-), benzyl nitrile, etc, which are originated from protein, were also found in the bio-oil derived from ovalbumin and the four algae except dunaliella. The bio-oil obtained from the two microalgae with protein content of 56 wt.% contained nitrogenated compounds as high as around 24-29 % and decreased to around 21-23 % when temperature was raised to 700 °C. Porphyra has a low protein content of 35.7 wt.% and resulted in the formation of 5-12 % of nitrogenated substances, much lower than that of spirulina and chlorella, which is similar to laminaria. Therefore, it is speculated that the yield of nitrogenated compounds correlates strongly to the protein content in raw materials. Moreover, biphenylene, fluoranthene and pyrene were found in the oil fraction yielded from the pyrolysis of cellulose and five algae, which suggests that the carbohydrates made noticeable contribution to the formation of PAHs in bio-oil. Porphyra with a carbohydrate content of 47.7 wt.%, produced 33-44 % PAHs, whereas microalgae only produced less than half of that amount. Since the algae samples has very low lipid content in the range of 1.5-5.4 wt.%, the heptadecane in bio-oil derived from spirulina was only around 4 % while others had almost no aliphatic carbohydrates. It is obvious in **Table 6-3** that the yield of phenols (phenol, p-Cresol) decreased with the increase in pyrolysis temperature. Protein content in algae is attributed to the formation of phenols compared with carbohydrate. Approximately 10-18 % in

bio-oil of spirulina and chlorella was phenols, while dunaliella and porphyra only contained 1.5-10 % of phenols.

Therefore, it is evident that protein-rich spirulina and chlorella produced more bio-oil compared with dunaliella, laminaria and porphyra. As the composition of bio-oil is very complex, further upgrading of the liquid products is necessary for its direct use as a transporting fuel or a value-added product, which normally leads to extra processing costs.

6.5 Characteristics of char

6.5.1 Morphologies of char by SEM

The morphologies of char of five algae and two model compounds pyrolyzed at 400, 550 and 700 °C were shown using SEM as **Figure 6-2** to **Figure 6-8** in three magnifications. After pyrolysis, it appeared some original pores, carbon structure and fibres. **Figure 6-8** showed the pyrolysis of ovalbumin under different pyrolysis temperatures, which contained fibres, so as laminaria and porphyra (**Figure 6-5** and **Figure 6-6**). Some porous blocky structures were spotted on chars derived from chlorella and laminaria as indicated in **Figure 6-3** and **Figure 6-5**, which formed from the devolatilization. Since most of the pyrolysis process performed best under 600 °C, the char formed small pores at 400 °C and the number increased when the temperature reached 550°C. However, when the temperature

raised to 700°C, most of the samples rarely have porous structure except for chlorella (**Figure 6-3**).

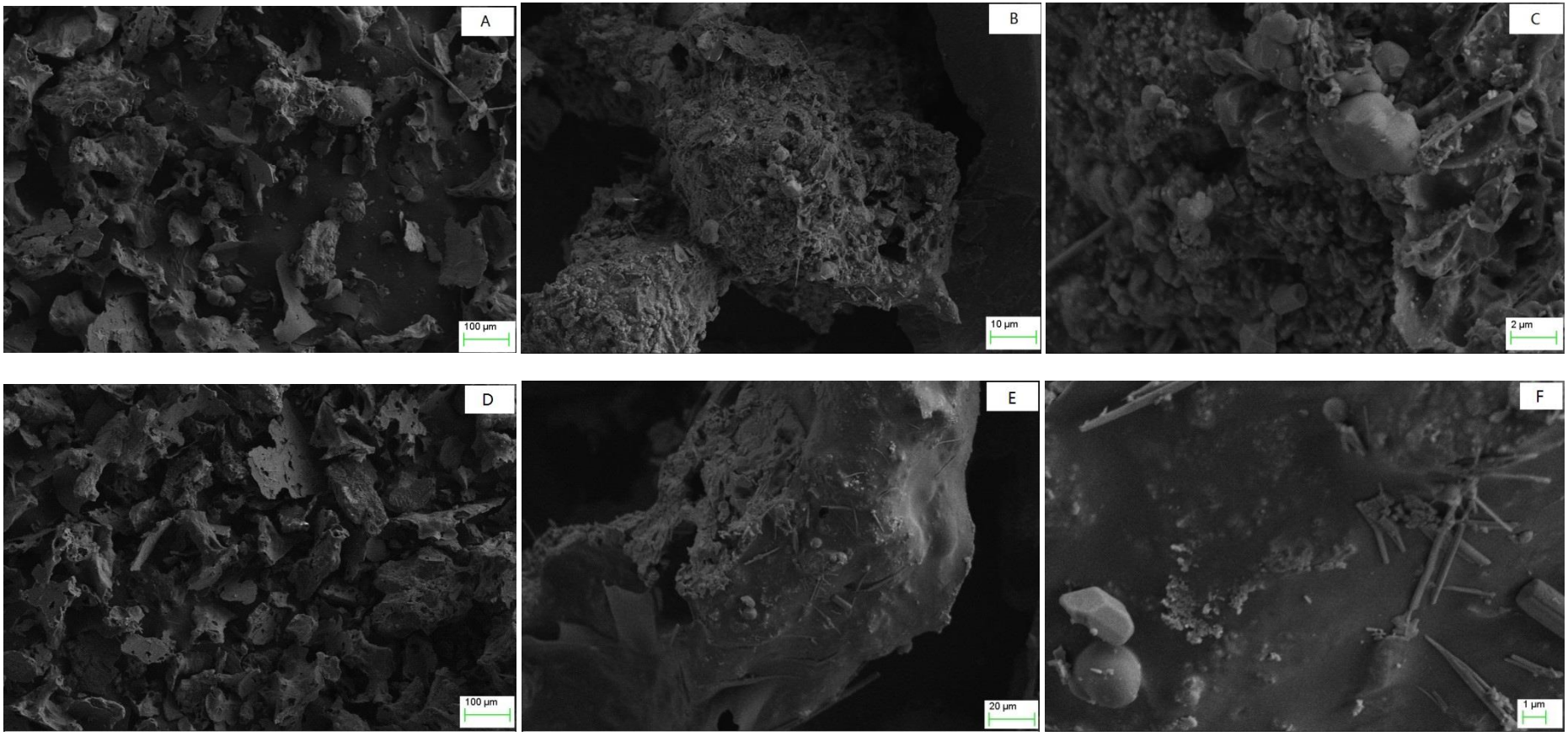
A
100 µm
B
10 µm
C
2 µm
D
100 µm
E
20 µm
F
1 µm

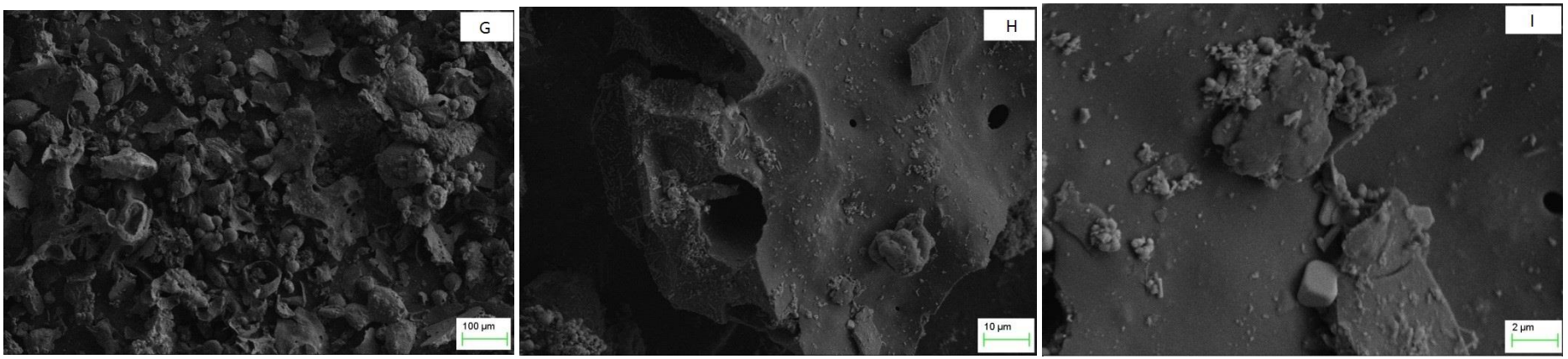

Figure 6-2 SEM images of char pyrolyzed from spirulina at 400 °C with magnification of A x 100, B x 1000, C x 5000; at 550 °C, D x 100, E x 1000, F x 5000; at 700 °C, G x 100, H x 1000, I x 5000

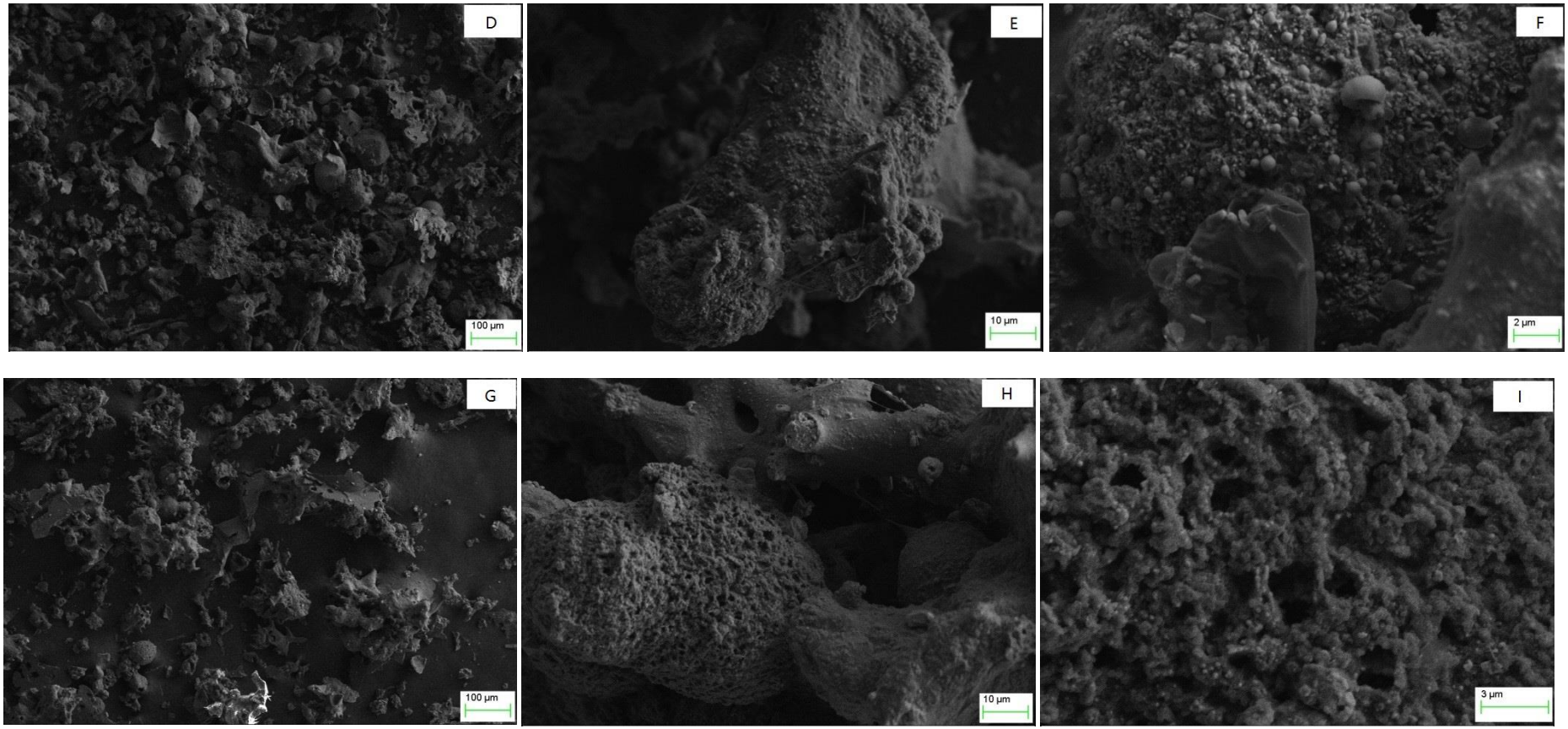

Figure 6-3 SEM images of char pyrolyzed from chlorella at 400 °C with magnification of A x 100, B x 1000, C x 5000; at 550 °C, D x 100, E x 1000, F x 5000; at 700 °C, G x 100, H x 1000, I x 5000

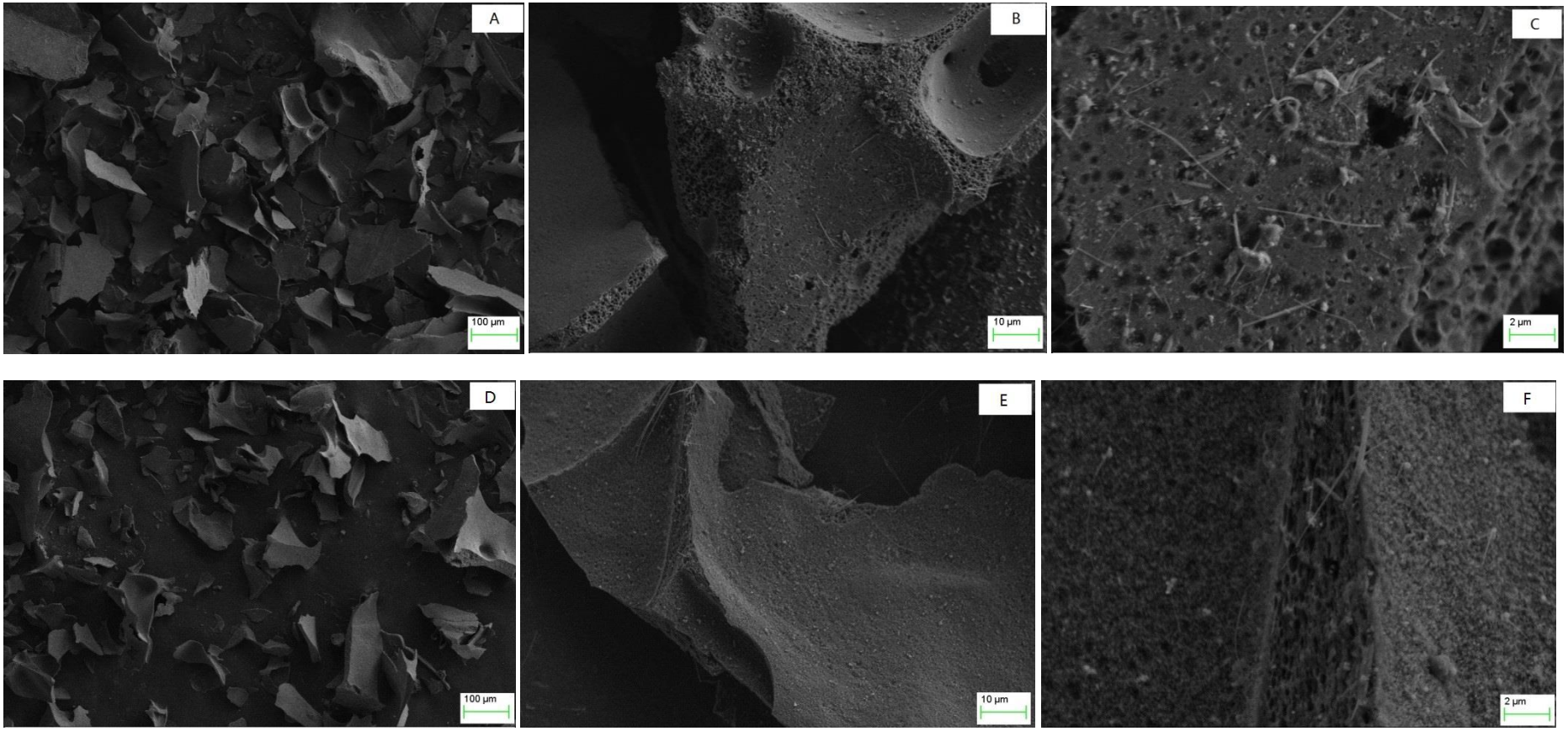
A
100 µm
B
10 µm
C
2 µm
D
100 µm
E
10 µm
F
2 µm

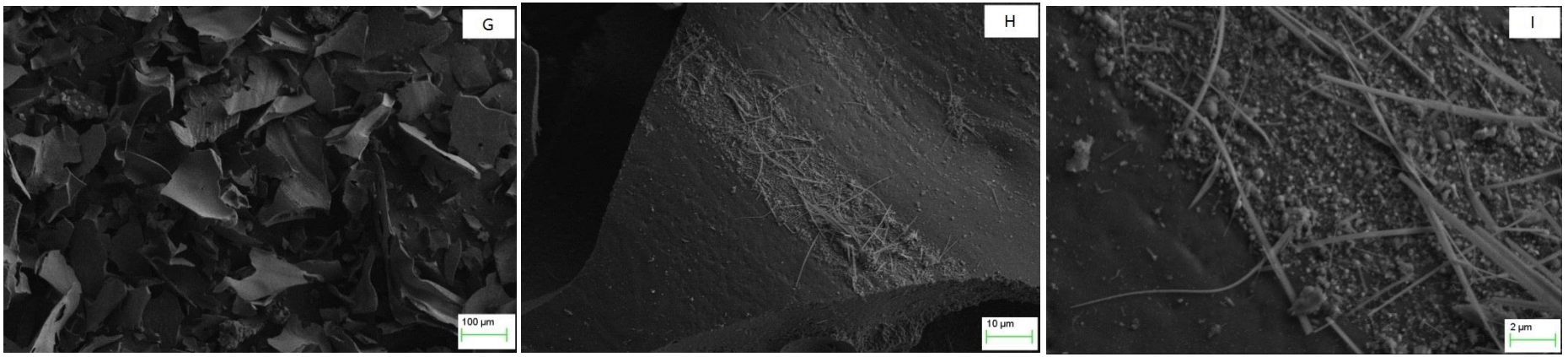

Figure 6-4 SEM images of char pyrolyzed from dunaliella at 400 °C with magnification of A x 100, B x 1000, C x 5000; at 550 °C, D x 100, E x 1000, F x 5000; at 700 °C, G x 100, H x 1000, I x 5000

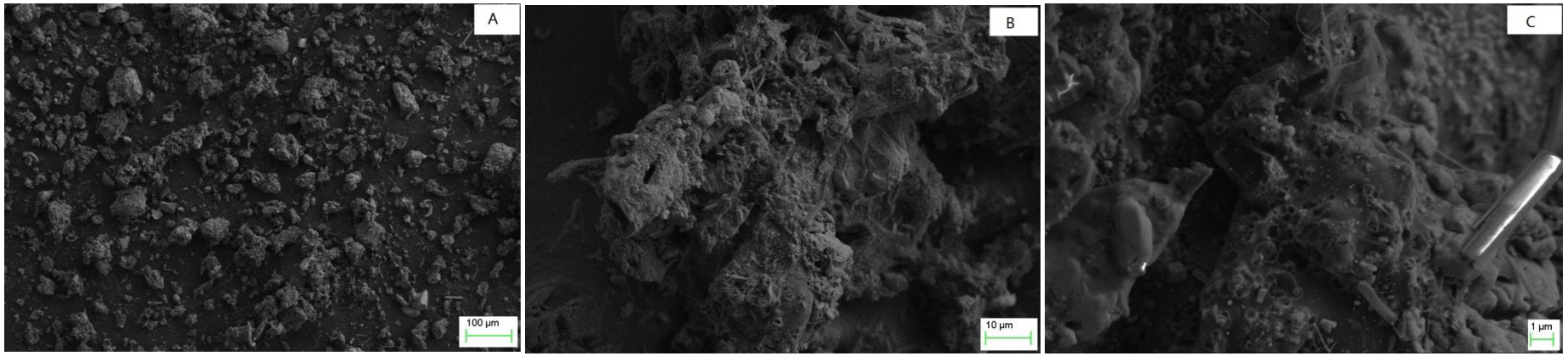

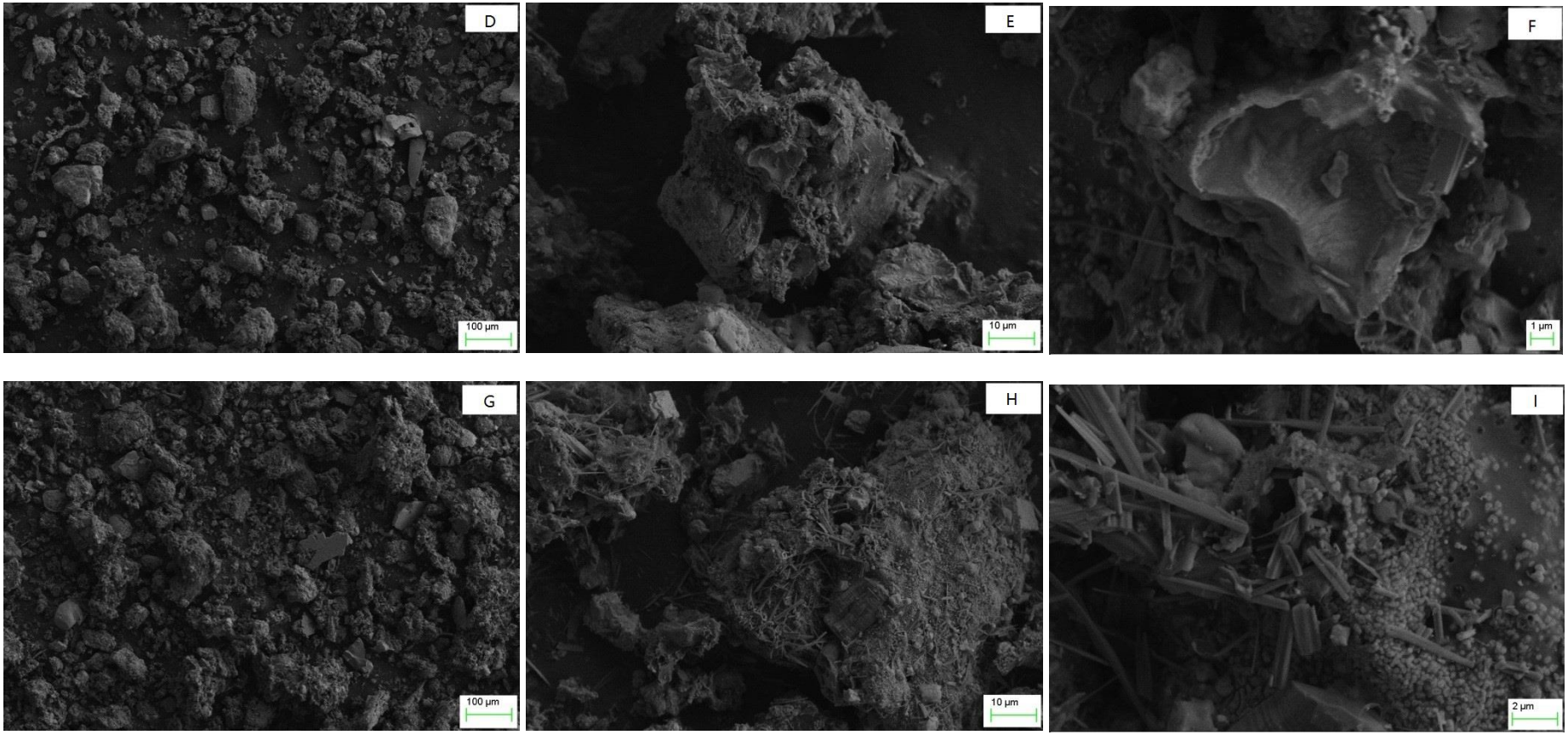

Figure 6-5 SEM images of char pyrolyzed from laminaria at 400 °C with magnification of A x 100, B x 1000, C x 5000; at 550 °C, D x 100, E x 1000, F x 5000; at 700 °C, G x 100, H x 1000, I x 5000

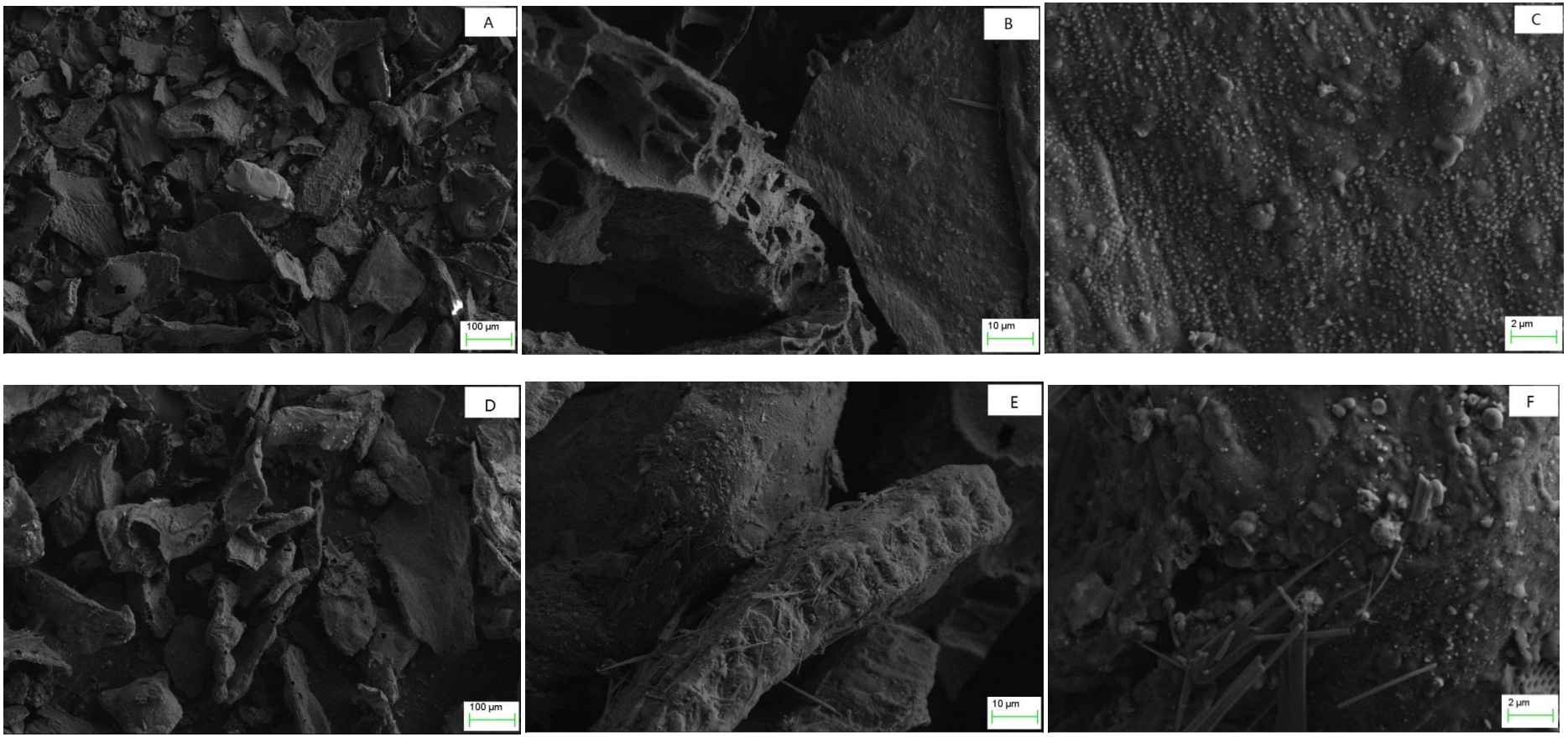
A
100 µm
B
10 µm
C
2 µm
D
100 µm
E
10 µm
F
2 µm

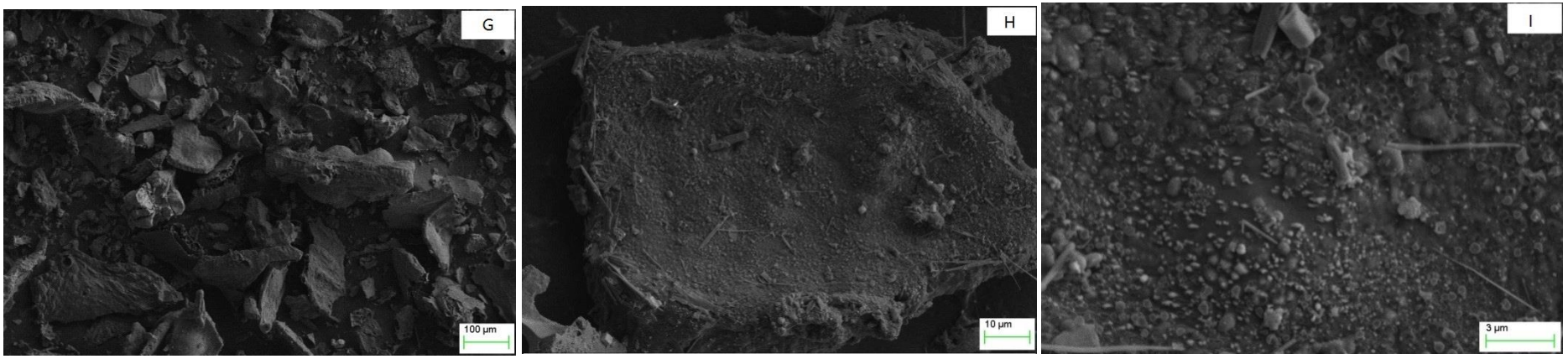

Figure 6-6 SEM images of char pyrolyzed from porphyra at 400 °C with magnification of A x 100, B x 1000, C x 5000; at 550 °C, D x 100, E x 1000, F x 5000; at 700 °C, G x 100, H x 1000, I x 5000

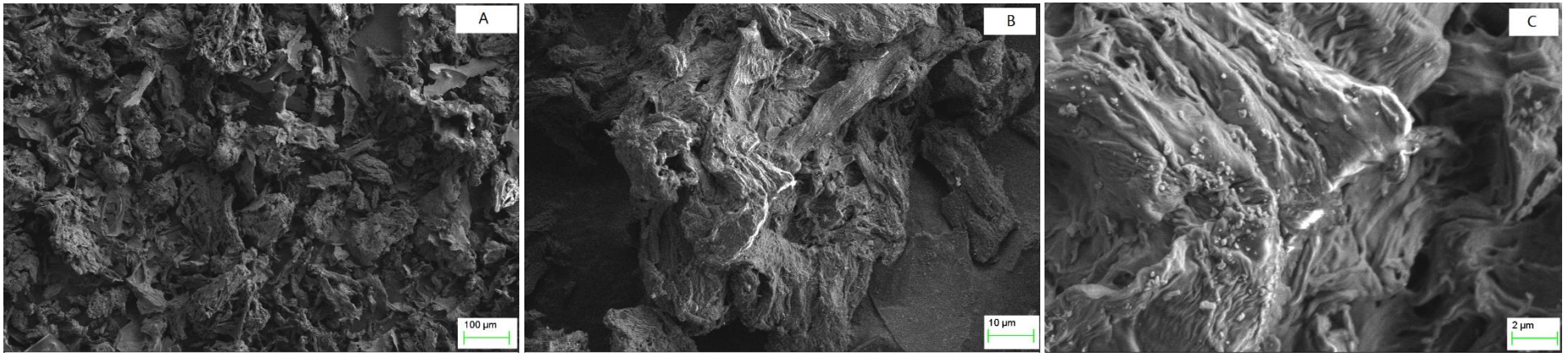

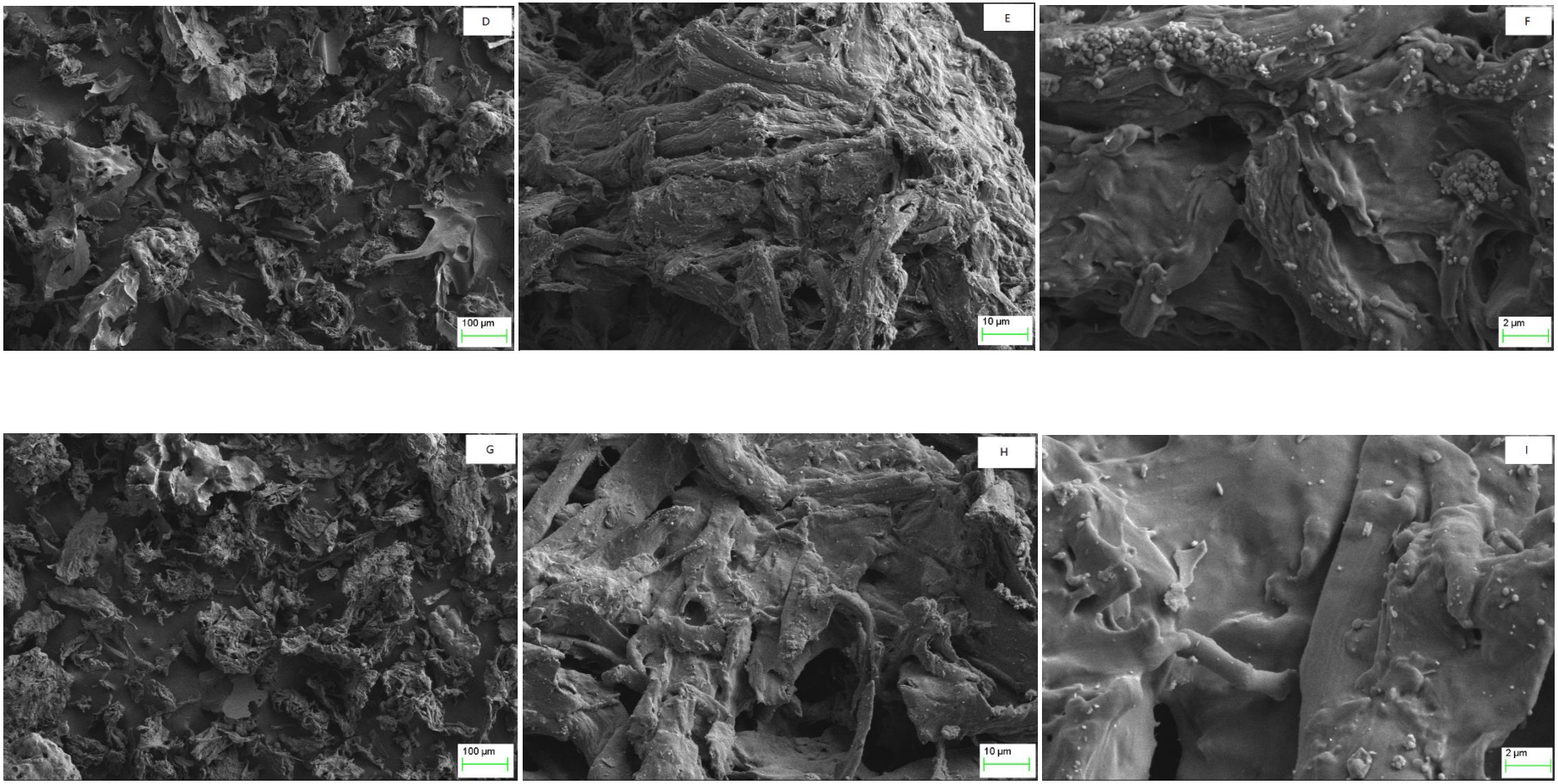

Figure 6-7 SEM images of char pyrolyzed from cellulose at 400 °C with magnification of A x 100, B x 1000, C x 5000; at 550 °C, D x 100, E x 1000, F x 5000; at 700 °C, G x 100, H x 1000, I x 5000

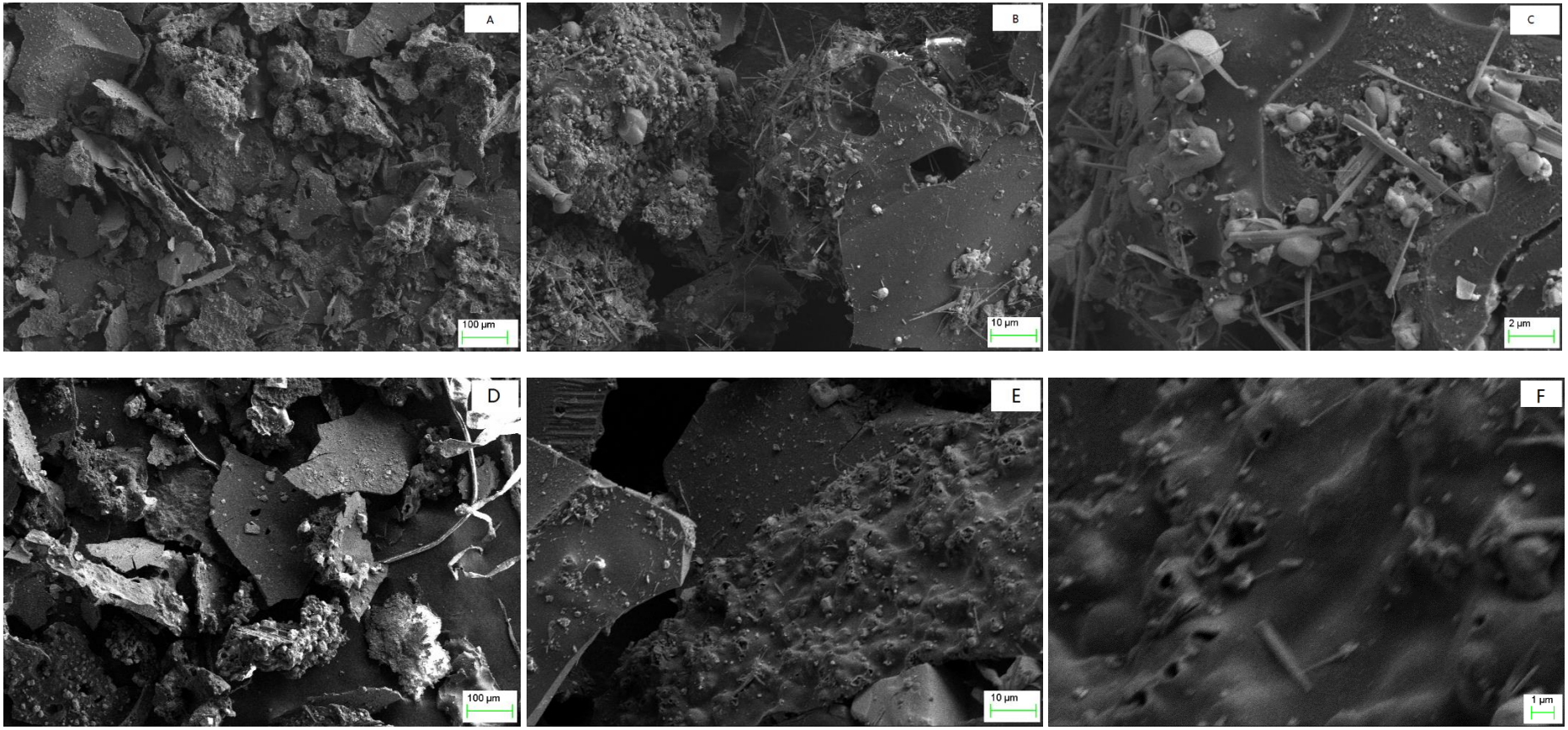
A
100 µm
B
10 µm
C
2 µm
D
100 µm
E
10 µm
F
1 µm

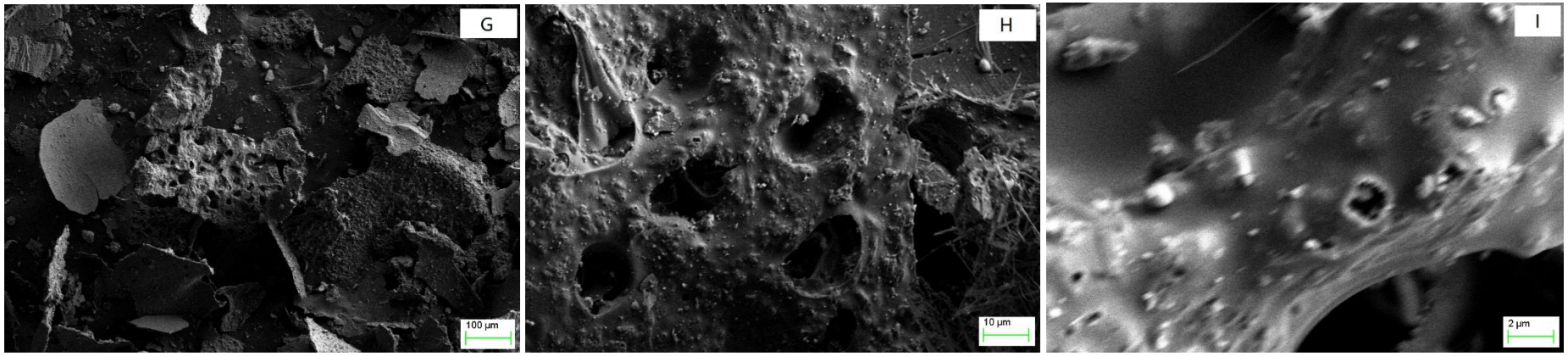

Figure 6-8 SEM images of char pyrolyzed from ovalbumin at 400 °C with magnification of A x 100, B x 1000, C x 5000; at 550 °C, D x 100, E x 1000, F x 5000; at 700 °C, G x 100, H x 1000, I x 5000

6.5.2 Composition of char by EDS

Elemental compositions of bio-chars were determined by using EDS and are summarised in **Table 6-4**. As for spirulina and chlorella, the C content in char decreased with the increase in temperature as a result of the enhanced reaction between carbon and CO_2 at high temperatures (R. 7), which leads to a higher CO content and lower CO_2 content in gas product at higher temperatures as shown in **Table 6-2**. This indicated that the amount of carbon could be reduced by continuously reacting with CO_2 if bio-char is fed back to the reaction system.

Normally, char is a good microwave absorber. Bio-char can also be used as a catalyst to catalyze the reactions between vapor and solids since bio-chars are normally enriched with minerals [248, 249], and therefore affect product distribution as well as the quality of products. In addition, bio-chars can also be used as a reactant to react with CO_2 and H_2O (R. 3). In this study, to further improve overall conversion efficiency and minimize the yield of solid, it is proposed that chars derived from algae are re-utilized as a microwave absorbent to enhance the pyrolysis process, as a catalyst to promote the pyrolysis of algae [250, 251], as well as a reactant to react with CO_2, H_2O and other gas components in pyrolytic gas mixture since biochars are normally porous and highly reactive and synergistic effect exists when chars are co-processed with materials of low

reactivity [252-254]. By the recycling and co-processing of biochars with algae, it could improve overall conversion efficiency by the enhanced interactions between biochar and algae.

6.5.3 Proximate and intrinsic analysis of char

According to **Table 6-1**, laminaria had the highest char yield (18.9-20.7 wt.%) and was reduced slightly when pyrolysis temperature was raised to 550 °C but increased when the temperature rose to 700 °C, while microalgae produced a relatively smaller amount of char (4.7-11.7 wt.%). Characterization of bio-char was also carried out in this study following the methods described elsewhere [253, 255]. The results of proximate and intrinsic analysis of five algal char together with two model compounds derived under 400, 550, 700 °C are summarized in **Table 6-5**. It is evident that dunaliella has the largest content of volatiles and fixed carbon among the five algae char samples, which was corresponding to its highest carbon content detected by EDS. Moreover, the dunaliella-derived char also had relatively higher HHVs (18.3-18.5 MJ/kg), compared with that of other algae such as spirulina (13.5-14.4 MJ/kg) and chlorella (13.1-16.3 MJ/kg), which is attributed to the higher content of carbonaceous substances.

Table 6-4 EDS Compositions of pyrolyzed char (wt.%)

	Spirulina			Chlorella			Dunaliella			Laminaria			Porphyra			Cellulose			Ovalbumin		
	400°C	550°C	700°C	400°C	550°C	700°C	400°C	550°C	700°C	400°C	550°C	700°C	400°C	550°C	700°C	400°C	550°C	700°C	400°C	550°C	700°C
C	69.2	61.7	50.7	58.6	56.1	38.9	27.1	27.1	27.3	-	-	19.2	70.6	51.8	65.4	27.2	27.3	27.3	25.0	24.7	13.9
O	18.4	19.6	24.8	14.5	17.7	12.8	72.6	72.5	72.7	15.8	14.8	54.9	8.4	16.2	8.4	72.8	72.7	72.7	70.0	68.9	68.6
Na	2.6	1.3	1.3	4.4	1.6	4.7	0.1	0.1	-	17.2	18.4	5.3	2.7	4.5	3.1	-	-	-	1.1	0.5	3.3
Mg	2.8	3.3	2.4	1.8	0.6	3.0	-	-	-	3.0	1.8	0.2	1.5	3.0	1.3	-	-	-	0.1	-	0.2
Al	0.4	3.0	5.2	0.3	0.5	-	-	-	-	-	-	-	-	-	0.1	-	-	-	-	-	-
P	5.8	4.9	5.5	7.1	9.3	12.6	-	-	-	0.4	0.2	-	2.8	5.6	7.2	-	-	-	0.2	-	0.8
Si	-	5.3	9.9	-	2.9	0.7	0.2	0.1	-	0.5	0.4	-	1.6	0.4	2.2	-	-	-	-	-	0.3
S	0.4	-	-	-	0.8	-	-	-	-	1.7	1.7	0.1	8.0	3.3	7.2	-	-	-	-	-	0.1
K	0.5	0.8	-	-	0.7	-	-	0.1	-	18.5	19.5	-	1.9	0.3	1.5	-	-	-	0.6	1.5	2.7
Fe	-	-	-	-	0.5	-	-	-	-	-	0.1	-	-	-	1.0	-	-	-	-	-	-
Ti	-	-	-	9.5	-	18.8	-	-	-	-	-	-	-	-	-	-	-	-	-	-	-
Ca	-	-	-	2.1	8.7	6.1	-	-	-	0.7	0.4	-	-	-	-	-	-	-	0.1	0.2	0.8
Cl	-	-	-	1.6	0.6	2.4	-	0.1	-	41.4	42.1	-	2.4	7.1	2.6	-	-	-	1.9	2.3	5.9

Table 6-5 Proximate and intrinsic analyses of algal chars

	Spirulina			Chlorella			Dunaliella			Laminaria			Porphyra			Cellulose			Ovalbumin		
	400°C	550°C	700°C	400°C	550°C	700°C	400°C	550°C	700°C	400°C	550°C	700°C	400°C	550°C	700°C	400°C	550°C	700°C	400°C	550°C	700°C
Proximate analysis (Dry basis, wt.%)																					
Volatile matters	14.0	16.3	11.4	26.9	27.2	13.0	13.6	10.1	7.1	74.9	74.2	73.3	25.5	26.2	21.4	12.2	14.6	6.3	47.4	43.8	47.5
Fixed carbon	44.5	45.7	47.6	40.5	42.0	61.3	83.4	86.0	90.3	11.2	10.6	11.3	50.7	49.1	51.6	85.6	83.6	91.2	43.5	47.3	43.1
Ash content	41.5	38.0	41.0	32.6	30.8	25.7	3.0	3.9	2.6	14.0	15.2	15.4	23.8	24.7	27.0	2.3	1.7	2.5	9.1	8.9	9.4
Intrinsic analysis (Temperature, °C)																					
Ignition	378	385	375	390	382	481	453	496	535	381	385	379	440	449	414	536	485	572	395	409	429
Peak	423	431	423	423	431	531	521	544	567	407	430	437	491	491	489	587	554	652	437	452	499
Burnout	618	621	648	642	629	869	606	582	596	469	480	487	680	685	654	614	688	694	583	593	613
HHV (MJ/kg)	13.5	14.4	14.0	13.1	13.8	16.3	18.5	18.8	18.3	4.1	3.9	2.9	17.4	13.8	18.2	16.3	13.4	12.8	10.7	11.7	11.0

6.6 Algae-derived syngas and its applications

It is clear that for most of the algae investigated in this study, the gas product percentages increased slightly while solid residue reduced gradually from 400 to 550 °C. Syngas in gaseous fraction increased steadily from 400 to 550°C, but the content of CO surged when the pyrolysis temperature was raised to 700 °C, as shown in **Table 6-2**. Therefore, optimal temperature for microwave-enhanced pyrolysis was 550 °C, which led to the formation of relatively higher amount of syngas-enrich gas product and less char residue. Compared with syngas produced via coal-water-slurry or pulverised-coal gasification, the gas products produced via MEP of algae are of high HHVs (12.1-19.4 MJ/Nm^3) and comparable H_2+CO percentage (46.6–79.3 vol. %, dry basis). Normally for coal-water-slurry gasification, the yield of syngas (H_2+CO) is around 75 mol per kg coal. For MEP of algae, the yield of syngas was around 20.2 - 41.2 mol per kg each algae sample, which is in the range of 1/3 to 1/2 of that of coal-water-slurry gasification. If bio-oil is further reformed together with C1-C3 compounds in gaseous fraction, the syngas production could be further improved. In addition, it has the virtue of eliminating costly air separation units, which are essential for large-scale coal gasification processes. Therefore, MEP of algae a very promising alternative option for hydrogen production, especially for small-scale production to be used as the feed for fuel cells.

6.7 Summary

In this chapter, the yield and compositions of gaseous, liquid and solid products from microwave-enhanced pyrolysis process of five algae and two model compounds at 400, 550 and 700 °C were investigated which indicated that porphyra is more suitable raw materials for syngas-enriched gas production (85.6-87.1 wt.%), while commonly-used microalgae-spirulina and chlorella favored oil production (6.3-12.8 wt.% and 8.0-15.4 wt.% respectively) owing to higher protein proportion of 57.8 and 55.6 wt.% respectively. Meanwhile, dunaliella, which contained a significant amount of carbohydrate (94 wt.%), converted most of its carbohydrates into C1-C3 gas, compared with the pyrolysis of porphyra. Laminaria has a high portion of incombustible components; therefore, it only has gaseous production less than 80 wt.%. It also indicated that most of the samples (except for spirulina) generated most gaseous fraction under the target temperature around 400-550 °C, which could be regarded as the optimal pyrolysis temperature.

Porphyra showed the highest reactivity amongst five algae with an average heating rate as high as 100 °C/min, which lead to higher yield in gaseous fraction. For the production of bio-oil, protein-enrich microalgae were considered to favor to be the raw materials with larger HHVs (>20 MJ/kg), compared to macroalgae (<18MJ/kg), and less amount of PAHs and phenols formed. The MEP of algae produced

high gas yield with higher HHVs and comparable H_2+CO percentage with conventional coal gasification processes. It was also found that microalgae favors the formation of more phenols, while nitrogenated compounds and PAHs are mainly derived from protein and carbohydrate respectively. Thus, porphyra is more appropriate for the production of syngas-rich gas product among the five algae.

Chapter 7. Microwave-enhanced reforming of algae

In this chapter, CO_2 replaces N_2 as the carrier gas for the microwave-enhanced reforming of microalgae and macroalgae. Meanwhile, the mechanism of the reforming process of algae under CO_2 is investigated via using algal primary model compounds, ovalbumin as protein content and cellulose as carbohydrates. The distribution of gaseous, liquid and solid products together with their compositions are characterized. Secondly, algal ash is prepared and used as catalysts for the microwave-enhanced pyrolysis of algae under N_2. Since dunaliella has only 0.2 wt.% ash content, spirulina, chlorella, laminaria and porphyra are used to prepare corresponding ash to perform as catalysts. The weight percentages of gas, bio-oil and char are calculated and the compositions of gas and bio-oil are detected and listed.

7.1 CO_2 as carrier gas

The pyrolysis of algae under N_2 and CO_2 atmosphere using TGA has been compared and analysed in **Section 0**. It is noticeable that compared to N_2, CO_2 atmosphere favoured the pyrolysis of protein content in algae, rather the lipid content. Microwave-enhanced pyrolysis of algae under N_2 has been carried out and discussed in **Chapter 6**.

7.1.1 Distribution of products

The distribution of algal gaseous, liquid and solid products pyrolysed under CO_2 at 400, 550 and 700 °C was listed in **Table 7-1**. It is apparent that gaseous product has the largest proportion (63.2-90.8 wt.%), followed by liquid and solid products (1.6-20.0 wt.% and 3.3-34.3 wt.% respectively). As the pyrolysis temperature increasing from 400 to 550°C, the gas portions derived from all samples rose slightly (2.2-11.2 wt.%) except for dunaliella and ovalbumin which decreased 0.3 and 8.5 wt.% respectively. The growth of gaseous product of chlorella, laminaria, porphyra and cellulose could be explained by the smaller amount of char yielded, while others are owing to the oil conversion. According to kinetic analysis (**Table 5-1** and **Table 5-2**), CO_2 atmosphere could significantly reduce the char yield when the heating rate was less than 50 °C/min because of the larger contacting and reaction time between carbon content in char and CO_2 [$C(s) + CO_2(g) \leftrightarrow 2CO(g)$]. Furthermore, the CO_2 atmosphere resulted in higher syngas production, especially CO, because of the presence of CO_2 could increase the thermal cracking of volatile organic compounds (VOCs) and the reaction between VOCs and CO_2 via some unidentified reaction. Meanwhile, compared with results carried out under N_2 in **Table 6-1**, the production of gas from most samples decreased by 1.0 to 15.1%, except for dunaliella and laminaria at higher pyrolysis temperature; while liquid product of these samples increased by 2 to 170%. This indicated that CO_2

atmosphere could inhibit the bio-oil production for dunaliella and laminaria and raise the conversion to char, while it favoured the bio-oil yield from other samples with slight decrease of gas production, especially for porphyra with an increment around 150% in bio-oil. The results showed similar distribution as literature, where the liquid yield under CO_2 was found to be slightly higher than that under N_2, while the gas production was higher under N_2 atmosphere [27].

Table 7-1 Product distribution of MEP of algae at 400, 550 and 700°C in CO_2 (100 wt.%)

	Temperature(°C)	Solid	Liquid	Gas
Spirulina	400	6.5±0.3	16.1±1.4	77.4±1.7
	550	6.4±0.8	10.1±1.1	83.5±1.9
	700	6.9±1.1	10.6±0.8	82.5±1.9
Chlorella	400	12.0±2.1	13.4±1.3	74.6±3.4
	550	7.1±0.5	14.2±1.9	78.7±2.4
	700	8.2±0.9	15.7±2.3	76.1±3.2
Dunaliella	400	7.6±1.0	5.0±0.7	87.4±1.7
	550	7.6±1.2	5.3±1.3	87.1±2.5
	700	7.4±0.8	4.0±0.8	88.6±1.6
Laminaria	400	34.3±3.1	2.4±0.4	63.3±3.5
	550	24.0±2.2	1.6±0.3	74.4±2.5
	700	20.7±1.5	2.5±1.0	76.8±2.5
Porphyra	400	15.3±1.2	4.9±0.9	79.8±2.1
	550	12.0±1.4	6.0±1.5	82.0±2.9
	700	13.5±1.1	3.3±0.8	83.2±1.9
Cellulose	400	7.4±1.2	5.4±0.9	87.2±2.1
	550	4.3±0.5	4.9±0.7	90.8±1.2
	700	6.5±1.0	5.0±1.7	88.5±2.7
Ovalbumin	400	3.3±0.5	12.2±2.1	84.5±2.6
	550	4.0±0.2	20.0±2.0	76.0±2.2
	700	5.3±0.4	18.6±1.7	76.1±2.1

7.1.2 Composition of gas product

According to **Table 7-2**, N_2, CO and H_2 were the primary component in gas production. Compared with gas production derived under N_2 atmosphere (**Table 6-2**), the syngas yield from spirulina decreased by 60.8 to 69.7%, while that from dunaliella increased by 23.4 to 30.4%, especially the increase of CO_2. Syngas from other samples remained similar amount. The composition of C1-C3 also decreased significantly by 7-94%, especially for methane and ethane production (decreased by 1.0-93.3% and 20.0-98.4% respectively). This might due to the higher production of N_2 generated from pyrolysis of samples, compared with the CO_2 composition when using nitrogen as carrier gas. Moreover, since the CO_2 atmosphere could decrease tar formation by 40-60% [37, 103], there were less decomposition of tar to generate volatiles, water vapours and hydrogen via R1. Therefore, the reaction of volatiles with water vapours via R2-R6 reduced and thus led to less yield of combustible gas in gasous fraction. With less production of volatiles, less hydrogen would be produced through reaction of R8 and R10. Additionally, the generation of CO from the pyrolysis of laminaria increased by 16.4-37.1%, while the H_2 from decomposition of dunaliella raised by 49.8-72.2% as the pyrolysis temperature increasing via the reaction of R7, R9, and R10. CO and H_2 from other algae slight reduced or remained nearly unchanged. Hence, most of the HHVs of gas product decreased, since combustible

gas compositions reduced. The primary and secondary cracking reactions in CO_2 (R.1 - 11) are listed as follow [245],

$$\mathrm{Tar(g)} \rightarrow \mathrm{CH_4}(g) + H_2O(g) + H_2(g) + C_mH_n(g) \quad (1)$$

$$\mathrm{CH_4}(g) + H_2O(g) \leftrightarrow \mathrm{CO(g)} + 3H_2(g) \quad (2)$$

$$\mathrm{C}(s) + H_2O(g) \leftrightarrow \mathrm{CO(g)} + H_2(g) \quad (3)$$

$$\mathrm{C}_m\mathrm{H}_n(g) + 2mH_2O(g) \rightarrow \mathrm{mCO_2(g)} + [2\mathrm{m} + \tfrac{\mathrm{n}}{2}]H_2(g) \quad (4)$$

$$\mathrm{C}_m\mathrm{H}_n(g) + mH_2O(g) \rightarrow \mathrm{mCO(g)} + [\mathrm{m} + \tfrac{\mathrm{n}}{2}]H_2(g) \quad (5)$$

$$\mathrm{CO}(g) + H_2O(g) \leftrightarrow \mathrm{CO_2(g)} + H_2(g) \quad (6)$$

$$C(s) + CO_2(g) \leftrightarrow 2CO(g) \quad (7)$$

$$\mathrm{CH_4}(g) \leftrightarrow \mathrm{C(s)} + 2H_2(g) \quad (8)$$

$$\mathrm{CH_4}(g) + CO_2(g) \leftrightarrow \mathrm{2CO(g)} + 2H_2(g) \quad (9)$$

$$\mathrm{C}_m\mathrm{H}_n(g) + mCO_2(g) \rightarrow \mathrm{2mCO(g)} + [\tfrac{\mathrm{n}}{2}]H_2(g) \quad (10)$$

$$\mathrm{C}_m\mathrm{H}_n(g) \rightarrow \mathrm{mC(s)} + [\tfrac{\mathrm{n}}{2}]H_2(g) \quad (11)$$

Table 7-2 Compositions of gaseous fraction from different algae at 400, 550 and 700°C in CO_2. (100 vol. %)

	Temperature(°C)	CH_4	C_2H_6	C_2H_4	C_3H_8	N_2	CO	H_2	Others	Syngas (CO+ H_2)	HHV (MJ/Nm^3)
Spirulina	400	1.1	0.1	0.3	0.0	84.4	4.5	9.6	0.0	14.1	2.5
	550	5.2	0.7	3.2	0.3	71.2	10.4	8.8	0.2	19.2	7.3
	700	7.7	0.7	4.1	0.2	64.2	11.9	11.1	0.1	23.0	9.3
Chlorella	400	14.6	1.2	4.2	0.2	30.2	20.3	29.2	0.1	49.5	15.8
	550	9.8	0.9	3.6	0.1	43.4	21.3	20.8	0.1	42.1	12.3
	700	19.6	1.7	6.7	0.3	22.4	23.6	25.6	0.1	49.2	19.8
Dunaliella	400	10.2	1.1	2.4	0.2	17.5	32.0	36.5	0.1	68.5	15.3
	550	8.6	0.8	2.1	0.1	15.3	36.3	36.6	0.2	72.9	14.8
	700	11.0	1.0	2.4	0.2	10.0	35.8	39.4	0.2	75.2	16.4
Laminaria	400	2.5	0.2	0.5	0.0	46.6	37.7	12.5	0.0	50.2	7.8
	550	3.5	0.3	0.4	0.0	9.4	42.5	43.7	0.2	86.2	12.9
	700	7.7	0.7	1.3	0.1	31.2	34.0	25.0	0.0	59.0	12.0
Porphyra	400	8.0	0.7	1.3	0.2	23.4	33.8	32.5	0.1	66.3	13.2
	550	7.3	0.8	2.1	0.2	21.3	30.9	37.2	0.2	68.1	13.7
	700	6.8	0.6	1.0	0.2	21.9	33.8	35.7	0.0	69.5	12.7
Cellulose	400	12.0	0.4	1.9	0.0	15.2	47.2	22.9	0.4	70.1	15.2
	550	8.0	0.4	2.2	0.0	14.1	54.9	19.9	0.5	74.8	14.4
	700	9.9	0.4	2.0	0.1	14.2	48.9	24.5	0.0	73.4	14.9
Ovalbumin	400	6.6	0.9	1.7	0.3	40.0	33.0	17.4	0.1	50.4	11.0
	550	14.0	1.3	3.6	0.3	41.2	22.7	16.9	0.0	39.6	14.0
	700	13.1	1.2	3.9	0.4	42.2	21.3	17.9	0.0	39.2	13.9

7.1.3 Bio-oil composition

The composition of bio-oil derived from the pyrolysis of samples was listed in **Table 7-3**. It was concluded in **Section 7.1.1** that CO_2 favoured higher yield of bio-oil, rather production of gas. Similar to **Table 6-3**, the bio-oil derived from cellulose under CO_2 has no nitrogenated-compounds, while that from ovalbumin still occupied the largest amount contained in oil. Similarly, in CO_2 atmosphere, the percentage of aldehyde, aromatics and glucose in bio-oil from cellulose increased to 44%, while that was only 4.8% in oil derived under N_2. Meanwhile, the amount of PAHs dramatically reduced to 3.3% under CO_2 and phenols slightly decreased. For ovalbumin, the fraction of phenols increased to around 15%, while other components including aromatics, nitrogenated compounds, PAHs decreased to about 2, 7, and 0% respectively. With relatively higher amount of protein, both of spirulina and chlorella seldom contained aldehyde in their derived oil. The contents of aromatics, aliphatics and phenol were found to increase slightly, whilst nitrogenated compounds and PAHs decreased dramatically (by 30 to 70% and 80 to 100% respectively). Since CO_2 favoured the oil from cellulose to form more aromatics, considerable increment of that occurred in liquid product of dunaliella and porphyra which involved higher carbohydrate content. However, the percentage of phenols and nitrogenated compounds almost remained the same or slightly reduces. This

showed an opposite trend described in literature, where CO_2 atmosphere increased higher yield of carboxylic acid while decreased the hydrocarbon and aromatics from pyrolysis of natural algae[27]. Due to seldom PAHs in oil with content of 0 to 6.4%, bio-oil yielded under CO_2 atmosphere from all five algae samples were regarded to be more environmental-friendly chemicals with high added value [256].

Table 7-3 GC-MS: Bio-oil compositions of α- Cellulose, ovalbumin, spirulina, chlorella, dunaliella, laminaria, porphyra at different pyrolytic temperatures of 400, 550 and 700°C. (100% area)

		α- Cellulose			Ovalbumins			Spirulina			Chlorella			Dunaliella			Laminaria			Porphyra		
Category	**Compounds**	**400**	**550**	**700**	**400**	**550**	**700**	**400**	**550**	**700**	**400**	**550**	**700**	**400**	**550**	**700**	**400**	**550**	**700**	**400**	**550**	**700**
Aldehyde	Furfural	7.8	5.4	2.2	-	-	-	-	-	-	-	-	-	-	-	-	-	2.5	-	-	-	-
	5-Hydroxymethylfurfural	6.1	4.1	-	-	-	-	-	-	-	-	-	-	-	-	-	-	1.5	-	-	-	-
	5-Norbornane-2-carboxaldehyde	3.0	5.2	-	-	-	-	-	-	-	-	-	-	-	-	-	-	1.3	-	-	-	-
	2-Furancarboxaldehyde, 5-methyl-	2.5	2.1	-	-	-	-	-	-	-	-	-	-	-	-	-	-	1.3	-	-	-	-
	Diethyltrisulphide	-	-	-	2.3	3.6	3.1	-	-	-	-	-	-	-	-	-	-	-	-	-	-	-
	Total	**19.4**	**16.8**	**2.2**	**2.3**	**3.6**	**3.1**	**0**	**0**	**0**	**0**	**0**	**0**	**0**	**0**	**0**	**0**	**6.6**	**0**	**0**	**0**	**0**
Aromatics	Styrene	1.6	5.0	2.1	-	1.2	2.2	1.7	-	1.2	5.0	0.8	3.4	1.4	2.1	4.9	-	1.0	-	3.7	4.9	2.7
	p-Xylene	-	-	-	-	-	-	1.1	-	0.9	3.9	1.1	2.2	5.8	7.0	12.7	-	2.9	-	3.2	3.8	2.8
	Ethylbenzene	1.9	2.4	-	-	-	1.8	1.8	2.0	2.0	3.9	1.5	2.6	2.0	2.6	4.4	-	1.5	-	4.0	4.8	3.1
	2-Furanmethanol	6.0	3.2	-	-	-	-	-	-	-	-	-	-	6.6	5.3	7.1	4.2	6.7	-	0.5	0.5	-
	o-Xylene	2.0	2.4	-	-	-	-	-	-	-	-	-	-	3.0	3.3	7.0	-	-	-	1.8	3.6	-
	t-Butylhydroquinone	-	-	-	-	-	-	-	-	-	-	-	-	2.7	-	-	-	-	-	-	-	-
	Mesitylene	-	-	-	-	-	-	-	-	-	-	-	-	-	-	7.0	-	-	-	0.4	0.8	-
	Total	**11.5**	**13.0**	**2.1**	**0**	**1.2**	**4.0**	**4.6**	**2.0**	**4.1**	**12.8**	**3.4**	**8.2**	**21.5**	**20.3**	**43.1**	**4.2**	**12.1**	**0**	**13.6**	**18.4**	**8.6**
Aliphatics	Tetradecane	-	-	-	-	-	-	-	-	4.5	-	-	0.3	-	-	-	-	-	-	-	0.3	-
	Hexadecane	-	-	-	-	-	-	4.6	-	-	-	1.2	0.8	0.8	-	-	-	-	-	-	-	-
	Heptadecane	-	-	-	-	-	-	-	4.3	-	-	-	-	-	-	-	-	-	-	-	-	-
	Neophytadiene	-	-	-	-	-	-	-	-	-	-	-	5.4	-	-	-	-	-	-	1.1	0.8	-
	1-Nonene	-	-	-	-	-	-	-	-	-	-	-		4.3	4.1	2.2	-	-	-	-	-	-
	Total	**0**	**0**	**0**	**0**	**0**	**0**	**4.6**	**4.3**	**4.5**	**0**	**1.2**	**6.5**	**5.1**	**4.1**	**2.2**	**0**	**0**	**0**	**1.1**	**1.1**	**0**
Phenols	p-Cresol	2.7	1.9	-	4.6	4.0	4.5	6.8	3.9	6.9	7.6	7.4	7.2	1.7	-	-	-	3.0	4.2	9.3	8.8	-
	Phenol	3.9	2.7	-	8.4	4.7	4.6	7.9	3.5	11.2	3.7	6.0	3.9	1.3	1.3	-	-	1.6	-	5.2	4.9	-
	Phenol, 2-methyl-	1.5	1.9	-	-	-	0.8	1.9	-	1.9	-	-	-	-	-	-	-	1.3	-	0.5	2.2	-
	Phenol, 4-amino-	-	-	-	-	-	0.3	-	-	-	-	2.4	1.0	-	-	-	-	-	-	1.9	-	-
	Phenol, 4-fluoro-	0.4	-	-	-	-	-	-	-	-	-	-	-	-	-	-	-	-	-	-	-	-
	Phenol, 3,5-dimethoxy-	-	-	-	2.3	3.7	3.3	-	-	-	-	-	-	-	-	-	-	-	-	-	-	-
	Total	**8.5**	**6.5**	**0**	**15.3**	**12.4**	**13.5**	**16.6**	**7.4**	**20.0**	**11.3**	**15.8**	**12.1**	**3.0**	**1.3**	**0**	**0**	**5.9**	**4.2**	**16.9**	**15.9**	**0**
Nitrogenated compounds	Indole	-	-	-	6.1	5.3	5.5	8.8	6.5	9.4	6.1	6.5	7.1	-	-	-	-	-	-	4.1	4.4	-
	Benzyl nitrile	-	-	-	-	-	1.0	2.3	-	2.5	-	-	0.6	-	-	-	-	-	-	0.8	0.6	-
	Benzonitrile	-	-	-	-	-	1.5	1.0	-	2.3	-	1.6	3.0	-	-	-	-	-	-	0.4	0.6	-
	Hexadecanenitrile	-	-	-	-	-	-	-	2.0	-	-	-	-	-	-	-	-	-	-	-	-	-
	Quinoline	-	-	-	-	-	1.4	1.2	-	2.1	1.2	1.9	2.4	-	0.6	-	-	-	-	1.4	1.1	-
	Total	**0**	**0**	**0**	**6.1**	**5.3**	**9.4**	**13.3**	**8.5**	**16.3**	**7.3**	**10**	**13.1**	**0**	**0.6**	**0**	**0**	**0**	**0**	**6.7**	**6.7**	**0**
Acids	Carbanic acid	-	-	-	-	-	-	0.6	-	1.5	-	6.7	-	-	-	-	-	-	-	-	-	-
	3-Methyl-2-furoic acid	-	-	-	-	-	-	-	-	-	-	-	-	5.4	3.3	-	-	-	-	-	-	-
	Octadecanoic acid	-	-	-	-	-	-	-	-	-	-	-	-	-	-	-	-	-	-	1.9	1.9	-
	Oxalic acid	-	-	-	-	2.8	-	-	-	-	-	-	-	-	-	-	-	-	-	-	-	-
PAHs	Naphthalene	1.4	2.0	3.1	-	1.7	2.3	2.3	-	6.5	-	5.8	8.1	2.1	5.5	2.2	-	1.7	2.9	2.2	1.8	-
	Naphthalene, 1,2,3,4-tetrahydro-1,1,6-trimethyl-	-	-	-	-	-	-	-	-	-	-	-	-	3.3	2.9	1.5	-	-	-	-	-	-
	Anthracene	1.3	2.7	-	-	-	0.8	0.6	-	-	-	0.4	1.5	0.5	0.5	1.4	-	1.2	-	1.0	1.1	-
	Pyrene	0.8	1.8	-	-	-	-	-	-	-	-	0.4	0.4	0.3	0.5	0.4	-	-	-	-	-	-
	Fluoranthene	0.4	1.3	-	-	-	0.4	-	-	-	-	0.4	0.6	-	0.3	-	-	1.2	-	-	-	-
	Indene	-	2.4	-	-	-	-	-	-	-	1.7	1.5	2.1	-	-	3.6	-	-	-	-	2.2	-
	Biphenylene	0.8	1.3	-	-	-	0.4	-	-	1.7	0.9	1.1	1.8	0.4	2.0	0.4	-	1.0	-	0.7	0.7	-
	1H-Indene, 1-ethylidene-	-	0.3	-	-	-	-	-	-	0.8	-	0.7	-	-	-	-	-	-	-	-	-	-
	1H-Indene, 3a,4,7,7a-tetrahydro-, trans-	-	-	-	-	-	-	-	-	-	-	-	-	3.0	-	-	-	-	-	-	-	-
	Total	**3.3**	**9.8**	**0**	**0**	**0**	**1.6**	**0.6**	**0**	**2.5**	**2.6**	**4.5**	**6.4**	**4.2**	**3.3**	**5.8**	**0**	**3.4**	**0**	**1.7**	**4.0**	**0**
Glucose	1,4:3,6-Dianhydro-.alpha.-d-glucopyranose	11.4	6.3	3.7	-	-	-	-	-	-	-	-	-	-	-	-	3.3	4.8	-	-	-	-
	D-Allose	-	7.9	2.8	-	-	-	-	-	-	-	-	-	-	-	-	-	3.3	-	-	-	-
Others	Cyclotrisiloxane, hexamethyl-	-	1.7	68.9	-	-	1.7	-	59.8	-	27.7	5.3				0.8	77.7	1.3	73.6	-	-	75.5
	Cyclotetrasiloxane, octamethyl-	-	-	8.6	-	-	-	-	9.9	-	-	-	-	-	-	-	7.1	-	16.4	-	-	13.4
	Dianhydromannitol	-	-	-	-	-	-	-	-	-	-	-	-	-	-	-	7.7	11.2	2.9	-	-	-
HHV (kJ/kg)		**3.0**	**5.4**	**3.5**	**2.3**	**2.6**	**2.7**	**2.7**	**2.4**	**1.7**	**3.5**	**2.8**	**3.1**	**4.2**	**3.8**	**1.4**	**4.6**	**2.4**	**2.6**	**4.1**	**2.8**	**4.2**

7.1.4 Characteristics of char

7.1.4.1 Morphology of char

Figure 7-1 to **Figure 7-7** show the morphology of char of the five algae and two model compounds pyrolyzed under CO_2 at 400, 550 and 700 °C using SEM in three magnifications. Compared with **Figure 6-2** to **Figure 6-8** in **Section 6.5.1**, the char derived under CO_2 showed larger porosity, which indicated CO_2 atmosphere could proliferate the volatilization process, especially for char of chlorella, dunaliella and porphyra. After the depletion of VOCs in CO_2, the morphology of char have been further modified with CO_2. Similar to N_2 atmosphere, when the temperature increased from 400 to 550 °C, the number of pore increased at first, and then decreased when the temperature was continuously raised to 700 °C by comparing the images derived under two atmospheres. The spirulina and laminaria char have more fibre and blocky structure, with less pores. However, the char would have less active sites due to the destruction of functional groups.

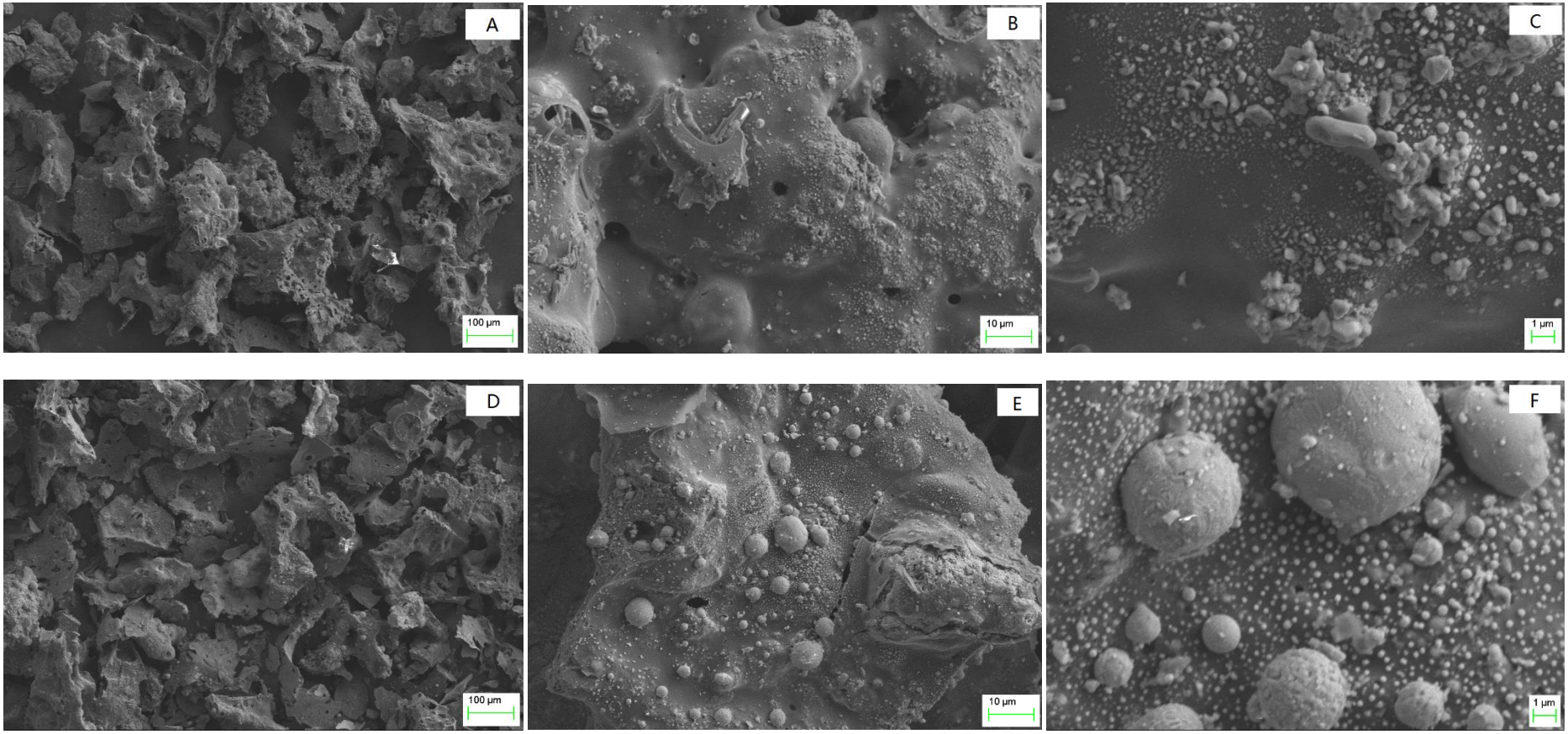
A
100 µm
B
10 µm
C
1 µm
D
100 µm
E
10 µm
F
1 µm

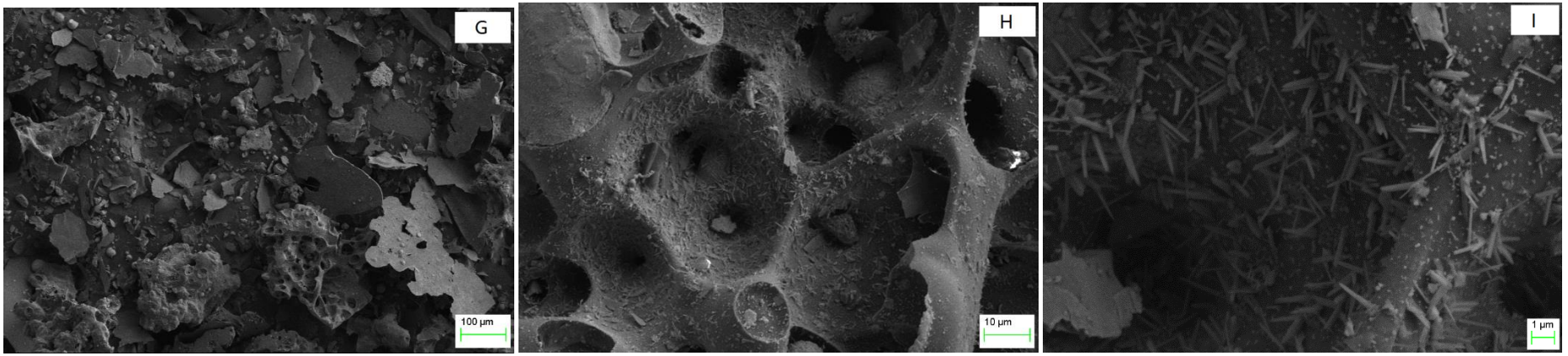

Figure 7-1 SEM images of char pyrolyzed from spirulina in CO_2 at 400 °C with magnification of A x 100, B x 1000, C x 5000; at 550 °C, D x 100, E x 1000, F x 5000; at 700 °C, G x 100, H x 1000, I x 5000

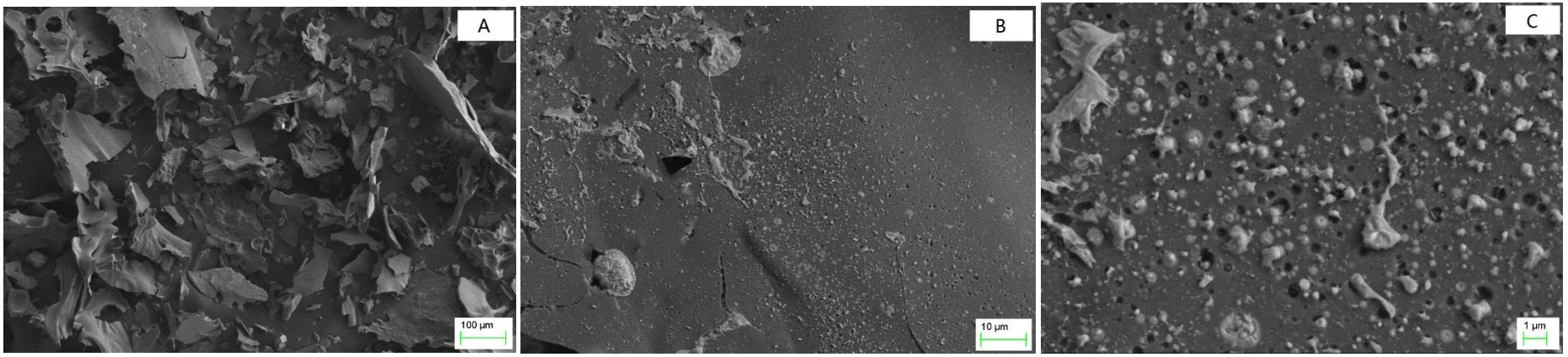

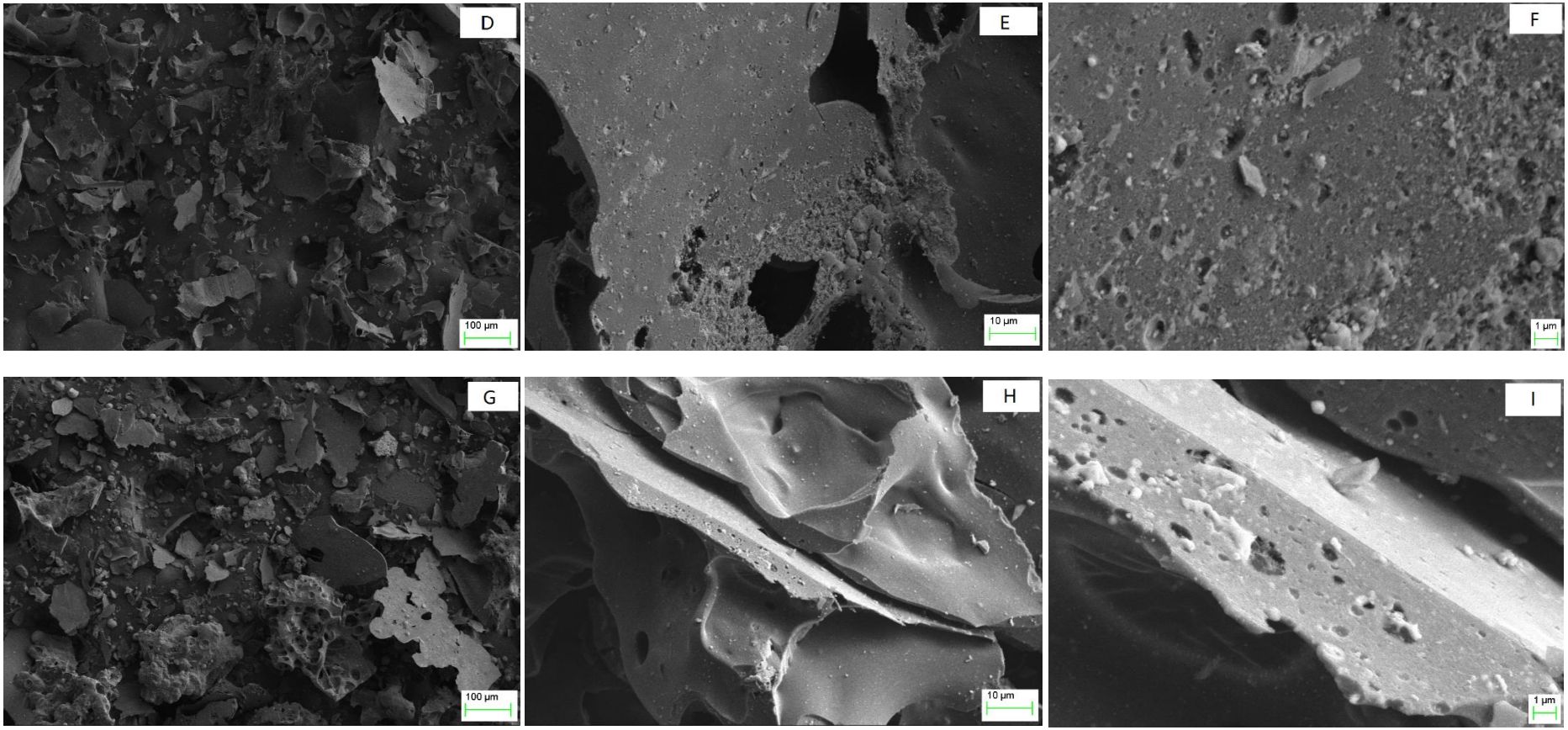

Figure 7-2 SEM images of char pyrolyzed from chlorella in CO_2 at 400 °C with magnification of A x 100, B x 1000, C x 5000; at 550 °C, D x 100, E x 1000, F x 5000; at 700 °C, G x 100, H x 1000, I x 5000

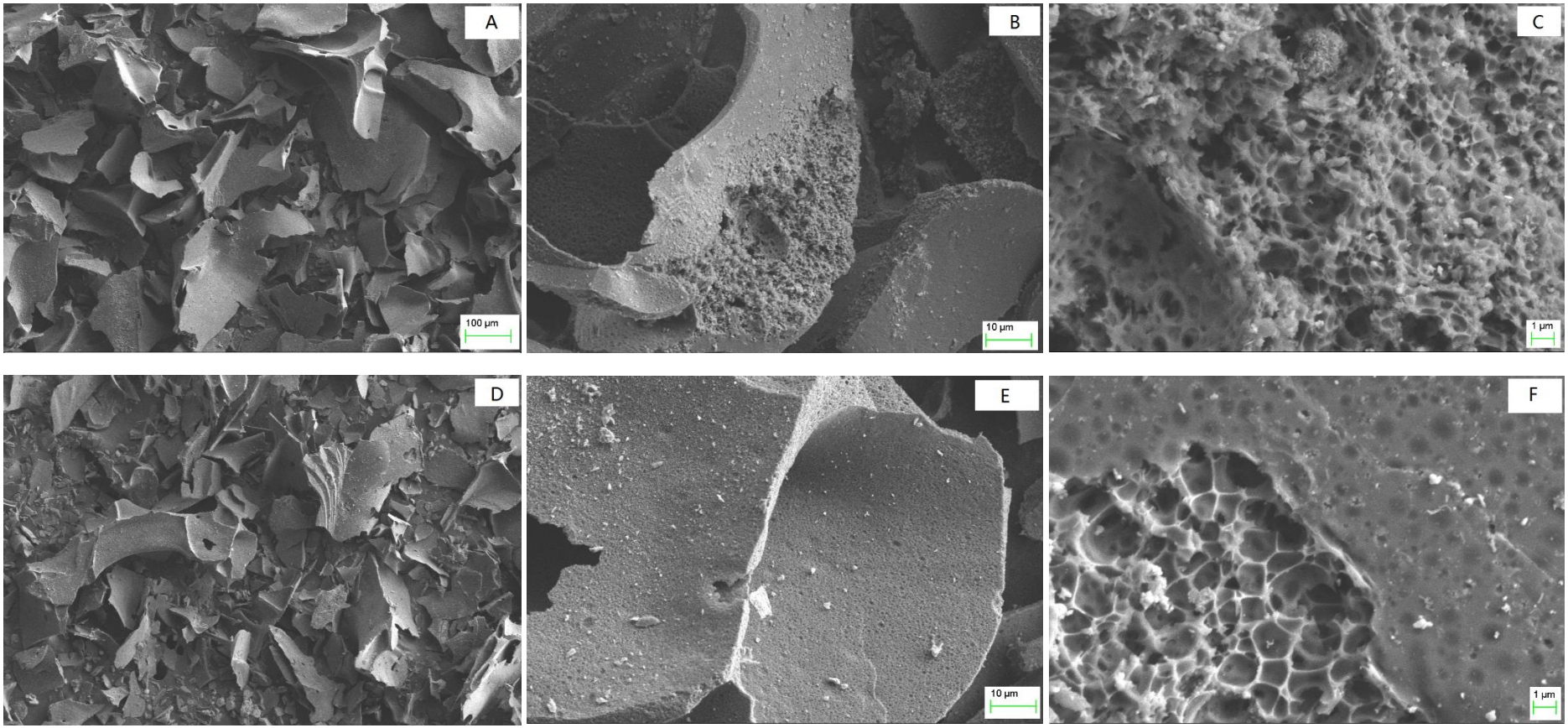
A
100 µm
B
10 µm
C
1 µm
D
E
10 µm
F
1 µm

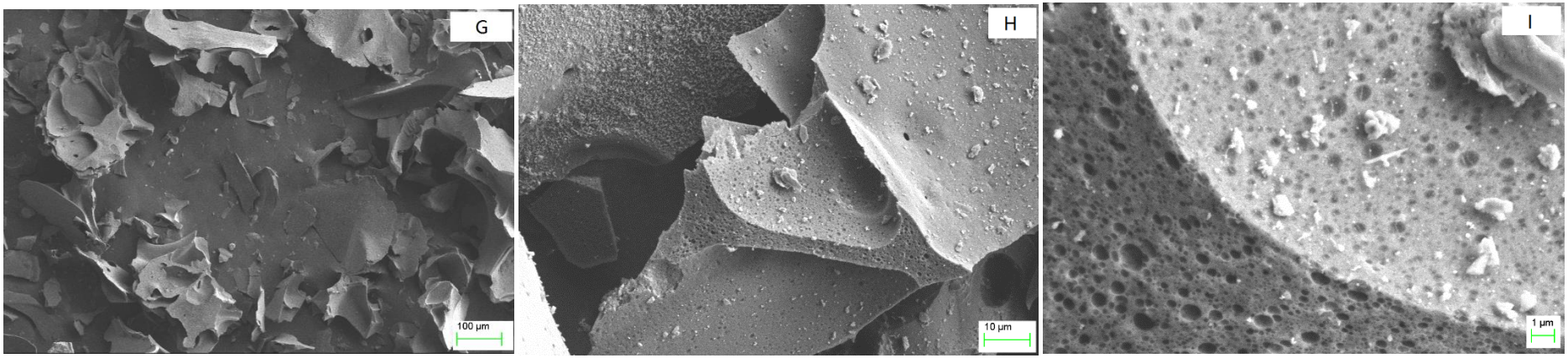

Figure 7-3 SEM images of char pyrolyzed from dunaliella in CO_2 at 400 °C with magnification of A x 100, B x 1000, C x 5000; at 550 °C, D x 100, E x 1000, F x 5000; at 700 °C, G x 100, H x 1000, I x 5000

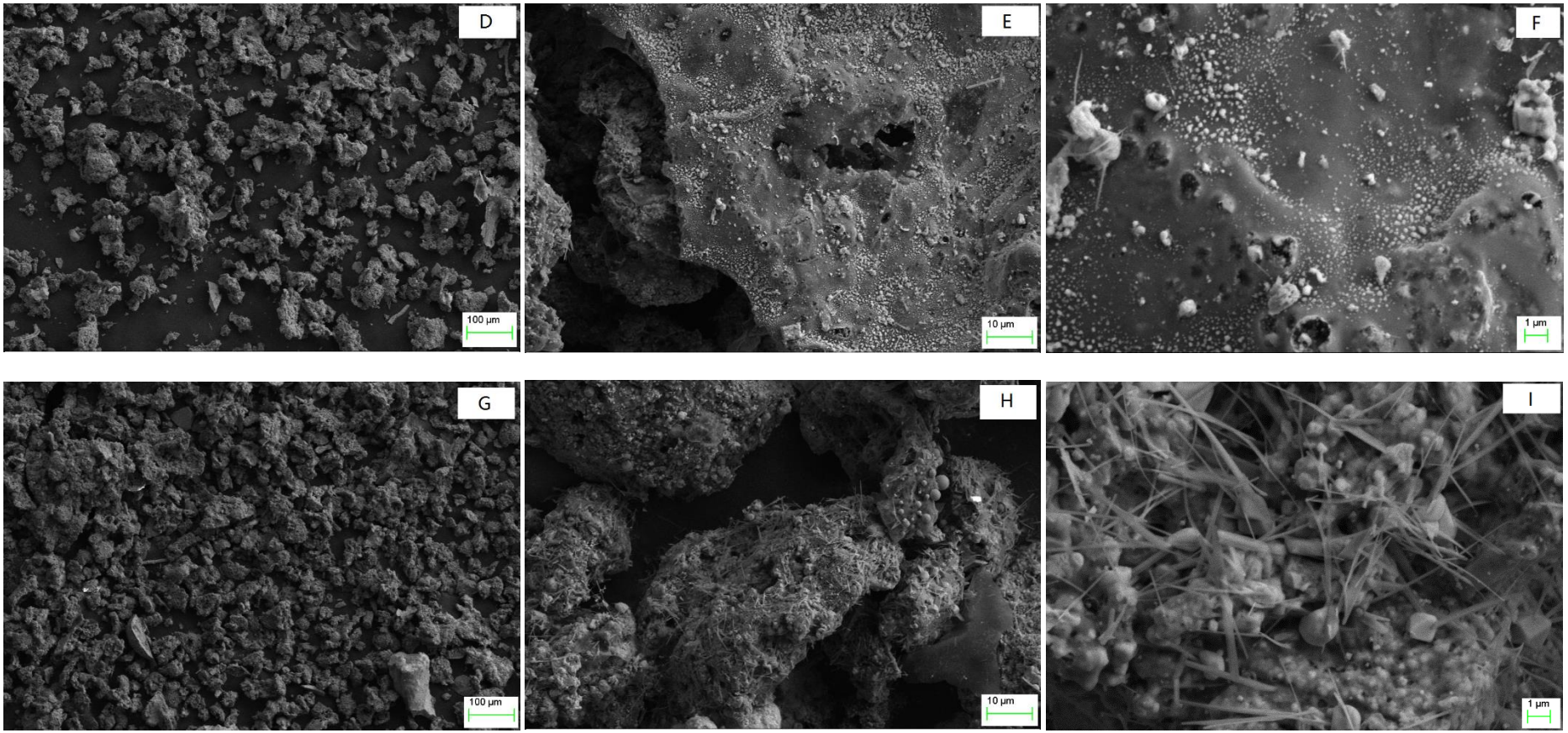

Figure 7-4 SEM images of char pyrolyzed from laminaria in CO_2 at 400 °C with magnification of A x 100, B x 1000, C x 5000; at 550 °C, D x 100, E x 1000, F x 5000; at 700 °C, G x 100, H x 1000, I x 5000

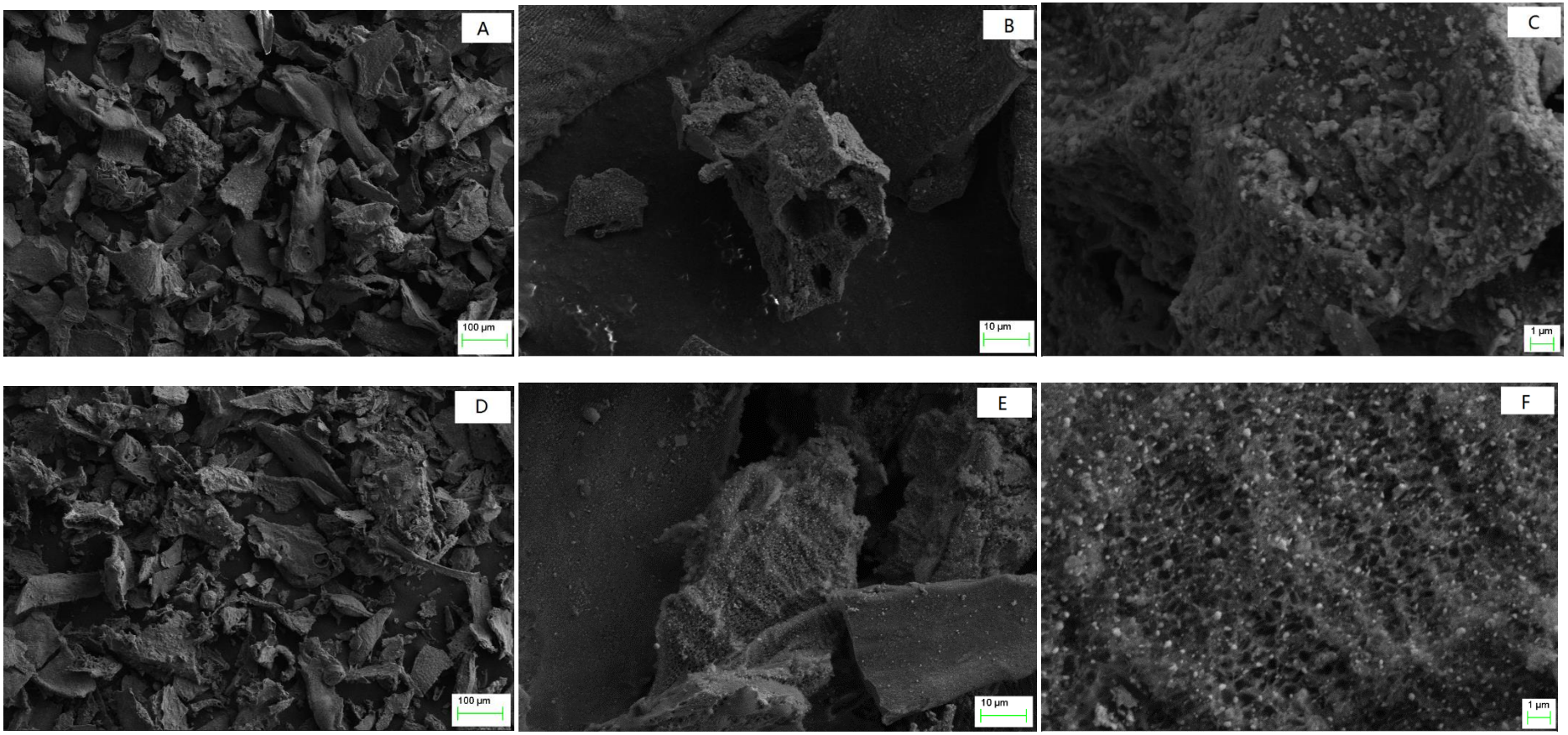
A
100 µm
B
10 µm
C
1 µm
D
100 µm
E
10 µm
F
1 µm

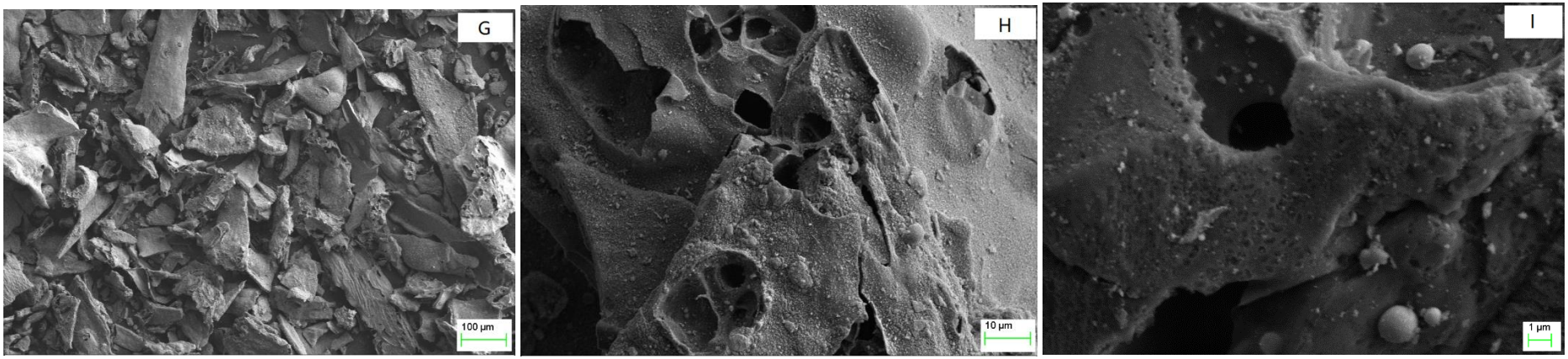

Figure 7-5 SEM images of char pyrolyzed from porphyra in CO_2 at 400 °C with magnification of A x 100, B x 1000, C x 5000; at 550 °C, D x 100, E x 1000, F x 5000; at 700 °C, G x 100, H x 1000, I x 5000

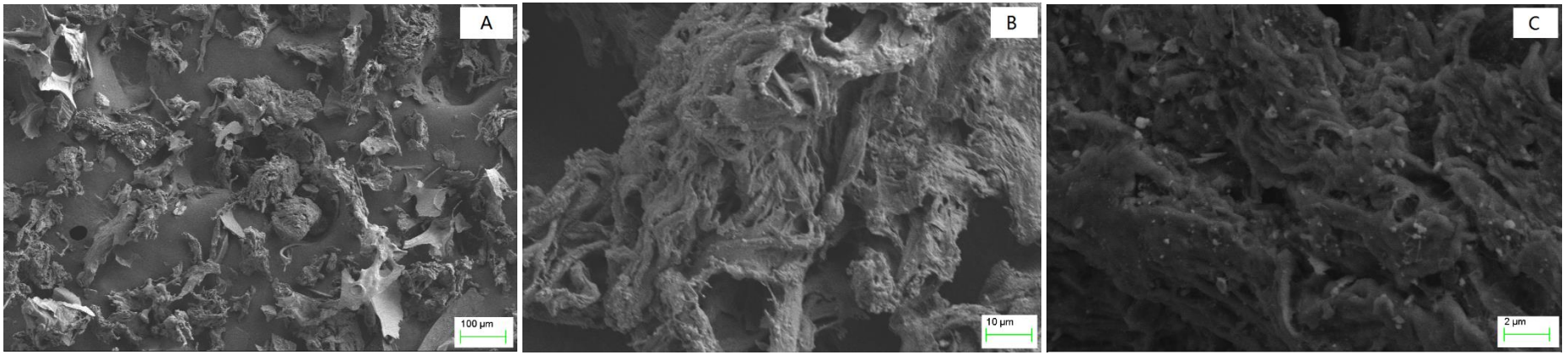

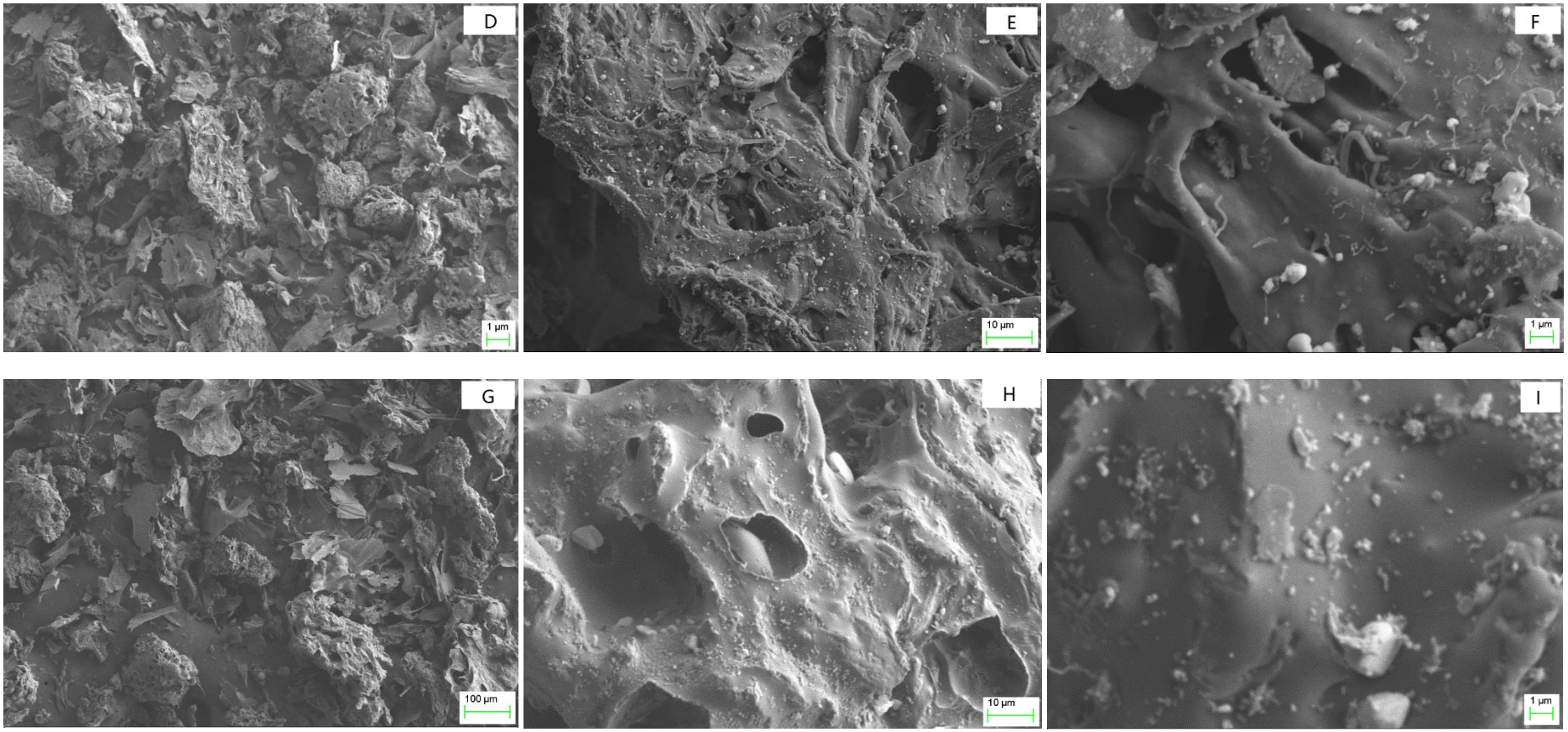

Figure 7-6 SEM images of char pyrolyzed from cellulose in CO_2 at 400 °C with magnification of A x 100, B x 1000, C x 5000; at 550 °C, D x 100, E x 1000, F x 5000; at 700 °C, G x 100, H x 1000, I x 5000

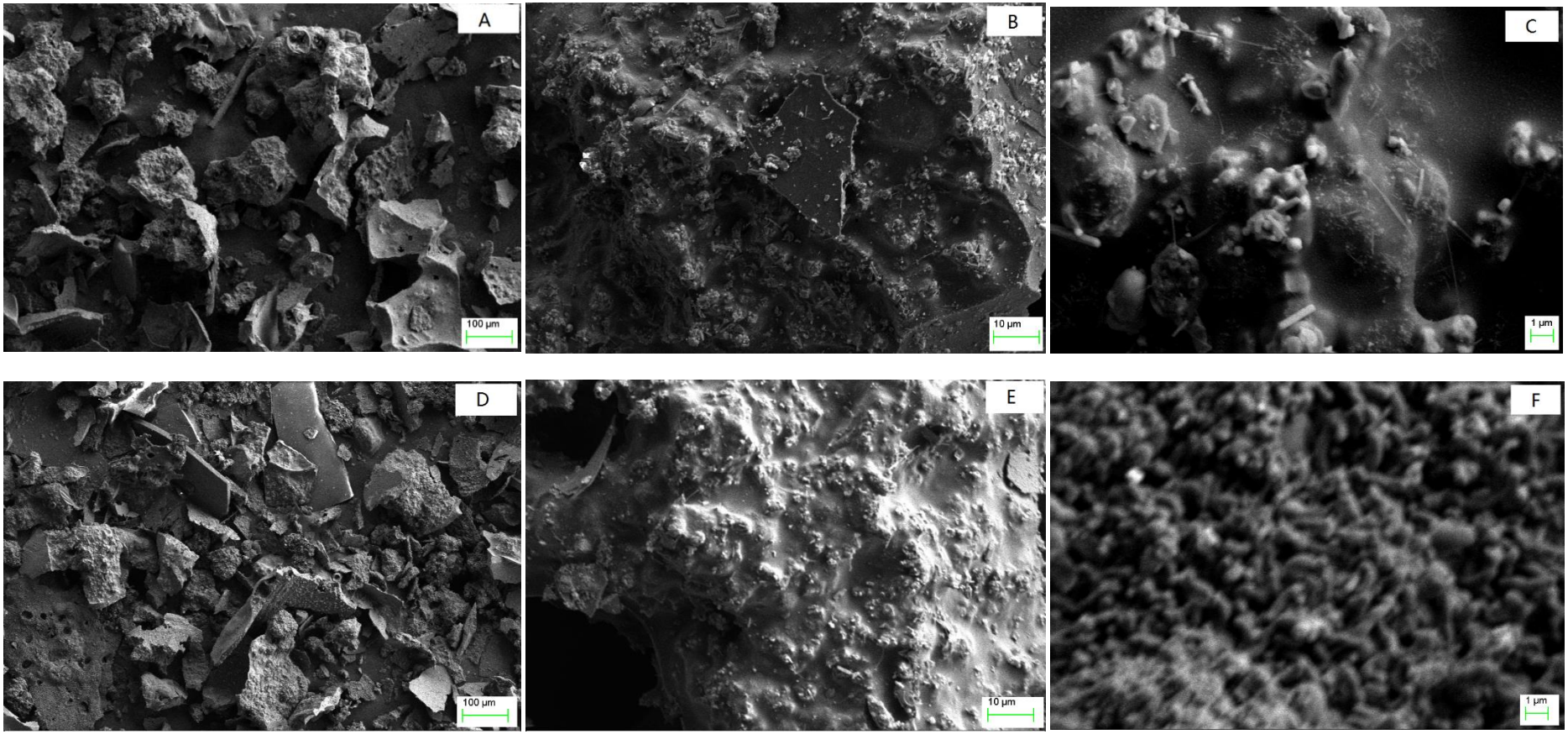
A
100 µm
B
10 µm
C
1 µm
D
100 µm
E
10 µm
F
1 µm

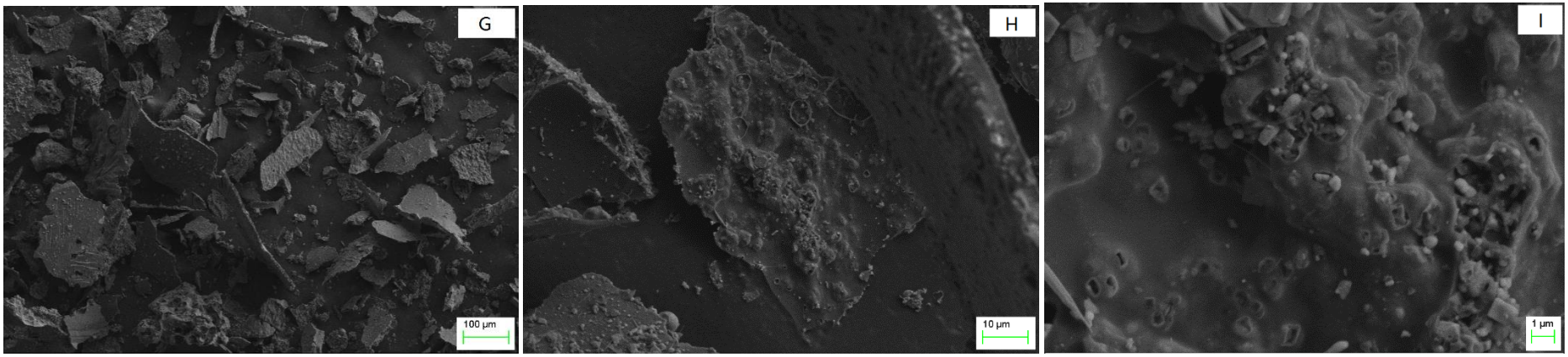

Figure 7-7 SEM images of char pyrolyzed from ovalbumin in CO_2 at 400 °C with magnification of A x 100, B x 1000, C x 5000; at 550 °C, D x 100, E x 1000, F x 5000; at 700 °C, G x 100, H x 1000, I x 5000

7.1.4.2 Composition of char by EDS

The element composition of char from five algae and two main model compounds in CO_2 atmosphere at 400, 550 and 700 °C was detected by EDS as shown in **Table 7-4**. Compared with **Table 6-5**, carbon content in char obviously reduced (17.9-27.2 wt.%), especially for spirulina, chlorella and porphyra. Meanwhile, oxygen percentage in char from spirulina, chlorella, laminaria and porphyra significantly increased to 53.1-70.3 wt.% under CO_2 atmosphere, rather around 10 wt.% under N_2. This might be explained by the reduction of tar amount via gasification reaction between carbon and CO_2. It is obvious that the content of other elements in the char of spirulina, chlorella, laminaria and porphyra including Na, Mg, Al, P, Si, K, Fe, Ca and Cl became much less under CO_2 carrier gas.

Table 7-4 EDS Compositions of pyrolyzed char (wt.%)

	Spirulina			Chlorella			Dunaliella			Laminaria			Porphyra			Cellulose			Ovalbumin		
	400°C	550°C	700°C	400°C	550°C	700°C	400°C	550°C	700°C	400°C	550°C	700°C	400°C	550°C	700°C	400°C	550°C	700°C	400°C	550°C	700°C
C	22.6	23.0	24.7	25.1	24.7	23.1	27.2	27.2	27.1	22.1	17.9	18.2	24.7	20.6	22.7	27.2	27.0	26.8	23.3	24.5	24.3
N	0.8	0.1	-	-	-	-	-	-	-	-	-	-	-	-	-	-	-	-	1.6	1.3	1.2
O	67.7	67.8	69.8	70.3	69.6	63.8	72.6	72.6	72.5	61.5	53.1	53.4	69.4	64.8	66.0	72.4	72.3	71.8	68.3	69.7	69.8
Na	0.8	0.7	0.4	0.4	0.9	0.4	-	0.1	-	2.9	4.8	6.6	1.0	-	-	-	0.1	0.3	2.0	1.1	1.1
Mg	0.6	1.0	0.4	0.2	0.5	0.2	-	-	-	0.2	0.2	0.3	0.6	-	-	-	-	-	-	-	0.1
Al	0.2	-	0.4	0.1	-	-	-	-	0.1	-	-	-	-	-	-	-	-	-	-	-	-
P	1.4	-	1.4	1.5	2.0	-	-	-	-	0.1	0.1	-	0.3	2.2	1.5	-	0.2	-	-	-	0.3
Si	0.2	-	0.6	0.6	0.2	-	-	-	-	0.3	0.3	0.2	-	0.8	0.3	-	0.1	0.1	-	-	0.1
S	-	0.3	-	-	-	-	-	-	-	0.4	0.4	-	-	0.5	0.8	-	-	-	0.1	0.1	-
K	0.5	1.5	-	-	-	0.9	-	-	0.1	-	-	-	1.2	3.5	5.3	0.1	0.1	-	1.2	0.9	-
Fe	0.2	0.7	0.3	0.1	0.1	-	-	-	-	-	-	0.1	0.1	0.1	0.3	-	-	-	-	-	-
I	-	-	-	-	-	-	-	-	-	0.2	0.2	0.2	-	-	-	-	-	-	-	-	-
Ca	0.2	1.3	0.3	0.4	0.3	0.1	-	-	-	-	-	-	0.3	0.9	0.4	-	-	-	0.2	0.1	0.4
Cl	0.3	0.3	-	-	-	-	-	-	-	-	-	-	0.2	0.2	1.1	0.1	0.2	-	2.9	2.2	-

Table 7-5 Proximate and intrinsic analyses of algal chars under CO_2 atmosphere

	Spirulina			Chlorella			Dunaliella			Laminaria			Porphyra			Cellulose			Ovalbumin		
	1	2	3	4	5	6	7	8	9	10	11	12	13	14	15	16	17	18	19	20	21
	400°C	550°C	700°C	400°C	550°C	700°C	400°C	550°C	700°C	400°C	550°C	700°C	400°C	550°C	700°C	400°C	550°C	700°C	400°C	550°C	700°C
Proximate analysis (Dry basis, wt.%)																					
Volatile matters	20.1	11.1	7.3	17.7	9.9	16.5	4.8	3.7	2.9	73.5	82.8	75.8	23.8	19.0	18.5	5.0	6.9	13.2	40.2	38.5	39.3
Fixed carbon	37.3	38.2	45.5	39.0	54.1	53.0	85.5	85.4	84.4	12.2	7.0	8.9	43.7	36.9	49.5	27.3	57.4	17.6	47.6	47.2	44.6
Ash content	42.6	50.7	47.2	43.3	36.0	30.5	9.7	10.9	12.7	14.3	10.2	15.3	32.5	44.1	32.0	67.8	35.7	69.2	12.2	14.3	16.1
Intrinsic analysis (Temperature, °C)																					
Ignition	553	466	464	442	484	465	518	563	556	366	344	377	439	429	408	491	404	451	426	433	419
Peak	597	519	518	504	534	551	575	616	592	424	420	417	489	495	494	561	441	557	520	510	504
Burnout	619	623	615	714	837	807	608	659	628	487	479	485	648	638	622	598	592	615	647	621	677
HHV (MJ/kg)	15.1	11.3	10.3	6.7	7.6	9.8	17.0	14.9	15.6	4.4	2.4	2.7	11.3	9.7	12.5	14.8	10.9	15.8	5.9	8.1	24.2

7.1.4.3 Proximate and Intrinsic analyses of char

The proximate and intrinsic analyses were carried out for pyrolyzed char obtained in CO_2 as shown in **Table 7-5**. Compared with the char derived under N_2 in **Table 6-4**, it is apparent that the percentage of volatile matters and fixed carbon decreased significantly, especially for dunaliella char, which indicated CO_2 could reduce the formation of solid residue and explained the greater corresponding content of ash in char. Based on intrinsic analysis, the ignition, peak and burnout temperatures and HHVs of the five algae and two model compound derived under two atmospheres were summarized and compared as **Figure 7-8**. These featured temperatures of cellulose char decreased while those of ovalbumin char increased when the carrier gas changed to CO_2. Meanwhile, the ignition and peak temperatures of microalgae char increased significantly, while those of macroalgae char remained almost the same. The HHVs of char reduced significantly by around 6.9-48.9% under CO_2 processing.

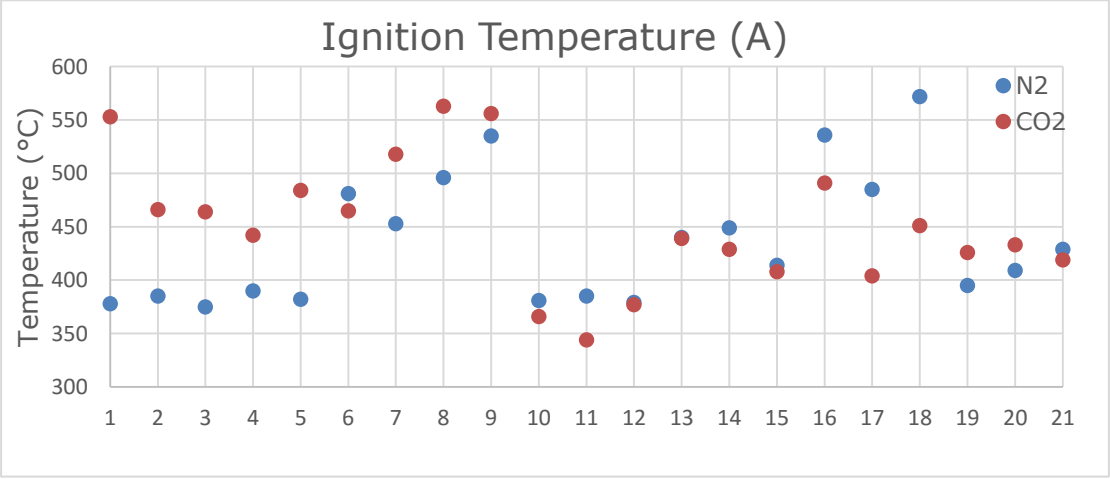

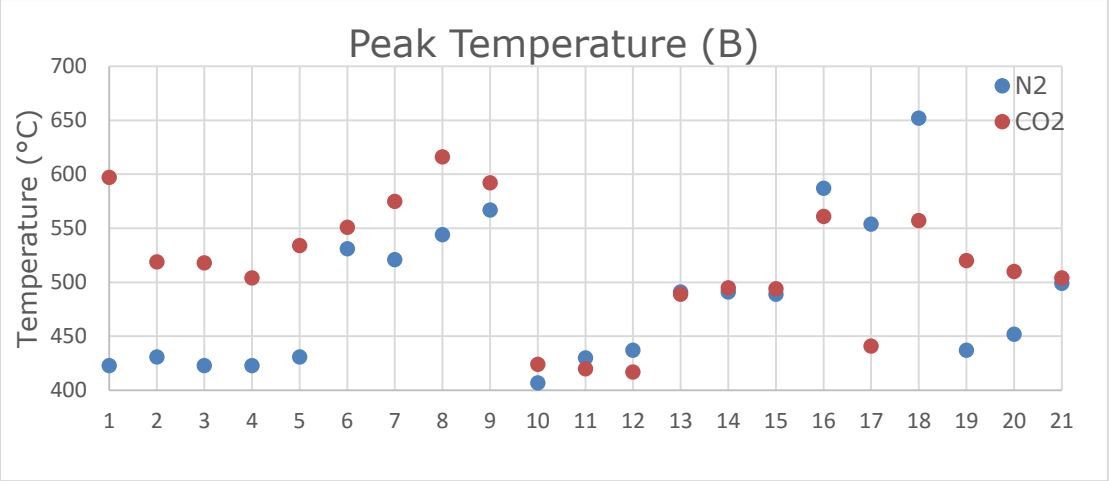

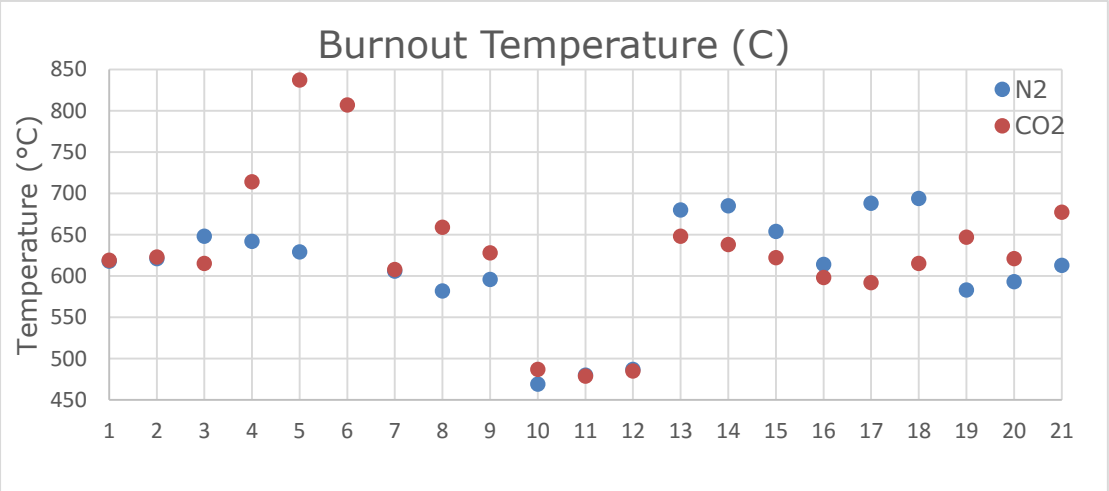

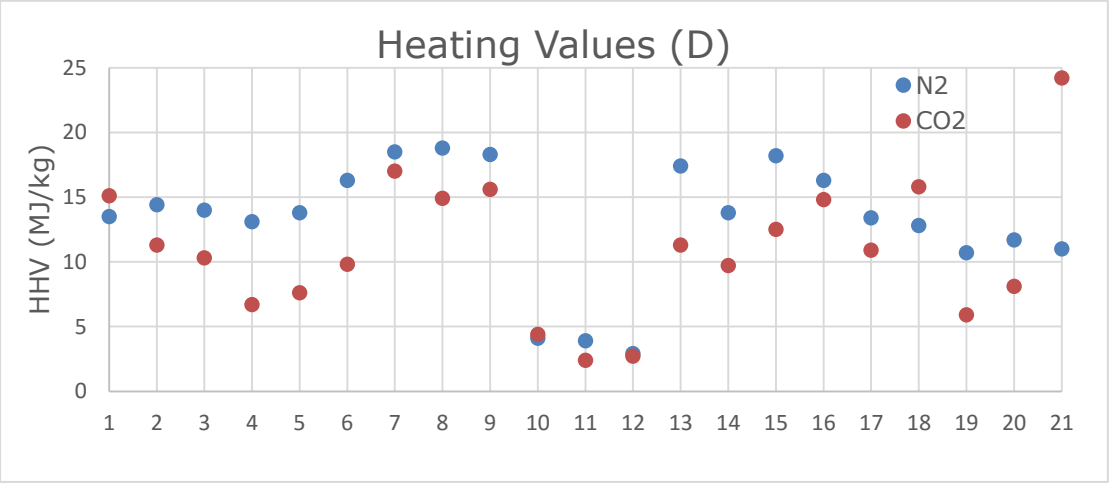

Figure 7-8 Ignition temperature (A), Peak temperature (B), Burnout temperature (C) and Heating values (D) of bio-oil under N_2 and CO_2. Spirulina: 1. 400°C; 2.550°C; 3. 700°C. Chlorella: 1. 400°C; 5. 550°C; 6. 700°C. Dunaliella: 7. 400°C; 8.550°C; 9. 700°C. Laminaria: 10. 400°C; 11. 550°C; 12. 700°C. Porphyra: 13. 400°C; 14. 550°C; 15. 700°C. Cellulose: 16. 400°C; 17. 550°C; 18. 700°C. Ovalbumin: 19. 400°C; 20. 550°C; 21. 700°C.

7.2 Algal ash as catalysts

7.2.1 Distribution of products

According to **Chapter 6**, the optimal pyrolysis temperature of most algae samples under nitrogen for maximum gaseous production is in the range of 400-550°C. Therefore, the catalysed pyrolysis of the five algae under nitrogen using spirulina, chlorella, laminaria and porphyra ash was conducted at 550°C. The distribution of gaseous, liquid and solid products was explicated in **Table 7-6**. Since dunaliella has only 0.2 wt.% ash content according to **Table 4-1**, its ash was not considered to be used as the catalyst in this section. Compared with non-catalysed pyrolysis, most of the additional ash increased the char yield after pyrolysis, while converted more long-chain compounds into more volatiles. Among four ash catalysts, porphyra and laminaria ash significantly enhanced the gas yield from the pyrolysis of spirulina, chlorella and dunaliella by around 6, 5, and 7% respectively, while decreased the bio-oil output by about 30, 60 and 20% respectively. These might due to the higher content of CaO, K_2O, and Fe_2O_3 in laminaria ash (30, 10, and 12 wt. % respectively), while larger amount of K_2O in porphyra ash (50 wt. %), according to the XRF analysis in **Table 4-8**. CaO could increase the hydrogen yield, thus the gas production raised, while the bio-oil amount reduced [124]. Meanwhile, the Fe_2O_3 contained in ash were regarded as good microwave absorbers, which could increase the microwave energy absorption capability of algae to increase the gas production from

pyrolysis [257]. Moreover, the oil production might be reduced, since the ash itself cannot be pyrolyzed into bio-oil [204]. However, ash from spirulina and chlorella, especially from spirulina, considerably increased the solid residues by 200%. It indicated that these ash contained P_2O_5, SO_3, and TiO_2 (30, 6 and 2 wt. % respectively) could inhibit the decomposition of algae samples, which significantly increased the solid yield while decreased the gaseous products correspondingly [258]. Since laminaria has only 67.7% volatiles, it yielded lower gaseous and liquid products with four ash catalysts. Similar product distribution occurred in the pyrolysis of porphyra using the same four ash catalysts, which led to enlarged char yield and lower amount of gaseous fraction and bio-oil.

Table 7-6 Product distribution of MEP of algae using spirulina ash, chlorella ash, laminaria ash and porphyra ash as catalysts at 550°C (100 wt.%)

Algae	Catalyst	Solid	Liquid	Gas
Spirulina	Spirulina Ash	17.2±1.7	7.9±0.7	74.9±2.4
	Chlorella Ash	11.0±1.2	15.6±1.1	73.4±2.3
	Laminaria Ash	7.7±1.1	10.7±2.0	81.6±3.1
	Porphyra Ash	6.8±1.2	6.5±1.7	86.7±2.9
	Non	**5.4±0.4**	**12.8±1.1**	**81.8±1.5**
Chlorella	Spirulina Ash	30.5±3.9	3.6±0.4	65.9±4.3
	Chlorella Ash	11.9±1.4	13.4±0.9	74.7±2.3
	Laminaria Ash	11.3±1.2	7.2±0.8	81.5±2.0
	Porphyra Ash	8.6±0.8	8.0±0.8	83.4±1.6
	Non	**11.7±2.4**	**8.9±0.8**	**79.5±3.2**
Dunaliella	Spirulina Ash	22.4±2.3	2.6±0.3	75.0±2.6
	Chlorella Ash	12.9±1.9	8.6±0.4	78.5±2.3
	Laminaria Ash	9.5±0.9	3.9±0.3	86.6±1.2
	Porphyra Ash	7.9±1.1	1.7±0.2	90.4±1.3
	Non	**6.0±0.9**	**9.3±2.0**	**84.7±2.9**
Laminaria	Spirulina Ash	43.0±3.8	0.7±0.1	56.3±3.9
	Chlorella Ash	28.7±2.9	2.6±0.4	68.7±3.3
	Laminaria Ash	36.3±3.1	0.8±0.1	62.9±3.2
	Porphyra Ash	33.8±3.9	2.6±0.4	63.6±4.3
	Non	**18.9±3.1**	**2.2±0.5**	**79.0±3.6**
Porphyra	Spirulina Ash	13.3±1.5	3.4±0.4	83.3±1.9
	Chlorella Ash	13.2±1.9	5.4±0.5	81.4±2.4
	Laminaria Ash	21.0±1.8	3.6±0.5	75.4±2.3
	Porphyra Ash	14.8±1.3	4.2±0.7	81.0±2.0
	Non	**11.2±2.1**	**2.4±0.1**	**86.4±2.2**

7.2.2 Composition of gas product

The compositions of gas product from the catalysed microwave-enhanced pyrolysis of algae using spirulina, chlorella, laminaria and porphyra ash as catalysts at 550°C were listed in **Table 7-7**. Compared with the results of non-catalysis process, the syngas percentage from microalgae increased greatly by 5-45%, while that from macroalgae decreased slightly by 2-20%, which catalysed by spirulina, chlorella and porphyra ash. Based on the XRF analysis in **Table 4-8**, these ash contained CaO, which could increase the overall syngas production by raising the H_2 yield while reducing the CO_2; MgO, which could decrease the CO and CO_2. Among these, the largest increment of syngas existed in the catalysis of spirulina by chlorella ash. The contents of C1-C3 gas from spirulina, chlorella, dunaliella and laminaria mostly reduced by 5-60%, with increment of CO_2, CO and H_2 proportions. However, syngas content reduced whilst CO_2 increased in the catalysed pyrolysis of porphyra under all four ash catalysts. Moreover, laminaria ash decreased the formation of syngas from spirulina, chlorella, laminaria and porphyra, while raised the CO_2 percent. It showed contrary gas composition from dunaliella, which yielded 76.4 vol. % of syngas and reduced CO_2 to only 15.7 vol. %.

Table 7-7 Compositions of gaseous fraction from different algae using spirulina ash, chlorella ash, laminaria ash and porphyra ash as catalysts at 550°C. (100 vol. %)

Algae	Catalyst	CH_4	C_2H_6	C_2H_4	C_3H_8	CO_2	CO	H_2	Others	Syngas (CO+ H_2)	HHV (MJ/Nm^3)
Spirulina	Spirulina Ash	9.5	1.0	2.8	0.3	17.0	29.4	39.8	0.2	69.3	15.4
	Chlorella Ash	4.0	0.4	1.1	0.2	23.4	29.4	41.5	0.0	70.9	11.8
	Laminaria Ash	15.0	1.5	6.6	0.4	29.3	20.4	26.4	0.5	46.7	17.5
	Porphyra Ash	6.8	0.7	2.6	0.2	19.4	32.7	37.4	0.2	70.0	14.0
	Non	**16.8**	**5.4**	**2.0**	**0.7**	**18.1**	**22.1**	**26.9**	**8.1**	**49.0**	**18.6**
Chlorella	Spirulina Ash	10.1	1.4	2.5	0.4	14.9	27.9	42.6	0.2	70.5	16.0
	Chlorella Ash	10.4	1.0	3.0	0.3	22.3	23.0	39.9	0.0	62.9	15.0
	Laminaria Ash	17.1	1.3	3.1	0.2	25.5	24.7	27.8	0.2	52.6	16.6
	Porphyra Ash	10.1	1.0	4.0	0.3	19.6	31.2	33.6	0.2	64.9	15.7
	Non	**16.6**	**5.6**	**1.3**	**0.7**	**12.4**	**23.6**	**26.1**	**13.7**	**49.7**	**18.4**
Dunaliella	Spirulina Ash	9.5	0.1	0.3	0.0	31.1	43.0	16.0	0.1	58.9	11.5
	Chlorella Ash	10.3	1.2	2.7	0.2	31.4	29.0	25.2	0.0	54.2	13.7
	Laminaria Ash	7.4	0.1	0.4	0.0	15.7	20.5	55.8	0.0	76.4	13.0
	Porphyra Ash	8.5	1.0	2.4	0.2	24.7	33.3	29.9	0.1	63.2	13.8
	Non	**9.6**	**2.6**	**1.2**	**0.3**	**17.5**	**33.3**	**22.6**	**12.9**	**55.9**	**13.8**
Laminaria	Spirulina Ash	5.0	0.4	0.6	0.1	21.0	32.1	40.7	0.1	72.9	11.9
	Chlorella Ash	5.1	0.3	1.0	0.1	20.7	37.5	35.2	0.1	72.7	12.1
	Laminaria Ash	12.1	0.0	0.2	0.0	30.2	32.9	24.5	0.0	57.4	12.3
	Porphyra Ash	4.2	0.4	0.7	0.1	24.4	26.8	43.3	0.0	70.1	11.4
	Non	**6.5**	**1.3**	**0.5**	**0.2**	**14.7**	**31.0**	**40.4**	**5.5**	**71.4**	**13.0**
Porphyra	Spirulina Ash	7.6	0.9	0.8	0.3	20.1	29.6	40.6	0.0	70.2	13.4
	Chlorella Ash	6.4	0.7	1.0	0.2	20.6	34.8	36.2	0.1	71.0	12.9
	Laminaria Ash	8.2	0.2	0.4	0.1	22.1	33.0	36.0	0.0	69.0	12.5
	Porphyra Ash	5.9	0.6	1.1	0.2	24.4	29.4	38.3	0.1	67.6	12.3
	Non	**6.4**	**0.3**	**0.1**	**0.1**	**7.5**	**40.7**	**38.6**	**6.3**	**79.3**	**13.0**

7.2.3 Bio-oil composition

Table 7-8 showed the composition of bio-oil using spirulina, chlorella, laminaria and porphyra ash as catalysts at 550°C, coupled with the non-catalysis pyrolysis results. In general, the catalysts assisted to reduce the yield of phenols, nitrogenated compounds, acids and PAHs, while increased the production of aromatics and aliphatics. Unlike other four algae, bio-oil from dunaliella reduced aromatics and larger percentages of aliphatics, phenols and PAHs, without nitrogenated compounds and acids. The ash of spirulina and porphyra significantly improved aromatic percent in the bio-oil of spirulina, chlorella, and porphyra, which made these liquid products desirable as fuels. Moreover, the PAHs of laminaria and porphyra oil decreased dramatically to 4.5-7.3 and 2.7-10.3 % from 35.4 and 43.8 % respectively. Meanwhile, the HHVs of laminaria and porphyra bio-oil increased by 84.2-163.2% and 27.3-81.8%, compared with the corresponding non-catalysis bio-oil. Similarly, the bio-oil of spirulina and chlorella reduced around half PAHs, while increased the amount of aromatics to 7.5-17.1 and 9.9-21.4 % from 2.1 and 4.3 % correspondingly.

Table 7-8 GC-MS: compositions of algae bio-oil using spirulina ash, chlorella ash, laminaria ash and porphyra ash as catalysts at 550°C. (100% area)

		Spirulina					Chlorella					Dunaliella					Laminaria					Porphyra				
Category	**Compounds**	**SA**	**CA**	**LA**	**PA**	**NON**	**SA**	**CA**	**LA**	**PA**	**NON**	**SA**	**CA**	**LA**	**PA**	**NON**	**SA**	**CA**	**LA**	**PA**	**NON**	**SA**	**CA**	**LA**	**PA**	**NON**
Aldehyde	5-Hydroxymethylfurfural	-	-	-	-	-	-	-	-	-	-	2.1	3.4	2.3	1.6	-	-	1.9	-	-	-	-	-	-	-	-
Aromatics	Benzene, 1,3-dimethyl-	-	1.4	-	-	-	2.5	1.1	3.6	6.8	-	1.9	4.0	4.5	6.0	1.6	2.3	1.3	1.1	1.4	-	2.4	-	-	-	2.3
	Benzene, 1-ethynyl-4-methyl-	-	-	-	-	-	-	-	-	-	-	-	-	-	-	-	-	-	-	-	-	-	-	-	-	3.3
	Styrene	6.4	2.2	5.2	8.2	1.5	6.1	2.7	3.2	8.7	2.9	1.3	1.2	2.4	2.0	-	2.6	2.8	2.9	1.1	8.8	3.4	2.3	4.4	5.1	5.4
	o-Xylene	3.4	-	2.3	3.9	-	6.1	2.9	1.6	-	-	4.6	4.0	2.0	2.9	0.4	6.7	5.2	4.1	4.1	5.2	4.1	2.4	3.4	4.7	2.3
	Ethylbenzene	4.8	2.7	3.6	4.4	0.6	5.6	2.7	3.3	5.4	1.4	1.9	2.3	1.8	2.2	-	2.5	2.0	2.3	1.0	1.5	4.7	3.4	3.5	4.4	1.2
	t-Butylhydroquinone	-	-	-	-	-	-	-	-	-	-	-	2.1	3.0	3.4	10.8	-	-	-	-	-	-	-	-	-	-
	2-Furanmethanol	0.6	1.2	0.7	0.6	-	1.1	0.5	0.5	0.5	-	4.1	5.1	4.2	4.8	7.0	6.0	5.6	3.9	3.9	-	0.6	0.7	-	0.7	-
	tert-Butyl-p-benzoquinone	-	-	-	-	-	-	-	-	-	-	2.1	-	-	-	7.0	-	-	-	-	-	-	-	-	-	-
	1-Dodecanol, 3,7,11-trimethyl-	-	-	-	-	-	-	-	-	-	-	-	-	-	-	4.6	-	-	-	-	-	-	-	-	-	-
	Total	**15.2**	**7.5**	**11.8**	**17.1**	**2.1**	**21.4**	**9.9**	**12.2**	**21.4**	**4.3**	**15.9**	**18.7**	**17.9**	**21.3**	**31.4**	**20.1**	**16.9**	**14.3**	**11.5**	**15.5**	**15.2**	**8.8**	**11.3**	**14.9**	**14.5**
Aliphatics	Heptadecane	2.6	4.8	3.0	3.3	4.1	0.9	1.6	1.6	1.3	-	0.7	0.7	0.4	0.6	-	-	-	-	-	-	0.8	0.6	0.6	0.7	-
	Neophytadiene	1.5	2.3	1.3	1.4	-	2.6	6.9	5.8	4.8	-	-	-	-	-	-	-	-	-	-	-	0.7	0.9	1.0	0.8	-
	1-Tetradecene	-	-	-	-	-	-	-	-	-	-	-	7.4	3.7	-	-	-	-	-	-	-	-	-	-	-	-
	Cyclopentadecane	-	-	-	-	-	-	-	-	-	-	2.1	2.5	1.8	4.7	-	-	-	-	-	-	0.5	-	-	-	-
	Cyclopropane, 1-methyl-2-octyl-	-	-	-	-	-	-	-	-	-	-	4.4	-	-	-	-	-	-	-	-	-	-	-	-	-	-
	Total	**4.1**	**7.1**	**4.3**	**4.7**	**4.1**	**3.5**	**8.5**	**7.4**	**6.1**	**0**	**7.2**	**10.6**	**5.9**	**5.3**	**0**	**0**	**0**	**0**	**0**	**0**	**2**	**1.5**	**1.6**	**1.5**	**0**
Phenols	p-Cresol	5.7	6.2	6.9	4.5	8.5	3.2	6.1	5.3	3.9	8.5	1.4	1.9	1.6	1.1	1.2	2.3	2.1	4.1	2.0	2.0	8.3	9.7	7.7	7.0	4.6
	Phenol	5.1	5.5	5.9	4.2	9.3	1.5	2.8	3.0	2.4	4	0.8	1.5	1.3	0.7	1.4	1.4	2.1	3.2	1.1	1.9	9.3	5.0	7.1	7.5	2.2
	Phenol, 2-methyl-	1.6	2.4	1.9	-	-	-	-	-	-	-	-	1.5	-	-	-	1.5	-	-	-	-	1.9	2.1	1.7	1.2	-
	Phenol, 4-amino-	-	-	-	-	-	0.8	1.7	1.0	1.1	-	-	-	-	-	-	-	-	2.0	-	-	1.2	1.2	-	1.6	-
	Total	**12.4**	**14.1**	**14.7**	**8.7**	**17.8**	**5.5**	**10.6**	**9.3**	**7.4**	**12.5**	**2.2**	**4.9**	**2.9**	**1.8**	**2.6**	**5.2**	**4.2**	**9.3**	**3.1**	**3.9**	**20.7**	**18**	**16.5**	**17.3**	**6.8**
Nitrogenated compounds	Indole	7.8	7.4	9.6	6.4	12.8	5.0	6.8	6.1	5.1	10.1	-	-	-	-	-	-	1.5	0.9	0.6	5.2	3.0	3.6	4.3	2.9	4.5
	1H-Indole, 4-methyl-	2.3	2.8	2.5	-	3.7	-	2.0	1.8	1.7	2.8	-	-	-	-	-	-	-	-	-	-	-	1.4	-	1.2	-
	Benzyl nitrile	1.1	1.3	1.6	1.5	2.5	0.6	1.1	1.5	1.1	2.2	-	-	-	-	-	-	-	-	-	0.5	1.0	2.0	1.4	1.0	-
	Benzonitrile	0.7	0.6	1.8	1.0	2.5	0.7	0.6	0.6	0.8	2.1	-	-	-	-	-	-	-	-	-	-	0.3	0.5	0.5	0.4	3.6
	Quinoline	1.2	0.7	2.0	1.7	4.1	2.2	1.3	1.3	1.5	3.7	-	-	-	-	-	-	-	0.8	-	-	1.4	1.1	1.6	1.3	2.3
	Hexadecanamide	2.6	3.9	1.8	2.0	-	0.6	1.9	1.1	0.6	-	-	-	-	-	-	-	-	-	-	-	-	1.0	-	-	-
	Hexadecanenitrile	2.1	1.6	0.9	1.4	-	1.2	-	1.9	-	-	-	-	-	-	-	-	-	-	-	-	2.0	1.6	0.9	1.1	-
	Total	**17.8**	**18.3**	**20.2**	**14.0**	**25.6**	**10.3**	**13.7**	**14.3**	**10.8**	**20.9**	**0**	**0**	**0**	**0**	**0**	**0**	**1.5**	**1.7**	**0.6**	**5.7**	**7.7**	**11.2**	**8.7**	**7.9**	**10.4**
Acids	n-Hexadecanoic acid	-	-	-	-	5.2	-	-	-	-	1.8	-	-	-	-	-	-	-	-	-	-	-	-	-	-	-
	Benzoic acid	-	-	-	-	-	-	-	-	-	-	19.0	0.4	-	-	3.0	-	-	-	-	-	-	-	-	0.3	-
	Octadecanoic acid, 2-propenyl ester	-	-	-	-	-	-	-	-	-	-	-	-	-	-	-	-	-	-	-	-	-	2.1	1.7	-	-
	Total	**0**	**0**	**0**	**0**	**5.2**	**0**	**0**	**0**	**0**	**1.8**	**19**	**0.4**	**0**	**0**	**0**	**0**	**0**	**0**	**0**	**0**	**0**	**2.1**	**1.7**	**0.3**	**0**
PAHs	Naphthalene	2.4	1.4	3.8	3.0	6.4	5.5	4.0	5.4	3.2	9.2	1.7	2.0	5.4	4.0	6.4	1.6	1.6	1.6	0.9	11.7	1.9	1.5	3.7	1.5	19.7
	Naphthalene, 1,2,3,4-tetrahydro-1,1,6-trimethyl-	0.4	-	-	0.3	-	0.6	-	-	-	-	3.1	4.4	3.5	3.8	-	-	-	-	-	-	-	-	-	-	-
	Naphthalene, 2-methyl-	-	-	-	-	-	2.5	-	-	-	-	2.8	-	-	3.7	-	0.3	-	-	0.5	-	1.7	-	-	0.9	-
	Anthracene	1.2	0.6	1.5	0.5	1.4	0.9	1.4	1.3	2.5	4.3	0.8	0.5	2.8	1.4	1.2	1.1	1.5	2.0	1.3	7.1	0.4	0.7	2.4	1.5	8.1
	Pyrene	-	-	-	0.5	-	0.5	0.6	0.6	0.9	1.1	-	0.5	1.2	0.4	-	0.7	0.5	1.2	0.8	2.5	-	-	1.1	0.4	3.2
	Fluoranthene	-	-	0.4	0.3	0.5	0.6	0.4	0.3	0.7	1.5	-	0.3	0.9	0.5	-	0.5	0.9	0.7	0.5	2.6	-	-	0.6	0.3	3.4
	Indene	-	-	-	1.6	1.3	2.0	1.8	1.4	1.5	1.4	-	-	2.1	1.6	-	1.8	1.8	-	-	4.2	-	-	-	1.7	-
	Biphenylene	0.8	-	1.2	0.9	1.8	2.1	1.1	1.1	1.8	3.2	-	0.9	2.8	1.2	1.1	0.7	1.0	1.7	0.5	7.3	0.7	0.5	2.5	1.2	9.4
	Total	**4.8**	**2.0**	**6.9**	**7.1**	**11.4**	**14.7**	**9.3**	**10.1**	**10.6**	**20.7**	**8.4**	**8.6**	**18.7**	**16.6**	**8.7**	**6.7**	**7.3**	**7.2**	**4.5**	**35.4**	**4.7**	**2.7**	**10.3**	**7.5**	**43.8**
Others	Dianhydromannitol	-	-	-	-	-	-	-	-	-	-	-	-	-	-	-	6.5	9.0	6.6	12.3	-	-	-	-	-	-
	1,4:3,6-Dianhydro-.alpha.-d-glucopyranose	-	-	-	-	-	-	-	-	-	-	0.7	-	-	0.7	-	4.0	4.4	4.0	7.0	-	-	-	-	1.1	-
	1,2-Cyclopentanedione, 3-methyl-	-	-	-	-	-	-	-	-	-	-	2.0	-	-	1.3	-	2.4	2.5	2.4	2.3	-	-	-	1.0	-	-
	[1,2,3,4]Tetrathiane	-	-	-	-	-	-	-	-	-	-	-	-	-	-	-	-	-	-	6.6	-	-	-	-	-	-
HHVs (MJ/kg)		**3.7**	**2.3**	**3.3**	**2.8**	**3.1**	**2.7**	**2.4**	**3.7**	**4.2**	**3.8**	**2.7**	**3.8**	**4.0**	**3.8**	**3.6**	**4.0**	**3.5**	**5.0**	**3.6**	**1.9**	**5.6**	**6.0**	**5.0**	**4.2**	**3.3**

7.3 Summary

In this chapter, microwave-enhanced reforming of algae under CO_2 atmosphere was conducted at 400, 550 and 700°C and the results including distribution and characterization of gas, bio-oil and char were compared with those obtained under N_2 atmosphere in **Section 7.1**. The bio-oil yield in CO_2 was slightly higher than that in N_2, whilst the production of gas was larger under N_2 atmosphere. The syngas in spirulina gas product decreased, while that from dunaliella increased. Syngas from other samples remained similar amount. Seldom PAHs occurred in bio-oil from all five algae samples under CO_2 atmosphere. Secondly, the ash of spirulina, chlorella, laminaria and porphyra was introduced into the pyrolysis of the five algae under N_2 atmosphere at 550°C in **Section 7.2**. Compared with the non-catalysis results, the amount of char increased. The syngas percentage from spirulina, chlorella and dunaliella increased greatly, while that from laminaria and porphyra decreased slightly with addition of spirulina, chlorella and porphyra ash. The content of PAHs in the bio-oil of spirulina, chlorella, laminaria and porphyra reduced, whilst the amount of aromatics increased.

Chapter 8. Conclusions and recommendations for future work

8.1 Conclusions

This study investigated kinetics of algae, microwave-enhanced pyrolysis of algae, microwave-enhanced reforming of algae under CO_2 and microwave-enhanced catalytic reforming of algae.

8.1.1 Kinetic analysis of algae pyrolysis under N_2 and CO_2

The pyrolysis behaviour and the kinetic characteristic of three primary algae components (lipid, carbohydrate and protein) and three representative algae (microalgae-spirulina and chlorella, macroalgae-porphyra), pyrolyzed under N_2 and CO_2 were carried out using TGA. On the basis of Arrhenius Law, Kissinger- Akahira-Sunose (KAS) method was introduced to determine activation energy (E_a) and pre-exponential factor (A). It is apparent that the time for the pyrolysis completion of algae and ovalbumin in CO_2 atmosphere was shorter, which suggested that CO_2 could attribute to the pyrolysis of algae and its protein content. However, the activation energy of cellulose pyrolysis performed similarly in both atmosphere. Moreover, oil droplets requested larger activation energy in CO_2 indicating the difficulty of lipid content pyrolysis under CO_2 atmosphere. This study shows that CO_2 atmosphere is favourable for algae pyrolysis when the protein content is high whilst lipid content is low. Furthermore, Coats-Redfern method was employed to optimize the calculation of

kinetic parameters (E_a and A) and define the mechanism and order of decomposition Events. By comparison of E_a derived under two gas conditions, ovalbumin and spirulina required the least amount of energy (66.8 and 20.7 kJ/mol) to initiate pyrolysis under CO_2. Additionally, the protein components in algae are the first to decompose followed by carbohydrates and lastly lipids.

8.1.2 Microwave-enhanced pyrolysis of algae for syngas production

The yield and compositions of gas product, bio-oil and char from microwave-enhanced pyrolysis process of five algae and two model compounds at 400, 550 and 700 °C were conducted. With gas production of 85.6-87.1 wt.%, porphyra is regarded to be more suitable as raw materials for syngas-enrich gas production, while widely-used spirulina and chlorella favored oil production of 6.3-12.8wt.% and 8.0-15.4 wt.% respectively, owing to their relatively higher protein content of 57.8 and 55.6wt.% respectively. With a high carbohydrate proportion of 94 wt.%, dunaliella converted most of its carbohydrates into C1-C3 gas, compared with the gas product of porphyra. Laminaria has a high portion of incombustible components; thus it only has gaseous production less than 80 wt.%. It also showed that the optimal temperature for most of the samples (except for spirulina) to maximize their gaseous fraction was around 400-550 °C.

By plotting the temperature profiles, porphyra showed the highest reactivity among five algae with an average heating rate as high as 100°C/min, which lead to higher yield in gaseous fraction. For the production of bio-oil, highly protein-contained microalgae were favored to be the raw materials with larger HHVs (>20 MJ/kg) and less formation of PAHs and phenols, compared to macroalgae (<18MJ/kg). The microwave-enhance pyrolysis of algae produced high gas yield with higher HHVs and comparable H_2+CO percentage with conventional coal gasification processes. It was also found that microalgae favors the formation of more phenols, while nitrogenated compounds and PAHs are mainly derived from protein and carbohydrate respectively. Therefore, porphyra is more appropriate for the production of syngas-rich gas product.

8.1.3 Microwave-enhanced reforming process of algae under CO_2

Microwave enhanced reforming process of algae coupled with its primary model compounds was conducted at 400, 550 and 700°C in CO_2 atmosphere. Compared with results derived in N_2, the production of bio-oil in CO_2 atmosphere increased, but the gas production was larger under N_2 atmosphere. The syngas in spirulina gas product decreased, while that from dunaliella increased. Syngas from other samples remained similar amount. For liquid product, rare PAHs formed in bio-oil of all five algae samples under CO_2 atmosphere.

8.1.4 Microwave-enhanced pyrolysis of algae with algal ash as catalysts

The ash of spirulina, chlorella, laminaria and porphyra was added into the pyrolysis of five algae under N_2 atmosphere at 550°C. Compared with the non-catalysis process, the weight percentage of algae char grew according to the product distribution. The syngas from microalgae-spirulina, chlorella and dunaliella dramatically increased, but that from macroalgae- laminaria and porphyra dropped slightly with addition of spirulina, chlorella and porphyra ash. The content of PAHs in the bio-oil of algae reduced, while the proportion of aromatics increased.

8.2 Future work

Although much research work has been conducted to study the microwave-enhanced pyrolysis as well as the catalytic reforming of algae to improve the gaseous production, there still remains some problems to be solved for further understanding and commercializing the process due to the limitations in resources and time. Some suggested future work are,

- The carrier gas for microwave-enhanced pyrolysis of algae can be altered to water steam gas, rather using nitrogen nor carbon dioxide. The investigation shows that water steam gas is favorable for algae pyrolysis which releases hydrogen ions and reforms into hydrocarbons. Hence, the water steam gas could

favor the bio-oil yield with improved quality from microwave-enhanced pyrolysis of algae.

- Due to inhomogeneous microwave field or dielectrics in the feedstock, microwave heating could form hot spots which would have crucial effects on the production. In order to control or even utilize the hot spot phenomenon, the software, COMSOL Multiphysics, can be used to conduct systematic modelling of the heating process in microwave cavity and waveguide, as well as the temperature distribution on the algae samples. Therefore, it could assist in the design and modification of microwave cavity to conduct the pyrolysis process of algae more effectively.
- The property of dielectrics of algae and its char is worthwhile further investigation, since it significantly affects the ability of substances to absorb microwave irradiation. Char, as carbonaceous material, could further promote the pyrolysis of algae as well. The derived dielectric parameters, i.e., dielectric constant and loss, also can be used in the COMSOL modelling of microwave-enhanced pyrolysis.

Bibliography

1. Koutinas, A., et al., *Biodiesel production from microbial oil.* Handbook of biofuels production: processes and technologies, 2011: p. 177-198.
2. Nautiyal, P., K.A. Subramanian, and M.G. Dastidar, *Production and characterization of biodiesel from algae.* Fuel Processing Technology, 2014. **120**(0): p. 79-88.
3. Gimpel, J., *Biofuels from algae: challenges and potential.* Biofuels, 2010. **1**(5): p. 763-784.
4. Fernand, F., et al., *Offshore macroalgae biomass for bioenergy production: Environmental aspects, technological achievements and challenges.* Renewable & Sustainable Energy Reviews, 2016.
5. McKendry, P., *Energy production from biomass (part 2): conversion technologies.* Bioresource Technology, 2002. **83**(1): p. 47-54.
6. Miao, X., Q. Wu, and C. Yang, *Fast pyrolysis of microalgae to produce renewable fuels.* Journal of Analytical & Applied Pyrolysis, 2004. **71**(2): p. 855-863.
7. Sami, M., K. Annamalai, and M. Wooldridge, *4 Co-firing of coal and biomass fuel blends.* Progress in Energy and Combustion Science, 2001. **27**(2): p. 171-214.
8. Lu, L., et al., *100 Char structural ordering during pyrolysis and combustion and its influence on char reactivity.* Fuel, 2002. **81**(9): p. 1215-1225.
9. Alonso, M.J.G., et al., *107 A reactivity study of chars obtained at different temperatures in relation to their petrographic characteristics.* Fuel Processing Technology, 2001. **69**(3): p. 257-272.
10. Alonso, M.J.G., et al., *109 Influence of pyrolysis temperature on char optical texture and reactivity.* Journal of Analytical and Applied Pyrolysis, 2001. **58-59**(0): p. 887-909.
11. Lester, E., et al., *117 The procedure used to develop a coal char classification—Commission III Combustion Working Group of the International Committee for Coal and Organic Petrology.* International Journal of Coal Geology, 2010. **81**(4): p. 333-342.

12. Bridgwater, A.V., *DIT/DITB Developments In Thermochemical Biomass Conversion Volume 2*. 1997: Blackie Academic and Professional. 1649.
13. Avila, C., et al., *123 Morphology and reactivity characteristics of char biomass particles.* Bioresource Technology, 2011. **102**(8): p. 5237-5243.
14. Colomba, D.B., *Combustion and gasification rates of lignocellulosic chars.* Progress in Energy and Combustion Science, 2009. **35**(2): p. 121-140.
15. Asadullah, M., et al., *101 Effects of biomass char structure on its gasification reactivity.* Bioresource Technology, 2010. **101**(20): p. 7935-7943.
16. Raveendran, K. and A. Ganesh, *Adsorption characteristics and pore-development of biomass-pyrolysis char.* Fuel, 1998. **77**(7): p. 769-781.
17. Mello, P.A., J.S. Barin, and R.A. Guarnieri, *Chapter 2 - Microwave Heating*, in *Microwave-Assisted Sample Preparation for Trace Element Analysis*, É.M.d.M. Flores, Editor. 2014, Elsevier: Amsterdam. p. 59-75.
18. Demirbas, A., *Combustion characteristics of different biomass fuels.* Progress in Energy & Combustion Science, 2004. **30**(2): p. 219-230.
19. Chisti, Y., *Biodiesel from microalgae.* Biotechnology Advances, 2007. **25**(3): p. 294-306.
20. Li, X., H. Xu, and Q. Wu, *Large-scale biodiesel production from microalga Chlorella protothecoides through heterotrophic cultivation in bioreactors.* Biotechnology & Bioengineering, 2007. **98**(4): p. 764-71.
21. Miao, X. and Q. Wu, *Biodiesel production from heterotrophic microalgal oil.* Bioresource Technology, 2006. **97**(6): p. 841-6.
22. Qi, Z., et al., *Review of biomass pyrolysis oil properties and upgrading research.* Energy Conversion & Management, 2007. **48**(1): p. 87-92.

23. Rodolfi, L., et al., *Microalgae for oil: Strain selection, induction of lipid synthesis and outdoor mass cultivation in a low-cost photobioreactor.* Biotechnology & Bioengineering, 2009. **102**(1): p. 100-12.
24. Alipour Moghadam Esfahani, R., et al., *H2-rich syngas production through mixed residual biomass and HDPE waste via integrated catalytic gasification and tar cracking plus bio-char upgrading.* Chemical Engineering Journal, 2017. **308**: p. 578-587.
25. Wan, Y., et al., *Experimental investigation on microwave assisted pyrolysis of algae for rapid bio-oil production.* Nongye Gongcheng Xuebao/Transactions of the Chinese Society of Agricultural Engineering, 2010. **26**(1): p. 295-300.
26. Xie, Q., et al., *Fast microwave-assisted catalytic co-pyrolysis of microalgae and scum for bio-oil production.* Fuel, 2015. **160**: p. 577-582.
27. Zhang, R., et al., *Microwave-enhanced pyrolysis of natural algae from water blooms.* Bioresource Technology, 2016. **212**: p. 311-317.
28. Saber, M., B. Nakhshiniev, and K. Yoshikawa, *A review of production and upgrading of algal bio-oil.* Renewable and Sustainable Energy Reviews, 2016. **58**: p. 918-930.
29. Hernández, I., et al., *Studies on the biofiltration capacity of Gracilariopsis longissima : From microscale to macroscale.* Aquaculture, 2006. **252**(1): p. 43-53.
30. Wu, H., et al., *Bioremediation efficiency of the largest scale artificial Porphyra yezoensis cultivation in the open sea in China.* Marine Pollution Bulletin, 2015. **95**(1): p. 289-296.
31. Yin, C., *Microwave-assisted pyrolysis of biomass for liquid biofuels production.* Bioresource Technology, 2012. **120**: p. 273-284.
32. Saxena, R.C., D.K. Adhikari, and H.B. Goyal, *Biomass-based energy fuel through biochemical routes: A review.* Renewable & Sustainable Energy Reviews, 2009. **13**(1): p. 167-178.
33. Wang, M., M. Wu, and H. Huo, *Life-cycle energy and greenhouse gas emission impacts of different corn ethanol plant types.* Environmental Research Letters, 2007. **2**(2): p. 24001-13.

34. Escobar, J.C., et al., *Biofuels: Environment, technology and food security.* Renewable & Sustainable Energy Reviews, 2009. **13**(6–7): p. 1275-1287.
35. Kwon, E.E., H. Yi, and Y.J. Jeon, *Sequential co-production of biodiesel and bioethanol with spent coffee grounds.* Bioresource Technology, 2013. **136**(3): p. 475-480.
36. Papa, G., et al., *Comparison of different pretreatments for the production of bioethanol and biomethane from corn stover and switchgrass.* Bioresource Technology, 2015. **183**: p. 101-110.
37. Kwon, E.E., H.R. Yi, and K. Hyunhan, *Energy recovery from microalgal biomass via enhanced thermo-chemical process.* Biomass & Bioenergy, 2014. **63**(2): p. 46-53.
38. Guo, M., et al., *The environmental profile of bioethanol produced from current and potential future poplar feedstocks in the EU.* Green Chemistry, 2014. **16**(11): p. 4680-4695.
39. Fu, X., et al., *A microalgae residue based carbon solid acid catalyst for biodiesel production.* Bioresource Technology, 2013. **146**(10): p. 767.
40. Truongxuan, D., et al., *Hierarchical economic potential approach for techno-economic evaluation of bioethanol production from palm empty fruit bunches.* Bioresource Technology, 2015. **189**: p. 224-235.
41. Ma, F. and M.A. Hanna, *Biodiesel production: a review.* Bioresource Technology, 1999. **70**(1): p. 1-15.
42. Wang, N., et al., *A Comparative study of microwave-induced pyrolysis of lignocellulosic and algal biomass.* Bioresource Technology, 2015. **190**: p. 89-96.
43. Grønli, M.G., G. Várhegyi, and C.D. Blasi, *Thermogravimetric Analysis and Devolatilization Kinetics of Wood.* Ind.eng.chem.res, 2002. **41**(17): p. 4201-4208.
44. Jiang, G., D.J. Nowakowski, and A.V. Bridgwater, *A systematic study of the kinetics of lignin pyrolysis.* Thermochimica Acta, 2010. **498**(1–2): p. 61–66.

45. Burhenne, L., et al., *The effect of the biomass components lignin, cellulose and hemicellulose on TGA and fixed bed pyrolysis.* Journal of Analytical & Applied Pyrolysis, 2013. **101**(101): p. 177-184.
46. Nautiyal, P., K.A. Subramanian, and M.G. Dastidar, *Production and characterization of biodiesel from algae.* Fuel Processing Technology, 2014. **120**: p. 79-88.
47. Ross, A.B., et al., *Classification of macroalgae as fuel and its thermochemical behaviour.* Bioresource Technology, 2008. **99**(14): p. 6494-6504.
48. Casoni, A.I., et al., *Valorization of Rhizoclonium sp. algae via pyrolysis and catalytic pyrolysis.* Bioresource Technology, 2016. **216**: p. 302-307.
49. Kim, S.S., et al., *Pyrolysis characteristics and kinetics of the alga Saccharina japonica.* Bioresource Technology, 2012. **123**(3): p. 445-451.
50. Minowa, T., et al., *Oil production from algal cells of Dunaliella tertiolecta by direct thermochemical liquefaction.* Fuel, 1995. **74**(12): p. 1735–1738.
51. *Renewable biological systems for alternative sustainable energy production / edited by Kazuhisa Miyamoto*. FAO agricultural services bulletin ; 128., ed. K. Miyamoto, Food, and N. Agriculture Organization of the United. 1997, Rome: Food and Agriculture Organization of the United Nations.
52. Gellenbeck, K.W. and D.J. Chapman, *Seaweed uses: the outlook for mariculture.* Endeavour, 1983. **7**(1): p. 31-37.
53. Schenk, P.M., et al., *Second generation biofuels: high-efficiency microalgae for biodiesel production.* Bioenergy Research, 2008. **1**(1): p. 20-43.
54. Chen, P., et al., *Review of the biological and engineering aspects of algae to fuels approach.* International Journal of Agricultural & Biological Engineering, 2009. **3483**(4): p. 261-268.
55. DOE, *National algal biofuels technology roadmap*. 2009.
56. Dimitriadis, A. and S. Bezergianni, *Hydrothermal liquefaction of various biomass and waste feedstocks for biocrude production: A*

state of the art review. Renewable and Sustainable Energy Reviews, 2017. **68, Part 1**: p. 113-125.

57. Brennan, L. and P. Owende, *Owende, P.: Biofuels from microalgae—a review of technologies for production, processing, and extractions of biofuels and co-products. Renew. Sustain. Energy Rev. 14(2), 557-577.* Renewable & Sustainable Energy Reviews, 2010. **14**(2): p. 557-577.
58. Chaiwong, K., et al., *Study of bio-oil and bio-char production from algae by slow pyrolysis.* Biomass and Bioenergy, 2013. **56**: p. 600-606.
59. Amin, S., *Review on biofuel oil and gas production processes from microalgae.* Energy Conversion and Management, 2009. **50**(7): p. 1834-1840.
60. Kamm, B., P.R. Gruber, and M. Kamm, *Biorefineries-Industrial Processes and Products: Status Quo and Future Directions*. 2008.
61. Kamm, B., P.R. Gruber, and M. Kamm, *Biorefineries-Industrial Processes and Products: Status Quo and Future Directions*. 2008. 8.
62. Demirbas, A., *Combustion characteristics of different biomass fuels.* Progress in Energy and Combustion Science, 2004. **30**(2): p. 219-230.
63. Chum, H.L. and R.P. Overend, *Biomass and renewable fuels.* Fuel Processing Technology, 2001. **71**(1–3): p. 187-195.
64. Kumar, A., S.C. Bhattacharya, and H.L. Pham, *Greenhouse gas mitigation potential of biomass energy technologies in Vietnam using the long range energy alternative planning system model.* Energy, 2003. **28**(7): p. 627-654.
65. Akhtar, J. and N.A.S. Amin, *A review on process conditions for optimum bio-oil yield in hydrothermal liquefaction of biomass.* Renewable & Sustainable Energy Reviews, 2011. **15**(3): p. 1615-1624.
66. Zhang, B., M.V. Keitz, and K. Valentas, *Thermochemical liquefaction of high-diversity grassland perennials.* Journal of Analytical & Applied Pyrolysis, 2009. **84**(1): p. 18-24.

67. Ramirez, J.A., R.J. Brown, and T.J. Rainey, *A Review of Hydrothermal Liquefaction Bio-Crude Properties and Prospects for Upgrading to Transportation Fuels.* Energies, 2015. **2015**(8): p. 6765-6794.
68. Zeb, H., A. Riaz, and J. Kim, *Understanding the effect of biomass-to-solvent ratio on macroalgae (Saccharina japonica) liquefaction in supercritical ethanol.* The Journal of Supercritical Fluids, 2017. **120, Part 1**: p. 65-74.
69. Gai, C., et al., *Co-liquefaction of microalgae and lignocellulosic biomass in subcritical water.* Bioresource Technology, 2015. **185**: p. 240-245.
70. Durak, H. and T. Aysu, *Thermochemical liquefaction of algae for bio-oil production in supercritical acetone/ethanol/isopropanol.* The Journal of Supercritical Fluids, 2016. **111**: p. 179-198.
71. Singh, R., B. Balagurumurthy, and T. Bhaskar, *Hydrothermal liquefaction of macro algae: Effect of feedstock composition.* Fuel, 2015. **146**: p. 69-74.
72. Gustafsson, E., *Characterization of particulate matter from atmospheric fluidized bed biomass gasifiers.* Biomass & Bioenergy, 2011. **35**(5): p. S71–S78.
73. Cho, S.H., et al., *Pyrolysis of microalgal biomass in carbon dioxide environment.* Bioresource Technology, 2015. **193**: p. 185-191.
74. Chen, W.H., et al., *Thermochemical conversion of microalgal biomass into biofuels: a review.* Bioresource Technology, 2015. **184**: p. 314-327.
75. Laboratory, N.E.T., *Gasification Technology R&D*. 2010 World Gasification Database.
76. Surridge, A., *Carbon sequestration leadership forum: South Africa status report*, in *Report to the National Committee on Climate Change*. 2004: Pretoria.
77. Schuster, G., et al., *Biomass steam gasification--an extensive parametric modeling study.* Bioresource Technology, 2001. **77**(1): p. 71-9.

78. Campoy, M., et al., *Air–steam gasification of biomass in a fluidised bed: Process optimisation by enriched air.* Fuel Processing Technology, 2009. **90**(5): p. 677-685.
79. Gil, J., et al., *Biomass Gasification in Fluidized Bed at Pilot Scale with Steam−Oxygen Mixtures. Product Distribution for Very Different Operating Conditions.* Energy & Fuels, 1997. **11**(6): p. 1109-1118.
80. Gao, Y., *HYDROGEN PRODUCTION FROM BIOMASS GASIFICATION IN INTERCONNECTED FLUIDIZED BEDS.* Acta Energiae Solaris Sinica, 2008. **32**(2): p. 120-127.
81. Duan, P., W. Bing, and Y. Xu, *Catalytic hydrothermal upgrading of crude bio-oils produced from different thermo-chemical conversion routes of microalgae.* Bioresource Technology, 2015. **186**: p. 58.
82. Cheng, J., et al., *Biodiesel production from lipids in wet microalgae with microwave irradiation and bio-crude production from algal residue through hydrothermal liquefaction.* Bioresource Technology, 2014. **151**(1): p. 415.
83. Demirbas, A., *The influence of temperature on the yields of compounds existing in bio-oils obtained from biomass samples via pyrolysis.* Fuel Processing Technology, 2007. **88**(6): p. 591-597.
84. Balat, M., et al., *Main routes for the thermo-conversion of biomass into fuels and chemicals. Part 1: Pyrolysis systems.* Energy Conversion and Management, 2009. **50**(12): p. 3147-3157.
85. Patel, M., X. Zhang, and A. Kumar, *Techno-economic and life cycle assessment on lignocellulosic biomass thermochemical conversion technologies: A review.* Renewable and Sustainable Energy Reviews, 2016. **53**: p. 1486-1499.
86. Fakhrhoseini, S.M. and M. Dastanian, *Predicting pyrolysis products of PE, PP, and PET using NRTL activity coefficient model.* Journal of Chemistry, 2014. **2013**(3).
87. Abnisa, F. and M.A.W.D. Wan, *A review on co-pyrolysis of biomass: An optional technique to obtain a high-grade pyrolysis oil.* Energy Conversion & Management, 2014. **87**: p. 71-85.
88. Anuar Sharuddin, S.D., et al., *A review on pyrolysis of plastic wastes.* Energy Conversion and Management, 2016. **115**: p. 308-326.

89. Vassilev, S.V. and C.G. Vassileva, *Composition, properties and challenges of algae biomass for biofuel application: An overview.* Fuel, 2016. **181**: p. 1-33.
90. Chen, C.-Y., et al., *Microalgae-based carbohydrates for biofuel production.* Biochemical Engineering Journal, 2013. **78**: p. 1-10.
91. Maurya, R., et al., *Non-isothermal pyrolysis of de-oiled microalgal biomass: Kinetics and evolved gas analysis.* Bioresource Technology, 2016. **221**: p. 251-261.
92. Beneroso, D., et al., *Microwave pyrolysis of microalgae for high syngas production.* Bioresource Technology, 2013. **144**: p. 240-246.
93. Rodolfi, L., et al., *Microalgae for Oil: Strain Selection, Induction of Lipid Synthesis and Outdoor Mass Cultivation in a Low-Cost Photobioreactor.* Biotechnology & Bioengineering, 2009. **102**(1): p. 100-112.
94. Sharma, R., P.N. Sheth, and A.M. Gujrathi, *Kinetic modeling and simulation: Pyrolysis of Jatropha residue de-oiled cake.* Renewable Energy, 2016. **86**: p. 554-562.
95. Wang, S., et al., *Kinetic modeling of biomass components pyrolysis using a sequential and coupling method.* Fuel, 2016. **185**: p. 763-771.
96. Hu, M., et al., *Kinetic study and syngas production from pyrolysis of forestry waste.* Energy Conversion and Management, 2017. **135**: p. 453-462.
97. Vyazovkin, S., et al., *ICTAC Kinetics Committee recommendations for performing kinetic computations on thermal analysis data.* Thermochimica Acta, 2011. **520**(1–2): p. 1-19.
98. Ceylan, S. and D. Kazan, *Pyrolysis kinetics and thermal characteristics of microalgae Nannochloropsis oculata and Tetraselmis sp.* Bioresource Technology, 2015. **187**: p. 1-5.
99. Ceylan, S., Y. Topcu, and Z. Ceylan, *Thermal behaviour and kinetics of alga Polysiphonia elongata biomass during pyrolysis.* Bioresource Technology, 2014. **171**(1): p. 193-198.

100. Gai, C., et al., *Thermogravimetric and kinetic analysis of thermal decomposition characteristics of low-lipid microalgae.* Bioresource Technology, 2013. **150**(3): p. 139-148.
101. Huang, Y.-F., et al., *Microwave pyrolysis of lignocellulosic biomass: Heating performance and reaction kinetics.* Energy, 2016. **100**: p. 137-144.
102. Cho, S.-H., et al., *Carbon dioxide assisted co-pyrolysis of coal and ligno-cellulosic biomass.* Energy Conversion and Management, 2016. **118**: p. 243-252.
103. Lee, J., et al., *Study on susceptibility of CO2-assisted pyrolysis of various biomass to CO2.* Energy.
104. Lee, J., et al., *Pyrolysis process of agricultural waste using CO2 for waste management, energy recovery, and biochar fabrication.* Applied Energy, 2017. **185, Part 1**: p. 214-222.
105. Lim, A.C.R., et al., *Kinetic Analysis of Rice Husk Pyrolysis Using Kissinger-Akahira-Sunose (KAS) Method ☆.* Procedia Engineering, 2016. **148**: p. 1247-1251.
106. Tian, L., A. Tahmasebi, and J. Yu, *An experimental study on thermal decomposition behavior of magnesite.* Journal of Thermal Analysis & Calorimetry, 2014. **118**(3): p. 1577-1584.
107. Yorulmaz, S.Y. and A.T. Atimtay, *Investigation of combustion kinetics of treated and untreated waste wood samples with thermogravimetric analysis.* Fuel Processing Technology, 2009. **90**(7-8): p. 939-946.
108. Pozar, D.M., *Microwave Engineering Addison.* Wesley Publishing Company, 1993.
109. Bianchi and Giovanni, *Microwave and RF engineering*. 2010: Wiley.
110. *Litton - For Heat, Tune to 915 or 2450 Megacycles*, in *Litton Industries*. 1965.
111. Hoogenboom, R., et al., *Microwave-Assisted Chemistry: a Closer Look at Heating Efficiency.* Australian Journal of Chemistry, 2009. **62**(3): p. 236-243.
112. Metaxas, A.C. and R.J. Meredith, *Industrial Microwave Heating.* 1988: p. 376.

113. Haque, K.E., *Microwave energy for mineral treatment processes—a brief review.* International Journal of Mineral Processing, 1999. **57**(1): p. 1-24.
114. Meredith, R., *Engineers' Handbook of Industrial Microwave Heating.* Power Engineer, 1998. **13**(1): p. 3-3.
115. Suriapparao, D.V. and R. Vinu, *Resource recovery from synthetic polymers via microwave pyrolysis using different susceptors.* Journal of Analytical & Applied Pyrolysis, 2015. **113**: p. 701-712.
116. Zlotorzynski, A., *The Application of Microwave Radiation to Analytical and Environmental Chemistry.* Critical Reviews in Analytical Chemistry, 1995. **25**(1): p. 43-76.
117. Fernández, Y. and J.A. Menéndez, *Influence of feed characteristics on the microwave-assisted pyrolysis used to produce syngas from biomass wastes.* Journal of Analytical & Applied Pyrolysis, 2011. **91**(2): p. 316-322.
118. Menéndez, J.A., et al., *Microwave heating processes involving carbon materials.* Fuel Processing Technology, 2010. **91**(1): p. 1-8.
119. Su, S.L. and H.A. Chase, *A Review on Waste to Energy Processes Using Microwave Pyrolysis.* Energies, 2012. **5**(10): p. 4209-4232.
120. Motasemi, F. and M.T. Afzal, *A review on the microwave-assisted pyrolysis technique.* Renewable and Sustainable Energy Reviews, 2013. **28**: p. 317-330.
121. Smith, R.D., *Microwave power in industry. Final report.* 1984.
122. *Making waves in food*, in *Technology Strategy Board*. 2012, Biosciences.
123. Kuan, W.-H., et al., *Catalytic pyrolysis of sugarcane bagasse by using microwave heating.* Bioresource Technology, 2013. **146**: p. 324-329.
124. Huang, Y.F., et al., *Catalytic and atmospheric effects on microwave pyrolysis of corn stover.* Bioresource Technology, 2013. **131**(3): p. 274-280.
125. Thostenson, E.T. and T.W. Chou, *Microwave processing: fundamentals and applications.* Composites Part A Applied Science & Manufacturing, 1999. **30**(9): p. 1055-1071.

126. Zhao, X., et al., *Microwave pyrolysis of wheat straw: Product distribution and generation mechanism.* Bioresource Technology, 2014. **158**(2): p. 278-285.
127. Fernandez, Y., A. Arenillas, and J.A. Menendez, *Microwave Heating Applied to Pyrolysis*. 2011.
128. Huang, Y.-F., P.-T. Chiueh, and S.-L. Lo, *A review on microwave pyrolysis of lignocellulosic biomass.* Sustainable Environment Research, 2016. **26**(3): p. 103-109.
129. Zhao, W., et al., *Effect of microwave irradiation on selective heating behavior and magnetic separation characteristics of Panzhihua ilmenite.* Applied Surface Science, 2014. **300**: p. 171-177.
130. Conner, W.C. and G.A. Tompsett, *How could and do microwaves influence chemistry at interfaces?* Journal of Physical Chemistry B, 2008. **112**(7): p. 2110.
131. Zhang, H. and A.K. Datta, *Microwave Power Absorption in Single - and Multiple - Item Foods ☆.* Food & Bioproducts Processing, 2003. **81**(3): p. 257-265.
132. Collins, J.M. and N.E. Leadbeater, *Microwave Energy: A Versatile Tool for the Biosciences.* Cheminform, 2007. **5**(8): p. 1141-1150.
133. Li, J., et al., *Biochar from microwave pyrolysis of biomass: A review.* Biomass and Bioenergy, 2016. **94**: p. 228-244.
134. Hayhurst, A.N., *Introduction to heat transfer*. 1958: McGraw-Hill. B37-B38.
135. Scott Jones, M.M., Marion Mixers, *Comparing Microwave to Conventional Heating and Drying Systems*, in *Chemical Product Processing*.
136. van de Voort, F.R., et al., *A Practical Thermocouple for Temperature Measurement in Microwave Ovens1.* Canadian Institute of Food Science and Technology Journal, 1987. **20**(4): p. 279-284.
137. Namazi, A.B., D.G. Allen, and C.Q. Jia, *Microwave-assisted pyrolysis and activation ofpulp mill sludge.* Biomass & Bioenergy, 2015. **73**: p. 217-224.

138. Wang, X.H., et al., *PROPERTIES OF GAS AND CHAR FROM MICROWAVE PYROLYSIS OF PINE SAWDUST.* Bioresources, 2009. **4**(3): p. 946-959.
139. Kappe, C.O. and A. Stadler, *Microwaves in organic and medicinal chemistry*. 2005: Wiley-VCH Verlag GmbH & Co. KGaA.
140. Salema, A.A. and F.N. Ani, *Microwave induced pyrolysis of oil palm biomass.* Bioresource Technology, 2011. **102**(3): p. 3388-3395.
141. Li, J., et al., *Biochar from microwave pyrolysis of biomass: A review.* Biomass and Bioenergy, 2016: p. 228–244.
142. Menéndez, J.A., et al., *Microwave-induced drying, pyrolysis and gasification (MWDPG) of sewage sludge: Vitrification of the solid residue.* Journal of Analytical & Applied Pyrolysis, 2005. **74**(1): p. 406-412.
143. Domínguez, A., et al., *Investigations into the characteristics of oils produced from microwave pyrolysis of sewage sludge.* Fuel Processing Technology, 2005. **86**(9): p. 1007-1020.
144. Menéndez, J.A., M. Inguanzo, and J.J. Pis, *Microwave-induced pyrolysis of sewage sludge.* Water Research, 2002. **36**(13): p. 3261-3264.
145. Harfi, K.E., et al., *Pyrolysis of the Moroccan (Tarfaya) oil shales under microwave irradiation.* Fuel, 2000. **79**(7): p. 733-742.
146. Borges, F.C., et al., *Fast microwave-assisted pyrolysis of microalgae using microwave absorbent and HZSM-5 catalyst.* Bioresource Technology, 2014. **166**: p. 518-526.
147. Borges, F.C., et al., *Fast microwave assisted pyrolysis of biomass using microwave absorbent.* Bioresource Technology, 2014. **156**: p. 267-274.
148. Bu, Q., et al., *Production of phenols and biofuels by catalytic microwave pyrolysis of lignocellulosic biomass.* Bioresource Technology, 2012. **108**: p. 274-279.
149. Mushtaq, F., R. Mat, and F.N. Ani, *The Performances of Intimately Mix and Layer Methods in Microwave Assisted Pyrolysis System.* Applied Mechanics & Materials, 2014. **554**: p. 150-154.

150. Mushtaq, F., et al., *Optimization and characterization of bio-oil produced by microwave assisted pyrolysis of oil palm shell waste biomass with microwave absorber.* Bioresource Technology, 2015. **190**: p. 442-450.
151. Huang, Y.F., et al., *Hydrogen-rich fuel gas from rice straw via microwave-induced pyrolysis.* Bioresource Technology, 2010. **101**(6): p. 1968-1973.
152. Guo, Z., et al., *Study on kinetics of coal pyrolysis at different heating rates to produce hydrogen.* Fuel Processing Technology, 2013. **107**: p. 23-26.
153. Fu, P., et al., *Evaluation of the porous structure development of chars from pyrolysis of rice straw: Effects of pyrolysis temperature and heating rate.* Journal of Analytical and Applied Pyrolysis, 2012. **98**: p. 177-183.
154. Hu, Z., X. Ma, and C. Chen, *A study on experimental characteristic of microwave-assisted pyrolysis of microalgae.* Bioresource Technology, 2012. **107**(3): p. 487-493.
155. Zhao, X., et al., *Effect of temperature and additives on the yields of products and microwave pyrolysis behaviors of wheat straw.* Journal of Analytical and Applied Pyrolysis, 2013. **100**: p. 49-55.
156. Du, Z., et al., *Microwave-assisted pyrolysis of microalgae for biofuel production.* Bioresource Technology, 2011. **102**(7): p. 4890-4896.
157. Kuan, W.H., et al., *Catalytic pyrolysis of sugarcane bagasse by using microwave heating.* Bioresource Technology, 2013. **146**(10): p. 324-329.
158. Yu, Y., et al., *Influence of catalyst types on the microwave-induced pyrolysis of sewage sludge.* Journal of Analytical & Applied Pyrolysis, 2014. **106**(3): p. 86-91.
159. Huang, Y.F., et al., *Microwave torrefaction of rice straw and pennisetum.* Bioresource Technology, 2012. **123**(123): p. 1-7.
160. Wornat, M.J., et al., *Single-particle combustion of two biomass chars.* Symposium on Combustion, 1996. **26**(2): p. 3075-3083.

161. Lin, K.C., Y.-C. Lin, and Y.-H. Hsiao, *Microwave plasma studies of Spirulina algae pyrolysis with relevance to hydrogen production.* Energy, 2014. **64**: p. 567-574.
162. S. Czernik, a. and A.V. Bridgwater‡, *Overview of Applications of Biomass Fast Pyrolysis Oil.* Energy & Fuels, 2004. **18**(2): p. 590--598.
163. Shoji, T., H. Kawamoto, and S. Saka, *Complete inhibition of char formation from cellulose in fast pyrolysis with aromatic substance.* Journal of Analytical and Applied Pyrolysis.
164. Du, Z., et al., *Microwave-assisted pyrolysis of microalgae for biofuel production.* Bioresour Technol, 2011. **102**(7): p. 4890-6.
165. Suriapparao, D.V., N. Pradeep, and R. Vinu, *Bio-Oil Production from Prosopis juliflora via Microwave Pyrolysis.* Energy & Fuels, 2015. **29**(4): p. 2571-2581.
166. Armaroli, N. and V. Balzani, *The Legacy of Fossil Fuels.* Chemistry – An Asian Journal, 2011. **6**(3): p. 768–784.
167. Overpeck, J.T., et al., *Paleoclimatic Evidence for Future Ice-Sheet Instability and Rapid Sea-Level Rise.* Science (New York, N.Y.), 2006. **311**(5768): p. 1747-50.
168. Pierantozzi, R., *Carbon Dioxide*, in *Kirk-Othmer Encyclopedia of Chemical Technology*. 2000, John Wiley & Sons, Inc.
169. Rubin, E.S., *Summary of the IPCC Special Report on Carbon Dioxide Capture and Storage.* Economics & Politics of Climate Change, 2006: p. 35-41.
170. Ravikumar, C., et al., *Microwave assisted fast pyrolysis of corn cob, corn stover, saw dust and rice straw: Experimental investigation on bio-oil yield and high heating values.* Sustainable Materials and Technologies, 2017. **11**: p. 19-27.
171. Halim, S.A. and J. Swithenbank, *Characterisation of Malaysian wood pellets and rubberwood using slow pyrolysis and microwave technology.* Journal of Analytical and Applied Pyrolysis, 2016. **122**: p. 64-75.

172. Cho, D.-W., et al., *Carbon dioxide assisted sustainability enhancement of pyrolysis of waste biomass: A case study with spent coffee ground.* Bioresource Technology, 2015. **189**: p. 1-6.
173. Lahijani, P., et al., *Microwave-enhanced CO2 gasification of oil palm shell char.* Bioresource Technology, 2014. **158**(0): p. 193-200.
174. Gao, S.P., et al., *Effect of CO 2 on pyrolysis behaviors of lignite.* Journal of Fuel Chemistry & Technology, 2013. **41**(3): p. 257-264.
175. Chen, M.-q., et al., *Catalytic effects of eight inorganic additives on pyrolysis of pine wood sawdust by microwave heating.* Journal of Analytical and Applied Pyrolysis, 2008. **82**(1): p. 145-150.
176. Beneroso, D., et al., *Integrated microwave drying, pyrolysis and gasification for valorisation of organic wastes to syngas.* Fuel, 2014. **132**: p. 20-26.
177. Wu, C., et al., *Conventional and microwave-assisted pyrolysis of biomass under different heating rates.* Journal of Analytical and Applied Pyrolysis, 2014. **107**: p. 276-283.
178. Pujadó, P.R., et al., *Industrial catalytic applications of molecular sieves.* Catalysis Today, 1992. **13**(1): p. 113-141.
179. Horne, P.A. and P.T. Williams, *The effect of zeolite ZSM-5 catalyst deactivation during the upgrading of biomass-derived pyrolysis vapours.* Journal of Analytical & Applied Pyrolysis, 1995. **34**(1): p. 65-85.
180. Pan, P., et al., *The direct pyrolysis and catalytic pyrolysis of Nannochloropsis sp. residue for renewable bio-oils.* Bioresource Technology, 2010. **101**(12): p. 4593-4599.
181. Vitolo, S., et al., *Catalytic upgrading of pyrolytic oils to fuel over different zeolites.* Fuel, 1999. **78**(10): p. 1147-1159.
182. Anand, V., V. Sunjeev, and R. Vinu, *Catalytic fast pyrolysis of Arthrospira platensis (spirulina) algae using zeolites.* Journal of Analytical and Applied Pyrolysis, 2016. **118**: p. 298-307.
183. Ojha, D.K. and R. Vinu, *Resource recovery via catalytic fast pyrolysis of polystyrene using zeolites.* Journal of Analytical & Applied Pyrolysis, 2015. **113**: p. 349-359.

184. Tripathi, A.K., D.K. Ojha, and R. Vinu, *Selective production of valuable hydrocarbons from waste motorbike engine oils via catalytic fast pyrolysis using zeolites.* Journal of Analytical & Applied Pyrolysis, 2015. **114**: p. 281-292.
185. Li, L., et al., *Influence of microwave power, metal oxides and metal salts on the pyrolysis of algae.* Bioresource Technology, 2013. **142**: p. 469-474.
186. Guo, J. and A.C. Lua, *Preparation of activated carbons from oil-palm-stone chars by microwave-induced carbon dioxide activation.* Carbon, 2000. **38**(14): p. 1985-1993.
187. Li, J., et al., *CaO/NaA combined with enzymatic catalyst for biodiesel transesterification.* Catalysis Communications, 2012. **28**: p. 52-57.
188. Zhu, T., et al., *Effect of calcium oxide on pyrolysis of coal in a fluidized bed.* Fuel Processing Technology, 2000. **64**(1–3): p. 271-284.
189. Wan, Y., et al., *Microwave-assisted pyrolysis of biomass: Catalysts to improve product selectivity.* Journal of Analytical & Applied Pyrolysis, 2009. **86**(1): p. 161-167.
190. Yuan, H., et al., *Influences of copper on the pyrolysis process of demineralized wood dust through thermogravimetric and Py–GC/MS analysis.* Journal of Analytical & Applied Pyrolysis, 2015. **112**: p. 325-332.
191. Yang, H., et al., *Influence of mineral matter on pyrolysis of palm oil wastes.* Combustion & Flame, 2006. **146**(4): p. 605-611.
192. Wang, T.J., et al., *The steam reforming of naphthalene over a nickel–dolomite cracking catalyst.* Biomass & Bioenergy, 2005. **28**(5): p. 508-514.
193. Zhang, S., et al., *High quality syngas production from microwave pyrolysis of rice husk with char-supported metallic catalysts.* Bioresource Technology, 2015. **191**: p. 17-23.
194. Shen, Y., et al., *In-situ catalytic conversion of tar using rice husk char-supported nickel-iron catalysts for biomass pyrolysis/gasification.* Applied Catalysis B: Environmental, 2014. **152–153**: p. 140-151.

195. Shen, Y., et al., *In situ catalytic conversion of tar using rice husk char/ash supported nickel–iron catalysts for biomass pyrolytic gasification combined with the mixing-simulation in fluidized-bed gasifier ☆.* Applied Energy, 2015. **160**: p. 808-819.
196. Popescu, S., et al., *New microwave reactor for paper-based waste neutralization.* Resources Conservation & Recycling, 2008. **52**(4): p. 671-677.
197. Miura, M., et al., *Rapid pyrolysis of wood block by microwave heating.* Journal of Analytical & Applied Pyrolysis, 2004. **71**(1): p. 187-199.
198. Nik-Azar, M., et al., *Mineral matter effects in rapid pyrolysis of beech wood.* Fuel Processing Technology, 1997. **51**(1–2): p. 7-17.
199. Zhang, Y., et al., *Effects of feedstock characteristics on microwave-assisted pyrolysis – A review.* Bioresource Technology, 2017. **230**: p. 143-151.
200. Keown, D.M., J.-i. Hayashi, and C.-Z. Li, *Effects of volatile–char interactions on the volatilisation of alkali and alkaline earth metallic species during the pyrolysis of biomass.* Fuel, 2008. **87**(7): p. 1187-1194.
201. Ying, Y., et al., *Influence of catalyst types on the microwave-induced pyrolysis of sewage sludge.* Journal of Analytical & Applied Pyrolysis, 2014. **106**(3): p. 86-91.
202. Liu, H., et al., *The catalytic pyrolysis of food waste by microwave heating.* Bioresource Technology, 2014. **166**(8): p. 45-50.
203. Li, L.J., et al., *Influence of microwave power, metal oxides and metal salts on the pyrolysis of algae.* Bioresource Technology, 2013. **142**(4): p. 469-474.
204. Domínguez, A., et al., *Bio-syngas production with low concentrations of CO2 and CH4 from microwave-induced pyrolysis of wet and dried sewage sludge.* Chemosphere, 2008. **70**(3): p. 397-403.
205. Hascakir, B. and S. Akin, *Recovery of Turkish Oil Shales by Electromagnetic Heating and Determination of the Dielectric Properties of Oil Shales by an Analytical Method.* Energy & Fuels, 2009. **24**(1): p. 503-509.

206. Cerqueira, H.S., et al., *Deactivation of FCC catalysts.* Journal of Molecular Catalysis A Chemical, 2008. **292**(1–2): p. 1-13.
207. Bridgwater, A.V. and A.V. Bridgwater, *Review of fast pyrolysis of biomass and product upgrading.* Biomass & Bioenergy, 2012. **38**(2): p. 68-94.
208. Yildiz, G., et al., *Effect of biomass ash in catalytic fast pyrolysis of pine wood.* Applied Catalysis B: Environmental, 2015. **168–169**: p. 203-211.
209. Shen, Y., et al., *Oil sludge recycling by ash-catalyzed pyrolysis-reforming processes.* Fuel, 2016. **182**: p. 871-878.
210. Cheng, S., et al., *Pyrolysis of oil sludge with oil sludge ash additive employing a stirred tank reactor.* Journal of Analytical and Applied Pyrolysis, 2016. **120**: p. 511-520.
211. Zhang, Y., et al., *Characteristics of biomass fast pyrolysis in a wire-mesh reactor.* Fuel, 2017. **200**: p. 225-235.
212. Singh, Y.D., P. Mahanta, and U. Bora, *Comprehensive characterization of lignocellulosic biomass through proximate, ultimate and compositional analysis for bioenergy production.* Renewable Energy, 2017. **103**: p. 490-500.
213. Oladejo, J.M., et al., *A novel index for the study of synergistic effects during the co-processing of coal and biomass.* Applied Energy, 2017. **188**: p. 215-225.
214. Li, X.-g., et al., *Thermogravimetric analysis of the co-combustion of the blends with high ash coal and waste tyres.* Thermochimica Acta, 2006. **441**(1): p. 79-83.
215. Guoqiang, L., *A Study on Pyrolysis and Combustion Characteristics of Municipal Solid Waste.* Shanghai Environmental Sciences, 2009.
216. Hong, Y., et al., *Microwave-enhanced pyrolysis of macroalgae and microalgae for syngas production.* Bioresource Technology.
217. Jimenez, G.D., et al., *New insights into microwave pyrolysis of biomass: Preparation of carbon-based products from pecan nutshells and their application in wastewater treatment.* Journal of Analytical and Applied Pyrolysis.

218. Moralı, U., N. Yavuzel, and S. Şensöz, *Pyrolysis of hornbeam (Carpinus betulus L.) sawdust: Characterization of bio-oil and bio-char.* Bioresource Technology, 2016. **221**: p. 682-685.
219. Adam, J., et al., *In situ catalytic upgrading of biomass derived fast pyrolysis vapours in a fixed bed reactor using mesoporous materials.* Microporous and Mesoporous Materials, 2006. **96**(1): p. 93-101.
220. Wang, X.H., et al., *Properties of gas and char from microwave pyrolysis of pine sawdust.* Bioresources, 2012. **4**(3): p. 946-959.
221. Zhang, H., et al., *Comparison of non-catalytic and catalytic fast pyrolysis of corncob in a fluidized bed reactor.* Bioresource Technology, 2009. **100**(3): p. 1428.
222. Kirtania, K. and S. Bhattacharya, *Pyrolysis kinetics and reactivity of algae–coal blends.* Biomass and Bioenergy, 2013. **55**: p. 291-298.
223. Wang, C., et al., *Thermogravimetric studies of the behavior of wheat straw with added coal during combustion.* Biomass and Bioenergy, 2009. **33**(1): p. 50-56.
224. Arias, B., et al., *Effect of biomass blending on coal ignition and burnout during oxy-fuel combustion.* Fuel, 2008. **87**(12): p. 2753-2759.
225. Channiwala, S.A. and P.P. Parikh, *A unified correlation for estimating HHV of solid, liquid and gaseous fuels ☆.* Fuel, 2002. **81**(8): p. 1051-1063.
226. Narayan, R. and M.J. Antal, *Thermal Lag, Fusion, and the Compensation Effect during Biomass Pyrolysis.* Industrial & Engineering Chemistry Research, 1996. **35**(5): p. 1711-1721.
227. Zhukova, N.V. and N.A. Aizdaicher, *Fatty acid composition of 15 species of marine microalgae.* Phytochemistry, 1995. **39**(2): p. 351-356.
228. Gressler, V., et al., *Lipid, fatty acid, protein, amino acid and ash contents in four Brazilian red algae species.* Food Chemistry, 2010. **120**(2): p. 585-590.
229. Kumari, P., et al., *Fatty acid profiling of tropical marine macroalgae: An analysis from chemotaxonomic and nutritional perspectives.* Phytochemistry, 2013. **86**(Supplement C): p. 44-56.

230. Amaral Debiagi, P.E., et al., *Algae Characterization and Multistep Pyrolysis Mechanism.* Journal of Analytical and Applied Pyrolysis, 2017.
231. And, R.N. and M.J. Antal, *Thermal Lag, Fusion, and the Compensation Effect during Biomass Pyrolysis†.* Industrial & Engineering Chemistry Research, 1996. **35**(5): p. 1711-1721.
232. Grønli, M., M.J. Antal, and G. Várhegyi, *A Round-Robin Study of Cellulose Pyrolysis Kinetics by Thermogravimetry.* Industrial & Engineering Chemistry Research, 1999. **38**(6): p. 2238-2244.
233. Du, Z., et al., *Catalytic pyrolysis of microalgae and their three major components: Carbohydrates, proteins, and lipids.* Bioresource Technology, 2013. **130**: p. 777-782.
234. Huang, Y.F., et al., *Microwave pyrolysis of lignocellulosic biomass: Heating performance and reaction kinetics.* Energy, 2016. **100**: p. 137-144.
235. Salema, A.A., et al., *Dielectric properties and microwave heating of oil palm biomass and biochar.* Industrial Crops and Products, 2013. **50**: p. 366-374.
236. Sait, H.H. and A.A. Salema, *Microwave dielectric characterization of Saudi Arabian date palm biomass during pyrolysis and at industrial frequencies.* Fuel, 2015. **161**: p. 239-247.
237. Torgovnikov, G.I., *Dielectric Properties of Wood and Wood-Based Materials*. 1993: Springer Berlin Heidelberg. 135-143.
238. Bridgwater, A.V., *Review of fast pyrolysis of biomass and product upgrading.* Biomass & Bioenergy, 2012. **38**(2): p. 68-94.
239. Diebold, J.P. and A.V. Bridgwater, *Overview of Fast Pyrolysis of Biomass for the Production of Liquid Fuels*. 1997: Springer Netherlands. 5-23.
240. Acıkgoz, C., O. Onay, and O.M. Kockar, *Fast pyrolysis of linseed: product yields and compositions.* Journal of Analytical & Applied Pyrolysis, 2004. **71**(2): p. 417-429.
241. Tsai, W.T., M.K. Lee, and Y.M. Chang, *Fast pyrolysis of rice straw, sugarcane bagasse and coconut shell in an induction-heating reactor.* Journal of Analytical & Applied Pyrolysis, 2006. **76**(1): p. 230-237.

242. Shinogi, Y. and Y. Kanri, *Pyrolysis of plant, animal and human waste: physical and chemical characterization of the pyrolytic products.* 2004. **90**(3): p. 241-7.
243. Yanik, J., et al., *Pyrolysis of algal biomass.* Journal of Analytical & Applied Pyrolysis, 2014. **103**(9): p. 134-141.
244. Wang, S., et al., *Research on Pyrolysis Characteristics of Seaweed.* Energy Fuels, 2007. **21**(6): p. 3723-3729.
245. Xianwen, D., et al., *The Fast Pyrolysis of Biomass in CFB Reactor.* Energy Fuels, 2000. **14**(3): p. 552-557.
246. Zheng, L. and E. Furinsky, *Comparison of Shell, Texaco, BGL and KRW gasifiers as part of IGCC plant computer simulations.* Energy conversion and management, 2005. **46**(11): p. 1767-1779.
247. Yuan, Y.n., T.j. Wang, and Q.x. Li, *Production of Low-carbon Light Olefins from Catalytic Cracking of Crude Bio-oil.* Chinese Journal of Chemical Physics, 2013. **26**(2): p. 237-244.
248. Jeong, H.M., et al., *Pyrolysis kinetics of coking coal mixed with biomass under non-isothermal and isothermal conditions.* Bioresource Technology, 2014. **155**: p. 442-445.
249. Skoulou, V. and A. Zabaniotou, *Fe catalysis for lignocellulosic biomass conversion to fuels and materials via thermochemical processes.* Catalysis Today, 2012. **196**(1): p. 56-66.
250. Ducousso, M., et al., *Reactivity enhancement of gasification biochars for catalytic applications.* Fuel, 2015. **159**: p. 491-499.
251. Raveendran, K., A. Ganesh, and K.C. Khilar, *Influence of mineral matter on biomass pyrolysis characteristics.* Fuel, 1995. **74**(12): p. 1812-1822.
252. Parvez, A.M. and T. Wu, *Characteristics and interactions between coal and carbonaceous wastes during co-combustion.* Journal of the Energy Institute, 2017. **90**(1): p. 12-20.
253. Wu, T., et al., *Characteristics and synergistic effects of co-firing of coal and carbonaceous wastes.* Fuel, 2013. **104**: p. 194-200.
254. Liu, Z. and R. Balasubramanian, *A comparison of thermal behaviors of raw biomass, pyrolytic biochar and their blends with lignite.* Bioresource Technology, 2013. **146**: p. 371-378.

255. Wu, T., et al., *Characterisation of residual carbon from entrained-bed coal water slurry gasifiers.* Fuel, 2007. **86**(7-8): p. 972-982.
256. Liu, Y., et al., *The production of diesel-like hydrocarbons from palmitic acid over HZSM-22 supported nickel phosphide catalysts.* Applied Catalysis B Environmental, 2015. **174-175**: p. 504-514.
257. Zhang, Y., et al., *Effects of feedstock characteristics on microwave-assisted pyrolysis - A review.* Bioresource Technology, 2017. **230**: p. 143-151.
258. Chen, M.Q., et al., *Catalytic effects of eight inorganic additives on pyrolysis of pine wood sawdust by microwave heating.* Journal of Analytical & Applied Pyrolysis, 2008. **82**(1): p. 145-150.